



Universitat Autònoma
de Barcelona

Contribution to lithiasic process knowledge

**Characterization of physiological aspect and novel
material to determine key inhibitors**

Tong Liu

Supervisors

Montserrat López-Mesas

Manuel Valiente Malmagro

2015



Contribution to lithiasic process knowledge

**Characterization of physiological aspect and novel
material to determine key inhibitors**

Tong Liu

Doctoral Thesis

PhD in Chemistry

Supervisors

Montserrat López-Mesas

Manuel Valiente Malmagro

Department of Chemistry

Faculty of Science

2015



Report submitted to aspire for the Doctor Degree by:

Tong Liu

Supervisors' approval:

Dr. Montserrat López-Mesas

Prof. Manuel Valiente Malmagro

Bellaterra, 30/09/2015

Acknowledgements

First and foremost, I wish to thank my supervisor Prof. Montserrat López Mesas for her guidance and support. Without her patient instruction, insightful criticism and expert guidance, the project would never matured into a typical thesis. I would also like to thank Prof. Manuel Valiente Malmagro for his invaluable advice and constant encouragement. Also he gave me a lot of opportunity to learn and many recommendations beyond the research. In addition, I would like to thank Prof. Olivier for providing me the short stay position in LCABIE, Pau, France, which make me to learn a lot of new techniques for analytical chemistry. Thank you very much Dr. Zoyne, who help me a lot when I was in Pau.

I would like to express my gratitude to Prof. Yongjun Zhang (my supervisor during Master), who inspired me to do further scientific research.

I would like to thank the friendly and generous staff and members of GTS for their help and guidance. My work could not have been proceeded without the assistance of several key staff members. Gustavo, Cristina Palet, Montserrat Resina Gallego, Maria dolors, Diego Morillo Martin, Fran Blanco, Pilar, Oriol, Julio, Olga Kotkowska, Maribel Restituyo Silis, Nurlin Abu Samah, Veronica Verdugo, Victor Marquina Garces, Maria Angles Subirana, Albert Pell Lorante, Maria Jesus sanchez Martin.

I take this opportunity to record my sincere appreciation to my doctoral colleagues, roommates, ball friends and playmates, Haijie Liu, Yangchun Xin, Zhikun Xu, Wusheng Guo, Zhiyu Jia, Guofen Ma, Helan Zhang, Muling Zeng, Yuanyuan Lu, Jian Li, Siming Yu, Min Cao, Qin Liu, Qinyi Tan, Luyan Teng, Ping Sun, for their valuable friendship. Additionally, thanks for the help of Caiyan Feng, Hongyao Yin, who are my friends in Pau, France.

I should especially acknowledge the encouragement, support and love given to me by my wife and my parents, without which I could have never reached this point in my life. And

finally, thanks for my boy “Pedro”, who comes to my life during my PhD study period and I want to say “I love you forever”.

Last but not least, I would like to gratefully acknowledge the financial support of Chinese scholarship council (CSC) for granting my personal expenses. In addition, the present thesis has been developed with the financial support of Projects: CHEMSYNCRO (Spanish Ministerio de Economía y Competitividad Ref, CTM2012-30970) and the EU project ORQUE-SUDOE (Interreg Program, project reference SOE3/P2/F591)

Summary

Urolithiasis is one of the most prevalent urological diseases, occurring in both industrialized and developing countries. The incidence rate is up to 15% of white men and 6% of all women and the recurrence affect about half of those people. Kidney stones are aggregates of crystals that cause obstruction of urine flow in the renal collecting system, ureters, or urethra and result in severe pain, bleeding or local erosion of kidney tissue. The etiological diversity of urinary stone formed as a result of different mechanisms which is still not well understood. The challenges posed by urinary lithiasis demands enhanced interdisciplinary diagnostic, therapeutic options and secondary prevention.

The purpose of this thesis is to offer knowledge to the previous mentioned challenges using novel scientific methods or materials. The dissertation exposes the work developed in three areas concerning urolithiasis, which embeds urolithiasis key inhibitors extraction from food, phosphorous inhibitors determination by using novel material, and copper isotopic fractionation analysis from urolithiasis patients

The first section in the dissertation is devoted to the use of microwave assisted extraction (MAE) technique to quantitatively extract the two phosphorous inhibitors of urolithiasis, phytic acid (IP₆) and pyrophosphate (PPi), from walnut since the existing extraction method and quantitative analysis show inconveniences. Walnuts were chosen since they are highly consumed, rich in polyunsaturated fatty acid and provide significant benefits due to the antioxidant capacity. Three main parameters were considered to optimize the condition of microwave-assisted extraction: acid content of extracting solvent, extraction time and treatment temperature. The hydrolysis of phytic acid by microwave treatment was also investigated for all the tested conditions. The extraction using mixture of 0.52 M H₂SO₄ and 0.66 M HCl under MAE condition (100°C, 10min) shows a better extract ability for both IP₆ and PPi. Compared with the conventional acid extraction method, the microwave-assisted extraction method developed reduces extraction time from 3h to 10 min obtaining the same recovery results.

The second section in the dissertation is devoted to develop a novel material based on molecular imprinted technology for selectively adsorb and separate the IP₆ and PPi. In this work, polymers have been molecularly imprinted using three organophosphorus compounds as template, phenylphosphonic acid (PA), Di-(2-ethylhexyl) phosphoric acid (DEHPA) and pyrophosphoric acid. The Molecularly Imprinted Polymer, MIP, was prepared by thermal polymerization using N-allylthiourea (AT) as functional monomer and ethylene glycol dimethacrylate (EGDMA) as cross-linker. The batch adsorption experiments show that the MIP using DEHPA has the best specific adsorption for IP₆ and the adsorption process is quite fast. The pH has a significant effect on the adsorption behavior of IP₆, PPi and phosphate. Through modification of the pH of the eluting solvent, IP₆, PPi and phosphate can be separated by SPE procedure using the developed MIP.

The third part of the thesis considers the physiological aspect of urolithiasis. In the literature Copper has shown inhibitory effect on the growth of kidney stone and disordered in copper metabolism may be important in the aetiology of disease. The blood Copper isotope fractionation from urolithiasis patients from Barcelona area was analyzed and compared to healthy controls. The serum and red cell samples Cu isotope compositions was measured by multi-collector ICP-MS after separation and purification by anion exchange chromatography. Our results show that, for the population considered in this study, Cu concentration and Cu isotopic ratio (⁶⁵Cu/⁶³Cu) show different value between the urolithiasis patients and the healthy people. Although further studies with a larger number of samples are needed, results are encouraging as far as the use of Cu isotopic analysis for the study of urolithiasis disease.

La urolitiasis es una de las enfermedades urológicas más frecuentes, que se producen tanto en los países industrializados como en vías de desarrollo. La tasa de incidencia es de hasta el 15% en hombres de raza blanca y el 6% de todas las mujeres. La recurrencia afecta aproximadamente a la mitad de los afectados. Los cálculos renales son agregados cristalinos que causan la obstrucción de la orina en el sistema colector renal, uréteres o uretra, resultando en dolor severo, sangrado o erosión local del tejido renal. La etiología del cálculo urinario formado es resultado de diferentes mecanismos que todavía no son bien entendidos. Los retos que plantea la litiasis urinarias son entre otros, mejores opciones terapéuticas, diagnóstico interdisciplinario y prevención secundaria.

El propósito de esta tesis es ofrecer conocimiento a los retos mencionados utilizando nuevos métodos científicos o materiales. La tesis expone el trabajo desarrollado en tres áreas relativas a la urolitiasis: extracción de inhibidores clave de alimentos, determinación de inhibidores de fósforo mediante un nuevo material desarrollado, y el análisis de fraccionamiento isotópico de cobre de pacientes de urolitiasis

En la primera sección se evalúa el uso de la extracción asistida por microondas (MAE) para extraer cuantitativamente los inhibidores de litiasis ácido fítico (IP_6) y pirofosfato (PPi) de nueces. Se escogieron nueces son un componente importante de la dieta humana, ricas en ácidos grasos poliinsaturados y tienen capacidad antioxidante. Se optimizaron los parámetros: concentración del ácido utilizado para la extracción, el tiempo y la temperatura de tratamiento. También se ha evaluado la hidrólisis del ácido fítico. Los mejores resultados se obtuvieron para una mezcla de 0,52 M de H_2SO_4 y 0,66 M HCl a 100 °C durante 10 min. En comparación con el método de extracción convencional, MAE reduce el tiempo de extracción de 3h a 10 min obteniendo los mismos resultados de recuperación.

La segunda sección de la tesis está dedicada a desarrollar un nuevo Polímero de Impresión Molecular (MIP) para adsorber y separar IP_6 y PPi. En este trabajo, los polímeros han sido desarrollados utilizando tres compuesto organofosforados como plantilla, ácido fenilfosfónico (PA), Di- (2-etilhexil) ácido fosfórico (DEHPA) y ácido pirofosfórico. El MIP se preparó mediante polimerización térmica utilizando N-aliltiourea (AT) como monómero y dimetacrilato de etilenglicol (EGDMA) como agente de reticulación. Los resultados muestran que el MIP formado usando DEHPA presenta la mejor adsorción para IP_6 y el proceso de adsorción es bastante rápido. El pH tiene un efecto significativo sobre el comportamiento de adsorción de IP_6 , PPi y fosfato por lo que utilizando diferentes concentraciones de pH IP_6 , PPi y fosfato pueden separarse mediante el uso del MIP en una extracción en fase sólida.

La tercera parte de la tesis considera un aspecto fisiológico de la urolitiasis. En la literatura se describe al Cobre como inhibidor del crecimiento de cálculos renales y una disfunción en el metabolismo del cobre puede estar relacionado con la etiología de la enfermedad. El estudio de la relación isotópica de cobre en sangre (suero y glóbulos rojos) de pacientes urolitiásicos del área de Barcelona se analizó y comparó con controles sanos. El Cu se separó y purificó mediante cromatografía de intercambio aniónico y analizó con un multi-colector ICP-MS. Los resultados muestran que, para la población considerada en este estudio, tanto la concentración como la relación isotópica ($^{65}Cu/^{63}Cu$) muestran diferencias entre pacientes y controles. Aunque se necesitan más estudios con un número mayor de muestras, los resultados son alentadores en cuanto a la utilización del análisis isotópico de Cu para el estudio de la enfermedad urolitiásica.

CONTENT

1. INTRODUCTION	1
1.1. DESCRIPTION OF UROLITHIASIS.....	3
1.1.1. <i>Epidemiology</i>	5
1.1.2. <i>Pathogenesis</i>	6
1.1.3. <i>Physicochemical aspect of urolithiasis</i>	8
1.1.3.1. <i>Supersaturation</i>	8
1.1.3.2. <i>Crystal formation</i>	9
1.2. CLASSIFICATION OF URINARY STONES	10
1.2.1. <i>Calcium oxalate stones</i>	12
1.2.2. <i>Uric acid stones</i>	13
1.2.3. <i>Struvite stones</i>	14
1.2.4. <i>Cystine stones</i>	15
1.2.5. <i>Brushite stones</i>	16
1.2.6. <i>Mixed stones</i>	17
1.2.7. <i>Other stones</i>	17
1.3. STONE ANALYSIS TECHNIQUES IN UROLITHIASIS.....	17
1.3.1. <i>Wet chemistry</i>	18
1.3.2. <i>Thermogravimetric analysis</i>	18
1.3.3. <i>Optical polarizing microscopy</i>	18
1.3.4. <i>Spectroscopy</i>	19
1.4. PROMOTERS AND INHIBITORS OF UROLITHIASIS	21
1.4.1. <i>Inhibitors</i>	22
1.4.1.1. <i>Phytic acid</i>	22
1.4.1.2. <i>Citrate</i>	25
1.4.1.3. <i>Pyrophosphate</i>	25

1.4.1.4.	Proteins	26
1.4.1.5.	Other macromolecules	29
1.4.2.	<i>Promoters</i>	29
1.5.	DETERMINATION OF PHOSPHOROUS INHIBITORS	31
1.5.1.	<i>Determination of IP6</i>	31
1.5.1.1.	Precipitation method	32
1.5.1.2.	Colorimetric method	33
1.5.1.3.	Ion-exchange method	33
1.5.1.4.	HPLC and HPIC method	34
1.5.2.	<i>Pyrophosphate determination</i>	36
1.5.2.1.	Chromatographic method	36
1.5.2.2.	Colorimetric method	36
1.5.2.3.	Enzymatic method	37
1.5.3.	<i>Drawbacks of the present analytic method for determination inhibitors of urolithiasis</i>	37
1.6.	COPPER IN THE PATHOGENESIS OF KIDNEY STONES	38
1.6.1.	<i>Cu in body</i>	38
1.6.2.	<i>Cu in the pathogenesis of kidney stones</i>	39
1.7.	REFERENCE	41
2.	OBJECTIVES	51
2.1.	GENERAL OBJECTIVE	53
2.2.	SPECIFIC OBJECTIVES	53
3.	INHIBITORS EXTRACTED FROM FOOD	55
3.1.	UROLITHIASIS INHIBITORS IN WALNUTS	57
3.2.	MICROWAVE ASSISTED EXTRACTION (MAE)	59
3.2.1.	<i>Introduction of MAE</i>	59
3.2.2.	<i>Basic principles</i>	63
3.2.3.	<i>Factors affecting MAE</i>	64

3.3.	EXPERIMENTAL	64
3.3.1.	<i>Walnuts materials</i>	64
3.3.2.	<i>Chemicals and reagents</i>	64
3.3.3.	<i>Preparation of walnut samples</i>	65
3.3.4.	<i>Microwave-assisted extraction (MAE)</i>	66
3.3.5.	<i>Solid-solvent extraction</i>	68
3.3.6.	<i>Separation of IP₆ and PP_i by solid phase extraction (SPE)</i>	69
3.3.7.	<i>Inductively coupled plasma mass spectrometry (ICP-MS)</i>	70
3.4.	RESULTS AND DISCUSSION	72
3.4.1.	<i>Effect of defatting process and acid solvent selection</i>	72
3.4.2.	<i>Effect of pH</i>	74
3.4.3.	<i>MAE parameters optimization</i>	75
3.4.4.	<i>Phytic acid hydrolysis in MAE</i>	77
3.4.5.	<i>Walnuts as a functional food</i>	78
3.5.	CONCLUSIONS	80
3.6.	REFERENCE	81
4.	NOVEL MATERIAL TO DETERMINE THE KEY INHIBITORS	85
4.1.	INTRODUCTION	87
4.1.1.	<i>Molecularly Imprinted Polymer (MIP)</i>	88
4.1.2.	<i>MIP preparation method</i>	89
4.1.2.1.	Monomer	89
4.1.2.2.	Cross-linker	90
4.1.2.3.	Solvent or porogen.....	91
4.1.3.	<i>Synthesis of MIP</i>	93
4.1.3.1.	Basic principle and approaches for the synthesis of MIP	93
4.1.4.	<i>Polymerization techniques</i>	93
4.1.4.1.	Bulk polymerization method.....	94

4.1.4.2.	Precipitation polymerization method	94
4.2.	EXPERIMENTAL	95
4.2.1.	<i>Reagents</i>	95
4.2.2.	<i>Preparation of Molecular Imprinted Polymer</i>	96
4.2.2.1.	Polymer of N-allylthiourea	96
4.2.2.2.	Polymer of MAA	97
4.2.2.3.	Soxhlet extraction	98
4.2.3.	<i>Batch mode studies</i>	99
4.2.3.1.	Influence of the initial pH.....	100
4.2.3.2.	Influence of temperature.....	100
4.2.4.	<i>Isotherm studies</i>	100
4.2.5.	<i>Kinetics studies</i>	101
4.2.6.	<i>Desorption experiments</i>	102
4.2.7.	<i>Solid phase extraction procedure on MIP</i>	102
4.2.8.	<i>ICP conditions</i>	102
4.3.	RESULTS AND DISCUSSION	104
4.3.1.	<i>The choice of monomer and cross-linker</i>	104
4.3.2.	<i>The effect of steric factors on recognition</i>	106
4.3.3.	<i>The impact of porogenic solvent</i>	108
4.3.4.	<i>The characterization of MIP</i>	109
4.3.5.	<i>The impact of molar ratio</i>	113
4.3.6.	<i>The effect of pH</i>	114
4.3.7.	<i>Adsorption isotherms</i>	115
4.3.7.1.	Langmuir isotherm	116
4.3.7.2.	Adsorption properties and Scatchard analysis.....	117
4.3.8.	<i>Adsorption kinetics</i>	119
4.3.9.	<i>The effect of temperature</i>	121

4.3.10.	<i>Separation section</i>	122
4.3.10.1.	The effect of pH	123
4.3.10.2.	MIP-Solid phase extraction	125
4.4.	CONCLUSION	127
4.5.	REFERENCE	128
5.	CU ISOTOPIC FRACTIONATION OF UROLITHIASIS	133
5.1.	INTRODUCTION	135
5.1.1.	<i>Cu in body</i>	135
5.1.2.	<i>Isotopic fractionation</i>	137
5.1.2.1.	Stable isotope	137
5.1.3.	<i>Stable isotope fractionation</i>	137
5.2.	EXPERIMENTS	138
5.2.1.	<i>Reagents and materials</i>	138
5.2.1.1.	Certified reference materials	139
5.2.1.2.	Chromatography materials	139
5.2.2.	<i>Equipment and methodology</i>	140
5.2.2.1.	Lyophilizer	140
5.2.2.2.	High Pressure Asher (HPA)	141
5.2.2.3.	Microwave digestion	142
5.2.2.4.	Hot block	143
5.2.2.5.	ICP-MS measurement	143
5.2.2.6.	Inductively Coupled Plasma Optical Emission Spectrometer (ICP-OES) measurement	146
5.2.2.7.	Multicollector-Inductively Coupled Plasma Mass Spectrometer (MC-ICP-MS) Instrumentation	147
5.2.3.	<i>Digestion procedure</i>	151
5.2.3.1.	Oyster samples	151
5.2.3.2.	Oyster sample digestion procedure	152
5.2.3.3.	Blood samples	152
5.2.3.4.	Sample digestion procedure	153

5.2.4.	<i>Clean-up procedure</i>	154
5.2.5.	<i>Isotopic fractionation measurement</i>	156
5.3.	RESULTS AND DISCUSSION	157
5.3.1.	<i>Cu extraction and clean-up procedure optimization</i>	157
5.3.2.	<i>Total Cu concentration in blood.</i>	161
5.3.3.	<i>Correction for mass discrimination</i>	162
5.3.4.	<i>Cu isotopic analysis of serum and red cell samples</i>	165
5.4.	CONCLUSION	168
5.5.	REFERENCE	169
6.	CONCLUSIONS	171
6.1.	GENERAL CONCLUSION	173
6.2.	KEY INHIBITORS MAE EXTRACTION FROM FOOD	173
6.3.	NOVEL MATERIAL FOR DETERMINATION OF KEY INHIBITORS	174
6.4.	CU ISOTOPIC ANALYSIS IN THE BLOOD OF UROLITHIASIS PATIENTS	175

ANNEX I

ANNEX II

ANNEX III

Abbreviations:

ACM, acrylamide	ICP-OES, inductively coupled plasma optical emission spectrometry
ACN, acetonitrile	IP ₆ , phytic acid
AEC, anion exchange column	LF, Langmuir-Freundlich
AIBN, 2, 2'-azobisisobutyronitrile	MAA, methacrylic acid
AT, N-Allylthiourea	MAE, microwave assisted extraction
BRU, brushite	MBAm, <i>N,N'</i> -Methylenebisacrylamide
CaOx, calcium oxalate	MC-ICP-MS, multicollector inductively coupled plasma mass spectrometer
CaPh, calcium phosphate	MIP, molecular imprinted polymer
CAP, carbonate apatite	MISPE, molecule-imprinted solid-phase extraction
CEC, capillary electrochromatography	MIT, molecular imprinting technology
COD, calcium oxalate dihydrate	NIP, non-imprinted polymer
COM, calcium oxalate monohydrate	NIR, near infrared
COT, calcium oxalate trihydrate	OPN, Osteopontin
DEHPA, Di-(2-ethylhexyl) phosphoric acid	PPi, pyrophosphate
DVB, divinylbenzene	P, phosphate
EGDMA, ethylene glycol dimethacrylate	PTF1, Prothrombin fragment 1
ESWL, extracorporeal shock wave lithotripsy	RL, renal lithostathine
FTIR, Fourier transform infrared	SPE, solid phase extraction
GAGS, glycosaminoglycans	TGA, thermogravimetric analysis
HPA, High Pressure Asher	TRIM, trimethylolpropane trimethacrylate
HPLC, high performance liquid chromatography	THP, Tamm-Horsfall Protein
HPIC, High-performance ion chromatography	UP, uropontin
ICP-MS, inductively coupled plasma mass spectrometry	WDs, Wilson's diseases



1. Introduction

1.1. Description of urolithiasis

Urolithiasis is one of the most prevalent urological diseases, occurring in both industrialized and developing countries. Urinary stone disease has afflicted human for thousand years. The oldest renal stone on record was described by Professor S. G. Shattock in 1905 and was found in an Egyptian mummy in a grave dating to about 4400 BC¹. The description of urinary stones has been a process of intense scientific investigation culminating in a burst of activity in the 19th century, when essentially all urinary stones seen commonly today were described and named². Kidney stones are aggregates of crystals mixed with a protein matrix that cause obstruction of urine flow in the renal collecting system, ureters, or urethra and result in severe pain, bleeding or local erosion of kidney tissue.

The urinary tract has several main components: the kidneys, which form the urine, the ureters which transport the urine to the bladder, which then stores the urine until it passes out of the body through the urethra. The kidneys are paired, bean-shaped organs, located in the back, just below the ribs. They serve multiple functions in the body, but primarily the kidneys filter the blood to clear toxins and extra water from the body by producing urine. Blood is filtered by a specialized structure called the glomerulus. Filtered blood from the glomeruli passes into a complex and highly specialized tubular system that runs through the kidney called the nephron, which adjusts the concentration of the urine, and is responsible for the excretion or absorption of the various electrolytes, such as sodium and potassium³.

There are two main parts of the kidney. The cortex is the outer portion of the kidney where all the specialized filters (glomeruli) and tubular structures (nephrons) that filter the blood and concentrate the urine are located. The collecting system is where the urine empties before passing down the ureters, which are the long thin tubes (usually 25-30cm) that channel the urine into the bladder. The collecting system is comprised of a branch network of structures called calyces which all empty into the renal pelvis which then funnels the

urine into the ureters. Stones may be located in any of these structures (see figure 1.1). Pain may result from obstruction in any location in the collecting system of the kidney or the ureters. However, the most common cause of pain from kidney stones arises when the stones pass down the ureter toward the bladder⁴. There are three narrow areas in the ureter which typically cause stones to get stuck and cause obstruction. The first is called the ureteropelvic junction, which is where the ureter and renal pelvis join. The second narrowed area is where the ureter passes over the large blood vessels in the pelvis called the iliac artery and vein. The final, and narrowest portion of the ureter, is at the ureterovesical junction where the ureter empties into the bladder⁵.

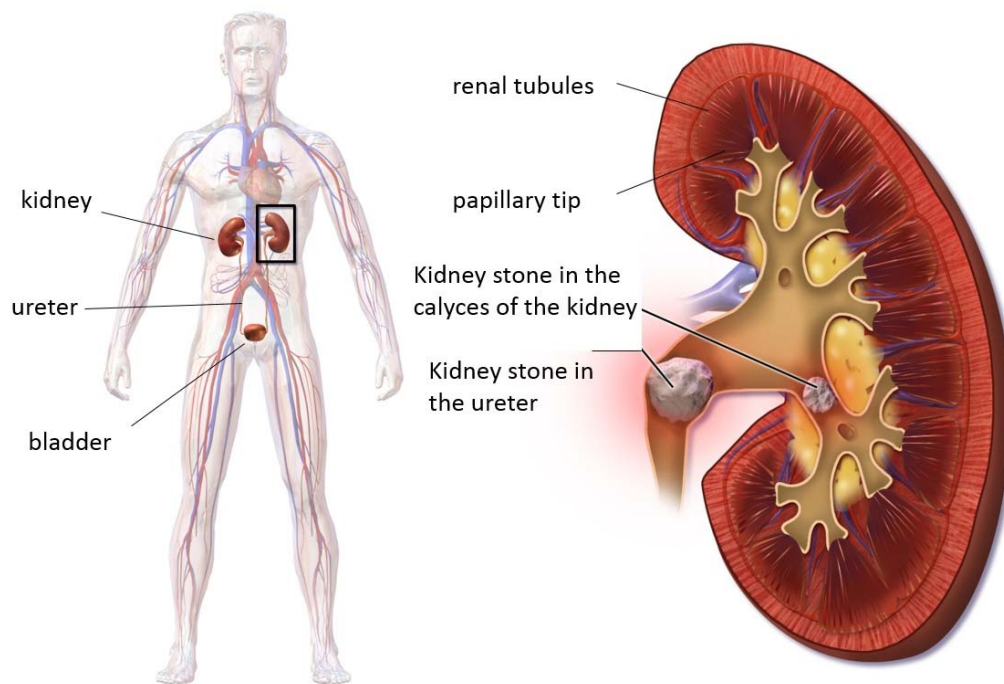


Figure 1.1. A schematic representation of a kidney cross-section with stones^{6,7}.

Many calculi cause no symptoms and are found incidentally. Most such calculi are in the kidney. A small calculus in the kidney may never grow or move, and never cause trouble. Some stones will remain in the kidney and grow. They may reach several centimeters in

size. They will cause a dull pain in the loin, bleeding in the urine and an increased risk of urinary infection. Kidney stones are dealt with either by non-invasive disintegration by shock waves generated outside the body and focused on the stone (lithotripsy), or by “key-hole surgery” through a single puncture in the loin (percutaneous nephrolithotomy)⁸. Small kidney calculi may leave the kidney in the flow of urine. If they are very small (say, less than 3mm in diameter) they may pass unnoticed down the ureters, into the bladder and out along the urethra with the next act of passing urine. Calculi between 3mm and 6mm in diameter, and which leave the kidney, will probably eventually pass through the urinary tract but are likely to be held up temporarily at some point in the ureter. Calculi between 6mm and about 1cm can leave the kidney but will be held up in the ureter and may not progress, requiring removal. Shockwave disintegration has much reduced effectiveness for stones greater than 2cm in diameter, and the success rate falls rapidly as size increases beyond this⁸.

1.1.1. Epidemiology

Between 120 and 140 per 1000,000 will develop urinary stones each year with a male/female ratio of 3:1. The lifetime prevalence of kidney stone in North America is 8% to 20%, with an annual incidence exceeding 1 per 1000 persons. Characteristically, patients present their first stone are in the range 20 - 50 years of age and 80% are men⁹. Furthermore, the recurrence rates may be as high as 10% to 23% per year and may reach 50% within 5 years and 75% in 20 years if a proper management, stone analysis, and follow-up are not applied¹⁰. Urolithiasis is one of the most common diseases, with approximately 750 000 cases per year in Germany¹¹.

Renal stone formation and the predominant chemical stone composition are age and gender dependent¹². Most stones are formed in older patients. However, clinical observations have indicated not only a change in frequency and composition of urinary calculi but also a shift in gender and age-related incidences^{13,14}. Urinary stone disease remains rare in children with a stable overall incidence in most series¹⁵.

Diet plays an important role in the pathogenesis of kidney stones. As a group, older stone formers excrete less urinary calcium than their younger counterparts and may exhibit defects in urinary inhibitors of crystallization. Animal protein and potassium intake also may influence the risk of calcium kidney stone formation. Ingested animal protein generates an acid load that increases urinary calcium excretion and reduces the excretion of citrate, an inhibitor of calcium stones. Some observational studies have shown a positive association between animal protein intake and stones, whereas others have not. Dietary potassium restriction increases and potassium supplementation may decrease urinary calcium excretion. It was recommended that calcium oxalate stone formers abstain from consuming supplemental vitamin C¹⁶.

The annual cost of stone disease in 2000, adjusted for inflation to 2014 US dollars, was approximately \$2.81 billion. After accounting for increases in population and stone prevalence from 2000, the estimated cost of stones in 2007 in 2014 US dollars was \$3.79 billion. The rising prevalence of obesity and diabetes, together with population growth, is projected to contribute to dramatic increases in the cost of urolithiasis, with an additional \$1.24 billion/yr estimated by 2030¹⁷.

The concomitant rise in comorbid conditions associated with stone disease, including obesity and type 2 diabetes mellitus, has been proposed as a possible explanation for this rise in stone prevalence. In US adults, the increase prevalence of obesity and diabetes have been linked to an increased risk of uric acid and calcium oxalate stone formation by a variety of proposed pathophysiologic mechanisms¹⁸.

1.1.2. Pathogenesis

Urinary stone formation is a result of different mechanisms. Whereas exceeding supersaturation is the cause of some types of kidney stones, infection stones result from bacterial metabolism. The formation of the most common fraction, the calcium-containing calculi, is more complex and, surprisingly, is not yet completely understood¹¹. The long accepted simple explanation of exceeding the solubility product of lithogenic substances in the urine cannot describe these complex processes sufficiently. Deviating from the hypothesis that claims the initial crystal deposition takes place in the lumens of renal

tubules¹⁹, new insights suggest a primary plaque formation in the interstitial space of the renal papilla²⁰. Calcium phosphate (CaPh) crystals and organic matrix initially are deposited along the basement membranes of the thin loops of Henle and extend further into the interstitial space to the urothelium, constituting the so-called Randall plaques, which are regularly found during endoscopy of patients who form calcium oxalate(CaOx) stones. These CaPh crystals seem to be the origin for the development of future CaOx stones, which form by the attachment of further matrix molecules and CaOx from the urine to the plaque²¹. The driving forces, the exact pathogenetic mechanisms, and the involved matrix molecules are still largely unknown¹¹.

The pathogenesis of kidney stones with calcium oxalate stones are presented in figure 1.2. Using calcium oxalate stones as a model, three categories of factors (genetic, metabolic, and dietary) act in conjunction or in isolation to lead to kidney stone formation. The process probably needs an initiating nidus on the epithelium, which provides the platform for crystallization and growth. The defect probably includes lesions in the cells and luminal factors²².

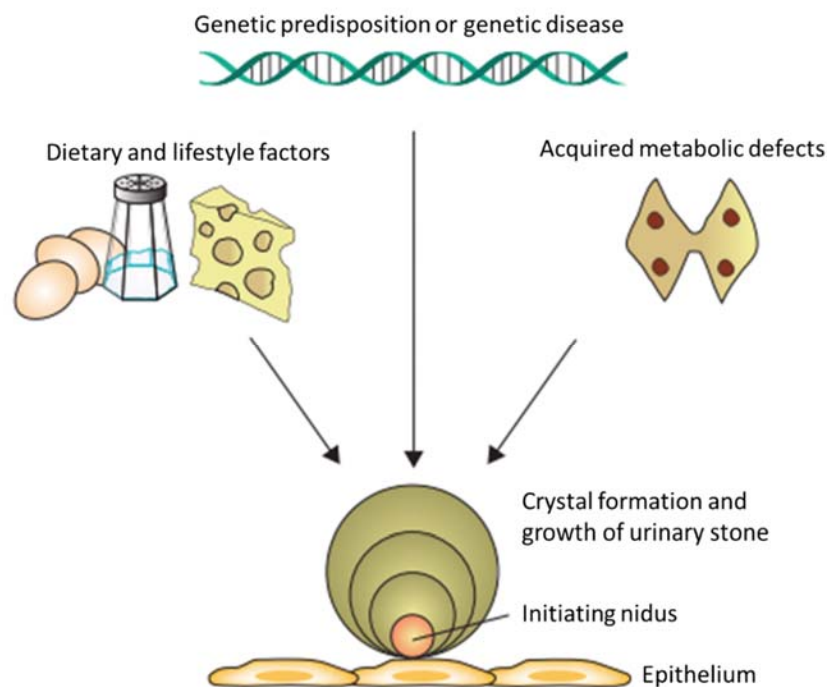


Figure 1.2. Pathogenesis of kidney stones.

1.1.3. Physicochemical aspect of urolithiasis

Urinary stone formation is a result of different mechanisms but it is not till well understood. The long accepted simple explanation of exceeding the solubility product of lithogenic substances in the urine may not describe the process. The known physicochemical features of urolithiasis are readily divided into four interrelated subjects: the driving force (supersaturation), nucleation, the growth of crystals and particles, and aggregation.

1.1.3.1. Supersaturation

Supersaturation of urine with respect to the salts that stones will consist of gives rise to the thermodynamic driving force for the formation of stones. This driving force can be expressed as free energy, by equation 1-1

$$\Delta G = RT \ln \left(\frac{A_i}{A_0} \right) \quad (1-1)$$

Where R is the gas constant, T is the temperature, and A_i and A_0 are the activities of the unionized salt species in solution at given condition and at equilibrium, respectively. The activity A is can be expressed as the equation 1-2

$$A = fC \quad (1-2)$$

When $A_i/A_0 > 1$, then $\Delta G > 0$, and the urine is said to be supersaturated with respect to the stone salt. In this circumstance, there is available free energy. If stones are already present, then they may grow, but if stone crystals are not present, then precipitation will not occur, unless A_i/A_0 exceeds the metastable limit, it is possible both new stone formation or old stone growth²³.

But urine is a complex solution, and crystallization does not occur in urine when the solubility product in water is reached. This is because urine has the capacity to hold more solute than water as it contains a mixture of many electrically active ions that interact with each other, affecting their solubility. The presence of organic molecules, such as urea, uric acid and citrate, affects the solubility of other substances. Urine is therefore described as

being 'metastable'. As the concentration of the substance is further increased, a point is reached when it eventually crystallizes and this concentration is known as the 'formation product' (K_F) of the substance. Therefore, the metastable range can be described as the range between the K_{sp} (thermodynamic solubility product) and the K_F ²⁴.

1.1.3.2. Crystal formation

There are three processes of crystallization: nucleation (formation of crystals), crystal growth and agglomeration (crystals aggregate together to form larger particles). Nucleation is the initial event in a phase transformation, stone-salt precipitation in urolithiasis. The onset of nucleation is governed by the energy given up in forming a new phase volume (ΔG_v) and by the energy required to form the surface of the new phase^{25,26}.

Two types of nucleation exist: 'homogeneous nucleation', which is the formation of the earliest crystals that will not dissolve, and 'heterogeneous nucleation', which is the formation of crystals on surfaces (e.g. cells, debris, urinary casts and other crystals)²⁴. Unless extraordinary precautions are made, most clean solutions contain 10^6 to 10^8 submicroscopic particles per milliliter. Many of these particles have high catalytic potency for nucleating precipitation of a variety of salts, including stone salts. Urine is rich in cellular debris that probably can catalyze nucleation²⁷. Therefore, it should be concluded that most of stone-salt nucleation in urine are heterogeneous or non-classical, or both²³. Particle retention caused by adherence to cells or disturbed urinary flow conditions must play an important role in stone formation²⁸.

There are two theories behind crystal formation (Figure 1.3):

The *free-particle theory*: it describes the spontaneous precipitation of crystals in supersaturated urine. Crystals grow/aggregate sufficiently during the transit time of urine in the kidney. One of the newly formed nuclei grows enough to be trapped at a narrow point in the renal tract to form a nidus for stone formation.

The *fixed-particle theory*: it claims that nuclei cannot grow sufficiently during the transit time of urine in the kidney but, if a crystal forms, it adheres to the renal epithelium, possibly

because of increased stickiness of the epithelium or damage to the cell walls (caused by crystals or by viruses and bacteria).

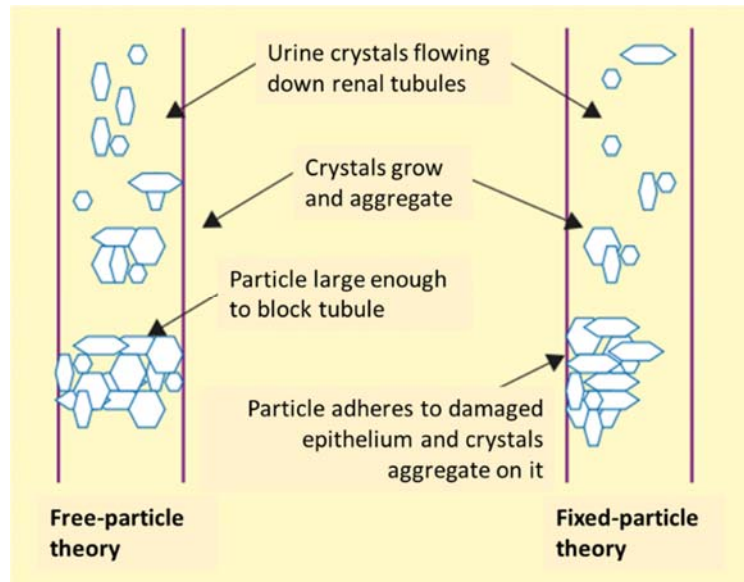


Figure 1.3. Stone initiation by the free-particle theory vs the fixed-particle theory²⁴

1.2. Classification of urinary stones

Urolithiasis is a complex disease that depends on a considerable list of factors and kidney stones consist of several kinds of minerals, alone or in combination. Correct classification of stones is important since it will impact treatment decisions and outcome. Urinary stones can be classified according to the following aspects: stone size, stone location, X-ray characteristics of stone, etiology of stone formation, stone composition, and risk group for recurrent stone formation²⁹.

The most frequent component of urinary calculi is calcium, which is the major constituent of nearly 75% of stones. Urinary stone is mostly composed of calcium oxalate about 60%, mixed calcium oxalate and hydroxy apatite 20%, uric acid approximately 10%, struvite (magnesium ammonium phosphate) about 10%, brushite 2%, and cystine 1%³⁰.

Considering the nature of the majority components, the presence of minute substances and their location, as well as the etiologic factors that could be deduced from the calculus macro and microstructure, renal calculi have been classified into groups that appear in table 1.1.

Table 1.1. Composition of urinary stones²²

Stone types	Percentage of stones	Characteristics	causes
Calcium oxalate monohydrate	40-60%	Radio-opaque	Primary hyperparathyroidism Idiopathic hypercalciuria
Calcium oxalate dihydrate	40-60%	Well circumscribed	Low urine citrate level Hyperoxaluria hyperuricosuria
Apatite	20-60%		Renal tubular acidosis
Brushite	2-4%		
Uric acid	5-10%	Radiolucent	Low urine pH Hyperuricosuria
Struvite	5-15%		Infection with bacteria that express urease
Cystine	1.0-2.5%	Mildly opaque	cystinuria
Ammonium urate	0.5-1.0%		
Mixed stones			
Mixed calcium oxalate-phosphate	35-40%		
Mixed uric acid-calcium oxalate	5%		

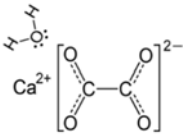
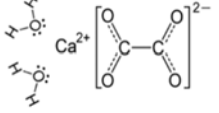


1.2.1. Calcium oxalate stones

Calcium oxalate stones are black, gray, or white. They are the principal crystalline constituents of kidney stones, and there are various forms of calcium oxalate crystals. Calcium oxalates crystallize as three hydrates— calcium oxalate monohydrate (COM, also known as whewellite), calcium oxalate dihydrate (COD, also known as weddellite)³¹, and calcium oxalate trihydrate (COT)³², a less common form in pathological stone formation. Table 1.2 shows the chemical structure, formula, and some pictures of COD and COM. A study of over 10,000 kidney stones from patients has shown that calcium oxalate monohydrate (COM) occurs about twice as frequently as calcium oxalate dihydrate (COD), although many stones contain both crystal forms³³. On the other hand, asymptomatic crystals in urine are a common occurrence, even in many individuals who do not form stones, and these crystals are usually COD³⁴. COM is known to have affinity for renal tubule cell surfaces³⁵, and theoretical calculations suggest that COM may have a stronger affinity for these cell membranes than COD³⁶. COM and COD crystals are readily distinguished by their crystal habits: COM usually exhibits hexagonal lozenge morphology, but COD crystallizes as bipyramids, reflecting its tetragonal crystal point group symmetry. COD appears to form in vitro in the presence of various inhibitors of COM growth, including many urinary proteins³⁷.

It was proposed that a change in calcium oxalate crystal structure could affect the formation of kidney stones by favoring the formation of COD, the less adherent crystal, and that normal urine contains factors that influence calcium oxalate crystal structure in the direction of COD³⁸.

The pathological origins of calcium oxalate stones have received considerable attention in the clinical research area and researchers start to understand the critical steps in their formation at a fundamental and microscopic level. The organic matter embedded within stones is thought to promote aggregation and crystal attachment to cells by acting as an adhesive. Urinary proteins with substantial anionic functionalities and other anionic macromolecules may serve as adhesives that promote COM aggregation and attachment to epithelial cells³⁹.

Table 1.2. Calcium oxalate general characteristics

Chemical formula	CaC ₂ O ₄ •H ₂ O, COM	CaC ₂ O ₄ •2H ₂ O, COD
Chemical structure		
Stone sample ^{40, 41}		

1.2.2. Uric acid stones

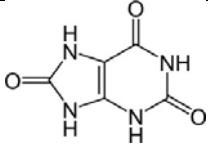

Uric acid stones are white or orange, and uric acid gravel is orange but nearly transparent radiographically unless mixed with calcium crystals or struvite. Uric acid stones are typically seen as filling defects on intravenous pyelograms. CT scanning can distinguish them from kidney tissue or blood clots and reveal their sizes and shapes. Table 1.3 shows the chemical structure, formula, and some pictures of uric acid stone.

A low urine pH is the predominant metabolic abnormality in uric acid stone disease. At a urine pH < 5.5, uric acid is sparingly soluble and will precipitate at concentrations >200 mg/L⁴². It was found that mean pH of urine in patients who form uric acid stone was 5.5 ± 0.4, as compared with 6.0 ± 0.4 among patients who form calcium oxalate stones and 5.7 ± 0.4 among patients whose stones contain both materials⁴³. Other urinary abnormalities also predispose to uric acid stone formation, including hyperuricosuria and a low urine volume¹⁸.

The etiologic cause of uric acid stone formation is complex⁴⁴. There are three urinary contributors to uric acid nephrolithiasis—hyperuricosuria, low urine volume and aciduria.

The latter is considered necessary, as the precipitation of uric acid is unlikely at a higher urine pH⁴⁵.


Table 1.3. Uric acid general characteristics

Chemical formula	C ₆ H ₁₂ N ₂ O ₄ S ₂
Chemical structure	
Stone sample ⁷	

1.2.3. Struvite stones

Struvite is a crystalline substance composed of magnesium ammonium phosphate. Struvite stones seem gnarled and laminated on radiographs; they look like ginger root. Table 1.4 shows the chemical structure, formula, and some pictures of struvite stone. They are associated with substantial morbidity including bleeding, obstruction, and urinary tract infection. Signs of struvite stones include urinary pH greater than 7, staghorn calculi, and urease that grows bacteria on culture. Stones develop if urine is alkaline, has a raised concentration of ammonium, contains trivalent phosphate, and contains urease produced by bacteria⁴⁶.

Table 1.4. Struvite general characteristics

Chemical formula	$\text{NH}_4\text{MgPO}_4 \cdot 6\text{H}_2\text{O}$
Chemical structure	$\begin{array}{c} \text{O} \\ \\ \text{O}-\text{P}-\text{O}^- \\ \quad \\ \text{NH}_4^+ \quad \text{Mg}^{2+} \end{array}$
Chemical name	magnesium ammonium phosphate
Stone sample ⁷	

1.2.4. Cystine stones

Cystine stones are multiple, greenish yellow and flecked with shiny crystallites, can form staghorn stones and are radio-opaque. Table 1.5 shows the chemical structure, formula, and some pictures of cystine stone. Cystine stones account for 1% of all stones, and occur only in patients with cystinuria, an autosomal recessive disorder. Cystinuria, an autosomal recessive disease causing decreased cystine resorption in the proximal tubule, affects 1 in 20,000 individuals; the peak age of incidence is 20–30 years. More than half the stones in cystinuria are of mixed composition, and many patients have associated physiological problems such as hypercalciuria (19% of patients), hyperuricosuria (22%), and hypocitraturia (44%)⁴⁷.

Table 1.5. Cystine general characteristics

Chemical formula	$C_6H_{12}N_2O_4S_2$
Chemical structure	
Chemical name	2-amino-3-(2-amino-2-carboxyethyl)disulfanyl-propanoic acid
Stone sample ⁷	

1.2.5. Brushite stones

Brushite (BRU), represents a minor incidence in the general count of urinary stones, has increase during last decades. Table 1.6 shows the chemical structure and formula of brushite stone. Brushite is considered the precursor phase of hydroxyapatite. If brushite does not convert to hydroxyapatite, brushite stones will form. Unlike hydroxyapatite, brushite stones are hard making them difficult to remove and are particularly resistant to shock wave lithotripsy (SWL).

Table 1.6. Brushite general characteristics

Chemical formula	$CaHPO_4 \cdot 2H_2O$
Chemical structure	
Chemical name	Calcium hydrogenphosphate dihydrate

1.2.6. Mixed stones

Urinary calculi with a mixed composition of CaOx and carbonate apatite (CAP) are found normally. The existence of CAP has been reported in 32% of the total amount of calculi; also considering stones that have just CAP heart (this value includes also mixtures with struvite). Another study set the total count for the combination of COD/COM with CAP, also including ternary mixtures in 19%. In any case, this numbers stand for a representative amount of urinary stones. The structure of mixed calculi can be usually classified as layers or as pattern-lacking stones. As it can be deduced, stones that have been formed by adding layers of both components alternatively respond to varying urine conditions, which clearly promote either CAP or CaOx precipitation.

1.2.7. Other stones

Although a precise description can be made on these main types of kidney stones, which account for more than 99% of the stones, in some particular conditions, other substances can form a kidney stone. Ammonium Urate uroliths can be formed when an alkaline urine pH is combined with hyperuricosuria and, usually, infection in the urinary tract. Another one is the drug-related stones, which include less than 1% of cases, and are divided into crystallization of poorly soluble drugs or stones resulting from a side effect from the drug intake.

1.3. Stone analysis techniques in urolithiasis

The knowledge of urinary stone composition is important for understanding pathophysiology, choice of treatment modality, and prevention of recurrences of urolithiasis. The correct stone analysis has to identify not only all stone components, but also the molecular structure and crystalline forms of them with the exact quantitative determination of each component. Although there are many techniques available for identifying the urinary stone composition and structure, no single method can provide all

the requiring information. Therefore, a combination of structural and morphological tests is needed for this purpose⁴⁸. The most used techniques are wet chemistry, thermogravimetric analysis, optical polarizing microscopy and spectroscopy.

1.3.1. Wet chemistry

The analysis of renal calculi implying wet chemistry qualitative reactions in order to identify the different anions and cations present in the calculus was the unique methodology used during the first four decades of the twentieth century and in fact, this process is still often applied in routine clinical laboratories using specifically designed kits⁴⁹. However, this method can only identify the presence of individual ions and some radicals, so, it is hard to differentiate a specific compound in many urinary stone types and the mixtures⁵⁰.

1.3.2. Thermogravimetric analysis

Thermogravimetric analysis(TG or TGA) is a fast, simple and viable technique which based on the continuous recording of both the weight loss and temperature of the material during a progressive temperature increase to about 1000 °C in an oxygen atmosphere⁵¹. This technique was widely used since 1970s and always coupled with other technique (such as electron dispersive spectroscopy (EDS)⁵¹ and Fourier transform infrared (FTIR) spectroscopy)⁵² to provide a deeper understanding to the mineralogical composition of kidney stones⁵³. Based on this approach, the exact material decomposed is known and recorded at each specific temperature. This proved to be an excellent routine method employed by many laboratories today⁵¹.

1.3.3. Optical polarizing microscopy

The base of this method is the interaction of stone crystals with polarized light. After the urinary calculi is fractured and the material is removed from various points of it, it can be assessed under the polarizing microscope using a drop of the appropriate refractive index liquid⁵⁴. Parameters which identify the stone minerals include the color, refraction of light, and double refraction.

1.3.4. Spectroscopy

The current generation of Fourier transform infrared (FTIR) spectrophotometers provide data of extremely high signal-to-noise ratio that can be manipulated easily by computer, enabling analyses of the components of complex overlapping peaks⁵⁵. However, the IR methodology require grinding the sample losing so the possibility of any spatial analysis. Recently, Blanco et al. have developed a near infrared (NIR)-hyperspectral imaging technique, which showed a probability higher than 90% for right classification of the stones⁵⁶.

The advantages and main drawbacks of the most common techniques are summarized in table 1.7. Although there are many techniques available for identifying the urinary stone composition and structure, no single method can provide all the requiring information.

Table 1.7. comparison of the urinary stone analysis techniques⁴⁸

Method	Advantage	drawbacks
Chemical analysis	Easy Low cost	Time-consuming Require large stone sample; hence, unsuitable for tiny stones Only identification of the presence of individual ions and radicals rather than a specific compound, eg, unable to distinguish between the two commonly occurring calcium stones (COD/COM)
Polarization microscopy	Cost-efficient Quick examinations Possibility to analyze very small samples Ability to detect very small contents of components in the stone	High subjective experience is necessary Differentiation of components is difficult in some cases in the groups of uric acid, purine derivates, and calcium phosphates
Infrared spectroscopy	Moderate cost Quick examination	Time-consuming; Need pre-analytic preparation;

	<p>Possibility to examine small samples</p> <p>Semiautomatic evaluations are possible applying search-match functions</p> <p>Useful for identification of organic components or noncrystalline substances, eg, purines, proteins, or fat and drug metabolites</p>	<p>The proper homogenization of the sample with potassium bromide may effect the IR spectrum quality</p> <p>Resolution of the apparatus and reproducibility of the spectrum bands may affect its reliability</p> <p>Difficulty in detection of small amounts of components in same cases, eg, whewellite in weddellite or reverse, or urates and uric acid dihydrate in uric acid</p> <p>Difficulty in detection of some components, such as carbonate in struvite stones or cystine in whewellite or uric acid stone</p>
X-ray diffraction	<p>Easy preparation</p> <p>Automatic measurement</p> <p>Quantitative analysis</p> <p>Exact differentiation of all crystalline components is possible</p>	<p>High cost</p> <p>Unable to detect noncrystalline or amorphous substances</p>
Thermogravimetry	<p>Fast</p> <p>simple</p>	<p>Requiring relatively large amount of sample</p> <p>Non-recovery of sample</p> <p>Difficulty in identifying closely related compounds, eg, purines</p>
Scanning electron microscopy	<p>Non-destructive</p> <p>Possibility to visualize the components without alerting their spatial orientation and specific morphology</p>	<p>High cost</p>

1.4. Promoters and inhibitors of urolithiasis

In general, the crystallization of stone-forming salts is due to an abnormal urinary composition that is either higher in crystallization promoters, lower in inhibitors, or both. Urine excreted by normal individuals, as well as stone-formers, is often supersaturated with respect to calcium oxalate. However, the complex process of stone formation is inhibited by substances in urine that raise the concentrations of calcium and oxalate that are required for new crystal formation, growth and aggregation and inhibit adhesion of crystals to renal epithelial cells⁵⁷. The mechanisms of crystallization need to be understood to outline the basis of stone formation, as it was described previously. The states of saturation of ions in a solution are governed by their concentrations. Figure 1.4 shows the urinary stone promoters and inhibitors effect. For example, when concentrations of calcium and oxalate reach saturation (the saturation product), stone formation begins with association of small amounts of crystalloid to form nuclei (nucleation). The main urinary stone promoters and inhibitors are shown in Figure 1.5.

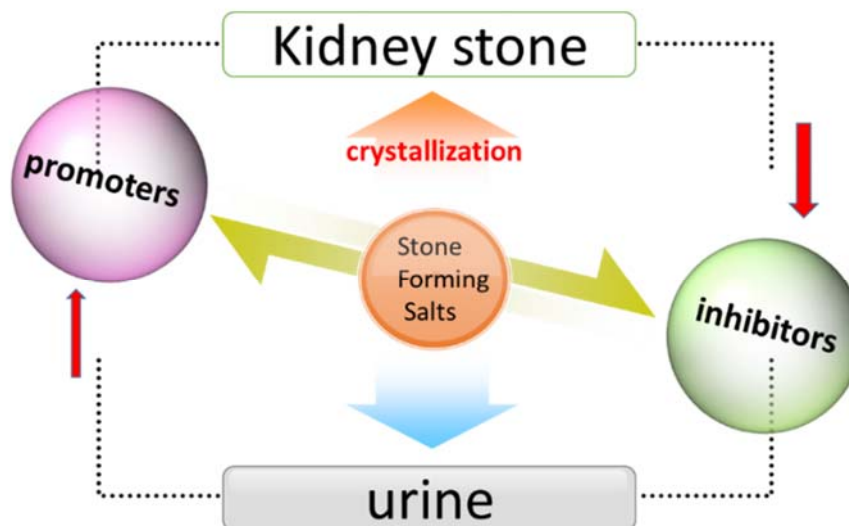


Figure 1.4. Schematic representation of the effect of promoters and inhibitors.

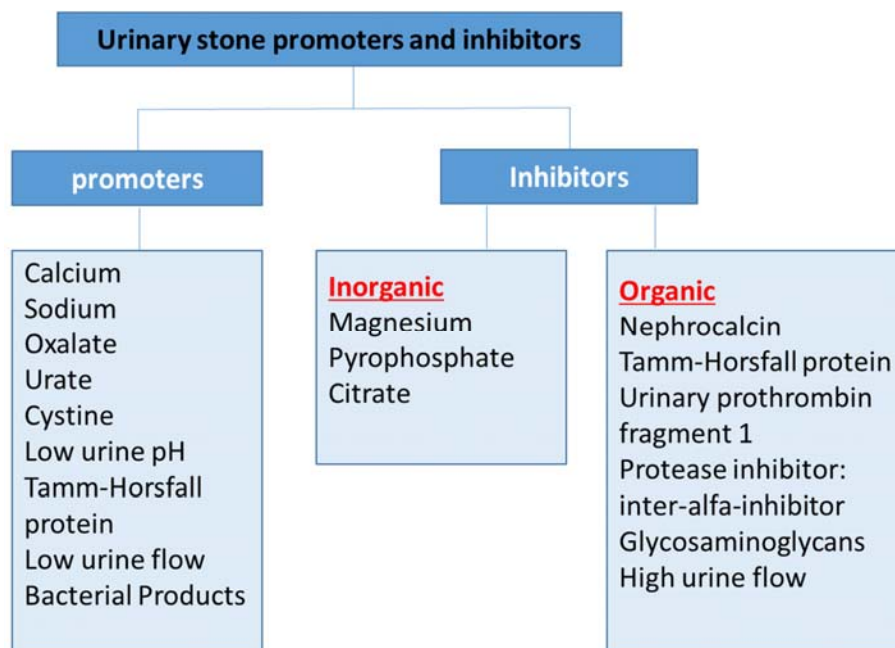


Figure 1.5. Urinary stone promoters and inhibitors⁵⁸

1.4.1. Inhibitors

Urine contains a range of low and high molecular weight components that are able to inhibit the nucleation of crystals that could block the renal collecting tubules. Inhibitors slow or inhibit the rate of growth or the aggregation of crystals or reduce adherence of crystals to the renal epithelium. The same molecule may also affect the likelihood that crystals attach to, or nucleate directly upon the renal epithelium. Some are also occluded within the mineral bulk of urinary crystals, and by disrupting their crystalline structure they may assist their intra-renal degradation, dissolution, and disposal⁵⁹. The most important are phytic acid⁶⁰ and pyrophosphate⁶¹.

1.4.1.1. Phytic acid

Phytic acid (*myo*-inositol hexaphosphoric acid, IP₆, figure 1.6) is abundantly present in many plant sources and in certain high-fiber diets, comprising 1-5% by weight of edible legumes, cereals, oil seeds, pollens, and nuts⁶². It was suggested that phytic acid acts as a store of phosphorus, of cations, of glucuronate (a cell wall precursor), or of high energy

phosphoryl groups⁶³. Phytic acid is a main reserve form for phosphorus in cereal grains. It occurs in a form of mixed salts (phytate). This phosphorus form is hardly digestible for monogastric animals and humans.

The presence of *myo*-inositol hexakisphosphate (IP₆) in tissues and biological fluids (blood, urine, saliva, interstitial fluid) of mammals is well known. The existence of intracellular IP₆ in mammalian cells has also been established, despite the problem of determining its exact subcellular localization. The role of IP₆ in mammalian cells is a complex matter that, in spite of recent research, leaves a lot of key questions unanswered, such as the exact pathways of IP₆ synthesis and metabolism and their mechanisms of control, the detailed biological function inside the cell and the relationship with the other inositol polyphosphates. Nevertheless, it seems that the presence of IP₆ inside the cell is important⁶¹.

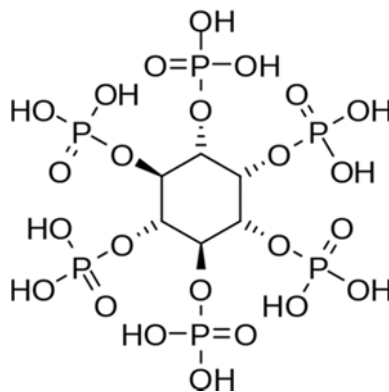


Figure 1.6. Chemical structure of phytic acid

Phytic acid is considered to be a strong antinutrient because it forms at physiological pH partly insoluble complexes with bi- and trivalent minerals (such as Zn²⁺, Mg²⁺, Fe²⁺, Mn²⁺, Ca²⁺) and so reduces the bioavailability of essential elements⁶⁴. When passing through the digestive tract, phytate can bind some essential trace elements and minerals, thus affecting negatively usability of nutrients and other nutritiously valuable substances. This led to controversial discussion about the nutrition of vegetarians and their supply with essential elements.

On the other hand, phytic acid exhibits a number of positive impacts on health. The role of phytic acid in numerous biochemical pathways and physiological processes is manifold. It is a strong antioxidant⁶⁵. High concentrations of phytic acid prevent browning and putrefaction of various fruits and vegetables by inhibiting polyphenol oxidase⁶⁰. It might act as an antioxidant in mammalian cells. Chelation of Fe³⁺ leads to suppression of formation of OH[·], a highly reactive oxyradical which indiscriminately attacks most biomolecules⁶⁶. It is claimed to have the ability to enhance the anticancer effect of conventional chemotherapy and control cancer metastases^{65,67}. It also positively affects a blood glucose level and cholesterol. Therefore, a phytate role in human diet and its effect on health have been studied intensively⁶⁸.

Phytic acid acts as an effective inhibitor of calcium salts crystallization in urine and soft tissues, and prevents the formation of kidney stones (urolithiasis)⁶⁸. Urinary phytic acid has an interesting beneficial action on some pathological processes such as calcium urolithiasis by preventing, at very low concentrations, the development of renal solid concretions. Consequently, it has been proposed as a promising drug to treat calcium oxalate and phosphate stone formers⁶⁹. Phytate exerted the most remarkable effects on the heterogeneous nucleation of COM crystals and when the phytate was present at 1.43×10^{-7} M, it totally prevented the development of COM crystals, which is in agreement with reported articles in which the effects on crystal growth⁷⁰ and crystal nucleation^{71,72} was shown. Since in humans between 1 and 10% of the total ingested phytic acid is excreted by the urine⁷³, increasing the urinary excretion of phytic acid is recommended to diminish the risk of calcium oxalate and calcium phosphate kidney stone recurrence⁷⁴. In taking into account the molecular structure of phytic acid, its inhibitory capacity can be justified as consequence of the affinity of the phosphate groups to bind calcium ions. The strong adsorption of phytate on the surface of the nucleous and/or calcium oxalate crystals blocks further development. This inhibitory action is enhanced by zinc, due to the formation of a complex with phytate, which is a more effective inhibitor⁷³.

1.4.1.2. Citrate

The inhibitory effect of urine citrate on calcium oxalate crystallization is well known, being the principal mechanism of action a reduction of calcium oxalate supersaturation by forming complexes with calcium and so a direct inhibition of crystal growth and aggregation happens⁷⁵. Such activities might also be expected to prevent stone enlargement and there has been recent interest in the use of citrate therapy to prevent regrowth of residual fragments⁷⁶. The chemical structure of citric acid are show in figure 1.7. Citrate is excreted in normal urine at a mean of about 3.3 mmol/day. It is measured clinically, and low levels are treated as a cause of stones⁷⁶. Because citrate lowers calcium oxalate supersaturation by binding calcium, a low citrate concentration can be a risk factor for the formation of stones and treatment with citrate should prevent stones⁷⁷.

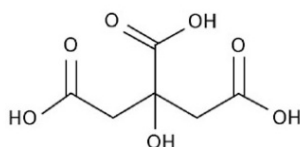


Figure 1.7. Chemical structure of citric acid

It was demonstrated that alkaline citrate therapy increases the clearance rate of residual fragments in patients with calcium oxalate and infectious stones following extracorporeal shock wave lithotripsy (ESWL)⁷⁸. Potassium citrate provides physiological and physicochemical correction and inhibits new stone formation, not only in hypocitraturic calcium nephrolithiasis but also in uric acid nephrolithiasis⁷⁹.

1.4.1.3. Pyrophosphate

Pyrophosphate (PPi, see figure 1.8) was one of the first component of urine to be isolated and identified as having a clear capacity to inhibit the crystallization of insoluble calcium salts (oxalate and phosphate)⁸⁰. In inorganic solutions, pyrophosphate inhibits CaOx crystal nucleation, growth, and a combination of growth and aggregation. It has also been shown to inhibit crystal aggregation under the same inorganic conditions. Its inhibitory effect can

be attributed to its irreversible binding to the CaOx crystal surface. Pyrophosphate excretion has been reported to be significantly reduced in stone formers, as compared with healthy controls^{81,82}.

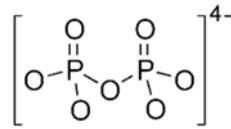


Figure 1.8. Chemical structure of pyrophosphate anion

1.4.1.4. Proteins

Proteins are also inhibitors of kidney stone growth. Those detected in calcium oxalate stones include Tamm-Horsfall glycoprotein, albumin, α and γ -globulins, haemoglobin, neutrophil elastase, transferrin, α_1 -microglobulin, CD59 protein (protectin), superoxide dismutase, α_1 -antitrypsin, uropontin, nephrocalcin, β_2 -microglobulin, α_1 -acid glycoprotein, apolipoprotein A1, retinol-binding protein, renal lithostathine, urinary prothrombin fragment 1, and inter α - trypsin inhibitor. However, although the presence of these proteins may imply that they fulfil some function in stone formation, it is equally possible that their inclusion in the stone structure may simply have been fortuitous, effects of the stone itself. For instance, haemoglobin is almost certainly the product of the haematuria that almost inevitably accompanies the presence of a stone in the urinary tract⁸³. The many proteins found in stones could cause, be the result of, or have no role in their formation⁸⁴. The most important described are:

Uropontin (UP) is the urinary form of osteopontin, an aspartic acid-rich phosphorylated glycoprotein. It has been shown as a potent inhibitor of nucleation, growth and aggregation of calcium oxalate crystals, as well as crystal attachment to renal epithelial cells^{84, 85}. The physiologic characteristic of an inverse relationship of uropontin concentration to urine volume favors protection from urinary crystallization of calcium oxalate by uropontin⁵⁷. The urinary concentration of UP is in the range in which its contribution to inhibition of growth and aggregation are likely to be substantial. Thus, UP appears to be an important natural defense against renal crystallizations and nephrolithiasis⁸⁶.

Prothrombin fragment 1 (PTF1) is a peptide generated from sequential cleavage fragments of the blood clotting factor prothrombin (the other two are thrombin and fragment 2)⁸⁷. Prothrombin fragment 1 is excreted in urine and is a potent inhibitor of calcium oxalate stone formation in vitro⁸⁸. The organic matrix of calcium oxalate crystals contains prothrombin fragment 1, providing evidence that links the role of blood coagulation proteins with urolithiasis. Prothrombin fragment 1 is an important inhibitor of calcium oxalate crystal aggregation and adherence of crystals to renal cells⁸⁹. The incidence of urolithiasis in blacks is significantly less compared to whites in South Africa. Prothrombin fragment 1 from the black population has a better inhibitory activity over it from the white population⁹⁰. Further studies show that sialylated glycoforms of prothrombin fragment 1 afford protection against calcium oxalate stone formation, possibly by coating the surface of calcium oxalate crystals⁹¹. PTF1 is a more potent inhibitor of calcium oxalate crystal aggregation and confirmed by scanning electron microscopy, which also revealed that the smaller particles deposited in the presence of the proteins resulted from reduced crystal aggregation rather than a decrease in the size of the individual crystals⁸³.

Tamm-Horsfall Protein (THP), also known as uromucoid, is an 80-kDa glycoprotein synthesized exclusively in the thick ascending limb of the loop of Henle's loop with exception the of the macula densa. Released THP is the most abundant protein in the urine of normal mammals under physiological conditions, the production ranges from 30 to 60 mg daily in humans⁹². It exclusively produced in the kidney and secreted into the urine via proteolytic cleavage. THP remains on crystal surfaces, and thus mainly affects aggregation of preformed crystals, although controversy still exists about whether this protein is a promoter or inhibitor of crystallization⁹³. Studies in knockout mice demonstrated that it has a protective role against urinary tract infections and renal stone formation⁹⁴. THP is supposed to involve in the pathogenesis of urolithiasis and tubulointerstitial nephritis⁹⁵. Lan Mo et al. ⁹⁶ provide the first in vivo evidence that THP is a critical urinary defense factor and suggest that its deficiency could be an important contributing factor in human nephrolithiasis. According to its well-known physico-chemical properties, THP has a dual role in modifying crystal aggregation: at high pH and low ionic strength (IS). THP is a powerful crystal aggregation inhibitor. Upon lowering pH and raising IS, THP viscosity

increases, leading to reduced crystal aggregation inhibition. In the presence of additional calcium ions, some THPs even become strong promoters of crystal aggregation⁹⁷.

Osteopontin (OPN) is an acidic phosphorylated glycoprotein initially isolated from bone matrix. It is a versatile regulator of inflammation and biomineralization. It is believed to play a role in modulating mineralization of normal bone by enhancing osteoclast activity and halting hydroxyapatite crystal growth. In addition to being expressed in bone, OPN is also expressed by normal renal epithelial cells, and it is secreted into the urine at about 4 mg/day. Purified OPN inhibits the nucleation, growth, and aggregation of calcium oxalate crystals in vitro and reduces the binding of the crystals to renal epithelial cells in vitro.

Peptide chain of inter-alfa-trypsin inhibitor (IaI) belongs to the Kunitz-type protein superfamily, a group of proteins possessing a common structural element and the ability to inhibit serine proteases⁹⁸. IaI has been isolated from urine and is considered to be a nephrolithiasis-related protein because it is present in the matrix of calcium crystals generated in human urine. It has been reported to inhibit calcium oxalate crystallization⁹⁹. Furthermore, the potent inhibition of CaOx crystal growth by these proteins, coupled with the known presence of bikunin and its fragments in urine, suggested the possible existence of a relationship between IaI and CaOx stone formation¹⁰⁰.

Lithostathine is a protein of pancreatic secretion inhibiting calcium carbonate crystal growth. A protein immunologically related to lithostathine is actually present in urine of healthy subjects and in renal stones, renal lithostathine (RL)¹⁰¹. Immunocytochemistry of kidney sections localized the protein to cells of the proximal tubules and thick ascending limbs of the loop of Henle. Because of its structural and functional similarities with pancreatic lithostathine, it was called renal lithostathine. RL seems to control growth of calcium carbonate crystals. Several reports showing the presence of calcium carbonate (CaCO₃) in renal stones suggested that crystals of CaCO₃ might be present in the early steps of stone formation. Such crystals might therefore promote CaOx crystallization from supersaturated urine by providing an appropriate substrate for heterogeneous nucleation^{102,89}.

Lastly, *Glycosaminoglycans* (GAGS) are highly negatively charged urinary macromolecules and play an important role on the calcium oxalate crystallization. GAGS have been isolated from the urinary stone matrix¹⁰³. Various glycosaminoglycans are found in the urinary tract of healthy people, such as chondroitin sulphate (55%), heparin sulphate (20%) and hyaluronic acid (4-10%) and so forth¹⁰⁴. Lower GAGS levels were found in urine of adult patients with urolithiasis, compared with healthy controls, GAGS concentration in the urine is too low to decrease calcium¹⁰⁵. In vitro, GAGS have exhibited to act as inhibitors of calcium oxalate crystal growth and crystal aggregation. However, researchers have failed to demonstrate any qualitative and/or quantitative significant difference in total excretion of GAGS between stone formers and health controls¹⁰⁶.

1.4.1.5. Other macromolecules

Human urinary trefoil factor (THF1) belongs to the trefoil factor family proteins. It is synthesised by mucosal epithelial cells and is expressed in gastric mucosa. It has been described as an antiapoptotic agent with mitogenic activities¹⁰⁷. It may also act as a potent inhibitor of CaOx crystal growth¹⁰⁸. Calgranulin, an S100 protein, is present in the kidney and human urine and can inhibit growth of CaOx crystals, which is the major component of kidney stones. There are 3 monomers (A, B and C) all mapped to chromosome 1. The inhibitory properties of calgranulin may be due to its ability to bind to the crystal surface^{109,89}.

1.4.2. Promoters

Basically the substances usually found in urine which act as crystallization promoters are the same ionic components that form the stone itself. Thus, each type of stone will be affected by a different type of promoter. In addition, other substances have also been considered as promoters. Promoters stimulate crystallization; examples include calcium, oxalate, sodium, urate, cystine, bacterial products, etc. Other urinary glycoproteins, such as uromucoid, the polymerized form of Tamm–Horsfall protein which as previously said can act as inhibitor or promoter.

Organic matter, often found in urine in the shape of small biological particles, can become a suitable starting point for the precipitation of some urinary components. In particular, calcium oxalate monohydrate is usually deposited on such organic seeds, so the core of the stone becomes a mixture of organic matter and calcium oxalate. Also some protein aggregates have been proven to act as nucleation point for the further precipitation of crystals.

The close relation between calcium and oxalate is described in Figure 1.9. The combined promoter effect for these ions can be appreciated here. Naturally, the increase of the concentration of calcium or oxalate ions affects the crystallization potential by increasing urine saturation respect calcium oxalate CaOx. In this Figure, the blue line represents the limit calcium concentration to consider hypercalciuria (3.8 mmol/l), while the grey line describes hyperoxaluria (0.31 mmol/l). When calcium concentration reaches hypercalciuria, an increase in oxalate concentration leads to the rise of CaOx activity product, while the $[Ca]/[Ox]$ value decreases. This situation ends up, after a critical point, in hypercalciuria and hyperoxaluria. Thus, the risk areas correspond to the upper, lower and right regions in this figure.

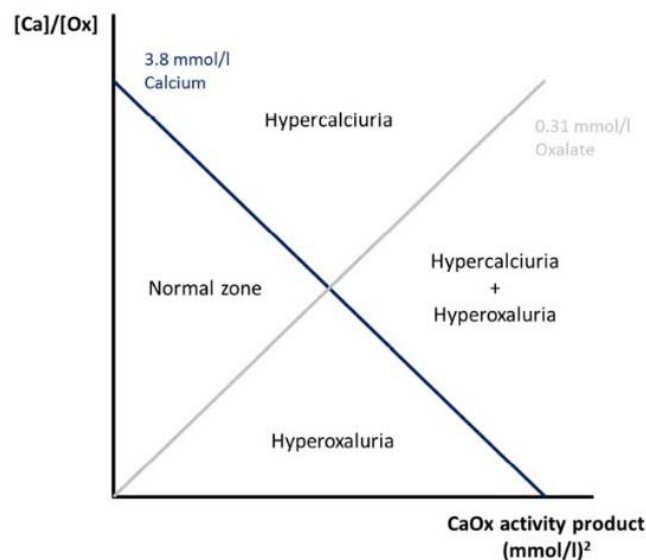


Figure 1.9. Schematic representation of the urinary saturation state in regard to calcium oxalate stones¹⁰⁹.

1.5. Determination of phosphorous inhibitors

Recently, the quantitative analysis of inorganic and organic phosphate ions has become an important issue in many research laboratories. In the human body, phosphate plays an important role not only in control of the pH in blood or lymph fluid, but also in the energy and nitrogen metabolism in cells¹¹⁰.

Although many analytical methods for phytic acid and pyrophosphate have been reported, most method are quantified by spectrophotometric or HPLC methods, which are either less sensitive or timing consuming.

1.5.1. Determination of IP6

The myo-inositol hexakisphosphate isomer is referred to by a number of different names: ‘phytic acid’ is the alternative name for the free acid form, whilst ‘phytate’ refers to the salt of phytic acid¹¹². The pK_a data for myo-inositol hexakisphosphate are listed in table 1.8. They exist as inositols in various states of phosphorylation (bound to between one and six phosphate groups) and isomeric forms (e.g. myo, d-chiro, scyllo, neo), although myo-inositol hexakisphosphate is by far the most prevalent form in nature¹¹². Despite the prevalence of inositol phosphates in the environment, their cycling, mobility and bioavailability are poorly understood. This is largely related to analytical difficulties associated with the extraction, separation and detection of inositol phosphates in environmental samples¹¹¹.

Table 1.8. pK_a data for myo-inositol hexakisphosphate(IP₆)¹¹⁴

pK_1	pK_2	pK_3	pK_4	pK_5	pK_6	pK_7	pK_8	pK_9	pK_{10}	pK_{11}	pK_{12}
1.1	1.5	1.5	1.7	2.1	2.1	5.7	6.9	7.6	10.0	10.0	12.0

In mature plant seeds, the inositol phosphates occur mainly as hexaphosphate, but during food processes involving prolonged heat treatment, it is likely that other inositol phosphates are formed. The structure of inositol and some of its polyphosphate derivates are showed in Figure 1.10. During digestion of phytate in the stomach and small intestine it is most

likely that lower inositol phosphates are formed and that food processing affects the digestibility¹¹⁵.

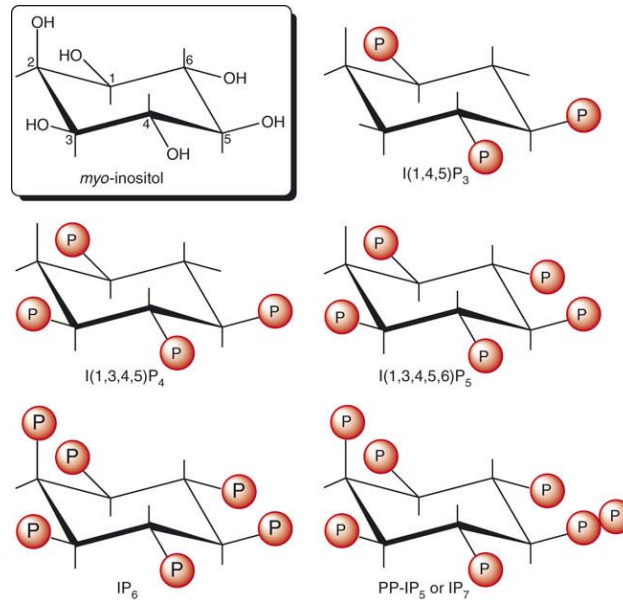


Figure 1.10. Structure of inositol and some of its polyphosphate derivatives¹¹³

This study summarizes the development of analytical methods for the determination of phytic acid. There are many methods for determining phytic acid which discussed below.

1.5.1.1. Precipitation method

At first, the determination of phytic acid was often based on the formation of a precipitate with iron(III). The first method generally accepted for the determination of phytic acid was proposed by Heubner & Stadtler (1914)¹¹⁶ which was based on a direct precipitation titration in the presence of ammonium thiocyanate. Also some researchers performed the same precipitation by titrating the iron(III) or copper(II) excess, using colorimetry and iodimetry¹¹⁷. One of the disadvantage of the iron precipitation methods is that not only phytate (inositol hexaphosphate), but other phosphorus-containing compounds are precipitated. It was found that all of the inositol phosphates from the di- to hexaphosphate form insoluble iron complexes. However, the mono-, di- and triphosphates are appreciably soluble and are not quantitatively precipitated. According to Mollgaard¹¹⁸, inositol mono- and diphosphates are not measured analytically by the iron precipitation methods.

1.5.1.2. Colorimetric method

Latta and Eskin developed a rapid colorimetric procedure for the determination of phytate based on the reaction between sulfosalicylic acid and ferric ion¹¹⁹. In this method they use 2.4% HCl to extract phytic acid from the matrix and then separated AG1-X8 chloride anion exchange column by 0.7M NaCl. They considered that the method had distinct advantages over the digestion procedure, with added simplicity and rapidity. In this paper, they showed that it was enough to use the commercial sodium phytate as a standard, without further purification.

1.5.1.3. Ion-exchange method

The official AOAC method (No. 986.11) for measuring the phytic acid contents in foods and feeds is based on the step gradient anion-exchange method developed by Harland and Oberleas¹²⁰. In this procedure, phytic acid is extracted directly from foods or feeds with 2.4% HCl, followed with elution through an anion-exchange resin. Most of the associated impurities are washed off the column while the phytic acid is retained on the column. Phytic acid is then eluted with a 0.7M NaCl solution and acid digested to inorganic phosphate¹²¹. Based on the ion-exchange separation, an inductively coupled plasma mass spectrometry (ICP-MS) method was developed. In this method, pretreatment of the sample is required to avoid interference in the ICP-MS detection from other phosphorus compounds accompanying phytic acid in urine such as phosphate or pyrophosphate. This treatment consists of a simple filtration of the urine sample followed by complete separation of phytic acid from the mentioned phosphorus components using an anion-exchange solid-phase extraction. An ICPMS method for the determination of phytic acid in human urine based on the total phosphorus measurement of purified extracts of phytic acid is described by Muñoz and Valiente¹²². Linear range (0.02- 0.6 mg of phytic acid L⁻¹) and limit of detection (5 µg/L phytic acid) are adequate for analysis of the usual amounts of phytic acid present in urine.

1.5.1.4. HPLC and HPIC method

Previously application HPLC to analysis of phytic acid used reserved- phase silica column (C-18 and refraction index detectors)^{123,124,125}. Sandberg and Ahderinne developed a HPLC method for separation and quantitative determination of inositol tri-, tetra-, penta-, and hexaphosphate in foods and intestinal contents. This method included the extraction of inositol phosphate by 0.5M HCl and separation of the inositol phosphate from the matrix by ion-exchange chromatography. For the HPLC step, they used 0.05M formic acid/methanol and 1.5ml/100ml of TBA-OH (tetrabutylammonium hydroxide) in the mobile phase. The ion-pair C-18 reverse column was used and inositol phosphates were detected by refractive index¹¹⁵. Unfortunately, the solvent front coincided with the phytic acid peak and made quantitation difficult. Lehrfeld¹²⁶ developed a HPLC method. In this method, ultrasonication for extraction, a commercially available silica-based anion exchange (SAX) column for concentration and purification, and the HPLC for analysis was used. This method used the pH—stable, macroporous polymer column PRP-1 and an eluting solvent composed of methanol, formic acid, sulfuric acid, and tetrabutylammonium hydroxide¹²⁷.

High-performance ion chromatography (HPIC) with gradient elution is the most commonly used method for separation of inositol phosphates and their isomers in foods, feeds and intestinal contents.¹²⁸ Halfrich and Bettmer developed a method for the determination of phytic acid (IP6) and its degradation products (IP₁-IP₅, see figure 1.10) by ion-pair chromatography coupled to a double focusing inductively coupled plasma-sector field-mass spectrometer (ICP-SF-MS). The separation of the six phosphorus species was enabled by a gradient elution using tetrabutylammonium hydroxide (TBA) as ion-pair reagent. In order to separate the ³¹P⁺ signal from the interfering cluster ions, a mass resolution (m/Δm) of 4000 was needed to detect the phosphorus species¹²⁹.

Determination of phytic acid in waters, urine and soils involves three distinct operations: extraction, separation and detection. Successful determination of inositol phosphates can be hindered in each or all of these steps. For example, the efficiency of inositol phosphate extraction from soils is highly dependent on the extraction conditions used and may involve

some hydrolysis of the inositol phosphate congeners present. Chromatographic separation of inositol phosphates may be incomplete because of the elution conditions chosen or specific interactions with the stationary phase, or could even entail some on-column hydrolysis. Detection of inositol phosphates after separation usually involves colorimetric determination of molybdate-reactive P following a digestion step, which may or may not be 100% efficient depending on the conditions selected¹¹².

Table 1.9. The compare of advantage and disadvantage of determination method of phytic acid¹¹¹

method	advantage	disadvantage
Precipitation method	They are most useful to measure the phytic acid contents in unprocessed products or to estimate the phytic acid content in a large numbers of samples when advanced instruments are not available, owing to overestimating the phytic acid contents in processed foods, because they cannot separate inositol hexaphosphate from the lower substituted inositol phosphates.	The methods are time consuming, require careful monitoring to minimise losses, and cannot avoid the presence of interfering substances such as reducing compounds. It is critical to avoid incomplete or excessive digestion.
Colorimetric method	These are more rapid and simple than precipitation methods, and are often based upon the reaction between ferric chloride and sulfosalicylic acid.	These methods are likely to be inaccurate, for the large and varying adsorption of iron(III) on the precipitate makes the method infeasible for many products, especially processed foods.
Ion exchange method	They are used in a step-gradient manner as the quantification of phytate is feasible, and can avoid the loss of minute quantities in the precipitation.	It is important to select a suitable resin for phytate analysis. The resin is expensive and cannot be used for many times.
HPLC and HPIC method	They have the sensitivity and reproducibility needed to measure low concentrations in various products, so they are suitable to quantify the phytic acid contents of processed foods. They can simultaneous separate and determine IP6 and the lower phosphorylated species by shortening the extraction and concentration procedures.	But these methods are also expensive and require considerable investment in equipment, and expertise to setup and operate them.

Synchronous fluorescence method	This method exhibits high precision and accuracy, and is simple, rapid, and exhibits excellent sensitivity	Selectivity need to be improved
---------------------------------	--	---------------------------------

1.5.2. Pyrophosphate determination

Pyrophosphate determination methods can be classified as chromatographic methods, colorimetric method and enzymatic method. Reagents used for chromatographic and colorimetric methods are cheaper than reagents required for enzymatic methods.

1.5.2.1. Chromatographic method

Yoza et al.¹³⁰ developed an HPLC method based on anion-exchange separation of pyrophosphate and orthophosphate and postcolumn spectrophotometric detection at 140°C with molybdenum (V)-molybdenum (VI) reagent. A photodiode-array detector for HPLC indicated the spectral characteristics of the heteropoly blue complex that was detectable at 330–800 nm. The HPLC method had a wide dynamic range from 3×10^{-7} to 5×10^{-4} M for both pyrophosphate and orthophosphate.

Henin and Barbier described a fast and simple capillary electrophoresis method to simultaneously determine the pyrophosphate and phosphate ions in aqueous solutions. They used the buffer containing metallic ions mimicking biological milieu. This method used indirect UV detection of the ATP electrophoretic chromophore at 254 nm and CTAB as an electroosmotic flow modifier. ATP has a strong UV absorption at 254 nm and its mobility was found to be between that of PPi and Pi. The method has been shown to be extensible to various media including pure water and salt-containing aqueous solutions¹³¹.

1.5.2.2. Colorimetric method

The colorimetric method was described by Flynn et al.¹³² for determination of 0.05 to 0.5 μmol of pyrophosphate in which use is made of a cysteine-catalyzed color effect with the molybdate reagent of Fiske and Subbarow¹¹⁶, which was used to determine the inorganic orthophosphate. Although this method is very sensitive, it does not allow the direct determination of PPi.

1.5.2.3. Enzymatic method

In the enzymatic method, inorganic pyrophosphate is converted to ATP by using the enzymes ATP sulfurylase and firefly luciferase¹³³. The assay is extremely sensitive, the linear range of the assay being $1 \times 10^{-9} - 5 \times 10^{-7}$ M PPi. The PPi formation in the DNA polymerase reaction is continuously monitored by a coupled enzymatic method¹³⁴. The method has been used for continuous monitoring of DNA synthesis in vitro¹³⁵.

March et al. developed an enzymatic method which is simple and showed much better selectivity. Enzymatic methods can be considered free from phosphate interference. The determination used is based on phosphorylation of D-fructose-6-phosphate using a fructose-6-phosphate kinase pyrophosphate dependent enzyme. Then, the D-fructose-1, 6-diphosphate is fragmented, by an aldolase, to D-glyceraldehyde-3-phosphate and dihydroxyacetone phosphate. Finally, a glycerophosphate dehydrogenase catalyzes the reduction of dihydroxyacetone phosphate by β -NADH. The reaction was monitored spectrophotometrically at 340 nm by measuring the diminution of β -NADH concentration. The method involves the preconcentration of pyrophosphate using anionic exchange resin and development of the enzymatic reactions with the pyrophosphate retained on the resin. The method was also successfully applied to the determination of pyrophosphate in human urine. Pyrophosphate in human urine was of the order of 4 mg/L¹³⁶.

With more and more interest in the human nutritional properties of phytic acid, we are looking forward to more rapid and simple procedures for the determination of the phytic acid contents of cereal grains and their products.

1.5.3. Drawbacks of the present analytic method for determination inhibitors of urolithiasis

The colorimetric method and precipitation methods were used to analyze phytic acid in foods and feeds. It requires extra experimental efforts to remove Fe-phytate precipitates before the Fe determination. High-performance liquid chromatography (HPLC), anion exchange column (AEC), and ³¹P nuclear magnetic resonance (NMR) spectroscopy

overcame the low accuracy, acid hydrolysis requirement, and other problems associated with the classic Fe(III) precipitation PA assay method and have also been used for PA assays. These methods, however, require sophisticated instruments, high maintenance, and specialized staff and are not readily adopted by plant breeders. Both HPLC and AEC methods can only analyze 10 to 30 samples per day, which makes them impractical for routine analysis involving large numbers of samples. To remove Pi interference, the HPLC procedure still needed to include the AEC step, which is time consuming. Although Vaintraub and Lapteva's method could omitted the anion exchange purification step by adding Wade reagent directly to acidified extracts, it is possibly caused by some unknown matrix interferences and underestimated PA content. The earlier AEC method also encountered these unknown matrix interferences¹³⁷. The official method for phytate in foods is elegant but rather lengthy and lacks the ability to identify and measure the lower phosphate esters of myo-inositol.

1.6. Copper in the pathogenesis of kidney stones

1.6.1. Cu in body

Copper (Cu) is an essential trace metal found in all living organisms in the oxidized Cu(II) and reduced Cu(I) states. It is required for survival and serves as an important catalytic cofactor in redox chemistry for proteins that carry out fundamental biological functions that are required for growth and development¹³⁸. The average intakes of copper by human adults, vary from 0.6 to 1.6 mg/d and the main sources are seeds, grains, nuts, and beans (concentrated in the germ and bran), shellfish and liver¹³⁹. Drinking water does not normally contribute significantly to intake. The concentration of free copper ions has been estimated to be of the order of 10^{-18} – 10^{-13} M in yeast cells and in human blood plasma, respectively. In excess of cellular needs, Cu can be cytotoxic^{140,141}. The nutritional biochemistry and metabolism of copper in adult human are summarized in Figure 1.11.

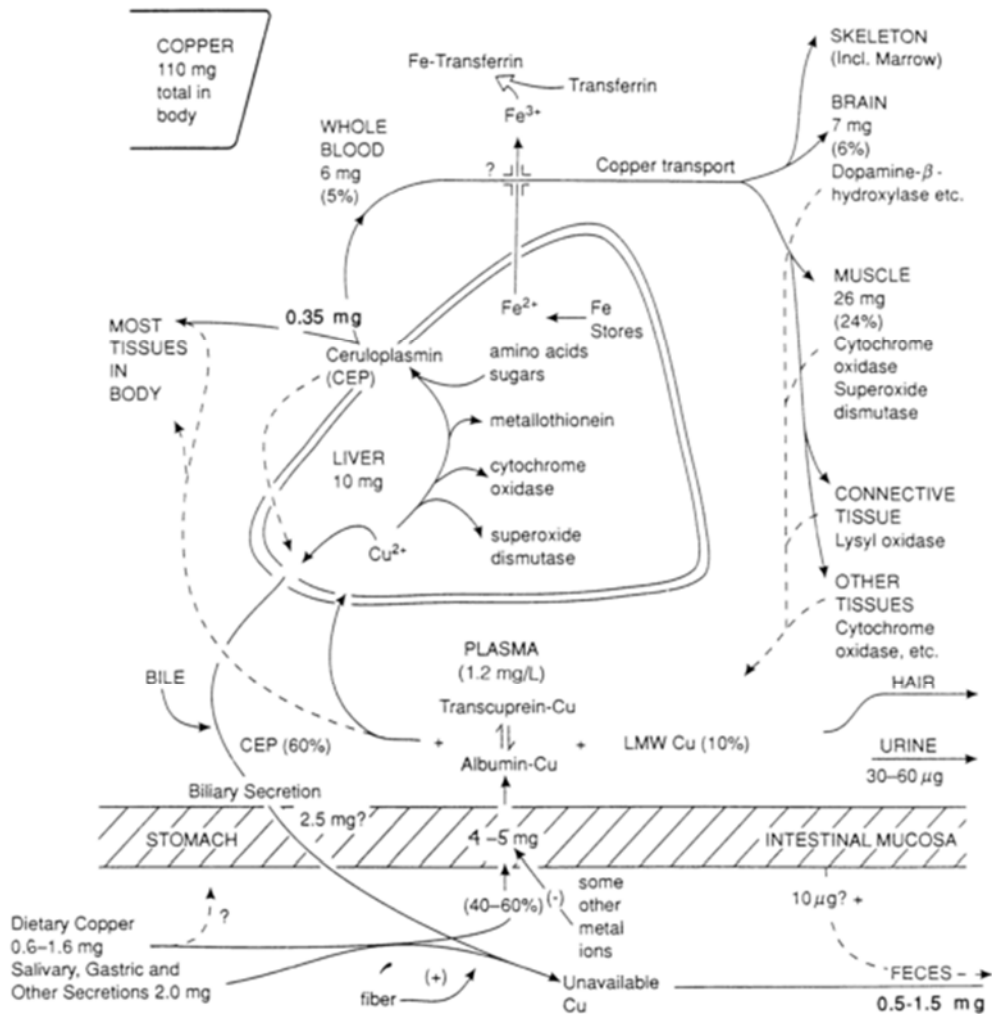


Figure 1.11. Summary of the nutritional biochemistry and metabolism of copper in adult humans¹⁴⁰. Values for copper indicate average daily amounts of copper ingested, absorbed, secreted into various fluids, and excreted by various routes; also shown are concentrations of copper in fluids, as well as total amounts of copper in various tissues. Percentages refer to that absorbed or percentage of total body copper accounted for by specific tissues. LMW, low molecular weight. Role of major and trace elements in the pathogenesis of kidney stone¹⁴²

1.6.2. Cu in the pathogenesis of kidney stones

Cu is an antioxidant and its highest concentration is found in the liver, kidney, heart and brain. Chronic (long-term) effect of Cu exposure can damage the liver and kidney. It was firstly pointed out by Bird et al.¹⁴³ that Cu shows the inhibitory effect on the mineralization process of rachitic rats' cartilage. It has been observed that the amount of Cu stored in the

stones is more relevant when compared to Zn, especially in oxalate stones¹⁴⁴. Cu and Mn urinary levels were found to be lower in stone formers than in normal subjects¹⁴⁵. The inhibitory activity of Cu against growth of calcium phosphate crystals was observed, but not on oxalate¹⁴⁶.

1.7. Reference

1. Modlin, M., A history of urinary stone. *S Afr Med J* **1980**, *58*, 652-655.
2. Stoller, M. L.; Meng, M. V., *Urinary stone disease: the practical guide to medical and surgical management*. Springer Science & Business Media: 2007.
3. Brenner, B. M., *Brenner & Rector's the kidney*. Saunders Philadelphia, PA: 2004; Vol. 1.
4. Layton, A. T.; Edwards, A., *Mathematical Modeling in Renal Physiology*. Springer: 2014.
5. Berger, A. D.; Stoller, M. L., Kidney stones.
6. Wesson, J. A.; Ward, M. D., Pathological biomineralization of kidney stones. *Elements* **2007**, *3* (6), 415-421.
7. <https://www.acvs.org/small-animal/urinary-stones>.
8. Baxby, M. K., Urinary Calculus. **2008**.
9. Monk, R. D. In *Clinical approach to adults*, Seminars in nephrology, 1996; pp 375-388.
10. Krepinsky, J.; Ingram, A. J.; Churchill, D. N., Metabolic investigation of recurrent nephrolithiasis: compliance with recommendations. *Urology* **2000**, *56* (6), 915-920.
11. Knoll, T., Epidemiology, pathogenesis, and pathophysiology of urolithiasis. *European Urology Supplements* **2010**, *9* (12), 802-806.
12. Daudon, M.; Doré, J.-C.; Jungers, P.; Lacour, B., Changes in stone composition according to age and gender of patients: a multivariate epidemiological approach. *Urol Res* **2004**, *32* (3), 241-247.
13. Strobe, S. A.; Wolf, J. S.; Hollenbeck, B. K., Changes in gender distribution of urinary stone disease. *Urology* **2010**, *75* (3), 543-546. e1.
14. Scales, C. D.; Curtis, L. H.; Norris, R. D.; Springhart, W. P.; Sur, R. L.; Schulman, K. A.; Preminger, G. M., Changing gender prevalence of stone disease. *The Journal of urology* **2007**, *177* (3), 979-982.
15. Rizvi, S.; Naqvi, S.; Hussain, Z.; Hashmi, A.; Hussain, M.; Zafar, M.; Sultan, S.; Mehdi, H., Pediatric urolithiasis: developing nation perspectives. *The Journal of urology* **2002**, *168* (4), 1522-1525.
16. Taylor, E. N.; Stampfer, M. J.; Curhan, G. C., Dietary factors and the risk of incident kidney stones in men: new insights after 14 years of follow-up. *Journal of the American Society of Nephrology* **2004**, *15* (12), 3225-3232.
17. Antonelli, J. A.; Maalouf, N. M.; Pearle, M. S.; Lotan, Y., Use of the National Health and Nutrition Examination Survey to calculate the impact of obesity and diabetes on cost and prevalence of urolithiasis in 2030. *European urology* **2014**, *66* (4), 724-729.
18. Cameron, M. A.; Maalouf, N. M.; Adams-Huet, B.; Moe, O. W.; Sakhaee, K., Urine composition in type 2 diabetes: predisposition to uric acid nephrolithiasis. *Journal of the American Society of Nephrology* **2006**, *17* (5), 1422-1428.

19. Verkoelen, C. F.; Van Der Boom, B. G.; Houtsmuller, A. B.; Schröder, F. H.; Romijn, J. C., Increased calcium oxalate monohydrate crystal binding to injured renal tubular epithelial cells in culture. *American Journal of Physiology-Renal Physiology* **1998**, *274* (5), F958-F965.
20. Evan, A. P.; Lingeman, J. E.; Coe, F. L.; Parks, J. H.; Bledsoe, S. B.; Shao, Y.; Sommer, A. J.; Paterson, R. F.; Kuo, R. L.; Grynepas, M., Randall's plaque of patients with nephrolithiasis begins in basement membranes of thin loops of Henle. *Journal of Clinical Investigation* **2003**, *111* (5), 607.
21. de Water, R.; Noordermeer, C.; Houtsmuller, A. B.; Nigg, A. L.; Stijnen, T.; Schröder, F. H.; Kok, D. J., Role of macrophages in nephrolithiasis in rats: an analysis of the renal interstitium. *American journal of kidney diseases* **2000**, *36* (3), 615-625.
22. Moe, O. W., Kidney stones: pathophysiology and medical management. *The Lancet* **2006**, *367* (9507), 333-344.
23. Finlayson, B., Physicochemical aspects of urolithiasis. *Kidney Int* **1978**, *13* (5), 344-360.
24. Sellaturay, S.; Fry, C., The metabolic basis for urolithiasis. *Surgery (Oxford)* **2008**, *26* (4), 136-140.
25. Walton, A. G.; Füredi, H.; Elving, P. J.; Kolthoff, I. M., The formation and properties of precipitates. **1967**.
26. Sears, G. W., The origin of spherulites. *The Journal of Physical Chemistry* **1961**, *65* (10), 1738-1741.
27. Trump, B.; Dees, J.; KIM, K.; Sahaphong, S., Some aspects of kidney structure and function, with comments on tissue calcification in the kidney. *Urolithiasis: Physical Aspects. B. Finlayson, LL Hench, and LH Smith, editors. National Academy of Sciences, Washington, DC* **1972**, *1*.
28. Kok, D. J.; Khan, S. R., Calcium oxalate nephrolithiasis, a free or fixed particle disease. *Kidney international* **1994**, *46* (3), 847-854.
29. Grases, F.; Costa-Bauzá, A.; Ramis, M.; Montesinos, V.; Conte, A., Simple classification of renal calculi closely related to their micromorphology and etiology. *Clinica Chimica Acta* **2002**, *322* (1), 29-36.
30. Pearle, M. S.; Lotan, Y., Urinary lithiasis: etiology, epidemiology, and pathogenesis. *Campbell-walsh urology* **2007**, *2*, 1363-92.
31. Sterling, C., Crystal structure analysis of weddellite, $\text{CaC}_2\text{O}_4 \cdot (2+x) \text{H}_2\text{O}$. *Acta Crystallographica* **1965**, *18* (5), 917-921.
32. Tomazic, B.; Nancollas, G., A study of the phase transformation of calcium oxalate trihydrate-monohydrate. *Invest Urol* **1979**, *16* (5), 329-335.
33. Mandel, N.; Mandel, G., Urinary tract stone disease in the United States veteran population. II. Geographical analysis of variations in composition. *The Journal of urology* **1989**, *142* (6), 1516-1521.
34. Elliot, J.; Rabinowitz, I., Calcium oxalate crystalluria: crystal size in urine. *The Journal of urology* **1980**, *123* (3), 324-327.
35. Lieske, J. C.; Leonard, R.; Toback, F. G., Adhesion of calcium oxalate monohydrate crystals to renal epithelial cells is inhibited by specific anions. *American Journal of Physiology-Renal Physiology* **1995**, *268* (4), F604-F612.

36. Mann, S.; Heywood, B.; Rajam, S.; Wade, V., Molecular recognition in biomineralization. In *Mechanisms and Phylogeny of Mineralization in Biological Systems*, Springer: 1991; pp 47-55.
37. Wesson, J. A.; Worcester, E. M.; Wiessner, J. H.; Mandel, N. S.; Kleinman, J. G., Control of calcium oxalate crystal structure and cell adherence by urinary macromolecules. *Kidney international* **1998**, *53* (4), 952-957.
38. Wesson, J.; Worcester, E., Formation of hydrated calcium oxalates in the presence of poly-L-aspartic acid. *Scanning microscopy* **1995**, *10* (2), 415-23; 423-4.
39. Christmas, K. G.; Gower, L. B.; Khan, S. R.; El-Shall, H., Aggregation and dispersion characteristics of calcium oxalate monohydrate: effect of urinary species. *Journal of colloid and interface science* **2002**, *256* (1), 168-174.
40. Photo of one of the renal stones (whewellite nephrolith) of the previous patient. <http://www.buc.hu/content/gallery.html>.
41. Calcium Oxalate Dihydrate <http://www.herringlab.com/photos/Urinary/Oxalates/Cod/>.
42. Pak, C. Y.; Sakhaee, K.; Peterson, R. D.; Poindexter, J. R.; Frawley, W. H., Biochemical profile of idiopathic uric acid nephrolithiasis. *Kidney international* **2001**, *60* (2), 757-761.
43. Millman, S.; Strauss, A. L.; Parks, J. H.; Coe, F. L., Pathogenesis and clinical course of mixed calcium oxalate and uric acid nephrolithiasis. *Kidney Int* **1982**, *22* (4), 366-370.
44. Sakhaee, K., Epidemiology and clinical pathophysiology of uric acid kidney stones. *Journal of nephrology* **2014**, *27* (3), 241-245.
45. Kenny, J.-E. S.; Goldfarb, D. S., Update on the pathophysiology and management of uric acid renal stones. *Current rheumatology reports* **2010**, *12* (2), 125-129.
46. Wierzbicki, A.; Sallis, J.; Stevens, E.; Smith, M.; Sikes, C., Crystal growth and molecular modeling studies of inhibition of struvite by phosphocitrate. *Calcified tissue international* **1997**, *61* (3), 216-222.
47. Krombach, P.; Wendt-Nordahl, G.; Knoll, T., Cystinuria and cystine stones. In *Urinary Tract Stone Disease*, Springer: 2011; pp 207-215.
48. Basiri, A.; Taheri, M.; Taheri, F., What is the state of the stone analysis techniques in urolithiasis? *Urology journal* **2012**, *9* (2), 445-454.
49. Daudon, M.; Bader, C.; Jungers, P., Urinary calculi: review of classification methods and correlations with etiology. *Scanning Microscopy* **1993**, *7*, 1081-1081.
50. Kasidas, G.; Samuell, C.; Weir, T., Renal stone analysis: why and how? *Annals of clinical biochemistry* **2004**, *41* (2), 91-97.
51. Lee, H. P.; Leong, D.; Heng, C. T., Characterization of kidney stones using thermogravimetric analysis with electron dispersive spectroscopy. *Urol Res* **2012**, *40* (3), 197-204.
52. Materazzi, S.; Curini, R.; D'Ascenzo, G.; Magri, A., TG-FTIR coupled analysis applied to the studies in urolithiasis: characterization of human renal calculi. *Thermochimica acta* **1995**, *264*, 75-93.
53. ROSE, G.; Woodfine, C., The thermogravimetric analysis of renal stones (in clinical practice). *British journal of urology* **1976**, *48* (6), 403-412.

54. Douglas, D.; Tonks, D., The qualitative analysis of renal calculi with the polarising microscope. *Clinical biochemistry* **1979**, *12* (5), 182-183.
55. Estepa, L.; Daudon, M., Contribution of Fourier transform infrared spectroscopy to the identification of urinary stones and kidney crystal deposits. *Biospectroscopy* **1997**, *3* (5), 347-369.
56. Blanco, F.; López-Mesas, M.; Serranti, S.; Bonifazi, G.; Havel, J.; Valiente, M., Hyperspectral imaging based method for fast characterization of kidney stone types. *Journal of Biomedical Optics* **2012**, *17* (7), 0760271-07602712.
57. Min, W.; Shiraga, H.; Chalko, C.; Goldfarb, S.; Krishna, G. G.; Hoyer, J. R., Quantitative studies of human urinary excretion of uropontin. *Kidney international* **1998**, *53* (1), 189-193.
58. Barbas, C.; Garcia, A.; Saavedra, L.; Muros, M., Urinary analysis of nephrolithiasis markers. *Journal of chromatography B* **2002**, *781* (1), 433-455.
59. Ryall, R. L., The possible roles of inhibitors, promoters, and macromolecules in the formation of calcium kidney stones. In *Urinary Tract Stone Disease*, Springer: 2011; pp 31-60.
60. Graf, E.; Empson, K. L.; Eaton, J. W., Phytic acid. A natural antioxidant. *Journal of Biological Chemistry* **1987**, *262* (24), 11647-11650.
61. Grases, F.; Costa-Bauzá, A.; Prieto, R., Intracellular and extracellular myo-inositol hexakisphosphate (InsP6), from rats to humans. *Anticancer research* **2005**, *25* (3C), 2593-2597.
62. Singh, P. K., Significance of phytic acid and supplemental phytase in chicken nutrition: a review. *World's Poultry Science Journal* **2008**, *64* (04), 553-580.
63. Maga, J. A., Phytate: its chemistry, occurrence, food interactions, nutritional significance, and methods of analysis. *Journal of Agricultural and Food Chemistry* **1982**, *30* (1), 1-9.
64. Zhou, J. R.; Erdman Jr, J. W., Phytic acid in health and disease. *Critical Reviews in Food Science & Nutrition* **1995**, *35* (6), 495-508.
65. Graf, E.; Eaton, J. W., Antioxidant functions of phytic acid. *Free Radical Biology and Medicine* **1990**, *8* (1), 61-69.
66. Reddy, N. R., Occurrence, distribution, content, and dietary intake of phytate. *Food phytates* **2002**, 25-51.
67. (a) Vucenik, I.; Shamsuddin, A. M., Protection against cancer by dietary IP6 and inositol. *Nutrition and cancer* **2006**, *55* (2), 109-125; (b) Rizvi, I.; Riggs, D. R.; Jackson, B. J.; Ng, A.; Cunningham, C.; McFadden, D. W., Inositol Hexaphosphate (IP6) Inhibits Cellular Proliferation In Melanoma. *Journal of Surgical Research* **2006**, *133* (1), 3-6; (c) Somasundar, P.; Riggs, D. R.; Jackson, B. J.; Cunningham, C.; Vona-Davis, L.; McFadden, D. W., Inositol Hexaphosphate (IP6): A Novel Treatment for Pancreatic Cancer¹. *Journal of Surgical Research* **2005**, *126* (2), 199-203.
68. Grases, F.; Isern, B.; Sanchis, P.; Perello, J.; Torres, J. J.; Costa-Bauza, A., Phytate acts as an inhibitor in formation of renal calculi. *Front Biosci* **2007**, *12* (1), 2580-7.
69. Grases, F.; Garcia-Ferragut, L.; Costa-Bauzá, A.; March, J., Study of the effects of different substances on the early stages of papillary stone formation. *Nephron* **1996**, *73* (4), 561-568.
70. Grases, F.; March, P., A study about some phosphate derivatives as inhibitors of calcium oxalate crystal growth. *Journal of crystal growth* **1989**, *96* (4), 993-995.

71. Grases, F.; Costa-Bauzá, A., Potentiometric study of the nucleation of calcium oxalate in presence of several additives. *Clin. Chem. Enzym. Comms* **1991**, *3*, 319.
72. Modlin, M., Urinary phosphorylated inositols and renal stone. *The Lancet* **1980**, *316* (8204), 1113-1114.
73. Grases, F.; Garcia-Gonzalez, R.; Torres, J.; Llobera, A., Effects of phytic acid on renal stone formation in rats. *Scandinavian journal of urology and nephrology* **1998**, *32* (4), 261-265.
74. Grases, F.; March, J.; Prieto, R.; Simonet, B.; Costa-Bauzá, A.; García-Raja, A.; Conte, A., Urinary phytate in calcium oxalate stone formers and healthy people: dietary effects on phytate excretion. *Scandinavian journal of urology and nephrology* **2000**, *34* (3), 162-164.
75. Coe, F.; Parks, J.; Nakagawa, Y., Inhibitors and promoters of calcium oxalate crystallization: their relationship to the pathogenesis of nephrolithiasis. Lippincott: 2002.
76. Chow, K.; Dixon, J.; Gilpin, S.; Kavanagh, J. P.; Rao, P. N., Citrate inhibits growth of residual fragments in an in vitro model of calcium oxalate renal stones. *Kidney international* **2004**, *65* (5), 1724-1730.
77. PAK, C. Y.; FULLER, C., Idiopathic hypocitraturic calcium-oxalate nephrolithiasis successfully treated with potassium citrate. *Annals of internal medicine* **1986**, *104* (1), 33-37.
78. Cicerello, E.; Merlo, F.; Gambaro, G.; Maccatrozzo, L.; Fandella, A.; Baggio, B.; Anselmo, G., Effect of alkaline citrate therapy on clearance of residual renal stone fragments after extracorporeal shock wave lithotripsy in sterile calcium and infection nephrolithiasis patients. *The Journal of urology* **1994**, *151* (1), 5-9.
79. Pak, C., Citrate and renal calculi: an update. *Mineral and electrolyte metabolism* **1993**, *20* (6), 371-377.
80. Grases, F.; Ramis, M.; Costa-Bauza, A., Effects of phytate and pyrophosphate on brushite and hydroxyapatite crystallization. *Urol Res* **2000**, *28* (2), 136-140.
81. Wikström, B.; Danielson, B.; Ljunghall, S.; McGuire, M.; Russell, R., Urinary pyrophosphate excretion in renal stone formers with normal and impaired renal acidification. *World journal of urology* **1983**, *1* (3), 150-154.
82. Ryall, R. L., Urinary inhibitors of calcium oxalate crystallization and their potential role in stone formation. *World journal of urology* **1997**, *15* (3), 155-164.
83. Grover, P. K.; Moritz, R. L.; Simpson, R. J.; Ryall, R. L., Inhibition of growth and aggregation of calcium oxalate crystals in vitro. *European Journal of Biochemistry* **1998**, *253* (3), 637-644.
84. Coe, F. L.; Parks, J. H.; Asplin, J. R., The pathogenesis and treatment of kidney stones. *New England Journal of Medicine* **1992**, *327* (16), 1141-1152.
85. Worcester, E. M.; Beshensky, A. M., Osteopontin Inhibits Nucleation of Calcium Oxalate Crystals. *Annals of the New York Academy of Sciences* **1995**, *760* (1), 375-377.
86. Asplin, J. R.; Arsenault, D.; Parks, J. H.; Coe, F. L.; Hoyer, J. R., Contribution of human uropontin to inhibition of calcium oxalate crystallization. *Kidney international* **1998**, *53* (1), 194-199.
87. Stapleton, A.; Ryall, U., Blood coagulation proteins and urolithiasis are linked: Crystal matrix protein is the F1 activation peptide of human prothrombin. *British journal of urology* **1995**, *75* (6), 712-719.

88. Grover, P. K.; Ryall, R. L., Inhibition of calcium oxalate crystal growth and aggregation by prothrombin and its fragments in vitro. *European Journal of Biochemistry* **1999**, *263* (1), 50-56.
89. Basavaraj, D. R.; Biyani, C. S.; Browning, A. J.; Cartledge, J. J., The role of urinary kidney stone inhibitors and promoters in the pathogenesis of calcium containing renal stones. *EAU-EBU update series* **2007**, *5* (3), 126-136.
90. Webber, D.; Rodgers, A. L.; Sturrock, E. D., Synergism between urinary prothrombin fragment 1 and urine: a comparison of inhibitory activities in stone-prone and stone-free population groups. *Clinical chemistry and laboratory medicine* **2002**, *40* (9), 930-936.
91. Webber, D.; Radcliffe, C. M.; Royle, L.; Tobiasen, G.; Merry, A. H.; Rodgers, A. L.; Sturrock, E. D.; Wormald, M. R.; Harvey, D. J.; Dwek, R. A., Sialylation of urinary prothrombin fragment 1 is implicated as a contributory factor in the risk of calcium oxalate kidney stone formation. *Febs Journal* **2006**, *273* (13), 3024-3037.
92. Padmanabhan, S.; Graham, L.; Ferreri, N. R.; Graham, D.; McBride, M.; Dominiczak, A. F., Uromodulin, an emerging novel pathway for blood pressure regulation and hypertension. *Hypertension* **2014**, *64* (5), 918-923.
93. El-Achkar, T. M.; Wu, X.-R., Uromodulin in kidney injury: an instigator, bystander, or protector? *American Journal of Kidney Diseases* **2012**, *59* (3), 452-461.
94. Rampoldi, L.; Scolari, F.; Amoroso, A.; Ghiggeri, G.; Devuyt, O., The rediscovery of uromodulin (Tamm-Horsfall protein): from tubulointerstitial nephropathy to chronic kidney disease. *Kidney international* **2011**, *80* (4), 338-347.
95. Raffi, H. S.; Bates, J. M.; Flournoy, D. J.; Kumar, S., Tamm-Horsfall protein facilitates catheter associated urinary tract infection. *BMC research notes* **2012**, *5* (1), 532.
96. Mo, L.; Huang, H.-Y.; Zhu, X.-H.; Shapiro, E.; Hasty, D. L.; Wu, X.-R., Tamm-Horsfall protein is a critical renal defense factor protecting against calcium oxalate crystal formation. *Kidney international* **2004**, *66* (3), 1159-1166.
97. Hess, B., Tamm-Horsfall glycoprotein-inhibitor or promoter of calcium oxalate monohydrate crystallization processes? *Urol Res* **1992**, *20* (1), 83-86.
98. Salier, J.-P., Inter- α -trypsin inhibitor: emergence of a family within the Kunitz-type protease inhibitor superfamily. *Trends in biochemical sciences* **1990**, *15* (11), 435-439.
99. Sørensen, S.; Hansen, K.; Bak, S.; Justesen, S., An unidentified macromolecular inhibitory constituent of calcium oxalate crystal growth in human urine. *Urol Res* **1990**, *18* (6), 373-379.
100. Atmani, F.; Opalko, F.; Khan, S., Association of urinary macromolecules with calcium oxalate crystals induced in vitro in normal human and rat urine. *Urol Res* **1996**, *24* (1), 45-50.
101. Verdier, J.; Dussol, B.; Casanova, P.; Daudon, M.; Dupuy, P.; Berthezene, P.; Boistelle, R.; Berland, Y.; Dagorn, J., Evidence that human kidney produces a protein similar to lithostathine, the pancreatic inhibitor of CaCO₃ crystal growth. *European journal of clinical investigation* **1992**, *22* (7), 469-474.
102. Grover, P. K.; Kim, D.-S.; Ryall, R. L., The effect of seed crystals of hydroxyapatite and brushite on the crystallization of calcium oxalate in undiluted human urine in vitro: implications for urinary stone pathogenesis. *Molecular medicine* **2002**, *8* (4), 200.

103. Poon, N. W.; Gohel, M. D. I., Urinary glycosaminoglycans and glycoproteins in a calcium oxalate crystallization system. *Carbohydrate research* **2012**, *347* (1), 64-68.
104. Torzewska, A.; Różalski, A., In vitro studies on the role of glycosaminoglycans in crystallization intensity during infectious urinary stones formation. *Apmis* **2014**, *122* (6), 505-511.
105. Akçay, T.; Konukoğlu, D.; DİNÇER, Y., Urinary glycosaminoglycan excretion in urolithiasis. *Archives of disease in childhood* **1999**, *80* (3), 271-272.
106. Ryall, R. L., Glycosaminoglycans, proteins, and stone formation: adult themes and child's play. *Pediatric Nephrology* **1996**, *10* (5), 656-666.
107. Ribieras, S.; Tomasetto, C.; Rio, M.-C., The pS2/TFF1 trefoil factor, from basic research to clinical applications. *Biochimica et Biophysica Acta (BBA)-Reviews on Cancer* **1998**, *1378* (1), F61-F77.
108. Chutipongtanate, S.; Nakagawa, Y.; Sritippayawan, S.; Pittayamateekul, J.; Parichatikanond, P.; Westley, B. R.; May, F. E.; Malasit, P.; Thongboonkerd, V., Identification of human urinary trefoil factor 1 as a novel calcium oxalate crystal growth inhibitor. *Journal of Clinical Investigation* **2005**, *115* (12), 3613.
109. Pillay, S. N.; Asplin, J. R.; Coe, F. L., Evidence that calgranulin is produced by kidney cells and is an inhibitor of calcium oxalate crystallization. *American Journal of Physiology-Renal Physiology* **1998**, *275* (2), F255-F261.
110. Aoki, H.; Hasegawa, K.; Tohda, K.; Umezawa, Y., Voltammetric detection of inorganic phosphate using ion-channel sensing with self-assembled monolayers of a hydrogen bond-forming receptor. *Biosensors and Bioelectronics* **2003**, *18* (2), 261-267.
111. Wu, P.; Tian, J.-C.; Walker, C. E.; Wang, F.-C., Determination of phytic acid in cereals - a brief review. *International Journal of Food Science & Technology* **2009**, *44* (9), 1671-1676.
112. Turner, B. L.; Paphazy, M. J.; Haygarth, P. M.; McKelvie, I. D., Inositol phosphates in the environment. *Philosophical transactions of the Royal Society of London. Series B, Biological sciences* **2002**, *357* (1420), 449-69.
113. Azevedo, C.; Saiardi, A., Extraction and analysis of soluble inositol polyphosphates from yeast. *Nature protocols* **2006**, *1* (5), 2416-2422.
114. Costello, A. J.; Glonek, T.; Myers, T. C., ³¹P Nuclear magnetic resonance pH titrations of myo-inositol hexaphosphate. *Carbohydrate Research* **1976**, *46* (2), 159-171.
115. Sandberg, A.-S.; Ahderinne, R., HPLC method for determination of inositol tri-, tetra-, penta-, and hexaphosphates in foods and intestinal contents. *J. Food Sci* **1986**, *51* (3), 547-550.
116. Fiske, C. H.; Subbarow, Y., The colorimetric determination of phosphorus. *J. Biol. Chem* **1925**, *66* (2), 375-400.
117. García-Villanova, R.; García-Villanova, R.; de Lope, C. R., Determination of phytic acid by complexometric titration of excess of iron (III). *Analyst* **1982**, *107* (1281), 1503-1506.
118. Møllgaard, H., On phytic acid, its importance in metabolism and its enzymic cleavage in bread supplemented with calcium. *Biochemical Journal* **1946**, *40* (4), 589.
119. Latta, M.; Eskin, M., A simple and rapid colorimetric method for phytate determination. *Journal of Agricultural and Food Chemistry* **1980**, *28* (6), 1313-1315.

120. Harland, B. F.; Oberleas, D., Anion-exchange method for determination of phytate in foods: collaborative study. *Journal-Association of Official Analytical Chemists* **1985**, *69* (4), 667-670.
121. Lehrfeld, J.; Morris, E. R., Overestimation of phytic acid in foods by the AOAC anion-exchange method. *Journal of Agricultural and Food Chemistry* **1992**, *40* (11), 2208-2210.
122. Muñoz, J. A.; Valiente, M., Determination of phytic acid in urine by inductively coupled plasma mass spectrometry. *Analytical chemistry* **2003**, *75* (22), 6374-6378.
123. Tangendjaja, B.; Buckle, K.; Wootton, M., Analysis of phytic acid by high-performance liquid chromatography. *Journal of Chromatography A* **1980**, *197* (2), 274-277.
124. Graf, E.; Dintzis, F. R., Determination of phytic acid in foods by high-performance liquid chromatography. *Journal of Agricultural and Food Chemistry* **1982**, *30* (6), 1094-1097.
125. Graf, E.; Dintzis, F. R., High-performance liquid chromatographic method for the determination of phytate. *Analytical biochemistry* **1982**, *119* (2), 413-417.
126. Lehrfeld, J., High-performance liquid chromatography analysis of phytic acid on a pH-stable, macroporous polymer column. *Cereal Chem* **1989**, *66* (6), 510-515.
127. Lehrfeld, J., HPLC separation and quantitation of phytic acid and some inositol phosphates in foods: problems and solutions. *Journal of agricultural and food chemistry* **1994**, *42* (12), 2726-2731.
128. Blaabjerg, K.; Hansen-Moller, J.; Poulsen, H. D., High-performance ion chromatography method for separation and quantification of inositol phosphates in diets and digesta. *Journal of chromatography. B, Analytical technologies in the biomedical and life sciences* **2010**, *878* (3-4), 347-54.
129. Helfrich, A.; Bettmer, J. r., Determination of phytic acid and its degradation products by ion-pair chromatography (IPC) coupled to inductively coupled plasma-sector field-mass spectrometry (ICP-SF-MS). *Journal of Analytical Atomic Spectrometry* **2004**, *19* (10), 1330.
130. Yoza, N.; Akazaki, I.; Nakazato, T.; Ueda, N.; Kodama, H.; Tateda, A., High-performance liquid chromatographic determination of pyrophosphate in the presence of a 20,000-fold excess of orthophosphate. *Analytical biochemistry* **1991**, *199* (2), 279-285.
131. Hénin, O.; Barbier, B.; Brack, A., Determination of phosphate and pyrophosphate ions by capillary electrophoresis. *Analytical biochemistry* **1999**, *270* (1), 181-184.
132. Flynn, R. M.; Jones, M. E.; Lipmann, F., A colorimetric determination of inorganic pyrophosphate. *Journal of Biological Chemistry* **1954**, *211* (2), 791-796.
133. Ronaghi, M.; Karamohamed, S.; Pettersson, B.; Uhlén, M.; Nyrén, P., Real-time DNA sequencing using detection of pyrophosphate release. *Analytical biochemistry* **1996**, *242* (1), 84-89.
134. Nyrén, P.; Lundin, A., Enzymatic method for continuous monitoring of inorganic pyrophosphate synthesis. *Analytical biochemistry* **1985**, *151* (2), 504-509.
135. Nyrén, P., Enzymatic method for continuous monitoring of DNA polymerase activity. *Analytical biochemistry* **1987**, *167* (2), 235-238.
136. March, J. G.; Simonet, B. M.; Grases, F., Determination of pyrophosphate in renal calculi and urine by means of an enzymatic method. *Clinica chimica acta* **2001**, *314* (1), 187-194.

137. Gao, Y.; Shang, C.; Maroof, M. A. S.; Biyashev, R. M.; Grabau, E. A.; Kwanyuen, P.; Burton, J. W.; Buss, G. R., A Modified Colorimetric Method for Phytic Acid Analysis in Soybean. *Crop Science* **2007**, *47* (5), 1797.
138. de Romaña, D. L.; Olivares, M.; Uauy, R.; Araya, M., Risks and benefits of copper in light of new insights of copper homeostasis. *Journal of Trace Elements in Medicine and Biology* **2011**, *25* (1), 3-13.
139. Scott, K. C.; Turnlund, J. R., Compartmental model of copper metabolism in adult men. *The Journal of Nutritional Biochemistry* **1994**, *5* (7), 342-350.
140. Linder, M. C.; Hazegh-Azam, M., Copper biochemistry and molecular biology. *The American journal of clinical nutrition* **1996**, *63* (5), 797S-811S.
141. Tapiero, H.; Townsend, D.; Tew, K., Trace elements in human physiology and pathology. Copper. *Biomedicine & pharmacotherapy* **2003**, *57* (9), 386-398.
142. Singh, V. K.; Rai, P. K., Kidney stone analysis techniques and the role of major and trace elements on their pathogenesis: a review. *Biophysical Reviews* **2014**, *6* (3-4), 291-310.
143. Bird, E. D.; Thomas, W. C., Effect of Various Metals on Mineralization in vitro. *Experimental Biology and Medicine* **1963**, *112* (3), 640-643.
144. Joost, J.; Tessadri, R., Trace element investigations in kidney stone patients. *European urology* **1986**, *13* (4), 264-270.
145. Komleh, K.; Hada, P.; Pendse, A.; Singh, P., Zine, copper and manganese in serum, urine and stones. *International urology and nephrology* **1990**, *22* (2), 113-118.
146. Meyer, J.; Angino, E., The role of trace metals in calcium urolithiasis. *Invest Urol* **1977**, *14* (5), 347-350.



2. Objective

2.1. General objective

The previous sections have illustrated a general picture of urinary lithiasis and many related aspects that show different relations to urinary disease. This complex, global description embraces the scientific and practice faces of the topic. There are still vast areas in nephrolithiasis that are poorly understood or even unexplored. To further the progression of research and clinical management of kidney stones, multilevel translational approaches are needed. Considering the state of the art previously described, the main purpose of the present work is focused on the contribution to the knowledge of urolithiasis: characterization of physiological aspect and novel material to determine key inhibitors.

2.2. Specific objectives

The present work aims to reach the defined objective through the application of separation chemistry on the analysis of solid and liquid samples for the study of lithogenesis. The global objective has been developed by accomplishing specific goals including:

1. Development of methodologies for quantitative extraction and determination of phosphorous inhibitors in walnuts. This aim involves the following purposes:
 - i. To use microwave- assisted extraction technique for the extraction of phytic acid and pyrophosphate from walnuts.
 - ii. To optimize the solvent contents, the temperature, the reaction time for the microwave-assisted extraction oven.
 - iii. To study the hydrolysis of phytic acid in the developed methodologies and compared with the published data.
 - iv. To test the developed methodologies against exiting, reference techniques to prove their suitability.
 - v. To study the potential of walnuts as functional food.
2. Development of molecularly imprinted polymer for selective extraction of phosphorous inhibitors of urolithiasis.

- i. To synthesize the molecularly imprinted polymer by appropriate choice of monomer, template, cross-linker, and solvent.
 - ii. To characterize the structure and function of both MIP and NIP using a variety of method.
 - iii. To determine the values including contact time, pH and target ions concentration of those that maximize the adsorption of the target analytes.
 - iv. To study the selectivity of the molecularly imprinted polymer in a wide range of pH and temperature.
 - v. To carry out a solid phase extraction based on the imprinted polymer to separate phytic acid, pyrophosphate and phosphate.
3. Study the isotopic of copper in the blood and urine of urolithiasic patients.
 - i. To optimize the copper column separation method
 - ii. To validate the copper column separation method by using oyster sample as reference materials.
 - iii. To establish links between copper isotope variation and other components in the serum and red cell sample.
 - iv. To compare the difference of copper isotope variation between urolithiasic patients and healthy control.



Chapter 3

Inhibitors extracted from food

3. Inhibitors extracted from food

3.1. Urolithiasis inhibitors in walnuts

Consumption of walnuts has been associated with a decreased risk of cardiovascular disease or events related to heart disease ¹. Walnuts (Figure 3.1) have been an important component of human diet from pre-agriculture times to the present day. A recent decline in the consumption of nuts was probably due to concerns about ingesting fatty food. Although total fat intake is related to health risks, there is now general agreement that the more important is the type of fat or fatty acids that are consumed ². Compared with most other nuts, walnuts in particular have a unique profile: they are rich in polyunsaturated fatty acids, especially highly enriched in omega-3 polyunsaturated fatty acids, which might have a significant role in the prevention of coronary heart disease (CHD) ³. Other reported results indicated that walnuts provide significant benefits for certain antioxidant capacity and inflammatory markers and had no adverse effects on body weight⁴. The versatility of walnuts, which allow their ready use in the diet as snacks or components of desserts, breads, or entrees, suggests that their consumption would be acceptable to most as part of a cholesterol-lowering diet ².



Figure 3.1. Walnuts

One of the bioactive compounds found in walnuts is phytic acid (myoinositol hexaphosphate, IP₆) which is abundantly present in many plant sources and in certain high-

fiber diets, such as cereals and legumes. It is claimed to have the ability to enhance the anticancer effect of conventional chemotherapy and control cancer metastases⁵. In addition, phytic acid acts as an effective inhibitor of calcium salts crystallization in urine and soft tissues, and prevents the formation of kidney stones (urolithiasis)⁶.

Inorganic pyrophosphate (PPi), can also be present in walnuts and can inhibit the formation of several crystallization reactions as for example the formation of calcium oxalate and hydroxyapatite, chemical composition of the 80% of kidney stones, serving so as natural inhibitor of urolithiasis⁷. In lithiasic patients, lower urinary PPi has been reported⁸ and its intake increase has been recommended⁹ as therapy. Thus, the determination of levels of both natural lithiasic inhibitors, IP6 and PPi, in walnuts is of interest for its healthy use.

The growing interest in the biomedical implications of phytic acid and pyrophosphate and the inherent problems with its poor separation are reflected in the tedious analytical techniques actually described and used in many laboratories. The quantitative extraction of phytate and pyrophosphate from foodstuff is not selective and always co-extract with cations, protein, or other nutrients leading to erroneous estimation, damage to the analytical instruments, or both¹⁰. But non-laborious method for the extraction and purification of the compounds from a fatty sample has not been developed.

Interest in microwave-assisted extraction (MAE) has increased significantly over the past years as a result of its inherent advantages (reduction in extraction time and solvent volume) over more traditional extraction techniques, such as Soxhlet extraction¹¹. Conventional extraction methods have been associated to higher solvent requirements, longer extraction times and increased risk of degradation of thermo-labile constituents. In MAE, the solvent and sample are contained in sealed extraction vessels under controlled temperature and pressure conditions. The closed vessels allow the temperature of the solvent to rise well above its boiling point, which shortens extraction time and subsequently increases extraction efficiency^{12,13}.

Development of robust, inexpensive, and reproducible techniques for accurate quantification of undigested phytate in complex food sample is essential to advance knowledge of the content of phytic acid and pyrophosphate. The objectives of the current

study were to investigate the effects of MAE on the extraction efficiency and optimize the parameters including microwave power, irradiation time and acid solvents. In this chapter, we present a rapid and simple procedure for extraction and determination of phytic acid and pyrophosphate content in walnuts.

3.2. Microwave assisted extraction (MAE)

3.2.1. Introduction of MAE

Although microwave energy has great potential for rapidly heating materials, microwave ovens have only recently appeared in analytical laboratories. In 1975 Abu-Samra et al.¹⁴ were the first researchers ever to use a microwave domestic oven in the laboratory, performing trace analysis of metals from biological samples. Since then microwave digestion methods have been developed for different sample types such as environmental, biological, geological, and metallic matrices, as well as for fly ashes and coal. Over the years procedures based on microwave ovens have replaced some of the conventional hot plate and other thermal digestion techniques that have been used for decades in chemical laboratories. Applications of microwave-assisted techniques can be found in other fields of analytical chemistry, such as sample drying, moisture measurements, chromogenic reactions, speciation and nebulization of sample solutions. There is a significant increase in the application of MAE in the last tween years (see figure 3.2).

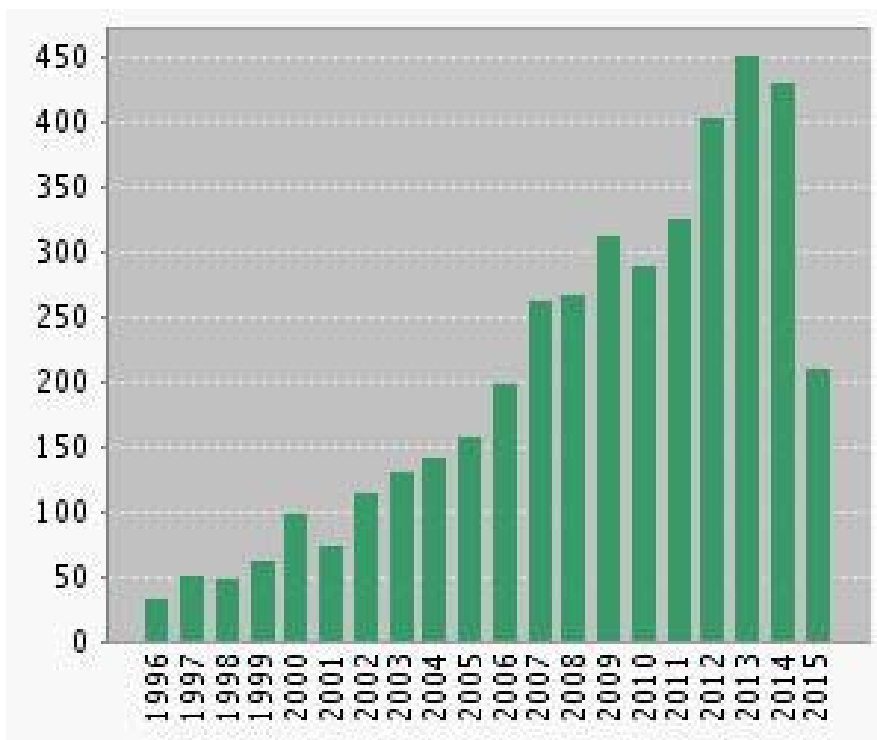


Figure 3.2. Number of scientific publications on microwave assisted extraction from 1996 to May 2015, based on a search in ISI web of Knowledge.

Compared with other extraction technique (such as Soxhlet extraction)(see table 3.1), one of the main advantages using MAE is the reduction of extraction time when applying microwaves. This can mainly be attributed to the difference in heating performance employed by the microwave technique and conventional heating. In conventional heating a finite period of time is needed to heat the vessel before the heat is transferred to the solution, while microwaves heat the solution directly. This keeps the temperature gradient to a minimum and accelerates the speed of heating. Additionally MAE allows for a significant reduction in organic solvent consumption as well as the possibility of running multiple samples. Consequently MAE is an attractive alternative to conventional techniques, as seen by the increasing number of scientific papers published during the last years (Figure 3.2.).

Table 3.1. comparison of MAE and recent extraction techniques¹².

Extraction technique	MAE	FMASE	PLE	SFE	Soxhlet	UAE
Brief description	Sample is immersed in a microwave-absorbing solvent in a closed vessel and irradiation with microwave energy.	Sample is immersed in a microwave-absorbing solvent in an open vessel and irradiation with microwave energy.	Sample and solvent are heated and pressurized in an extraction vessel. When the extraction is finished, the extract is automatically transferred into a vial	Sample is loaded in a high pressure vessel and extracted with supercritical fluid. The analytes are collected in a small volume of solvent or onto a solid-phase trap, which is rinsed with solvent in a subsequent step.	Sample is placed in a glass fibre thimble and, by using a Soxhlet extractor, the sample is repeatedly percolated with condensed vapors of the solvent.	Sample is immersed in solvent in a vessel and placed in an ultrasonication bath.
Extraction time	3-30 min	10-60 min	5-30 min	10-60 min	3-48 hrs	10-60 min
Sample size	1-10 g	1-30 g	1-30 g	1-5 g	1-30 g	1-30 g
Solvent usage	10-40 ml	10-150 ml	10-100 ml	2-5 ml(solid trap) 5-20 ml(liquid trap)	100-500 ml	30-200 ml
Investment	Moderate	Moderate	High	High	Low	Low
advantages	✓ Fast and multiple extractions	✓ Fast extractions	✓ Fast extractions	✓ Fast extractions ✓ Minimal solvent volumes	✓ No filtration required	✓ Multiple extractions

	<ul style="list-style-type: none"> ✓ Low solvent volumes ✓ Elevated temperature 	<ul style="list-style-type: none"> ✓ Low solvent volumes 	<ul style="list-style-type: none"> ✓ Low solvent volumes ✓ Elevated temperature ✓ No filtration required ✓ Automated systems 	<ul style="list-style-type: none"> ✓ Elevated temperature ✓ Relatively selective towards matrix interferences ✓ No clean-up required ✓ Concentrated extracts ✓ Automated systems 		
Drawbacks	<ul style="list-style-type: none"> • Extraction solvent must be able to absorb microwaves • Clean-up step needed • Waiting time for the vessels to cool down. 	<ul style="list-style-type: none"> • Extraction solvent must be able to absorb microwaves • Clean-up step needed • Waiting time for the vessels to cool down. 	<ul style="list-style-type: none"> • Clean-up step needed 	<ul style="list-style-type: none"> • Many parameters to optimize, especially analyte collection 	<ul style="list-style-type: none"> • Long extraction time • Large solvent volumes • Clean-up step needed 	<ul style="list-style-type: none"> • Large solvent volumes • Repeated extractions may be required • Clean-up step needed

MAE: microwave assisted extraction; SFE: supercritical fluid extraction; PLE: Pressurized liquid extraction; FMASE: focused microwave-assisted solvent extraction; UAE: ultrasound-assisted extraction.

Two types of microwave heating systems are commercially available for the analytical laboratory: an open- and a closed-vessel system. This paper focuses on closed-vessel MAE, which is normally used in analytical scale laboratories.

3.2.2. Basic principles

Microwaves are non-ionising electromagnetic (EM) waves located between the radio-frequency range at the lower frequency and infrared at the higher frequency in the electromagnetic spectrum, within the frequency band of 300 MHz to 300 GHz. 915 MHz is considered most useful for industrial applications with its greater penetration depth, while 2,450 MHz frequency is generally used in domestic microwave ovens and for extraction applications with a wide range of commercial units designed for analytical chemistry purposes¹⁵.

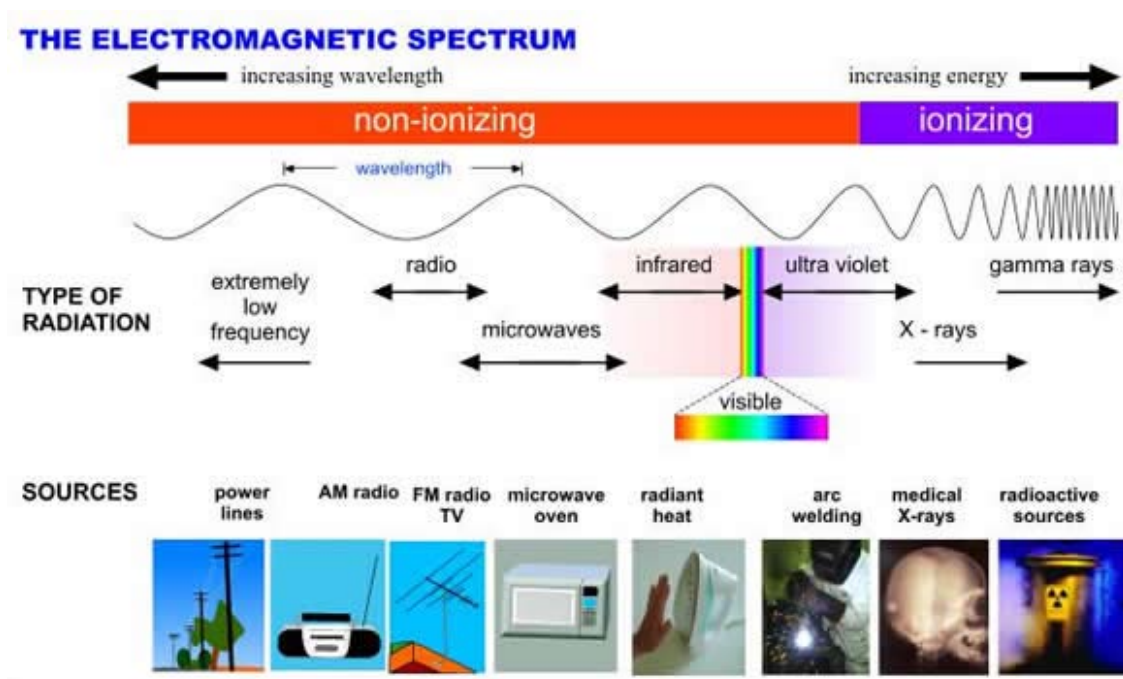


Fig 3.3. The electromagnetic spectrum¹⁶

The principle of heating using microwave energy is based on the direct effect of microwave on molecules by two mechanisms: dipole rotation and ionic conduction through reversals of dipoles and displacement of charged ions present in the solvent and solute. Dipole rotation means realignment of dipoles with the applied field. At the frequency used in

commercial systems, the dipoles align and randomize 4.9×10^9 times/second and this force molecular movement results in heating. Ionic conduction is the electrophoretic migration of ions when an electromagnetic field is applied. The resistance of the solution to this flow of ions will result in friction that heats the solution. When the microwaves interact with polar solvents, heating of substance is caused by due to any of the above mentioned phenomena, in many applications these two mechanisms occur simultaneously^{12,17}.

3.2.3. Factors affecting MAE

The efficiency of the extraction process is directly related to the operation conditions selected. Special attention should be given to usually studied parameters that may influence the performance of MAE such as solvent composition, solvent-to-feed ratio, extraction temperature and time, microwave power, and the characteristics of the matrix including its water content. Comprehension of the effects and interactions of these factors on the MAE process is significant.

3.3. Experimental

3.3.1. Walnuts materials

The walnuts (Lleida, Spain) were purchased from a local supermarket in Barcelona. The walnuts were packed in mesh package. Immediately after it reached the laboratory, the walnuts samples were stored in a sealed plastic container.

3.3.2. Chemicals and reagents

- Tetra-sodium pyrophosphate 10-hydrate (Panreac, Barcelona, Spain),
- myoinositol hexaphosphoric acid hexasodium salt from corn (Sigma, Steinheim, Germany),
- hydrochloric acid 37% (J.T. Baker, Deventer, Holland)

- sulphuric acid (J.T. Baker, Deventer, Holland)
- hexane (Merck, Germany)
- sodium dihydrogen phosphate (Panreac, Barcelona, Spain)

all these compounds were of analytical-reagent grade.

- AG 1x8 200–400 mesh, chloride form, and anion exchange resin was from Bio-Rad Laboratories (Hercules, CA, USA).

- Purified Milli-Q water of 18mΩ-cm resistivity was used for the preparation of all reagents.

3.3.3. Preparation of walnut samples

The walnuts were previously shelled and blended using an electrical grinding machine (corresponding equipment description is specified in table 3.2), then dried at 40°C until no further weight loss and stored into a desiccator until use. Total lipid was extracted from walnut samples by using hexane, based on the modified method of Saad et al.¹⁸. To do so, 5 ml of hexane was added to 1 g of walnut and soaked for 16 hours under a hood. Then after filtration, walnuts were evaporated to dryness using a vacuum pump apparatus.

Table 3.2. Electrical grinding machine description

Equipment	Coffee grinder
Models	MO-3250
Manufacturer	Sonifer, Murcia, Spain
Laboratory of analysis	Centre Grup de Tècniques de Separació en Química (GTS), UAB, Barcelona, Spain



3.3.4. Microwave-assisted extraction (MAE)

MAE experiments were carried out at a CEM Mars5 Accelerated Microwave System (Matthews, USA)(Table 3.3). Acid digestion is employed to break down the sample matrix leaving the compounds of interest in solution and ready for analysis. Samples (defatted as previously described) were transferred into a set of microwave extraction vessels. The samples were added to hydrochloric acid, sulphuric acid or mixture of both at the selected concentrations. Each mixture was placed in a 100 mL sealed perfluoroalkoxy Teflon reactor vessel and extracted for a certain time at selected temperatures using microwave oven which allowed accurate control of pressure, power and temperature. The control vessel (Figure 3.4) was used to monitor the temperature and pressure of the reaction using the sample and solvents under the same condition of standard vessel (Figure 3.5). Three replicates of each sample were extracted at the same time. After certain time of extraction, vessels were allowed to cool down prior to their removal from the extractor.

Table 3.3 Microwave system employed in the extraction procedure.

Equipment	CEM Mars 5 Accelerated Microwave System
Models	Mars 5
Manufacturer	CEM corporation, Matthews, USA
Laboratory of analysis	Centre Grup de Tècniques de Separació en Química (GTS),UAB, Barcelona, Spain

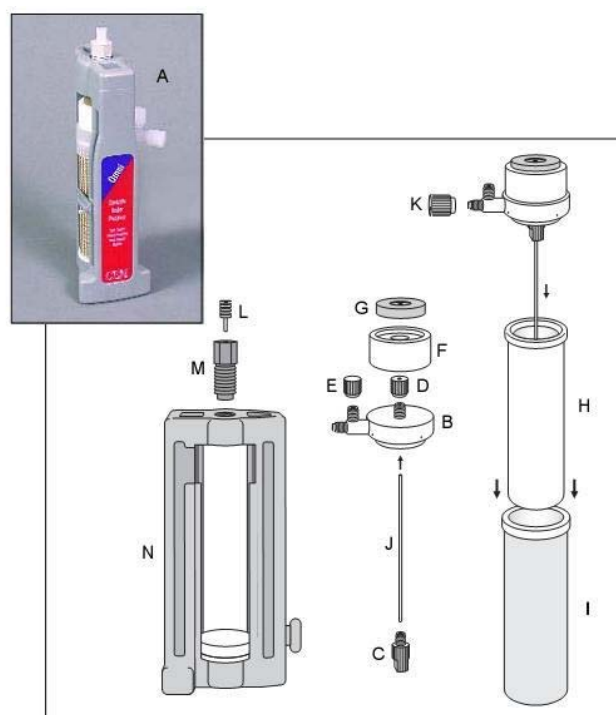


Figure 3.4. Main parts of a control vessel of MAE

A: control vessel assembly; B:pressure/temperature control cover; C:Thermowell locking nut, flat; D:thermowell locking nut, special; E:nut, plug ferrule; F: control spacer; G: control load disk; H: telfon reaction vessel; I:vessel sleeve; J:sapphire thermowell; K:vent nut; L:probe plug; M: control screw; N: control frame module;

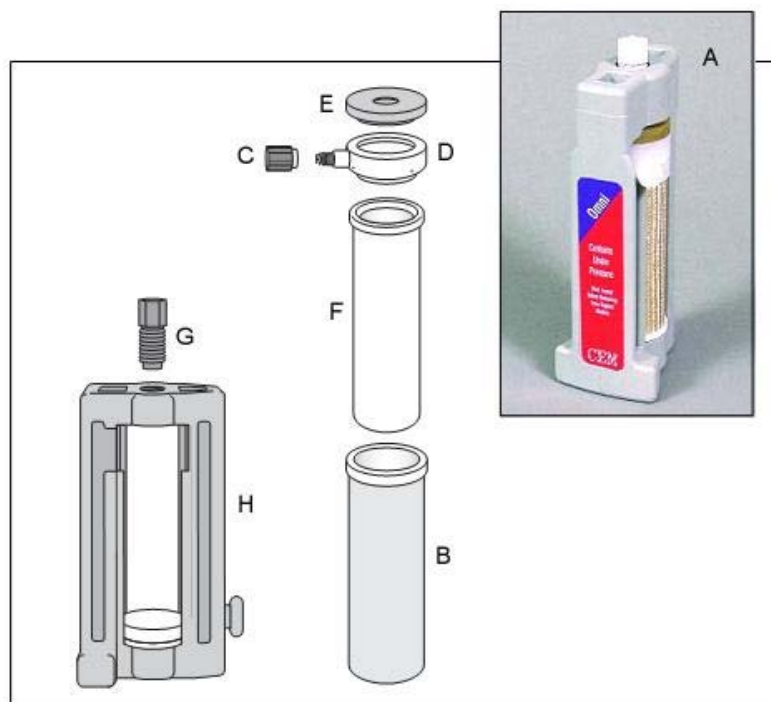


Figure 3.5. Main parts of a standard vessel of MAE


A: standard vessel assembly; B:vessel sleeve; C:solid vent fitting; D:standard vessel cover; E:standard load disk; F: teflon reaction vessel; G:screw; H:standard frame module.

Since the hydrolysis of phytic acid by using a domestic microwave oven has been reported¹⁹. In order to investigate the hydrolysis of phytic acid during the MAE process, 20ml of standard phytic acid (50mg/L) was treated by the microwave under different acid conditions (HCl and H₂SO₄) and microwave parameters(temperature and reaction time).

3.3.5. Solid-solvent extraction

In order to validate the results, the traditional solid-solvent extraction method from the AOAC office method 986.11²⁰ was followed. 0.66 M HCl used as extraction solvents. The extraction was carried out at room temperature with constant shaking at medium speed in an orbital mixer for 3 hours. The equipment description is specified in Table 3.4. The obtained creamy mixture was then processed in the same way as for the creamy extract obtained by microwave extraction.

Table 3.4 Rotary mixer system employed in the extraction procedure.

Equipment	Rotary mixer
Models	CE 2000 ABT-4
Manufacturer	SBS Instruments SA, Barcelona, Spain
Laboratory of analysis	Centre Grup de Tècniques de Separació en Química (GTS), UAB, Barcelona, Spain
Image	

3.3.6. Separation of IP₆ and PP_i by solid phase extraction (SPE)

The obtained creamy extracts from MAE were then centrifuged at 5000 rpm for 10 min. The supernatants were collected and used for separation and determination of total phytic acid and pyrophosphate content.

The SPE methodology followed was described elsewhere²¹. Before separation, the sample was diluted 25 times and then adjusted to pH 6.0 using 0.1M NaOH solution. To separate IP₆ and PP_i, 1.0 mL of the obtained cream was transferred quantitatively to a SPE cartridge, packed with 0.2 g of AG 1x8 resin, previously conditioned with 2mL of HCl 10mmol L⁻¹. First phosphate and some other matrix components of sample were eluted with 50 ml of HCl 50 mmol L⁻¹. Then PP_i were eluted with a second 5 ml HCl 100 mmol/ L eluting. Finally the column was washed with 2 mL of HCl 2 mol/L to elute phytic acid (IP₆). Figure 3.6 shows schematic view of the SPE procedure. The clean-up process was run by gravity, at a flow rate of 0.33 mL min⁻¹.

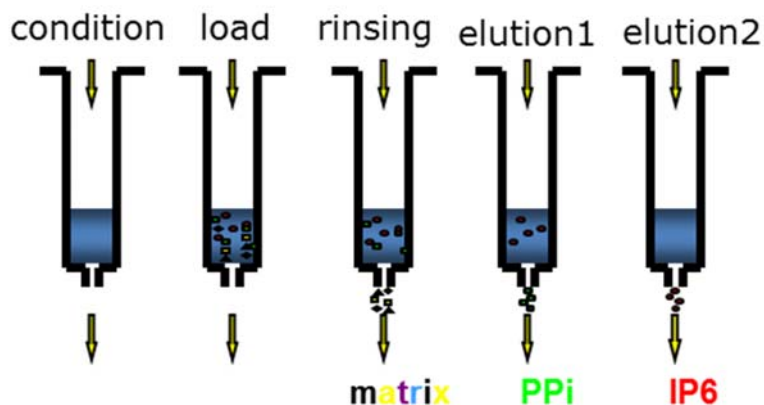


Figure 3.6. Schematic view of the SPE procedure.

3.3.7. Inductively coupled plasma mass spectrometry (ICP-MS)

Inductively coupled plasma mass spectrometry (ICP-MS) is an analytic technique used for metals and several non-metals at very low concentration (about ppb level). This is achieved by ionizing the sample with inductively coupled plasma and then using a mass spectrometer to separate and quantify those ions. Figure 3.7 shows the component of an ICP-MS system.

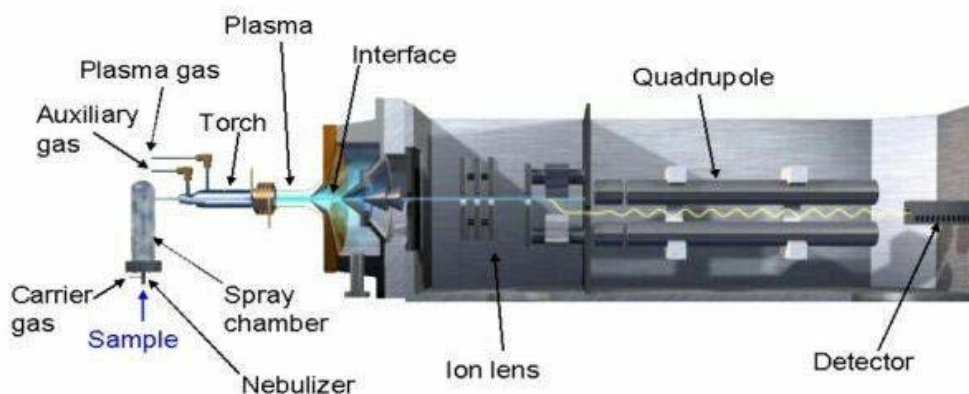


Figure 3.7. Components of an ICP-MS system.

The determination of PPi and IP₆ from the fraction obtained by SPE was carried out through ³¹P analysis of the purified extracts by ICP-MS using ⁴⁵Sc (5 µg L⁻¹) as internal standard. The ICP-MS equipment was X series II ICP-MS (Thermo Scientific, UK) and the equipment description is specified in Table 3.5. the ICP-MS work conditions were set as

follows — ICP system: RF power: 1400W; auxiliary gas flow: 0.92 L/min; coolant gas flow: 13.30 L/min; nebulizer: concentric nebulizer (Thermo) at a gas flow rate of 0.90 L/min; sample cone: nickel with 1.0 mm orifice; skimmer cone: nickel with 0.7 mm orifice; Sample introduction system: sample uptake flow rate 2ml/min; delay time: 60s; wash time: 50s (1% HCl); Data acquisition parameters: analyzer: quadrupole; scanning mode: peak jump; sweeps per reading: 30; dwell time: 10ms; number of replicates: 3.

Table 3.5. ICP-MS system employed in the determination procedure.

Equipment	ICP-MS
Models	Element XSeries 2
Manufacturer	Thermo Scientifics, UK
Laboratory of analysis	Centre Grup de Tècniques de Separació en Química (GTS),UAB, Barcelona, Spain
Image	

3.4. Results and discussion

3.4.1. Effect of defatting process and acid solvent selection

According to the food composition database published by the US Department of Agriculture, 100 g of walnuts contain 15.2 g protein, 65.2 g fat, and 6.7 g dietary fiber ⁴. That's means more than half weights of walnuts are fat (fresh weight).

The fat content can reduce the efficiency of the extraction and determination of the analytes so, it is important to defat the walnuts before any procedure and to analyze if the defatting process entails any loss of the analytes.

Since walnuts contain a lot of fat, it is important to investigate the effect of defatting on the extract process. In traditional acid extraction method procedure (AOAC), the defatted sample could extract 1.04% (dry weight) of phytic acid, while the no defatted sample could extract 1.16% of phytic acid. This phenomena also happened in the sample treated with microwave assisted extraction, it can be observed from table 3.6 that the non-defatted sample shows about 0.10% of higher content on phytic acid, which means that a small loss of the compound happened during the defatting procedure.

According to Oberleas and Harland²², fat content influences the extractability of phytate from food products and should be lowered below 5% before phytate extraction. As previously said, this kind of sample contains more than 50% weight in fat which can have an adverse effect on any posterior procedure (including SPE and ICP-MS). The organic compound from the fat could produce a lot of interferences during the phosphorous measurement by ICP-MS technique. So it is important to defat the walnuts before the extraction procedure and will be the sample used for subsequent experiment.

Table 3.6. Effect of sample defatting on the extraction of IP6 and PPI content from walnuts

<i>sample</i>	<i>extraction solvent</i>	<i>defatted</i>	<i>Extraction condition</i>	<i>Phytic acid content(% dry wt)</i>	<i>Pyrophosphate content(‰ dry wt)</i>
1	0.66M HCl	Yes	2 hours	1.04 ± 0.06	0.13 ± 0.02
2	0.66M HCl	Yes	3 hours	1.04 ± 0.02	0.15 ± 0.03
3	0.66M HCl	No	2 hours	1.16 ± 0.05	0.06 ± 0.02
4	0.66M HCl	Yes	MAE1	0.95 ± 0.02	0.07 ± 0.01
5	0.66M HCl	No	MAE1	1.07 ± 0.03	
6	0.52MH ₂ SO ₄ +0.66MHCl	Yes	MAE2	0.97 ± 0.05	0.09 ± 0.01
7	0.52MH ₂ SO ₄ +0.66MHCl	No	MAE2	1.01 ± 0.05	

MAE1: temperature set: 125 °C, hold time: 10 min; MAE2: temperature set: 50 °C, hold time: 10 min;

Results obtained by the traditional acid extraction method procedure (AOAC method) are shown in table 3.7. It is observed that after 2 hours of acid extraction the result shows no significant differences as 3 hours of extraction ($P>0.05$), although 3 hours extraction is recommended by the AOAC method. In addition, using sulphuric acid as solvent, 0.52M and 0.94M H₂SO₄ have been tested. It can be observed that 0.52M H₂SO₄ gave the same results as 0.66M HCl on IP6, while gave lower yield on PPI. In the same extraction condition, compared with 0.52M H₂SO₄, 0.94M H₂SO₄ give a lower yield on IP6 and a higher yield on PPI. So, H₂SO₄ will be also tested as acid solvent for the MAE procedure. The amount expected of phytic acid and pyrophosphate in the analyzed walnuts will be compare with 1.04% and 0.14‰ (dry weight).

Table 3.7. Study of the solvent nature on the determination of IP6 and PPI content from walnuts

<i>sample</i>	<i>extraction solvent</i>	<i>Extraction time</i>	<i>Phytic acid content(% dry wt)</i>	<i>Pyrophosphate content(‰ dry wt)</i>
1	0.66M HCl	2 hours	1.04 ± 0.06	0.13 ± 0.02
2	0.66M HCl	3 hours	1.04 ± 0.02	0.15 ± 0.03
3	0.52M H ₂ SO ₄	0.5 hour	1.04 ± 0.03	0.03 ± 0.01
4	0.52M H ₂ SO ₄	1 hour	1.05 ± 0.06	0.05 ± 0.02
5	0.94M H ₂ SO ₄	0.5 hour	0.90 ± 0.05	0.08 ± 0.02

3.4.2. Effect of pH

The complexes between phytate and mineral cations are pH sensitive. To minimize the effect of both metals and proteins some researchers treated the samples with NaOH - EDTA^{23,24}. For several minerals this complexation shows a maximum around pH 6²⁵. In that sense, the influence of adjusting the pH on the column separation was studied. pH was adjusted to 6.0 (above the isoelectric point of the proteins) just before the separation procedure (SPE).

From the results (figure 3.8) it is observed that for the no defatted sample, the pH adjustment has a significant effect ($P < 0.05$), obtaining a 0.09% higher content on phytic acid. While for the defatted samples, pH adjustment seems don't have significant difference ($P > 0.05$). Nevertheless, it is worthwhile to emphasize the fact that when the pH adjustments were carried out, the standard deviation was lower. For the defatted samples, the pH adjustment does not show a significant effect because this procedure eliminates the possible phytic acid complex²⁵. Therefore, in order to gain precision and accuracy in the final outcome, the pH of the diluted aliquot was adjusted to 6.0 with 1M NaOH just before running them through the SPE column.

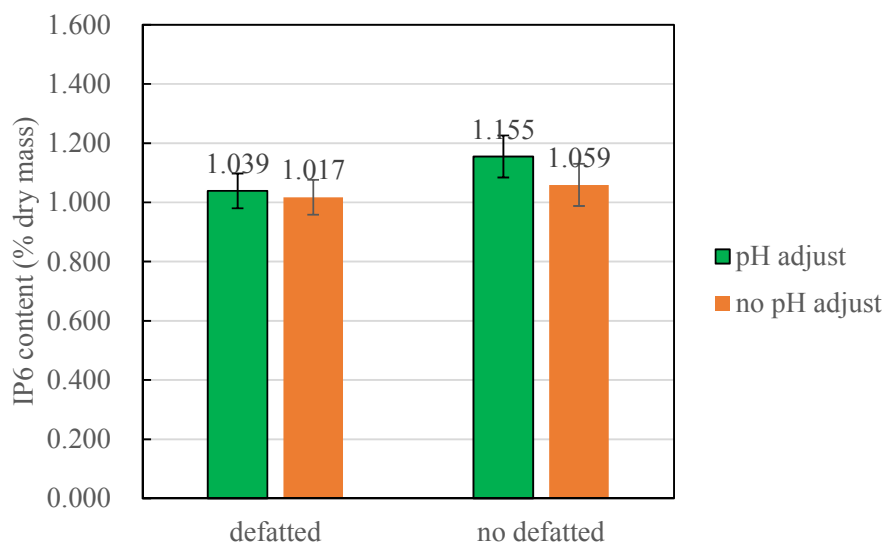


Figure 3.8. Effect of pH adjustment on separation of phytic acid from walnut

3.4.3. MAE parameters optimization

Three main parameters were considered to optimize the condition for microwave-assisted extraction: acid concentration of extracting solvent, extraction time and temperature. The results obtained by MAE will be compared with those obtained by the traditional method. As shown in table 3.8, when using the single acid as the extraction solvent, the 0.52 M H₂SO₄ shows poor extraction ability on PPi under the same condition compare with HCl. On the extract of IP6, 0.66 M HCl and 0.52 M H₂SO₄ didn't show significant different (0.925% and 0.989% respectively). While for the extraction of PPi, the use of 0.66 M HCl only recover 0.075‰ compared with the 0.145‰ of PPi obtained when using 0.52 M H₂SO₄. When temperature was raised from 100 °C to 125 °C, or increased the extraction time from 10 min to 20 min, there was a littler increase on the extraction of IP6 and PPi. Increasing the temperature to 150 °C, the extraction of IP6 was decreased and PPi was increased significantly, due to the hydrolysis of IP6 under this condition, confirmed later on by the study of the hydrolysis. The mixture acid solvent of HCl and H₂SO₄ (1:1) was also tested. It is observed that the MAE extraction by the mixture show a good recovery of both IP6 and PPi. The best extraction conditions were found to be 0.52 M H₂SO₄ + 0.66 M HCl at 100°C, 10 min irradiation time, and a solvent volume to walnut ratio of 20 ml/g.

For these conditions the hydrolysis was low (see table 3.9). Mixtures of HCl/H₂SO₄ provided results slightly higher than those determined by conventional extraction with no statistical difference ($P>0.05$) with the advantage that the extraction time decreased from 3 hours to 10 minutes. Compared with the traditional solid-solvent extraction, treatment of the walnut with MAE likely initiated cell rupture, which allowed more of the phytate and pyrophosphate compounds from the bulk to be extracted by the solvent. The dried material used for extraction contains minute traces of moisture and as microwave energy is absorbed and subsequently converted into heat, the moisture begins to evaporate. The vaporization of water generates pressure within the cell wall that eventually leads to cell rupture, thereby facilitating the leaching out of active constituents into the surrounding solvent and improving extraction efficiency and yield¹³.

Table 3.8. Study of the solvent and MAE work condition on the determination of IP6 and PPI content from walnuts

<i>sample</i>	<i>acid content of extracting solvent</i>	<i>MAE condition</i>	<i>Phytic acid content(% dry wt)</i>	<i>Pyrophosphate content(% dry wt)</i>
1	0.66M HCl	100°C 10min	0.925 ± 0.079	0.075 ± 0.021
2	0.66M HCl	125°C 10min	0.947 ± 0.018	0.070 ± 0.007
3	0.66M HCl	125 °C 20min	0.990 ± 0.029	0.094 ± 0.018
4	0.66M HCl	150°C 10min	0.706 ± 0.083	0.455 ± 0.045
5	0.52MH ₂ SO ₄	100°C 10min	0.989 ± 0.010	0.114 ± 0.018
6	0.94MH ₂ SO ₄	100°C 10min	0.977 ± 0.013	0.153 ± 0.029
7	0.52MH ₂ SO ₄ +0.66M HCl	50°C 10min	0.973 ± 0.048	0.089 ± 0.014
8	0.52MH ₂ SO ₄ +0.66M HCl	80°C 10min	1.057 ± 0.023	0.138 ± 0.021
9	0.52MH ₂ SO ₄ +0.66M HCl	100°C 10min	1.134 ± 0.081	0.145 ± 0.036
10	0.52MH ₂ SO ₄ +0.66M HCl	110°C 10min	1.138 ± 0.020	0.162 ± 0.002

3.4.4. Phytic acid hydrolysis in MAE

The possible hydrolysis of phytic acid by microwave extraction procedure has been studied under several work conditions to compare the yield of hydrolysis reaction. The MAE work condition and the hydrolysis was list in table 3.9.

Table 3.9 Yield of IP6 hydrolysis reaction^a

<i>Experiment</i>	<i>Inorganic acid</i>	<i>Concentration(M)</i>	<i>MAE condition</i>	<i>Hydrolysis (%)</i>
1	HCl	0.1	100°C 10 min	26
2	HCl	0.1	125°C 10 min	33
3	HCl	0.1	150°C 10 min	88
4	HCl	0.1	150°C 20 min	99
5	HCl	0.78	150°C 20 min	85
6	HCl	2.0	150°C 20 min	85
7	HCl	0.66	100°C 10 min	13
8	H ₂ SO ₄	0.52	100°C 10 min	7
9	H ₂ SO ₄	0.94	100°C 10 min	25

^aInitial concentration of phytic acid, 50 mg/L.

When comparing the different acid concentrations, it can be observed that the hydrolysis of phytic acid increased at lower acid concentration (see experiment 1, 7; 4-6; 8-9), in agreement with the known fact that the absorption of radiation of aqueous acid solutions is more effective at lower acid concentrations. The kinetics of heteropoly acid formation was affected by acidity conditions. Generally the fact is the higher the acid concentration, the faster the reaction. As expected, when comparing at the same molar concentration in acid, it can be observed that at higher temperature higher hydrolysis is observed (see experiments 1-3). The proposed hydrolysis of phytic acid can be compared with other reported hydrolysis method. When hydrolysis is carried out at 120 °C in 2 M HCl, 24 hours is necessary to reach quantitative hydrolysis²⁶. In our case, at the MAE condition of 150 °C in 0.1 M HCl, 99% of phytic acid was hydrolyzed in 10 min. When comparing the different

inorganic acid at the same microwave treatment conditions, it can be observed that 0.52 M H₂SO₄ gave lower yield of hydrolysis, following by 0.66 M HCl and 0.94 M H₂SO₄. For the purpose of extract phytic acid from walnuts, it is obligate to control the hydrolysis in an accept range. To minimize the hydrolysis of phytic acid in the MAE process, temperature of 100°C during 10 min were recommended.

3.4.5. Walnuts as a functional food

In the last decades consumer demands in the field of food production has changed considerably. Consumers more and more believe that foods contribute directly to their health. Today foods are not intended to only satisfy hunger and to provide necessary nutrients for humans but also to prevent nutrition-related diseases and improve physical and mental well-being of the consumers. The increasing demand on such foods can be explained by the increasing cost of healthcare, the steady increase in life expectancy, and the desire of older people for improved quality of their later²⁷.

The European Commission's Concerted Action on Functional Food Science in Europe (FuFoSE), coordinated by International Life Science Institute (ILSI) Europe defined functional food as follows: 'a food product can only be considered functional if together with the basic nutritional impact it has beneficial effects on one or more functions of the human organism thus either improving the general and physical conditions or/and decreasing the risk of the evolution of diseases. The amount of intake and form of the functional food should be as it is normally expected for dietary purposes. Therefore, it could not be in the form of pill or capsule just as normal food form²⁸.

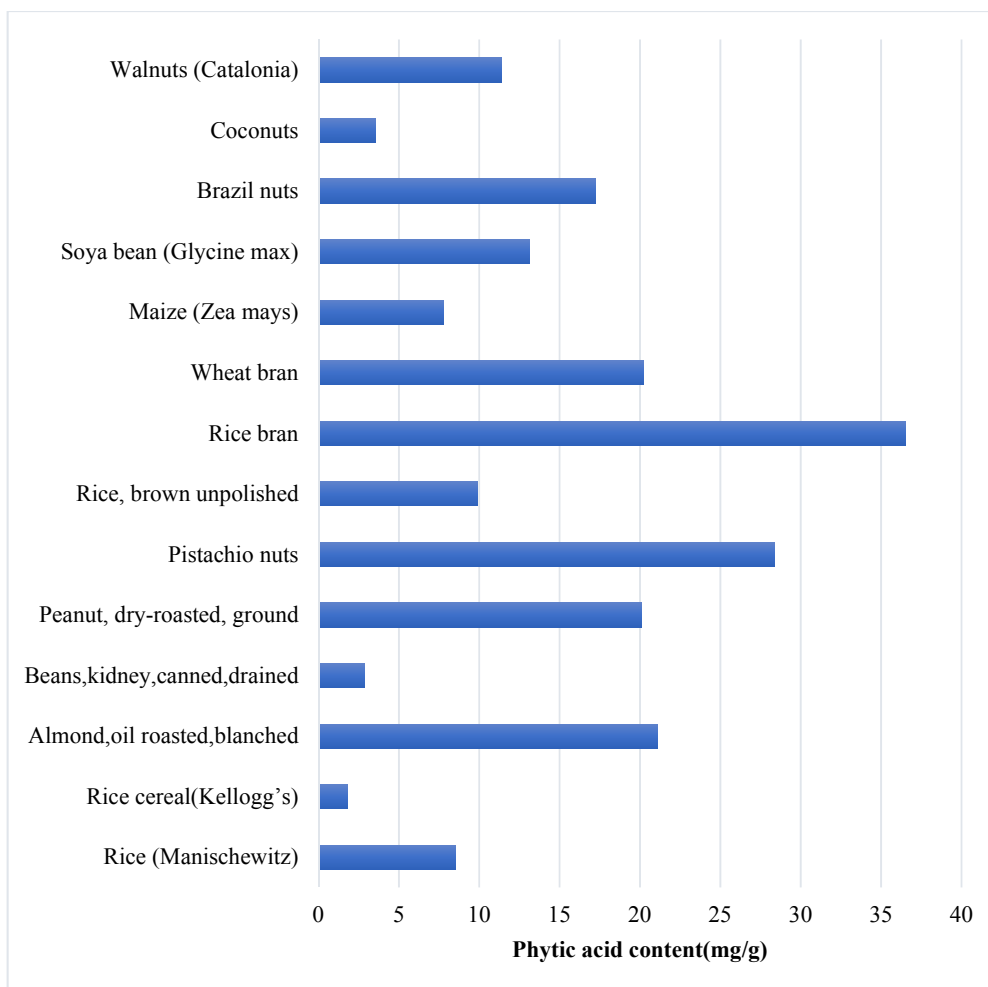


Figure 3.9. IP6 content of selected foods^{29,30,31}

In developing country situations where cereals and other plant-based foods provide a large proportion of the food consumption, the dietary phytate intake will be greater. Although dietary phytate has been ascribed as a potential way to reduce the risk of mineral deficiency, it exhibits beneficial health effects, such as protection against a variety of cancer and heart-related diseases, diabetes mellitus and renal stones. Pharmaceutical preparations containing phytic acid are used to treat relapsed urolithiasic patients¹⁹. These beneficial health effects are more significant for people from developed countries because of the higher incidence of cancer which is associated with higher fat and lower fibre-rich food intakes. Such populations generally do not suffer from mineral deficiencies³². Walnuts contains less phytate than other nuts, such as peanut and almond, and rich in polyunsaturated fatty acids, which make it is valuable to develop functional food based on it.

3.5. Conclusions

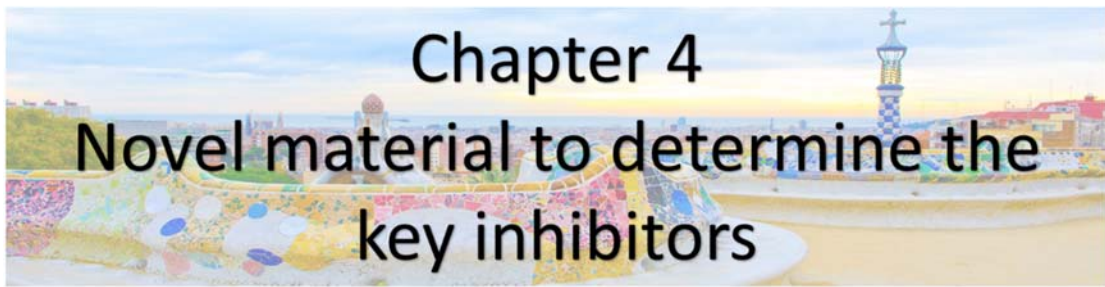
MAE proved to be an attractive alternative to conventional extraction methods, such as solid-liquid extraction, for the removal of phytic acid and pyrophosphate from walnuts. The predicted level of total phytic acid extracted with the MAE procedure was similar to those obtained from the traditional procedures reported in previous works. The extraction time required for optimal recovery of total phytic acid and pyrophosphate using MAE was significantly less than that required by traditional extraction techniques, thereby showing MAE to be a more rapid and efficient method of extraction. The development of a microwave-assisted extraction method for application in analyzing the concentration of total phytic acid and pyrophosphate may aid in increasing the healthy market potential for walnuts.

3.6. reference

1. Sabate, J.; Fraser, G. E.; Burke, K.; Knutsen, S. F.; Bennett, H.; Lindsted, K. D., Effects of walnuts on serum lipid levels and blood pressure in normal men. *New England Journal of Medicine* **1993**, *328* (9), 603-607.
2. Amaral, J. S.; Casal, S.; Pereira, J. A.; Seabra, R. M.; Oliveira, B. P., Determination of sterol and fatty acid compositions, oxidative stability, and nutritional value of six walnut (*Juglans regia* L.) cultivars grown in Portugal. *Journal of Agricultural and Food Chemistry* **2003**, *51* (26), 7698-7702.
3. Harper, C. R.; Jacobson, T. A., The fats of life: the role of omega-3 fatty acids in the prevention of coronary heart disease. *Archives of Internal Medicine* **2001**, *161* (18), 2185-2192.
4. Banel, D. K.; Hu, F. B., Effects of walnut consumption on blood lipids and other cardiovascular risk factors: a meta-analysis and systematic review. *The American journal of clinical nutrition* **2009**, *90* (1), 56-63.
5. (a) Vucenik, I.; Shamsuddin, A. M., Protection against cancer by dietary IP6 and inositol. *Nutrition and cancer* **2006**, *55* (2), 109-125; (b) Rizvi, I.; Riggs, D. R.; Jackson, B. J.; Ng, A.; Cunningham, C.; McFadden, D. W., Inositol Hexaphosphate (IP6) Inhibits Cellular Proliferation In Melanoma. *Journal of Surgical Research* **2006**, *133* (1), 3-6; (c) Somasundar, P.; Riggs, D. R.; Jackson, B. J.; Cunningham, C.; Vona-Davis, L.; McFadden, D. W., Inositol Hexaphosphate (IP6): A Novel Treatment for Pancreatic Cancer¹. *Journal of Surgical Research* **2005**, *126* (2), 199-203.
6. Grases, F.; Isern, B.; Sanchis, P.; Perello, J.; Torres, J. J.; Costa-Bauza, A., Phytate acts as an inhibitor in formation of renal calculi. *Front Biosci* **2007**, *12* (1), 2580-7.
7. Terkeltaub, R. A., Inorganic pyrophosphate generation and disposition in pathophysiology. *American Journal of Physiology-Cell Physiology* **2001**, *281* (1), C1-C11.
8. Sharma, S.; Vaidyanathan, S.; Thind, S.; Nath, R., Urinary excretion of inorganic pyrophosphate by normal subjects and patients with renal calculi in north-western India and the effect of diclofenac sodium upon urinary excretion of pyrophosphate in stone formers. *Urologia internationalis* **1992**, *48* (4), 404-408.
9. Breslau, N. A.; Padalino, P.; Kok, D. J.; Kim, Y. G.; Pak, C. Y., Physicochemical effects of a new slow - release potassium phosphate preparation (UroPhos - K) in absorptive hypercalciuria. *Journal of Bone and Mineral Research* **1995**, *10* (3), 394-400.
10. Ray, P.; Shang, C.; Maguire, R.; Knowlton, K., Quantifying phytate in dairy digesta and feces: Alkaline extraction and high-performance ion chromatography. *Journal of dairy science* **2012**, *95* (6), 3248-3258.
11. Li, H.; Deng, Z.; Wu, T.; Liu, R.; Loewen, S.; Tsao, R., Microwave-assisted extraction of phenolics with maximal antioxidant activities in tomatoes. *Food Chemistry* **2012**, *130* (4), 928-936.
12. Eskilsson, C. S.; Björklund, E., Analytical-scale microwave-assisted extraction. *Journal of Chromatography A* **2000**, *902* (1), 227-250.
13. Ballard, T. S.; Mallikarjunan, P.; Zhou, K.; O'Keefe, S., Microwave-assisted extraction of phenolic antioxidant compounds from peanut skins. *Food Chemistry* **2010**, *120* (4), 1185-1192.

14. Abu-Samra, A.; Morris, J. S.; Koirtiyohann, S., Wet ashing of some biological samples in a microwave oven. *Analytical chemistry* **1975**, *47* (8), 1475-1477.
15. Routray, W.; Orsat, V., Microwave-assisted extraction of flavonoids: a review. *Food and Bioprocess Technology* **2012**, *5* (2), 409-424.
16. Australian Radiation Protection and Nuclear Safety Agency Radiation Basics - Ionising and Non Ionising Radiation. http://www.arpana.gov.au/radiationprotection/basics/ion_nonion.cfm (accessed 15 June).
17. Thuéry, J., *Microwaves: industrial, scientific, and medical applications*. Artech House on Demand: 1992.
18. Saad, N.; Mohd Esa, N.; Ithnin, H.; Shafie, N. H., Optimization of optimum condition for phytic acid extraction from rice bran. *African Journal of Plant Science* **2011**, *5* (3), 168-176.
19. March, J.; Grases, F.; Salvador, A., Hydrolysis of phytic acid by microwave treatment: Application to phytic acid analysis in pharmaceutical preparations. *Microchemical journal* **1998**, *59* (3), 413-416.
20. AOAC office method 986.11, final action 1988. *Association of Official Analytical Chemists, Arlington, VA, USA*.
21. Munoz, J. A.; Lopez-Mesas, M.; Valiente, M., Minimum handling method for the analysis of phosphorous inhibitors of urolithiasis (pyrophosphate and phytic acid) in urine by SPE-ICP techniques. *Analytica chimica acta* **2010**, *658* (2), 204-8.
22. Oberleas, D.; Harland, B., *Analytical methods for phytate*. **1986**.
23. Bos, K. D.; Verbeek, C.; Van Eeden, C. P.; Slump, P.; Wolters, M. G., Improved determination of phytate by ion-exchange chromatography. *Journal of Agricultural and Food Chemistry* **1991**, *39* (10), 1770-1772.
24. Harland, B. F.; Oberleas, D., Anion-exchange method for determination of phytate in foods: collaborative study. *Journal-Association of Official Analytical Chemists* **1985**, *69* (4), 667-670.
25. Fruhbeck, G.; Alonso, R.; Marzo, F.; Santidrián, S., A modified method for the indirect quantitative analysis of phytate in foodstuffs. *Analytical biochemistry* **1995**, *225* (2), 206-212.
26. áde Koning, A. J., Determination of myo-inositol and phytic acid by gas chromatography using scyllitol as internal standard. *Analyst* **1994**, *119* (6), 1319-1323.
27. Siro, I.; Kapolna, E.; Kapolna, B.; Lugasi, A., Functional food. Product development, marketing and consumer acceptance—A review. *Appetite* **2008**, *51* (3), 456-467.
28. Action, E. C., Scientific concepts of functional foods in Europe: consensus document. *British Journal of Nutrition* **1999**, *81* (1).
29. Harland, B. F.; Smikle-Williams, S.; Oberleas, D., High performance liquid chromatography analysis of phytate (IP6) in selected foods. *Journal of Food Composition and Analysis* **2004**, *17* (2), 227-233.
30. Ravindran, V.; Ravindran, G.; Sivalogan, S., Total and phytate phosphorus contents of various foods and feedstuffs of plant origin. *Food Chemistry* **1994**, *50* (2), 133-136.

31. Macfarlane, B. J.; Bezwoda, W. R.; Bothwell, T. H.; Baynes, R. D.; Bothwell, J. E.; MacPhail, A. P.; Lamparelli, R. D.; Mayet, F., Inhibitory effect of nuts on iron absorption. *The American journal of clinical nutrition* **1988**, *47* (2), 270-274.
32. Kumar, V.; Sinha, A. K.; Makkar, H. P. S.; Becker, K., Dietary roles of phytate and phytase in human nutrition: A review. *Food Chemistry* **2010**, *120* (4), 945-959.



Chapter 4
**Novel material to determine the
key inhibitors**

4. Novel material to determine the key inhibitors

4.1. Introduction

Phytic acid (myoinositol hexaphosphate, IP₆) is a naturally occurring compound that is abundantly found in grains, cereals, nuts, and foods that are high in fiber content. It is claimed to have the ability to enhance the anticancer effect of conventional chemotherapy and control cancer metastases^{1,2}. In addition, phytic acid acts as an effective inhibitor of calcium salts crystallization in urine and soft tissues, and prevents the formation of kidney stones (urolithiasis)³.

Inorganic pyrophosphate (PPi), can inhibit the formation of several crystallization reactions as for example the formation of calcium oxalate and hydroxyapatite, chemical composition of the 80% of kidney stones, serving so as natural inhibitor of urolithiasis⁴. In lithiasic patients, lower urinary PPi has been reported⁵ and its intake increase has been recommended⁶ as therapy. Thus, the determination of levels of both natural lithiasic inhibitors, IP₆ and PPi, in urine is of interest for its healthy use.

The growing interest in the biomedical implications of phytic acid and pyrophosphate and the inherent problems with its poor separation are reflected in the tedious analytical techniques actually described and used in many laboratories. The quantitative extraction of phytate and pyrophosphate from urine is not selective and always co-extract with cations, protein, or other nutrients leading to erroneous estimation, damage to the analytical instruments, or both⁷.

For the determination of phytic acid, many methods have been developed. The frequently used measurement techniques include colorimetric method⁸, HPLC^{9,10,11,12}, HPIC¹³, ³¹P NMR spectroscopy¹⁴, synchronous fluorescence method¹⁵, inductively coupled plasma mass spectrometry (ICP-MS)¹⁶, and IPC-ICP-MS¹⁷. Indirect determination of phosphate after hydrolysis has been also used for the analysis of pharmaceutical formulations¹⁸. The traditional procedures employed for PPi determination are mainly based in chemical¹⁹ and enzymatic methods²⁰. Method including either chromatographic²¹ or electrophoretic²²

separation of PPI have also been reported. A method for the determination of IP₆ and PPI in urine by SPE-ICP-MS techniques was developed in our laboratory achieving a simple and easy measurement to simultaneously analyze IP₆ and PPI²³. But a non-laborious method for the extraction and purification from a fatty sample has not been developed.

4.1.1. Molecularly Imprinted Polymer (MIP)

Molecular Imprinting Technology (MIT) is today a viable synthetic approach to design robust molecular recognition materials able to mimic natural recognition entities, such as antibodies and biological receptors²⁴.

Molecular imprinted polymer (MIP) is prepared with a reaction mixture composed of the target analyte (the molecular template), a functional monomer (or two), a cross-linking monomer (or two), a polymerization initiator in a solvent²⁵. The functional monomers initially form a complex with the template molecule, and the complex is surrounded by the surplus cross-linking monomer, yielding a three-dimensional polymer network where the template molecules are trapped after completion of polymerization. By thorough washing, the template molecules are eliminated to leave cavities complementary to the template in size, shape, and molecular interactions. In that way, a molecular memory is introduced into the polymer, which is now capable of rebinding the analyte with a very high specificity²⁶. In essence, a molecular “memory” is imprinted on the polymer, which is now capable of selectively rebinding the template²⁷. Usually, intermolecular interactions like hydrogen bonds, dipole–dipole and ionic interactions between the template molecule and functional groups present in the polymer matrix drive the molecular recognition phenomena. Thus, the resultant polymer recognizes and binds selectively only the template molecules²⁴.

The main advantages of molecularly imprinted polymers (MIPs) are their high selectivity and affinity for the target molecule used in the imprinting procedure. Imprinted polymers compared to biological systems such as proteins and nucleic acids, have higher physical robustness, strength, resistance to elevated temperature and pressure and inertness towards acids, bases, metal ions and organic solvents. In addition, they are also less expensive to

be synthesized and the storage life of the polymers can be very high, keeping their recognition capacity also for several years at room temperature²⁴.

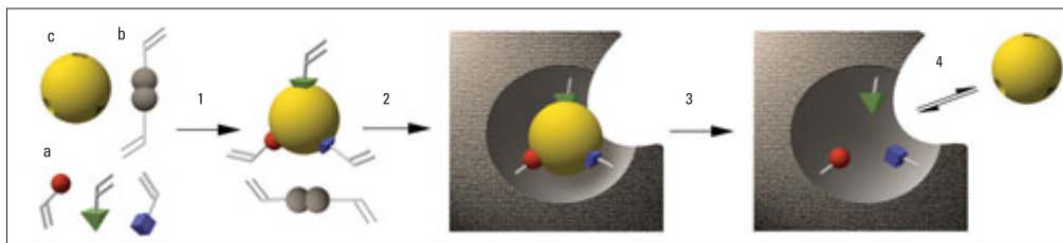


Figure 4.1. Creating a molecular imprint in a synthetic polymer²⁷.

(a) Functional monomers, (b) a cross-linker, and (c) a template molecule are mixed together. (1) The functional monomers form a complex with the template molecule. (2) The functional monomers copolymerize with the cross-linker. (3) As polymerization proceeds, an insoluble, highly cross-linked polymeric network is formed around the template. (4) Removing the template liberates complementary binding sites that can reaccommodate the template in a highly selective manner.

The schematic illustration of MIP formation is given in Fig. 4.1. Reaction conditions such as formulation of MIP reaction mixture including choice of cross-linking monomer, functional monomer, and porogenic solvent, reaction temperature, and time altogether govern the properties, physical appearance, morphology, and performance of MIP²⁵.

4.1.2. MIP preparation method

4.1.2.1. Monomer

Typical functional monomers are carboxylic acids (acrylic acid, methacrylic acid, vinylbenzoic acid), sulphonic acids (2-acrylamido-2-methylpropane sulphonic acid), heteroaromatic bases (vinylpyridine, vinylimidazole). In the non-covalent approach they are normally used in excess compared to the template to favor the formation of template-monomer assemblies. In fact, association between the monomer and the template is governed by an equilibrium, and the functional monomers normally have to be added in

excess, relative to the number of moles of the template to favor the formation of the complex. Consequently, this led to a number of different configurations of the template-functional monomer complex, which produced a heterogeneous binding site distribution in the final MIP, with a range of affinity constants. The best monomers for synthesizing imprinted materials are selected considering strength and nature of template-monomer interactions²⁴.

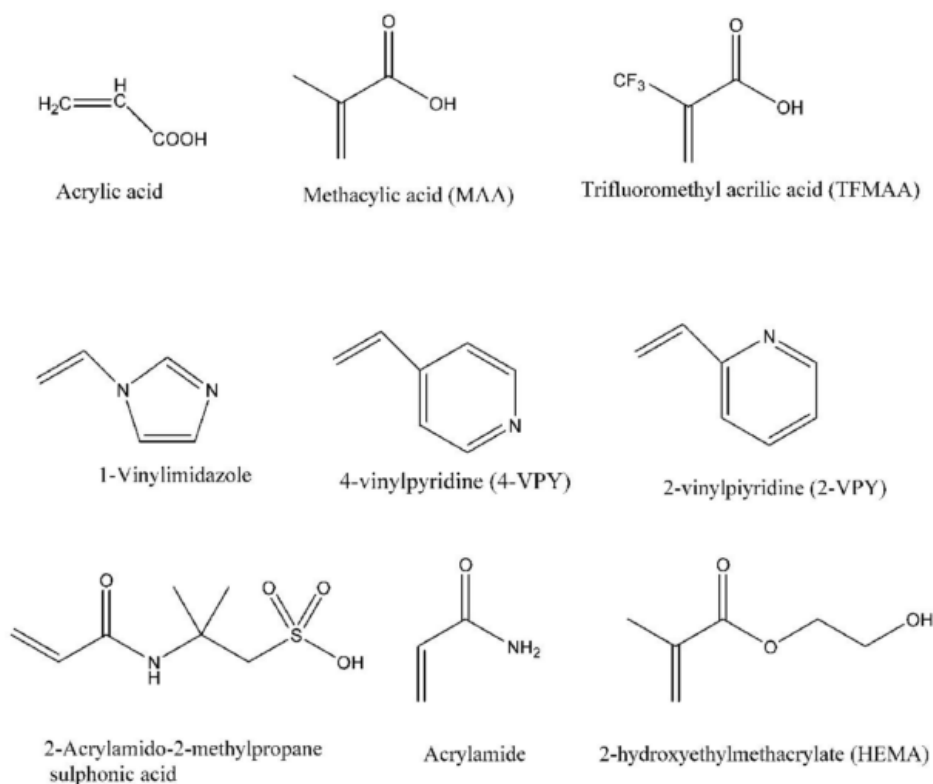


Figure 4.2. Structure of the most common monomers used for molecular imprinting

4.1.2.2. Cross-linker

In imprinted polymers synthesis, the cross-linker also fulfils important functions. The cross-linker is important in controlling the morphology of the polymer matrix, serves to stabilize the imprinted binding sites and imparts mechanical stability to the polymer matrix in order to retain its molecular recognition capability. Different cross-linkers have been used (Figure 4.3). High cross-link ratios are generally used in order to access permanently

porous (macroporous) materials with adequate mechanical stability. Ethylene glycol dimethacrylate (EGDMA) and trimethylolpropane trimethacrylate (TRIM) are the most commonly employed. Some authors found that cross-linker has a major impact on the physical characteristics of the polymers and much less effect on the specific interactions between the template and functional monomers (37,50,51)²⁴.

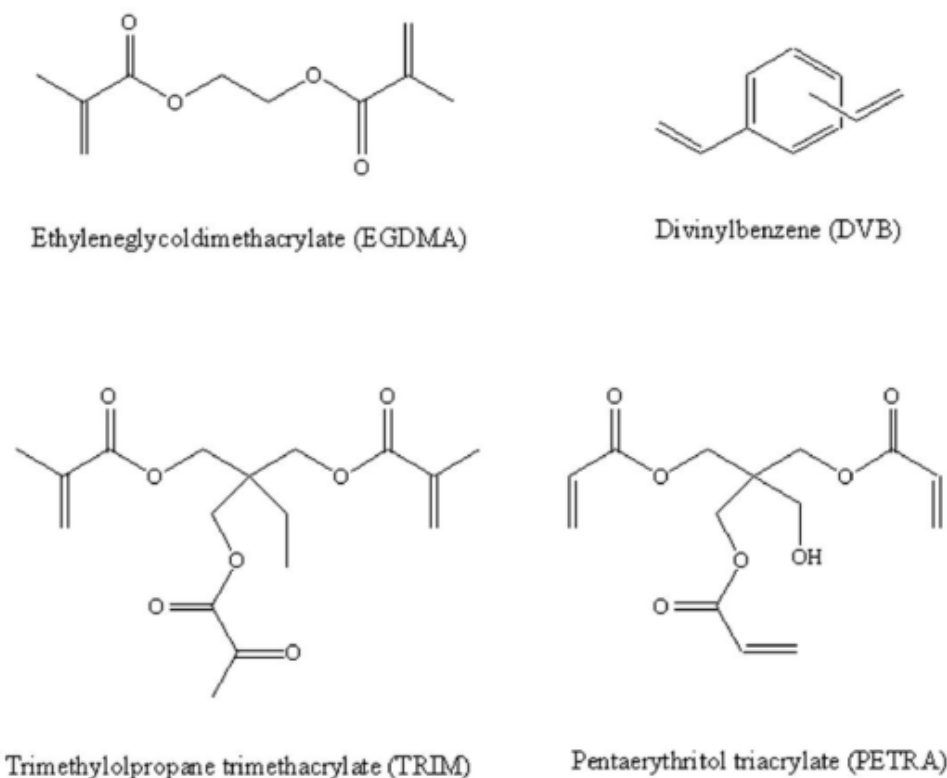


Figure 4.3. Structure of the most common cross-linkers used for molecular imprinting

4.1.2.3. Solvent or porogen

The solvent (or porogen) serves to bring all the components (monomer, template, initiator, and cross-linker) into one phase in the polymerization and it is responsible for creating the pores in macroporous polymers. The most common solvents used for MIPs synthesis are listed in table 4.1. The solvent should produce large pores to assure good flow through properties of the resultant MIP and increasing the volume of the solvents, the pore volume of the polymer enlarges. The porogen in a non-covalent imprinting polymerization should

also be chosen considering its role in promoting template-functional monomer complex formation: less polar solvents increase the complex formation facilitating polar non-covalent interactions such as hydrogen bonds; more polar solvents tend to dissociate the non-covalent interactions in the prepolymer complex. However in some papers efficient MIPs have been prepared in rather polar solvents (e.g., acetonitrile/water or methanol/water) since strong template-monomer interactions have been observed. Usually apolar, non-protic solvents, such as toluene or chloroform, are preferred in MIPs synthesis whereas, if hydrophobic forces are involved in the complexation process, water or other protic solvents could be selected as well²⁴.

Table 4.1. Type of solvent used for molecularly imprinted polymer²⁸

Type of solvent	solvent	Relative permittivity	Boiling point	references
Non-polar solvents	Toluene	2.379	110.6	29, 30
	chloroform	4.8069	61.1	31
Polar aprotic solvents	THF	7.52	65	32
	1,2-dichloroethane	10.10	83.5	
	Dichloromethane	9.08	39.6	33
	Acetonitrile	36.64	81.6	34, 35,36
Alcohols	Isopropanol	20.18	82.3	
	ethanol	25.3	78.2	
	methanol	33.0	64.4	
Mixture of solvents				
	Water/ethanol (3/1 v/v)			37
	Methylethyl ketone/heptane			35
	ACN/toluene			38
	Water/methanol(1/4,v/v)			39

4.1.3. Synthesis of MIP

4.1.3.1. Basic principle and approaches for the synthesis of MIP

Depending on the nature of adducts between templates and functional monomers, three different approaches for the synthesis of MIPs have been reported: covalent, semi-covalent and non-covalent.

- a) Covalent imprinting uses reversible covalent bonds to give specific binding sites. The functional monomer and the template are bound to each other by covalent linkage prior to polymerization. The high stability of the template-monomer conjugates leads to a rather homogenous population of binding sites, minimizing the occurrence of non-specific sites. But, the difficulty in designing an reversible covalent bonds and the synthesis is often troublesome and less economical make this approach rather restrictive⁴⁰.
- b) Finally, the non-covalent approach was based on the formation of non-covalent interactions (e.g., hydrogen bonding, coordination-bond formation and electrostatic interaction) between template molecule and selected monomers before polymerization. The procedure is quite simple and a wide variety of monomers are commercially available. This approach is by far the most used for the preparation of MIPs⁴¹.
- c) The semi-covalent approach is a hybrid of the two previous approach. The template is covalently bound to a functional monomer before polymerization, but once the templates have been removed, the rebinding of the analyte is based only on non-covalent interactions⁴².

4.1.4. Polymerization techniques

Commonly used polymerization technique for MIP preparation include bulk polymerization, suspension polymerization, emulsion polymerization, multistep swelling polymerization, and precipitation polymerization. Because of its simplicity, bulk polymerization and precipitation polymerization has become very attractive for preparation of MIP³⁵.

4.1.4.1. Bulk polymerization method

Bulk polymerization is a very convenient and easy way to produce MIPs. No particular skills or sophisticated equipment are required⁴³. For these reasons, it is extensively used for the preparation of MIPs. Except when the polymerization is realized in a column in order to use the materials in their monolithic form, the bulk materials usually need to be crushed, ground and sieved to obtain particles of the desired dimensions. Figure 4.4 shows the prepare process of MIP by bulk polymerization method. This process is tedious and time-consuming with usually less than 50% of the ground polymer being recovered. The irregular size and shape of the particles are not favorable for many chromatographic and separation applications. Moreover, some binding sites can be destroyed during the grinding which leads to a considerable loss of loading capacity of the MIPs²⁸.

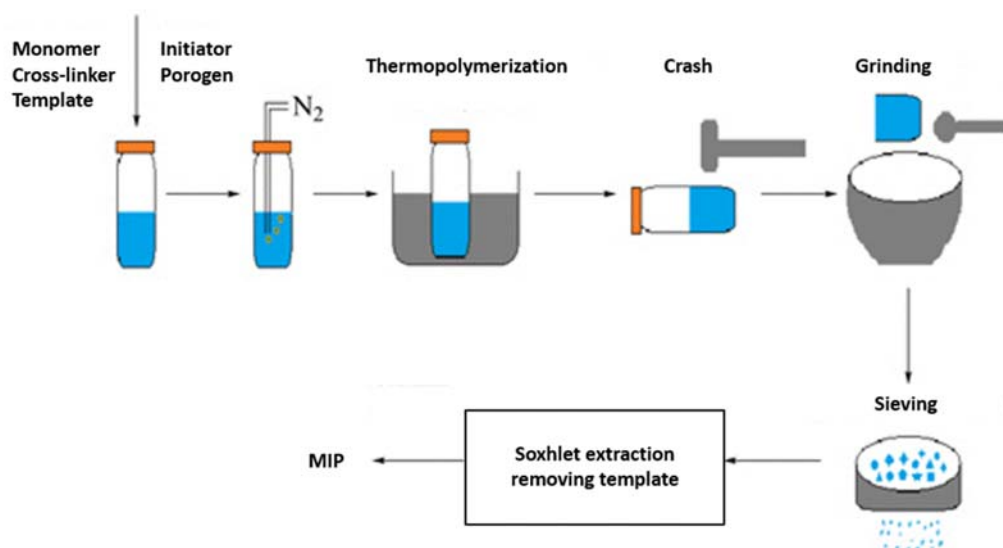


Figure 4.4. schematic representation of MIP preparation by bulk polymerization⁴⁴

4.1.4.2. Precipitation polymerization method

There have been many different synthetic approaches developed to overcome the irregular size and shape of the imprinted particles produced by bulk polymerization. The most streamlined protocol is precipitation polymerization, which produces spherical particles in a single preparative step within the normally used range of particle size for SPE

applications. This kind of polymerization uses a process in which all the components involved in the synthesis of the polymer are highly diluted within a solvent (or a mixture of two solvents). Not only must this solvent be able to solubilize all the components involved in the polymerization process at the temperature of polymerization but also, as the polymeric chains grow, to be able to solubilize this polymer too, but only to certain extent. Once the polymer reaches a certain critical mass, this solvent is no longer able to hold the polymeric chain in solution, thus precipitating the particles off the solution.

Interest in molecularly imprinted polymer technique has increased significantly over the past few years as a result of its inherent advantages over more traditional extraction techniques⁴⁵. The main advantages of MIPs are their high affinity and selectivity for the target molecule (template). MIPs have higher physical strength, robustness, resistance to elevated pressure and temperature and inertness against various chemicals (organic solvents, acids, bases, and metal ions) compared to biological media such as proteins and nucleic acids. Furthermore, their production costs are low and their lifetimes can be as long as several years at room temperature²⁵.

It has been demonstrated in many cases that MIP adsorption is an effective method to extract and separate compounds from matrix, but only few papers about IP6 separation using MIP were published, and the separation of PPI using the MIP adsorbent has also hardly been reported. Furthermore, the MIP mentioned above were prepared using methacrylic acid (MAA) as functional monomer and thus these MIP could not exhibit high selectivity for phytic acid.

4.2. Experimental

4.2.1. Reagents:

Compounds used for the synthesis of MIP and the non-imprinted polymer (NIP) were:

- N-Allylthiourea(AT) used as functional monomer,
- Methacrylic acid (MAA) used as functional monomer

- ethyleneglycol dimethacrylate (EGDMA) as crosslinker,
- phenylphosphonic acid as template molecule,
- pyrophosphoric acid as template molecule
- Di-(2-ethylhexyl) phosphoric acid (DEHPA) as template molecule.
- N, N'-Methylenebisacrylamide (MBAm), as crosslinker

All these compounds were purchased from Sigma-Aldrich (Steinheim, Germany).

- 2, 2'-azobisisobutyronitrile (AIBN), from Acros Organics (Geel, Belgium), was used as the free radical initiator.
- Myoinositol hexaphosphoric acid hexasodium salt from corn (Sigma, Steinheim, Germany),
- Acetonitrile (ACN) (Merck, Germany)
- hydrochloric acid (J.T. Baker, Deventer, Holland)
- sodium dihydrogen phosphate (Panreac, Barcelona, Spain)

All chemicals used were of analytical-reagent grade.

Purified Milli-Q water of 18mΩ-cm resistivity was used for the preparation of all reagents.

4.2.2. Preparation of Molecular Imprinted Polymer

4.2.2.1. Polymer of N-allylthiourea


The MIP synthesized using as functional monomer N-allylthiourea was prepared following the literature³⁴ with a few modification. A certain amount of template (0.5mmol or 1 mmol), the functional monomer N-Allylthiourea (464.8mg, 4.0mmol), and cross-linker EGDMA (3.96g, 20mmol) were dissolved in ACN (4.0mL). The preassembly solution was degassed in a sonicating bath for 5 min to get the prepolymerization solution. After sonication, AIBN (30mg, 0.18mm) was added into the prepolymerization solution as an initiator, purged with nitrogen for 10 min and sealed. The polymerization was carried out in a thermostatic water bath at 60 °C for 16 h, followed by heating at 80 °C for 3 h under nitrogen atmosphere. After the polymerization process, the obtained polymer was ground and sieved to yield a particle size of 50-100µm. In order to remove the template molecules, the polymer particles

were washed. To do so, the polymer was placed in a Soxhlet apparatus and washed with water/acetic acid (4:1, v/v) for 24 h, and then with ethanol for 24 h more. The polymer was washed to elute the template and then complete elution of template was confirmed from the eluent by ICPMS. As a reference, non-imprinted polymer (NIP), was prepared in parallel to the MIP by using the same procedure without addition of template.

4.2.2.2. Polymer of MAA

As previously, the MIP synthesized using as functional monomer MAA was prepared following the literature with modification³⁷. A certain amount of template (phytic acid, 0.5-1mmol), the functional monomer (MAA, 5-16mmol), cross-linker (MBAm, EGDMA, or MBA+ ACM) were dissolved in suitable porogenic solvent and ammonium persulfate as an initiator added. The reaction mixture was degassed in a sonicating bath for 20 min, purged with nitrogen for 10 min and sealed. The polymerization was carried out in a thermostatic water bath (see table 4.2) at 40 °C for 24 h. The polymer was ground and sieved to yield a particle size of 28-75µm. To wash the polymer, it was placed in a Soxhlet apparatus and washed with water/acetic acid (4:1, v/v) for at least 48 h, followed by water for others 48 hours and then ethanol 48 h more. Non-imprinted polymer (NIP) was prepared in parallel to the MIP by using the same procedure, in order to use it as a reference. The polymer was washed to elute the template and then complete elution of template was confirmed from the eluent by ICPMS. The particles were dried under vacuum at 40°C overnight and then used for further studies. Obtained creamy mixture was then processed in the same way as for the creamy extract obtained by microwave extraction.


Table 4.2 Heating system employed in the polymerization procedure.

Equipment	Heater
Models	CE 2000 ABT-4
Manufacturer	SBS Instruments SA, Barcelona, Spain
Laboratory of analysis	Centre Grup de Tècniques de Separació en Química (GTS),UAB, Barcelona, Spain
Image	

4.2.2.3. Soxhlet extraction

In order to validate the results, the traditional solid-solvent extraction method from the AOAC office method 986.11²⁰ was followed. 0.66 M HCl used as extraction solvents. The extraction was carried out at room temperature with constant shaking at medium speed in an orbital mixer for 3 hours. The equipment description is specified in Table 4.3. The obtained creamy mixture was then processed in the same way as for the creamy extract obtained by microwave extraction.

Table 4.3 Soxhlet system employed in the extraction procedure.

Equipment	Soxhlet
Manufacturer	SBS Instruments SA, Barcelona, Spain
Laboratory of analysis	Centre Grup de Tècniques de Separació en Química (GTS), UAB, Barcelona, Spain
Image	

4.2.3. Batch mode studies

The experimental parameters affecting the adsorption of IP₆ such as pH, contact time, initial concentration of IP₆ and temperature were studied in batch mode. Stock solutions (IP₆, PPI and P) were prepared by dissolving the reagents in Mill-Q water. 10mg of sorbent (MIPs or NIPs) was dispersed in standard solution of corresponding analyte (2 mL). The system was properly shaken on a rotary mixer at 25 rpm. After the desired time, MIPs and NIPs were isolated through 0.22µm Millipore filters (Millex-GS, Millipore, Ireland), and the concentration of analytes in the solvent phase was determined by ICP-MS.

4.2.3.1. Influence of the initial pH

The effect of initial pH on the equilibrium uptake of analytes (IP₆, PPI and P) was investigated in the pH range from 1.0 to 6.0. The solution pH was adjusted by the addition of 0.1 M HCl or 0.1 M NaOH, alternatively. In this study, each initial analyte concentration is 25 µM. 2 ml of this solution, at each selected pH, was agitated by a rotary mixer with 10 mg of MIP for 1 hour. The temperature was conducted at 20°C.

4.2.3.2. Influence of temperature

In order to study the temperature effect on the adsorption capacity of MIP, batch experiment also did at different temperatures (20°C, 50°C and 70°C). Experiments are all conducted at pH 4.0, and other conditions were kept equal as mentioned above.

4.2.4. Isotherm studies

Adsorption isotherm is critical to evaluate the sorption capacity of adsorbents as well as understand the sorbate–sorbent interactions. Two commonly used model, the Langmuir and Freundlich⁴⁶ equations were used to describe the experimental data of adsorption isotherms.

The Langmuir isotherm model can be expressed by the following equation:

$$Q_e = \frac{Q_m K_L C_e}{1 + K_L C_e} \quad (4-1)$$

Where C_e is the equilibrium concentration ($\mu\text{mol L}^{-1}$) of adsorbate in solution, Q_e represents the amount of IP₆ adsorbed at equilibrium ($\mu\text{mol g}^{-1}$), Q_m is the maximum adsorption capacity and K_L is the Langmuir constants related to adsorption capacity and energy of adsorption.

The Freundlich isotherm model is given as follows:

$$Q_e = K_F C_e^{1/n} \quad (4-2)$$

Where K_F is a constant representing the adsorption capacity ($\mu\text{mol g}^{-1}$), and n is a constant depicting the adsorption intensity.

To carry out the assays, 10 mg of MIP or NIP were added to 2 ml aqueous solution of phytic acid in the range of 0-100 μM of different concentrations and stirred for 1 hour at room temperature. The polymer particles were filtered off and filtrate was analyzed for phytic acid by ICP-MS. The quantity of phytic acid bounded was determined by subtracting the equilibrium amount of the compound to the initial measured quantity. The experimental binding data were fitted to the Langmuir-Freundlich (L-F) adsorption models.

4.2.5. Kinetics studies

The pseudo-first-order kinetic model can be generally described in the following equation:

$$\ln(q_{eq} - q_t) = \ln Q_e - k_1 t \quad (4-3)$$

Where q_{eq} and q_t are the amounts (mmol/g) of adsorbed analytes on the imprinted polymer at equilibrium and at time t , respectively. k_1 is the first order rate constant (1/min).

The pseudo-second-order kinetic model is expressed by Eq. (4-4).⁴⁷

$$dq_t/dt = k_2 (q_{eq} - q_t)^2 \quad (4-4)$$

where q_{eq} is the sorption capacity at equilibrium and q_t is the loading of the compound at time t . k_2 ($\text{g mg}^{-1} \text{h}^{-1}$) represents the pseudo-second-order rate constant for the kinetic model. By integrating Eq. (4-4) with the boundary conditions of $q_t=0$ at $t=0$ and $q_t=q_t$ at $t=t$, the following linear equation can be obtained:

$$\frac{t}{q_t} = \frac{1}{V_0} + \frac{1}{q_{eq}} t \quad (4-5)$$

$$V_0 = k_2 q_{eq}^2 \quad (4-6)$$

Where V_0 ($\text{mg g}^{-1} \text{h}^{-1}$) is the initial sorption rate. Therefore, the V_0 and q_{eq} values of kinetic tests can be determined experimentally by plotting t/q_t versus t .

To perform the adsorption kinetic experiments, 40 ml of IP_6 25 μM was added to 200 mg of MIP. The suspension was set at pH 5.6 and shaken for 120 min. Aliquots of 1 ml were taken at different times.

4.2.6. Desorption experiments

To perform the desorption experiments, 10 ml of 0.5 M HCl was added to the MIP and shaken for 60 min. This procedure repeat 3 times and then using 10 ml of M.Q. water for 3 times to elute the acid. The washed MIP was dry in oven at 40°C.

4.2.7. Solid phase extraction procedure on MIP

A 20 mg amount of polymer was poured into 1 mL-volume SPE cartridges (Bio-rad). The sorbent was conditioned with different pH solutions. A 1 mL-volume of IP_6 , PPi or P standard solution was loaded on the MIP-SPE cartridge. After a washing step with diluted HCl, the analytes were eluted with HCl. All fractions were collected and diluted prior to ICP analysis. All results were confirmed by triplicated experiments.

4.2.8. ICP conditions

The determination of P, PPi and IP_6 was carried out through ^{31}P analysis of the purified extracts by ICP-MS using ^{45}Sc ($5 \mu\text{g L}^{-1}$) as internal standard. The ICP-MS equipment was X series II ICP-MS (Thermo Fisher Corp., USA) and conditions were set as specified in table 4.4.

Table 4.4 Instrumental operating conditions for ICP-MS system

<i>ICP system</i>	
Instrument	Thermo X series II ICP-MS
RF power	1350W
Auxiliary gas flow	0.92 L min ⁻¹
Coolant gas flow	13.30 Lmin ⁻¹
Nebulizer gas flow	0.89 Lmin ⁻¹
Sample cone	Pt, 1.0 mm orifice
Skimmer cone	Pt, 0.7 mm orifice
Resolution	normal
Nebulizer	concentric nebulizer (Thermo)
<i>Sample introduction system</i>	
Sample uptake flow rate	2 mL min ⁻¹
Delay time	60s
Wash time	50s (HCl 1%)
<i>Data acquisition parameters</i>	
Analyzer	quadrupole
Scanning mode	peak jumping
Sweep per reading	30
Number of replicates	3
Dwell time	10ms

4.3. Results and discussion

4.3.1. The choice of monomer and cross-linker

Two different monomers were used, AT and MAA. The chemical structures of these two monomers are shown in figure 4.5.

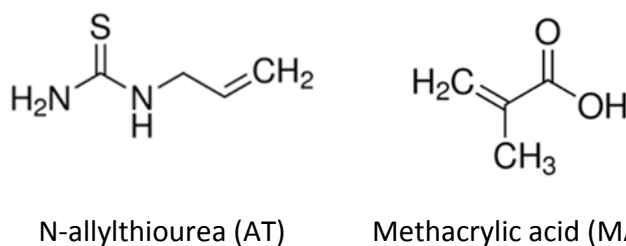


Figure 4.5. Structures of monomer used in this study

The choice of functional monomer is very important in order to forming more stable complexes with the template to generate MIPs with template-specific cavities.

The thiourea group has been used in the literature as anion binding sites through the hydrogen bond donors to recognize anions⁴⁸. It is known to have a strong binding ability to phosphate in hydrophilic solvent and aqueous media^{49,50}. For the present study, it was necessary to develop the molecularly imprinted polymers that had effective binding in a hydrophilic condition. For this purpose, functional monomer with a thiourea group, N-allylthiourea was chosen to prepare the molecularly imprinted polymer and the binding activities of the imprinted polymers was evaluated.

Methacrylic acid (MAA) is a conventional functional monomer in molecular imprinting. Three different cross linkers N, N'-Methylenebisacrylamide (MBAm), ethylene glycol dimethacrylate (EGDMA), Acrylamide (ACM), were used to synthesize the imprinted polymers in order to evaluate the imprinting effect.

Table 4.5 shows the polymers prepared imprinted (MIP) or non-imprinted (NIP) with the amount and type of functional monomer, solvent and crosslinker used.

Table 4.5. Imprinted and non-imprinted polymers prepared in this study

<i>Polymer</i>	<i>Template (mmol)</i>	<i>Functional monomer (mmol)</i>	<i>Crosslinker (mmol)</i>	<i>Solvent (ml)</i>
M3	Phytic acid (1.0)	MAA(16.0)	MBAm (12.5)	Water/ethane (3:1,V/V) 10ml
N3	None	MAA(16.0)	MBAm (12.5)	Water/ethane (3:1,V/V) 10ml
M13*	Phytic acid (1.0)	MAA(16.0)	EGDMA (20)	Water/ACN (80/8ml)
N13*	None	MAA(16.0)	EGDMA (20)	Water/ACN (80/8ml)
M15*	Phytic acid (0.5)	MAA(5.0)	MBA (12.5)+ ACM(5)	Water/ethane (3:1,V/V) 10ml
N15*	None	MAA(5.0)	MBA (12.5)+ ACM(5)	Water/ethane (3:1,V/V) 10ml
M29	DEHPA (1.0)	AT(4.0)	EGDMA (20)	ACN 4ml
N29	None	AT(4.0)	EGDMA (20)	ACN 4ml

Note* imprinted polymer prepared by suspension method due to the solubility of the template.

Adsorption results are shown in Figure 4.6. It is observed how one of the MIP has an adsorption capacity higher than the rest (M29) and differentiated from the corresponding NIP (N29) what indicates the effect of imprinting.

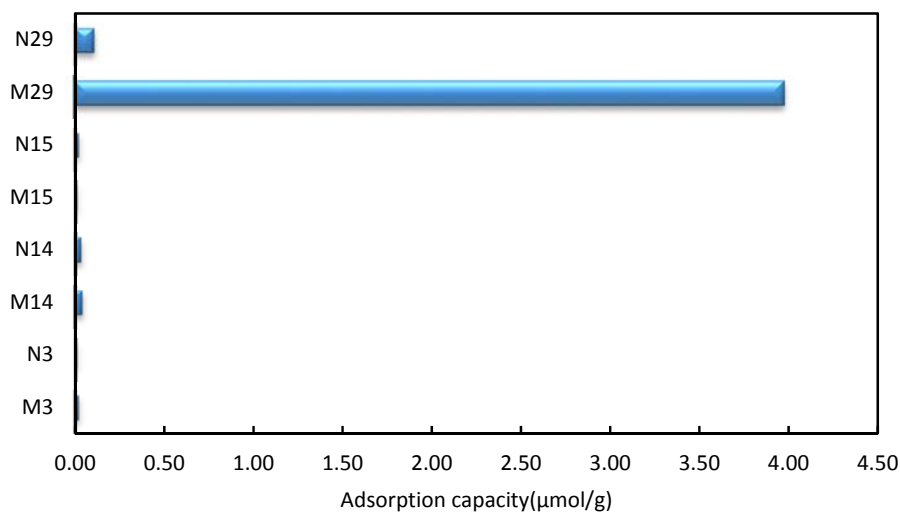


Figure 4.6. Binding activities of imprinted polymers towards IP₆ in water solutions.

When using N-allylthiourea as the functional monomer, the amount of IP₆ binding to the imprinted polymers was nearly 4 μmol/g, comparing that to the non-imprinted polymer was only 0.1 μmol/g (Fig 4.6).

However, for MAA none of the polymers showed affinity to IP₆. Though methacrylic acid is a powerful functional monomer in molecular imprinting in the organic solution system, the binding activities were quite low in aqueous media. N-allylthiourea, as the functional monomer, has both the strong binding ability to IP₆ in an aqueous condition and hydrophilicity. Thus, the imprinted polymer would successfully interact with IP₆³⁴.

4.3.2. The effect of steric factors on recognition

To prepare the MIP different compounds were used as template: DEHPA, pyrophosphoric acid and phenylphosphonic acid (see chemical structures in figure 4.7 and figure 4.8). The different MIPs prepared are shown in table 4.6.

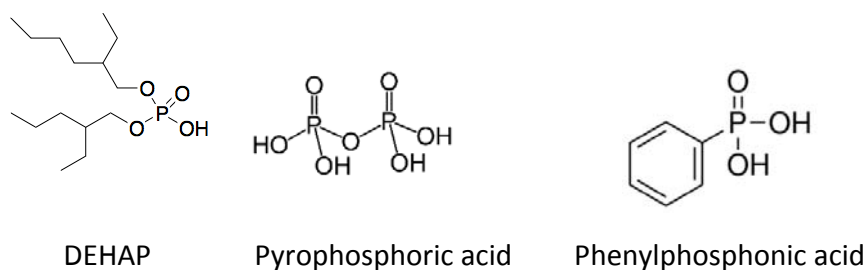


Figure 4.7. Structures of templates used in this study

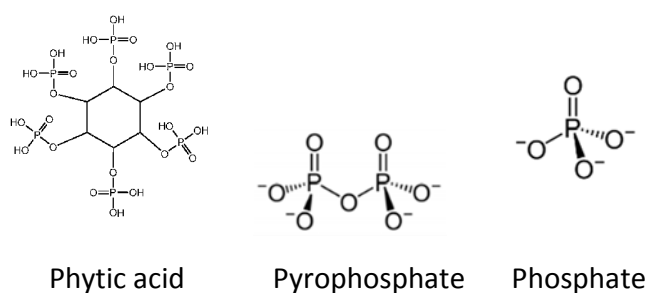


Figure 4.8. Structures of the objective analytes used in this study

Table 4.6. Imprinted and non-imprinted polymers prepared in this study

<i>Polymer</i>	<i>Template (mmol)</i>	<i>Functional monomer (mmol)</i>	<i>Crosslinker (mmol)</i>	<i>Solvent (ml)</i>
M-1	DEHPA (0.4)	AT(4.0)	EGDMA (16)	Acetonitrile 4ml
M-2	Pyrophosphoric acid (1.5)	AT(4.0)	EGDMA (16)	Acetonitrile 4ml + ethanol 1.5ml
M-3	Pyrophosphoric acid (1.5)	AT(4.0)	EGDMA (16)	Ethanol 4ml
M-4	Phenylphosphonic acid (1.0)	AT(4.0)	EGDMA (20)	Acetonitrile 4ml
M-5	DEHPA (1.0)	AT(4.0)	EGDMA (20)	Acetonitrile 4ml
NIP	None	AT(4.0)	EGDMA (20)	Acetonitrile 4ml

Comparing the imprinted polymers M-1, M-2, M-3, M-4 and M-5, bulk polymer prepared in the same functional monomer and cross-linker but using different templates, the synthesized polymer had different adsorption capacity for IP₆, PPI and P. The adsorption capacity of all the imprinted polymers is shown in Figure 4.11. It indicated that M-5 have the best adsorption capacity for IP₆, PPI, and P. This means that the imprinted polymer using DEHPA as template has the best specific adsorption ability which means the template has a great effect on the binding capacity of MIP for the adsorption of IP₆. This can be explained by the presence of steric factors in the template. This possibility of recognition based on steric factors was further suggested by the adsorption capacity of imprinted polymers. The template DEHPA is much bigger than phenylphosphonic acid and pyrophosphoric acid which may leave larger binding site on the surface of imprinted polymers. The effect of molecular shape on recognition was particularly pronounced in the case of imprinted polymer M-5 which had the highest adsorption capacity for IP₆, PPI and P.

4.3.3. The impact of porogenic solvent

We have tried to dissolve the phytic acid in various solvents in order to find the best solvent to prepare the molecularly imprinted polymer (see table 4.7). These solvents are commonly used for the synthesis of imprinted polymer, such as methanol, ethanol, acetonitrile and acetone. As show in table 10, the phytic acid is very hard to dissolve in organic solvent even though we added some part of water. With 0.5mmol of phytic acid, finally we found the phytic acid can dissolve in the mixture of ethanol and water with the volume ratio of 1:3, which is confirmed by the study of Cirillo et al.³⁷.

Table 4.7. The dissolve of phytic acid by different solvent.

0.5mmol phytic acid dissolved in different various								
20ml methanol/water (4:1 V/V)	15 ml methanol/water (1:1 V/V)	5ml acetonitrile	5ml ethanol/water (4:1 V/V)	10ml ethanol/water (4:1 V/V)	15 ml ethanol/water (1:1 V/V)	5ml ethanol/water (1:3 V/V)	5ml diethylamine/water(1:1 V/V)	5ml acetone
×	×	×	×	×	×	√	×	×

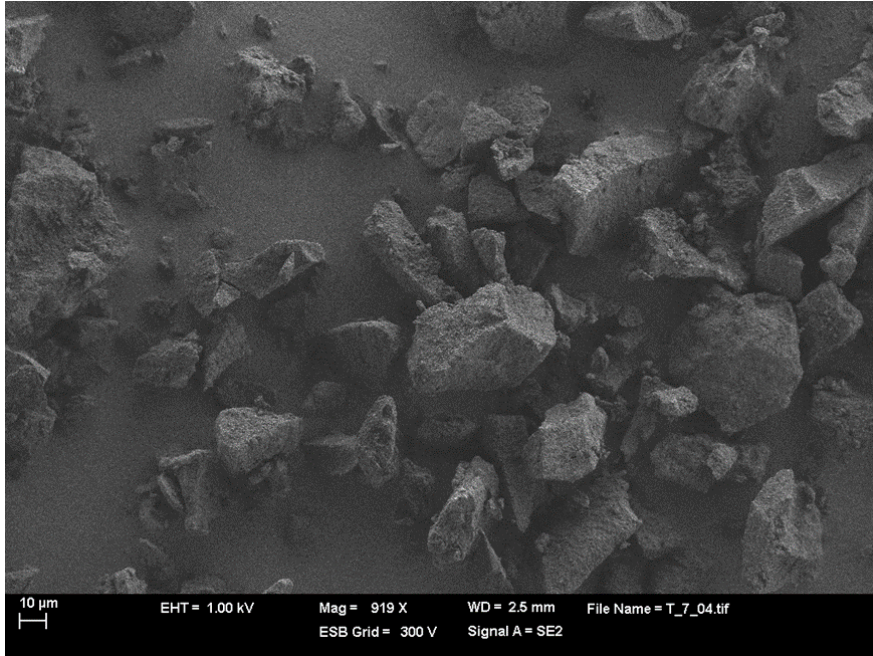
Nature and volume of the porogenic solvent is also a vital factor in molecular imprinting synthesis⁵¹. The typically solvents used were toluene, dichloromethane, chloroform, and acetonitrile. Less polar solvents are believed to enhance the complex formation by ensuring strong interactions such as hydrogen bonds²⁵. Although acetonitrile was shown by preliminary studies⁵² to be the optimum porogen for synthesizing EGDMA system polymers, in the present study, polymers M-2 and M-3 were prepared with the addition of ethanol as porogen solvent because the pyrophosphoric has a poor solubility in acetonitrile. Compared with acetonitrile, ethanol is a more polar solvent. The presence of ethanol reduced the imprinting effect which was observed in the adsorption capacity of M-2 (ethanol and ACN), which was better than M-3 (only ethanol) for all three compounds. These results suggest that the use of correct porogen can have a significant effect on the chemical performance.

Given the poor performance of these polymers, no further studies were carried out on it, yet it is worthy to mention the binding ability compared with the NIP polymer.

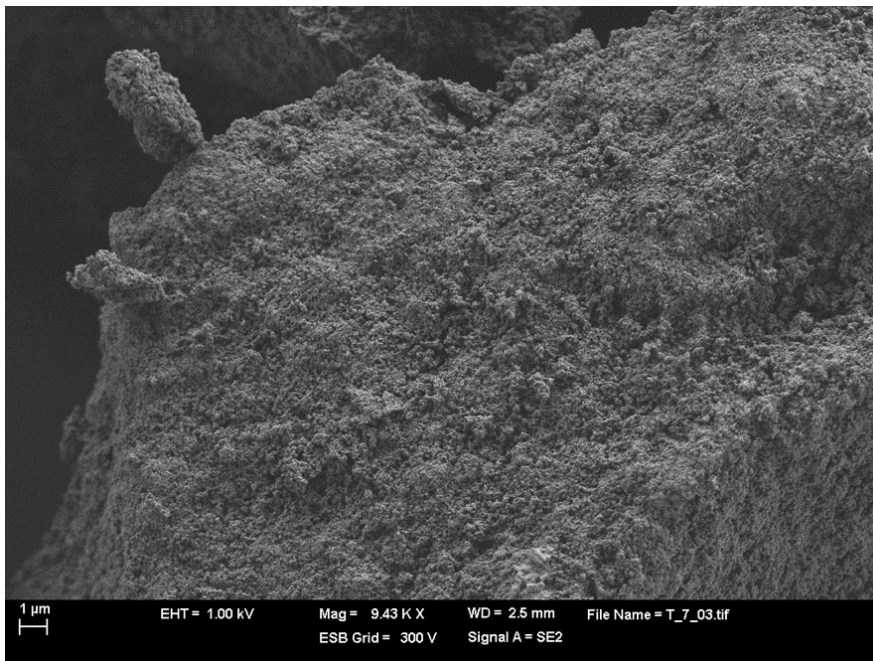
4.3.4. The characterization of MIP

The SEM image of M-29 shows irregular shaped and agglomerated particles with 25µm size are observed in the SEM images of (a). Fig. 4.9 (a) to (d) depicts the SEM images from 1000× to 61.30K× respectively. The morphology of these MIPs is highly agglomerated and

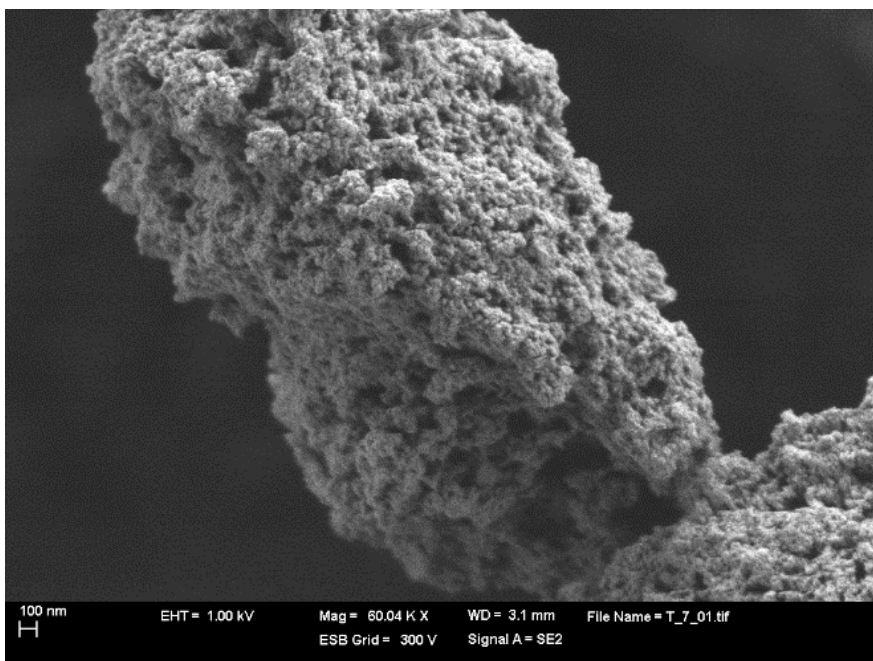
irregularly shaped with particle size in nanometers. We could observed a lot of holes on the surface of the polymer.



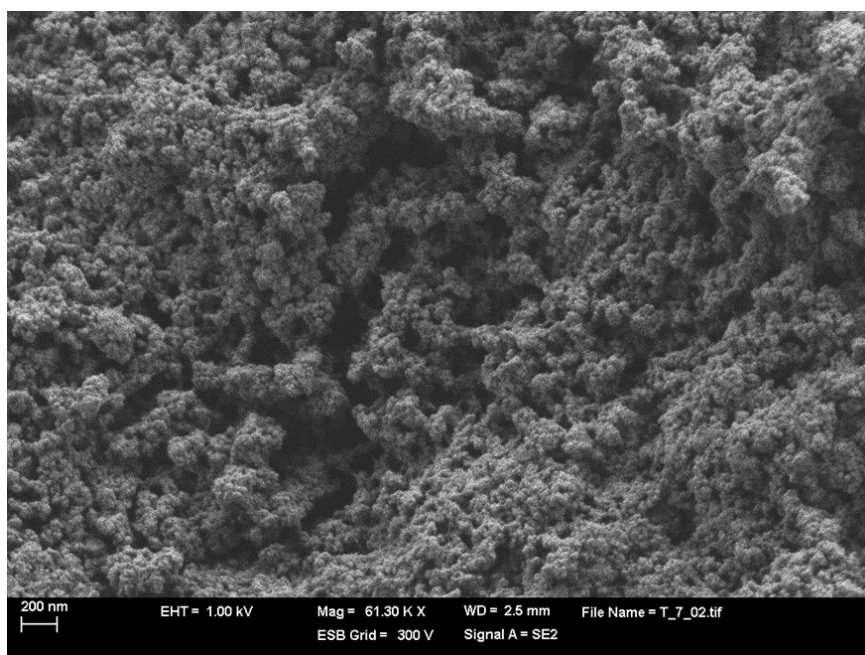
(a)



(b)



(c)



(d)

Figure 4.9. SEM of M29 prepared by bulk polymerization method

For the polymer prepared by the precipitation method, it was observed (figure 4.10) that when the quantities of toluene in the acetonitrile–toluene mixture were low (0% or 10%),

the MIPs were formed in the form of large beads with uniformity and monodispersity of the beads also maintained. However, as the percentage of toluene increased in the solvent mixture, the particle shape changed from globular to irregular and the polydispersity.



Figure 4.10. SEM of M36-02 prepared by precipitation polymerization method

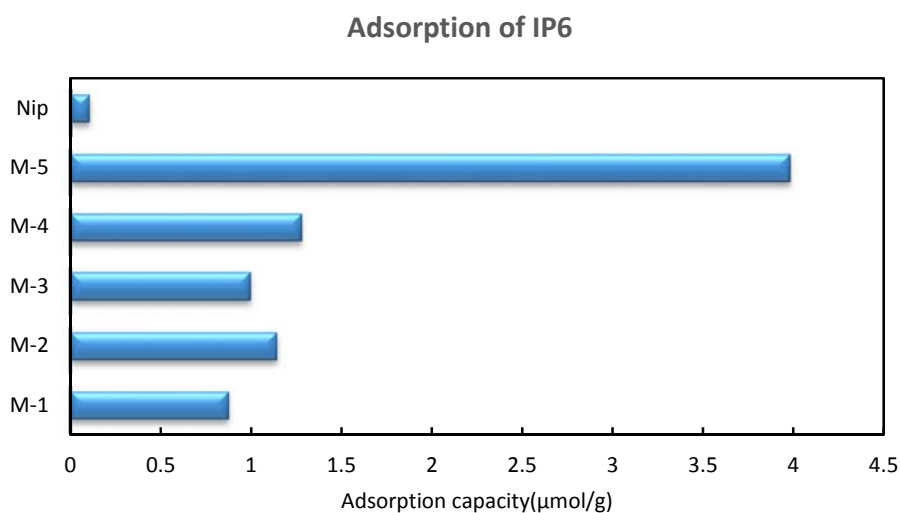
The solubility parameter of toluene is 8.9 MPa while, the solubility parameter of EGDMA is 18.2 MPa. When the concentration of toluene in the system increased the mismatch between the solubility parameters of components in the system also increased resulting in the formation of irregular MIPs nanoparticles. This is also expressed in the earlier investigations on MIPs, wherein divinylbenzene (DVB) was used as a crosslinker for MIPs.

Even though the polymerized bead has a good shape and size, our batch experiments showed that it has no adsorption capacity for IP₆. So we will not discuss this kind of materials in this chapter.

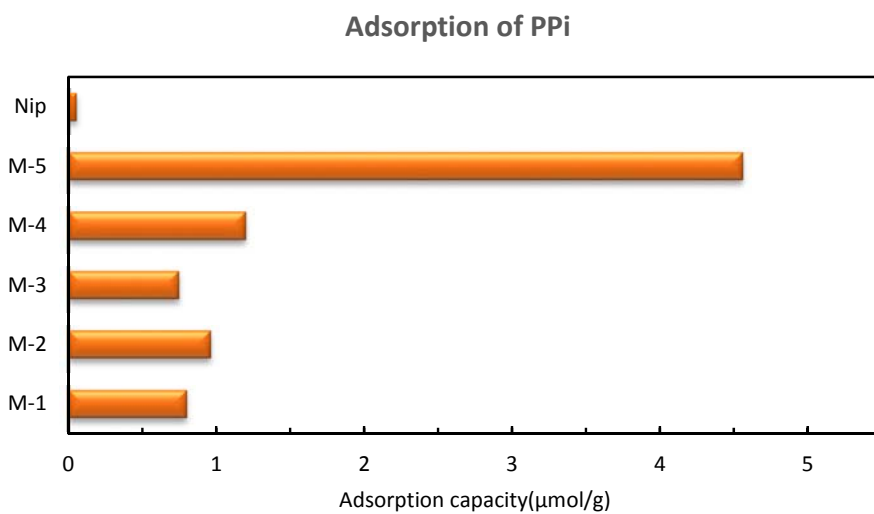
4.3.5. The impact of molar ratio

It is known that the molar ratio template: functional monomer: cross-linker affects polymer porosity which determines the substrate accessibility, size and shape of active binding site, which at the end will affect the sorption capacity. On the other hand, the arrangement of functional groups in the recognition sites of the polymeric network will determine the degree of specific binding interactions⁵³.

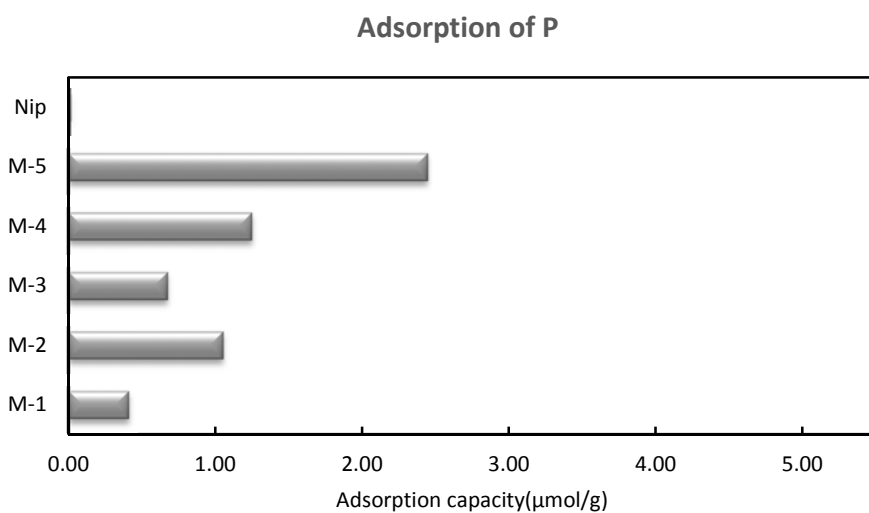
This can be observed comparing M1 and M5 (figure 4.11), where the same template but with different molar ratio were used (0.4:4:16 and 1:4:20 respectively). For the second polymer a higher performance is obtained being the best molar ratio 1:4:20 which was the chosen in the present work.



(a)



(b)



(c)

Figure 4.11 Adsorption capacity of MIP for polymers shown in Table 4.6

4.3.6. The effect of pH

Solution pH usually influences the adsorption to a large extent, as it affects the properties of both adsorbent and adsorbate. Optimization of pH value for adsorption medium plays a

vital role in the adsorption studies. The pH of the adsorption medium is the most significant parameter in the treatment of phytic acid by the adsorbent. The pH of the solution affects the degree of ionization and speciation of phytic acid which subsequently leads to a change in adsorption kinetics and equilibrium characteristics⁵⁴. Then, the effect of pH on the adsorption of phytic acid was study and results are shown in Figure 4.12.

It was observed that adsorption of IP₆ between pH 2.0 to 5.6 did not cause any change in adsorption capacity. Figure 4.12 also showed that adsorption of IP₆ at pH 1.0 was significantly low and indicates that the MIP loss the adsorption capacity. The fact neutral molecules of phytic acid are benefit for the adsorption process has also been reported previously for other sorbent by Muñoz et al.²³. For subsequent studies, pH 5.6 was selected for the adsorption medium since is the pH closer to the natural pH of environmental water samples and urine.

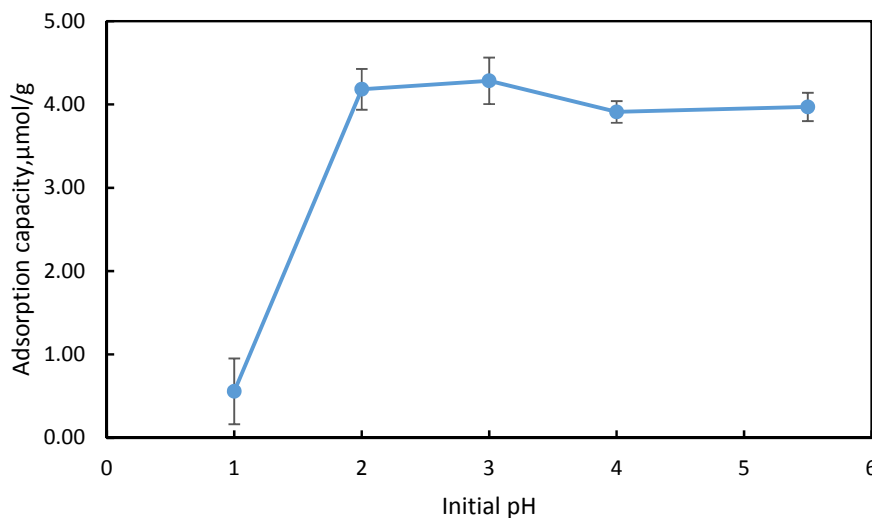


Figure 4.12. Effect of pH on adsorption of IP₆.

4.3.7. Adsorption isotherms

From previous results, MIP 5 was selected as the best for the adsorption and separation of phytic acid and so isotherm study was performed on it.

4.3.7.1. Langmuir isotherm

The Langmuir adsorption isotherm has been successfully applied to many MIP adsorption processes and has been the most widely used to describe the adsorption of a solute from a liquid solution. A basic assumption of the Langmuir theory is that adsorption takes place at specific homogeneous sites on the surface of the adsorbent. It is then assumed that once adsorbate molecule occupies a site, no further adsorption can take place at that site. The rate of adsorption to the surface should be proportional to a driving force and area. The driving force is the concentration in the solution, and the area is the amount of bare surface⁵⁴.

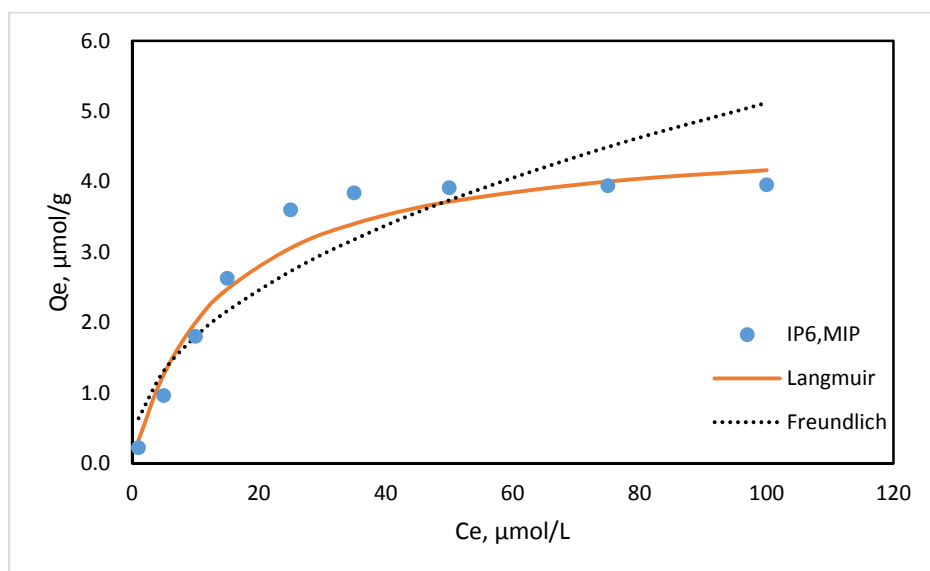


Figure 4.13. Adsorption isotherm of the imprinted polymer.

In order to investigate the binding properties of the IP₆ imprinted polymer, the saturation adsorption experiments were carried out and the corresponding adsorption isotherms were shown in Figure 4.13.

In Figure 4.13, the adsorption capacity, Q_e is shown against initial concentrations of IP₆. From Figure 4.13, when the concentration of IP₆ increased, the adsorption capacity (Q_e) firstly increased sharply, then increased slowly, to finally reach a saturation profile at

higher concentration. It could be ascribed to the molecular-imprinting effect, which could recognize the templates via multiple point electrostatic interaction and shape complementarity formed in the MIP by the polymerization⁵⁵.

Equations 4-1 and 4-2 were applied to the experimental data and results are shown in Figure 4.13. It shows the adsorption isotherms of the MIP adsorbents for IP₆, and Langmuir and Freundlich models. As shown the adsorption isotherms of IP₆ on the MIP can be fitted better by the Langmuir model than the Freundlich. Freundlich isotherm has been observed for a wide range of heterogeneous surfaces, including activated carbon, silica, clays, metals, and polymers⁵⁶. Freundlich equation is suitable for heterogeneous surfaces and has been applied in the adsorption process using the non-covalently imprinted polymers. In this study, the correlation coefficients suggest that the Langmuir isotherm model is suitable for describing the adsorption equilibrium of IP₆ by the imprinted polymer. The fitting data in table 4.8 shows that the maximum adsorption capacity (Q_{max}) for IP₆ was 4.675 $\mu\text{mol/g}$.

Table 4.8. Parameters in adsorption isotherm of imprinted polymer

Isotherm models	Constants	
	Langmuir equation	$Q_m(\mu\text{mol g}^{-1})$
$K_L(\text{L } \mu\text{mol}^{-1})$		0.074
r^2		0.9783
Freundlich equation	$K_F(\mu\text{mol g}^{-1})$	0.633
	n^{-1}	0.454
	r^2	0.8199

4.3.7.2. Adsorption properties and Scatchard analysis

The adsorption capacity of MIP is an important parameter to determine the amount of MIP required to quantitatively adsorb a specific amount of imprinted templates from solution⁵⁷.

Scatchard analysis is a method to linearize data from a saturation binding experiment in order to determine binding constants. To investigate the binding ability of the imprinted polymer in aqueous media, a Scatchard analysis was carried out. This tool has been already applied in molecularly imprinted polymer in the bibliography⁵⁸.

Scatchard analysis was conducted using the following equation⁵⁹:

$$\frac{Q_e}{F} = \frac{Q_{max}-Q_e}{K_D} \quad (4-7)$$

Where Q_e ($\mu\text{mol/g}$) is the amount of IP₆ bounded to the polymer and F ($\mu\text{mol/L}$) is equilibrium concentration of free IP₆ in solution (approximated by the analytical concentration of IP₆). Q_{max} ($\mu\text{mol/g}$) is the apparent maximum number of binding sites of the polymer and K_D ($\mu\text{mol/L}$) represents the dissociation constant of the complex IP₆-MIP.

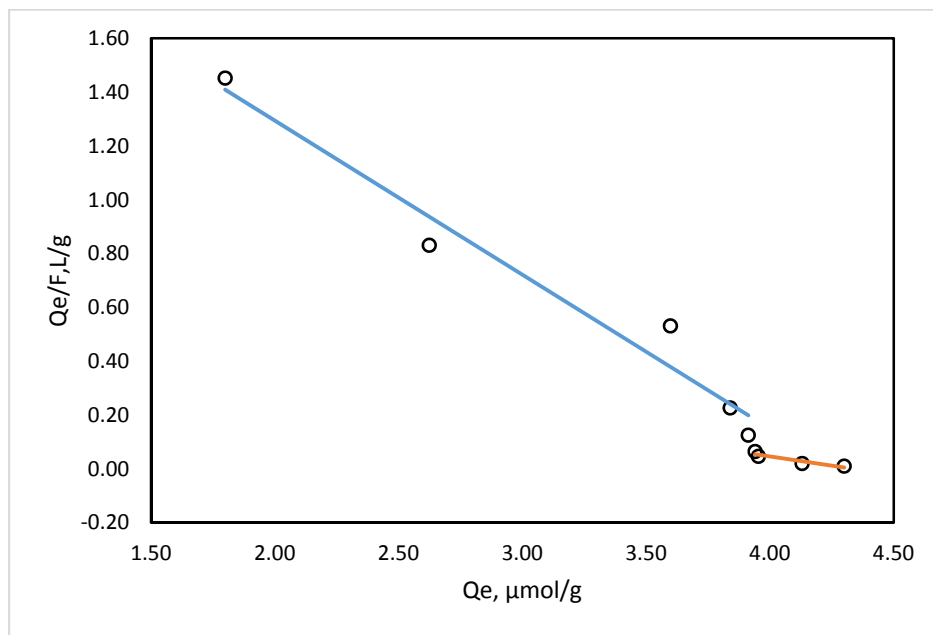


Figure 4.14. Scatchard plot of the imprinted polymer to estimate the binding ability calculated from the saturation profile.

The Scatchard plot was shown in Fig.4.14. The dissociation constant K_D and the number of binding sites Q_{max} can be estimated from the obtained binding data which was plotted in Figure 4.14. As shown in the Scatchard plot, the relationship between Q_e/F and Q_e was not

a single linear curve, but consisted of two linear curves with different slopes, suggesting that the binding sites in MIP are heterogeneous in respect to the affinity for IP₆⁵⁸. Since there are two distinct parts within the plot which can be considered as straight lines, it would be reasonable to assume that the binding sites configuration in the MIP can be classified into two distinct groups with specific binding properties. This kind of non-intervalence-type molecular imprinting polymer has been reported by other researches⁶⁰. Under the assumptions, the respective dissociation constant, K_D , was estimated by Scatchard analysis calculated from the saturation profile. The K_D of the highest affinity binding site was estimated to be 1.75 μM and 7.32 μM . The respective theoretical binding site, Q_{max} were calculated on 4.26 $\mu\text{mol/g}$ and 4.34 $\mu\text{mol/g}$ of dry polymer.

4.3.8. Adsorption kinetics

The kinetics of adsorption that describe the solute adsorption rate governing the residence time of the sorption reaction is one of the important characteristics that define the efficiency of adsorption.

Figure 4.15 shows the adsorption kinetics of IP₆ on the MIP at different time intervals and the simulation of the pseudo-second-order kinetic model. It can be seen that the adsorption equilibrium was almost achieved after 10 min. Adsorption of IP₆ on the MIP approach pseudo-equilibrium rapidly. For IP₆, more than 70% removal of IP₆ was achieved within 1 min of contact and the adsorption equilibrium was approached in 10 min. The greater surface area and smaller particle size raise the probability of the adsorption reactions. The sorption amount of the MIP for IP₆ reached 3.85 $\mu\text{mol g}^{-1}$ after 10 min sorption, suggesting the good imprinting effect of the MIP. The short contact time needed to reach equilibrium as well as the high adsorption capacity suggests that the MIP possess highly potential applications for the removal of IP₆ from urine.

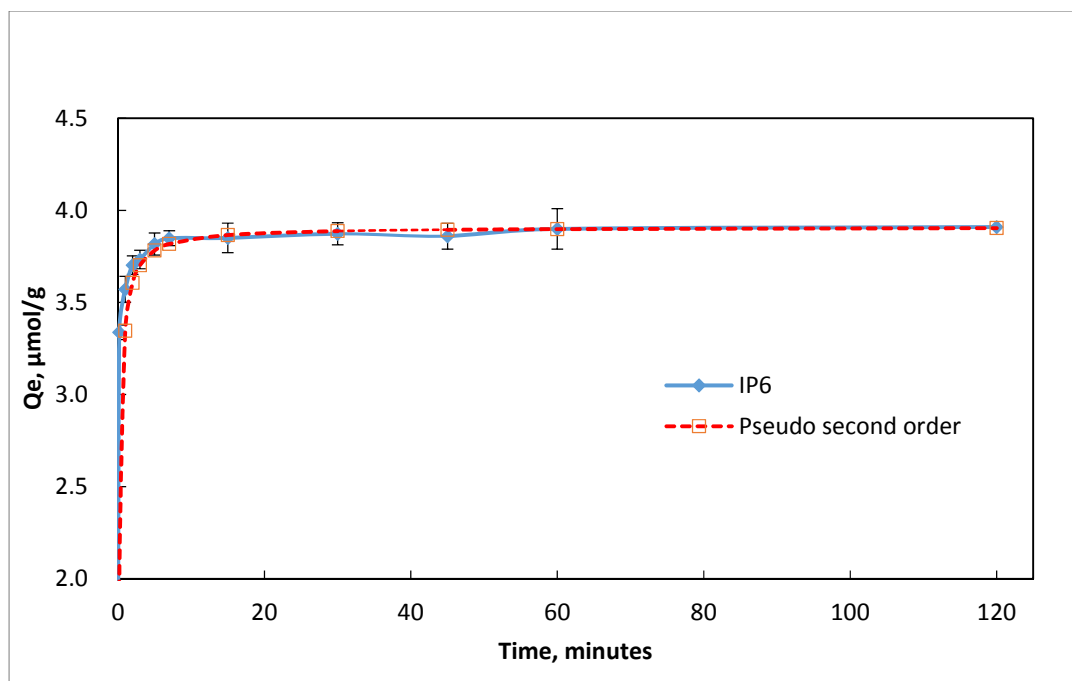


Figure 4.15. Adsorption kinetics of IP₆ on the MIP at pH5.6.

Table 4.9 shows the determination coefficients (r^2) and the other parameters obtained from the pseudo-second-order kinetic model by the plot of t versus t/q_t to determine the V_0 and q_{eq} values for all the media. The pseudo-second-order model fits the kinetic data in our system very well ($r^2 > 0.999$). The initial adsorption rate of IP₆ over MIP is $23.3 \mu\text{mol g}^{-1} \text{h}^{-1}$. The fitting data show that the MIP has a good affinity for IP₆, which takes less time to reach equilibrium in the process.

Table 4.9 Kinetic parameters of a pseudo-second-order kinetic model fitting IP₆ adsorption by the MIP.

	V_0	q_{eq}	k_2	
system	$\mu\text{mol g}^{-1} \text{h}^{-1}$	$\mu\text{mol g}^{-1}$	$\text{g } \mu\text{mol}^{-1} \text{h}^{-1}$	r^2
IP ₆ /MIP	23.25	3.91	1.52	0.99998

4.3.9. The effect of temperature

The temperature has two major effects on the adsorption process. Increasing the temperature is known to increase the rate of diffusion of the adsorbate molecules across the external boundary layer and in the internal pores of the adsorbent particle, owing to the decrease in the viscosity of the solution. In addition, changing the temperature will change the equilibrium capacity of the adsorbent for a particular adsorbate⁵⁴. In this phase study, a series of experiments were conducted at 20, 50, and 70°C to study the effect of temperature on the rate and the kinetics. The results are present in Fig 4.16. As can be seen, the adsorption decrease with the rise of temperature, indicating the exothermic nature of these adsorptions⁶¹.

Also we can see that PPI have a little more capacity than IP₆, this is may be because the size the PPI is smaller than IP₆, so it is easier to go into the MIP body and occupy a lot of the active space. P is less adsorb on MIP and well release from MIP as the temperature arise.

Since these prepared imprinted polymer could be used in high performance liquid chromatography (HPLC) or capillary electrochromatography (CEC) for the separations of phosphate compounds, there will have some obstacles leading to loss of separation power, such as the effects of temperature on the polymer syntheses and chiral recognition characters⁶². During the last 10 years, most molecularly imprinted polymers were prepared by using thermal initiator, especially the typically used free radical initiator is AIBN (2,2'-azobisisobutyronitrile) which undergoes thermal decomposition at 60°C. It is also reported⁶³ that the azobisnitriles are used to prepare molecular imprints as thermal initiators between 30 and 60°C and as photo-initiators at 0°C. Their results indicated that the chemical interactions between the functional monomer and the template could be stronger at lower temperature. On the other hand, since host functional monomers binding to the specific guest templates are chemically solidified by cross-linking polymerization, the host-guest complexation mechanism is also a kinetically driven process. The temperature effect is assumed to be an important factor for CEC filled with molecularly imprinted

polymer since there potential Joule heating within the capillary under usual voltage setting of 5–30 kV⁶². The developed MIP in our study have a good adsorption capacity for IP₆ even at 70°C means that it can be used in the higher temperature for HPLC. For P and PPI the adsorption capacity decrease more dramatically with the rise of temperature. This interesting finding let us to think about using heat to separate the IP₆, PPI and P from the matrix.

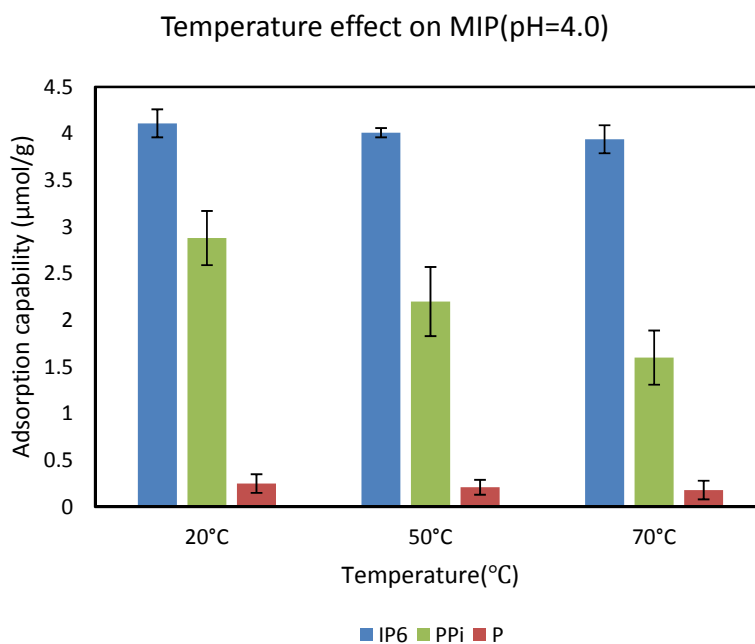


Figure 4.16. IP₆, PPI and P adsorption capacity on MIP at different temperature at pH=4.0

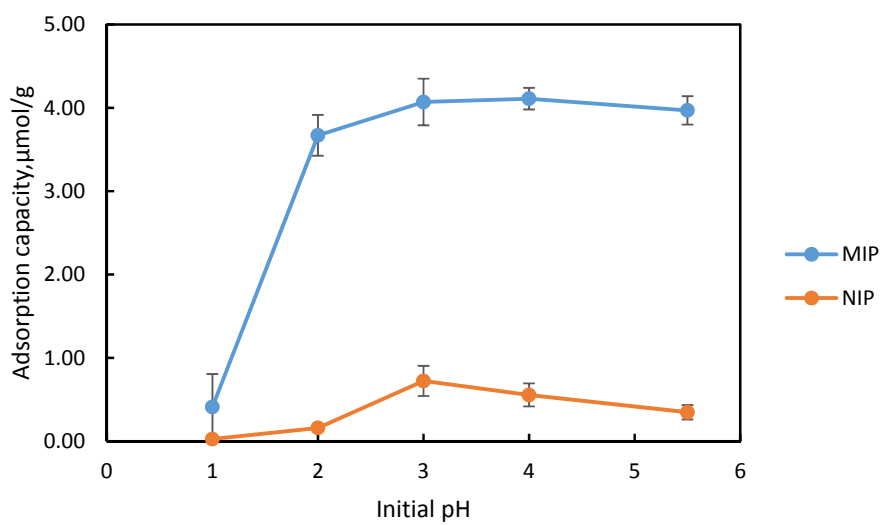
4.3.10. Separation section

Since we found the pH have a significant effect on the adsorption of IP₆ on the developed MIP, therefore, a separation procedure based on acid elution was developed. For this purpose, different concentrations of HCl were used (0.1 M, 0.01M and 0.005M) and the obtained results were compared. With the addition of acid solution, the interactions

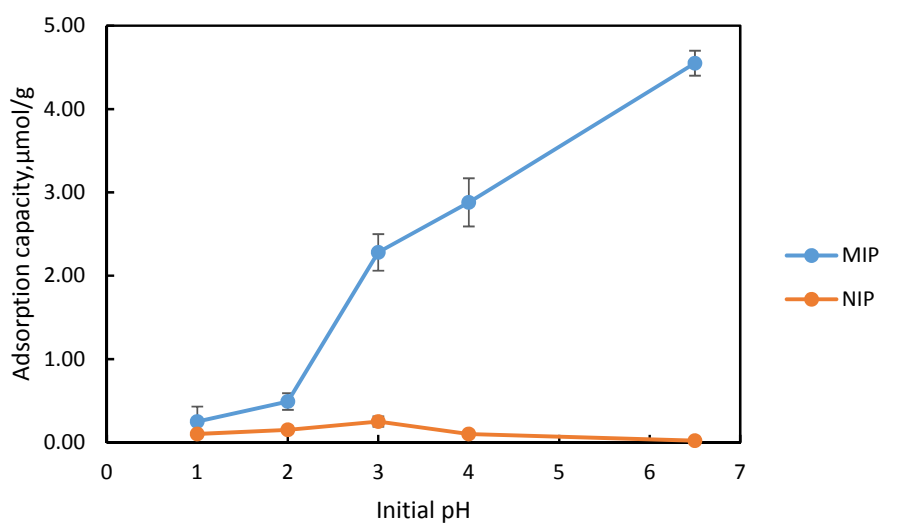
established between the analytes and the MIP was disrupted so that the adsorbed analytes were almost completely eluted upon the introduction of the washing step.

4.3.10.1. The effect of pH

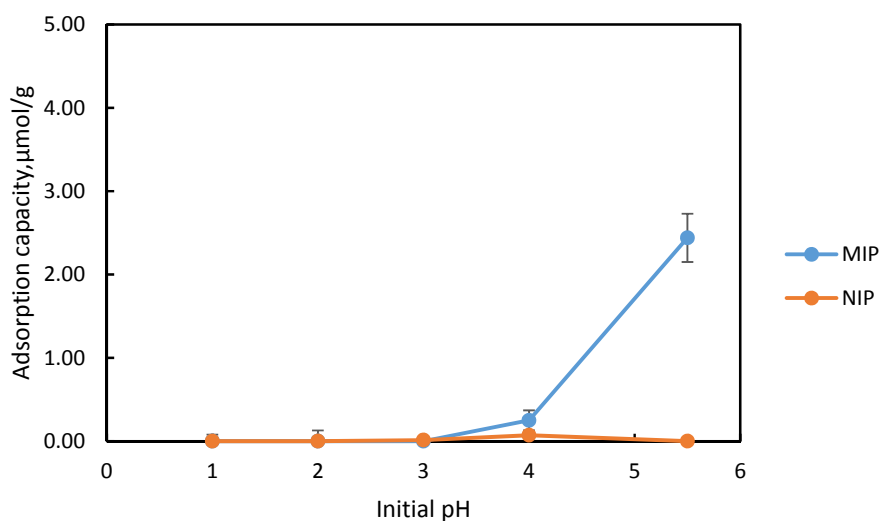
In order to selectively elute the IP₆, PPI and P from the SPE column, it is necessary to investigate the effect of pH on the adsorption of MIP which will be used for the separation procedure. It is indicated in figure 4.17(a) that the MIP start to desorb the IP₆ below pH 2.0, and 95% of the IP₆ was desorbed form the imprinted polymer at pH 1.0. While for PPI, desorption started below pH 6.0 slowly and sharply desorbed from pH 3.0 to pH 2.0. Figure 4.17(c) show that the P cannot adsorbed on the imprinted blow pH 4.0. This phenomena let us to think about separate the three compounds by just tuning the pH of the elute solution.



(a) IP6



(b) PPI



(c) P

Figure 4.17. IP₆, PPI and P adsorption capacity on MIP at different pH

The different desorption phenomena of IP₆, PPI and P can be explained by the different dissociate constant of these three compounds. IP₆ is highly selectively adsorbed in the imprinted polymer as a consequence of its strongest dissociation at low pH values (pKa₁ = -0.15, pKa₂ = 0.41, pKa₃ = 0.85, pKa₄ = 1.84). PPI is strongly dissociated at low pH values (pKa₁ = 0.85, pKa₂ = 1.49, pKa₃ = 5.77, pKa₄ = 8.22) being strongly retained by the polymer above pH 3.0, whereas P (pKa₁ = 2.12, pKa₂ = 7.20, pKa₃ = 12.36) is easier desorbed from the polymer by lower the pH or use diluted HCl. Thus, separation is pH-dependent and a suitable selection of the eluting condition according to their acidity will lead to highly purified extracts of PPI and IP₆, respectively²³. Due to the different dissociation degree of the phosphorous species depending on the pH a separation system based on pH gradient can be designed where P can be separated from IP₆ and PPI at pH 3.0 and the PPI can be separated from IP₆ at the pH 2.0, then the IP₆ could eluted at pH 1.0 by the use of molecularly imprinted polymer solid phase extraction system.

4.3.10.2. MIP-Solid phase extraction

Based on the discovery of the effect of pH, we did the SPE separation to separate IP₆, PPI and P by elute the cartridge with HCl solution. In order to do this, loading of P, IP₆ and PPI on the prepared MIP-SPE cartridge was achieved just by passing the defined concentration of standard analytes through the cartridge. After a washing step with HCl, the analytes were eluted with different concentration of HCl. All fractions were collected and analyzed by ICP-MS. All results were confirmed by triplicated experiments.

As mentioned previously, the adsorption of P on MIP will not happen below pH 4.0. So it is easily elute form the cartridge by just passing pH=3.0 diluted HCl solution. After loaded the PPI, the 1mM HCl can only elute 6.5% of the loaded analytes, this means the acid at this concentration are not strong enough to disrupt the interaction between PPI and MIP(table 4.10). While when increase the HCl to 5mM, 71.9% of the PPI can be eluted and this recovery increase to 97.8% at 10mM HCl. From figure 4.18 we can clearly observed that the PPI eluted efficiently from the matrix by HCl solution (concentrated more than 10mM (pH=2)), since at this pH the MIP has very poor adsorption capacity which observed in the batch experiments. While for the IP₆, under the condition of 10mM HCl, the recovery is only 38.2%, which means at this condition the cartridge still retain most of the IP₆. However, when we using the more concentrated HCl, at 100mM conditions, the recovery of IP₆ can achieve 103.7%, which means all of the IP₆ has release to the acid solution. From figure 4.18 we can observe clearly that the separation of IP₆ and PPI can be achieved at 10mM HCl elution.

Table 4.10. Recovery of IP₆ and PPI by the SPE process under different elute condition.

Analyte	Elute solution (HCl)	Recovery,%
PPI	1mM	6.5
	5mM	71.9
	10mM	97.8
	50mM	107.5
IP ₆	10mM	38.2
	100mM	103.7
	200mM	113.6

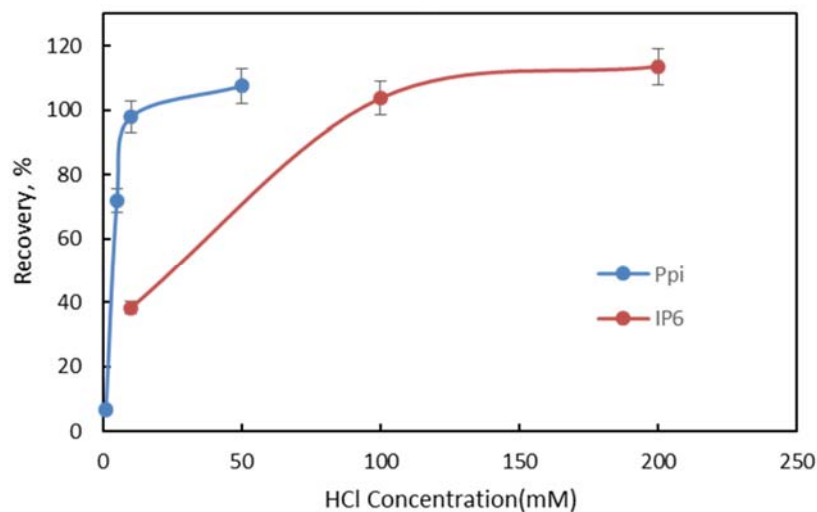


Figure 4.18. IP6 and PPI MIP-SPE elution curve.

4.4. Conclusion

MIP were successfully synthesized using the bulk polymerization method. The polymer prepared using MAA as functional monomer showed no affinity for IP6. The polymer synthesis with N-allylthiourea showed high adsorption for IP6 with the capacity nearly 4 $\mu\text{mol/g}$, comparing that to the non-imprinted polymer was only 0.1 $\mu\text{mol/g}$. The MIP prepared using DEHPA as template show the best adsorption capacity compared with the polymer prepared with pyrophosphoric acid and phenylphosphonic acid. The solution pH has a significant effect on the adsorption of IP6, PPI and Phosphate on the developed MIP. The separation of IP6, PPI and Phosphate was achieved by SPE procedure which using the synthesized MIP as adsorbent.

This work demonstrates a new method for extracting phosphorous inhibitors of urolithiasis (phytic acid and pyrophosphate) using molecularly imprinted polymers and could be used for nephrolithiasis related analysis. The developed polymer can be applied as specific stationary phases in solid-phase extraction or liquid chromatography. The development of methods to extract and recover phosphorous inhibitors from urine is very much desired. With improvements in the binding ability and selectivity of the molecularly imprinted polymers proposed in this study, these materials could be put into clinic use.

4.5. Reference

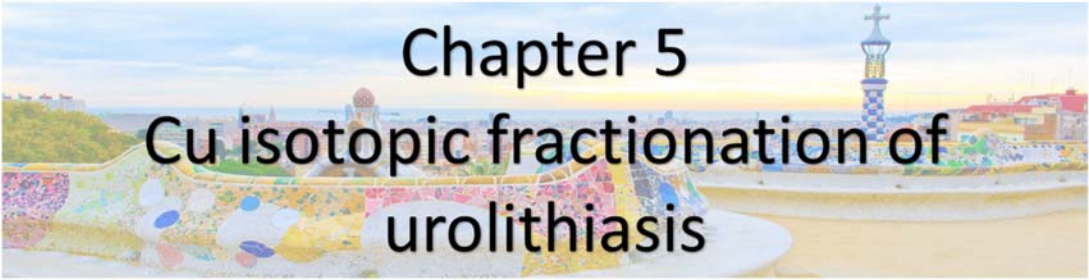
1. Rizvi, I.; Riggs, D. R.; Jackson, B. J.; Ng, A.; Cunningham, C.; McFadden, D. W., Inositol Hexaphosphate (IP6) Inhibits Cellular Proliferation In Melanoma. *Journal of Surgical Research* **2006**, *133* (1), 3-6.
2. Somasundar, P.; Riggs, D. R.; Jackson, B. J.; Cunningham, C.; Vona-Davis, L.; McFadden, D. W., Inositol Hexaphosphate (IP6): A Novel Treatment for Pancreatic Cancer1. *Journal of Surgical Research* **2005**, *126* (2), 199-203.
3. Grases, F.; Isern, B.; Sanchis, P.; Perello, J.; Torres, J. J.; Costa-Bauza, A., Phytate acts as an inhibitor in formation of renal calculi. *Front Biosci* **2007**, *12* (1), 2580-7.
4. Terkeltaub, R. A., Inorganic pyrophosphate generation and disposition in pathophysiology. *American Journal of Physiology-Cell Physiology* **2001**, *281* (1), C1-C11.
5. Sharma, S.; Vaidyanathan, S.; Thind, S.; Nath, R., Urinary excretion of inorganic pyrophosphate by normal subjects and patients with renal calculi in north-western India and the effect of diclofenac sodium upon urinary excretion of pyrophosphate in stone formers. *Urologia internationalis* **1992**, *48* (4), 404-408.
6. Breslau, N. A.; Padalino, P.; Kok, D. J.; Kim, Y. G.; Pak, C. Y., Physicochemical effects of a new slow - release potassium phosphate preparation (UroPhos - K) in absorptive hypercalciuria. *Journal of Bone and Mineral Research* **1995**, *10* (3), 394-400.
7. Ray, P.; Shang, C.; Maguire, R.; Knowlton, K., Quantifying phytate in dairy digesta and feces: Alkaline extraction and high-performance ion chromatography. *Journal of dairy science* **2012**, *95* (6), 3248-3258.
8. Latta, M.; Eskin, M., A simple and rapid colorimetric method for phytate determination. *Journal of Agricultural and Food Chemistry* **1980**, *28* (6), 1313-1315.
9. Skoglund, E.; Carlsson, N.-G.; Sandberg, A.-S., High-performance chromatographic separation of inositol phosphate isomers on strong anion exchange columns. *Journal of agricultural and food chemistry* **1998**, *46* (5), 1877-1882.
10. Rounds, M.; Nielsen, S., Anion-exchange high-performance liquid chromatography with post-column detection for the analysis of phytic acid and other inositol phosphates. *Journal of Chromatography A* **1993**, *653* (1), 148-152.
11. Perello, J.; Isern, B.; Munoz, J.; Valiente, M.; Grases, F., Determination of Phytate in Urine by High-Performance Liquid Chromatography–Mass Spectrometry. *Chromatographia* **2004**, *60* (5-6), 265-268.
12. Sandberg, A. S.; Ahderinne, R., HPLC Method for Determination of inositol Tri - , Tetra - , Penta - , and Hexaphosphates in Foods and Intestinal Contents. *Journal of Food Science* **1986**, *51* (3), 547-550.
13. Blaabjerg, K.; Hansen-Møller, J.; Poulsen, H. D., High-performance ion chromatography method for separation and quantification of inositol phosphates in diets and digesta. *Journal of Chromatography B* **2010**, *878* (3), 347-354.

14. Kemme, P. A.; Lommen, A.; De Jonge, L. H.; Van der Klis, J. D.; Jongbloed, A. W.; Mroz, Z.; Beynen, A. C., Quantification of inositol phosphates using ³¹P nuclear magnetic resonance spectroscopy in animal nutrition. *Journal of agricultural and food chemistry* **1999**, *47* (12), 5116-5121.
15. Chen, Y.; Chen, J.; Luo, Z.; Ma, K.; Chen, X., Synchronous fluorescence analysis of phytate in food. *Microchimica Acta* **2009**, *164* (1-2), 35-40.
16. Muñoz, J. A.; Valiente, M., Determination of phytic acid in urine by inductively coupled plasma mass spectrometry. *Analytical chemistry* **2003**, *75* (22), 6374-6378.
17. Helfrich, A.; Bettmer, J., Determination of phytic acid and its degradation products by ion-pair chromatography (IPC) coupled to inductively coupled plasma-sector field-mass spectrometry (ICP-SF-MS). *Journal of Analytical Atomic Spectrometry* **2004**, *19* (10), 1330-1334.
18. March, J.; Grases, F.; Salvador, A., Hydrolysis of phytic acid by microwave treatment: Application to phytic acid analysis in pharmaceutical preparations. *Microchemical journal* **1998**, *59* (3), 413-416.
19. Chang, G.-G.; Denq, R.-Y., Determination of inorganic pyrophosphate concentration in urine. *International Journal of Biochemistry* **1985**, *17* (6), 733-735.
20. Baykov, A.; Avaeva, S., A sensitive method for measuring pyrophosphate in the presence of a 10,000-fold excess of orthophosphate using inorganic pyrophosphatase. *Analytical biochemistry* **1982**, *119* (1), 211-213.
21. Yoza, N.; Akazaki, I.; Nakazato, T.; Ueda, N.; Kodama, H.; Tateda, A., High-performance liquid chromatographic determination of pyrophosphate in the presence of a 20,000-fold excess of orthophosphate. *Analytical biochemistry* **1991**, *199* (2), 279-285.
22. Hénin, O.; Barbier, B.; Brack, A., Determination of phosphate and pyrophosphate ions by capillary electrophoresis. *Analytical biochemistry* **1999**, *270* (1), 181-184.
23. Munoz, J. A.; Lopez-Mesas, M.; Valiente, M., Minimum handling method for the analysis of phosphorous inhibitors of urolithiasis (pyrophosphate and phytic acid) in urine by SPE-ICP techniques. *Analytica chimica acta* **2010**, *658* (2), 204-8.
24. Vasapollo, G.; Sole, R. D.; Mergola, L.; Lazzoi, M. R.; Scardino, A.; Scorrano, S.; Mele, G., Molecularly imprinted polymers: present and future prospective. *International journal of molecular sciences* **2011**, *12* (9), 5908-5945.
25. Cheong, W. J.; Yang, S. H.; Ali, F., Molecular imprinted polymers for separation science: a review of reviews. *Journal of separation science* **2013**, *36* (3), 609-28.
26. Haupt, K.; Mosbach, K., Molecularly imprinted polymers and their use in biomimetic sensors. *Chemical reviews* **2000**, *100* (7), 2495-2504.
27. Haupt, K., Peer reviewed: molecularly imprinted polymers: the next generation. *Analytical chemistry* **2003**, *75* (17), 376 A-383 A.
28. Branger, C.; Meouche, W.; Margailan, A., Recent advances on ion-imprinted polymers. *Reactive and Functional Polymers* **2013**, *73* (6), 859-875.
29. Cacho, C.; Turiel, E.; Martin-Esteban, A.; Ayala, D.; Perez-Conde, C., Semi-covalent imprinted polymer using propazine methacrylate as template molecule for the clean-up of triazines in soil and vegetable samples. *Journal of chromatography. A* **2006**, *1114* (2), 255-62.

30. Cacho, C.; Turiel, E.; Martín-Esteban, A.; Pérez-Conde, C.; Camara, C., Clean-up of triazines in vegetable extracts by molecularly-imprinted solid-phase extraction using a propazine-imprinted polymer. *Analytical and bioanalytical chemistry* **2003**, *376* (4), 491-6.
31. balamurugan, K.; Gokulakrishnan, K.; Prakasam, T., Preparation and evaluation of molecularly imprinted polymer liquid chromatography column for the separation of ephedrine enantiomers. *Arabian Journal of Chemistry* **2011**.
32. Byun, H.-S.; Yang, D.-S.; Cho, S.-H., Synthesis and characterization of high selective molecularly imprinted polymers for bisphenol A and 2,4-dichlorophenoxyacetic acid by using supercritical fluid technology. *Polymer* **2013**, *54* (2), 589-595.
33. Caro, E.; Marcé, R. M.; Cormack, P. A. G.; Sherrington, D. C.; Borrull, F., Direct determination of ciprofloxacin by mass spectrometry after a two-step solid-phase extraction using a molecularly imprinted polymer. *Journal of separation science* **2006**, *29* (9), 1230-1236.
34. Kugimiya, A.; Takei, H., Preparation of molecularly imprinted polymers with thiourea group for phosphate. *Analytica chimica acta* **2006**, *564* (2), 179-183.
35. Ara, B.; Chen, Z.; Shah, J.; Rasul Jan, M.; Ye, L., Preparation and characterization of uniform molecularly imprinted polymer beads for separation of triazine herbicides. *Journal of Applied Polymer Science* **2012**, *126* (1), 315-321.
36. Brüggemann, O.; Visnjeviski, A.; Burch, R.; Patel, P., Selective extraction of antioxidants with molecularly imprinted polymers. *Analytica chimica acta* **2004**, *504* (1), 81-88.
37. Cirillo, G.; Curcio, M.; Parisi, O. I.; Puoci, F.; Iemma, F.; Spizzirri, U. G.; Picci, N., Gastro-intestinal sustained release of phytic acid by molecularly imprinted microparticles. *Pharmaceutical development and technology* **2010**, *15* (5), 526-31.
38. Beltran, A.; Marce, R. M.; Cormack, P. A.; Borrull, F., Synthesis by precipitation polymerisation of molecularly imprinted polymer microspheres for the selective extraction of carbamazepine and oxcarbazepine from human urine. *Journal of chromatography. A* **2009**, *1216* (12), 2248-53.
39. Caro, E.; Marcé, R. M.; Cormack, P. A. G.; Sherrington, D. C.; Borrull, F., Molecularly imprinted solid-phase extraction of naphthalene sulfonates from water. *Journal of Chromatography A* **2004**, *1047* (2), 175-180.
40. Hu, Y.; Pan, J.; Zhang, K.; Lian, H.; Li, G., Novel applications of molecularly-imprinted polymers in sample preparation. *TrAC Trends in Analytical Chemistry* **2013**, *43*, 37-52.
41. Martín-Esteban, A., Molecularly-imprinted polymers as a versatile, highly selective tool in sample preparation. *TrAC Trends in Analytical Chemistry* **2013**, *45*, 169-181.
42. Puoci, F.; Cirillo, G.; Curcio, M.; Iemma, F.; Parisi, O. I.; Spizzirri, U. G.; Picci, N., Molecularly Imprinted Polymers (MIPs) in Biomedical Applications. *Biopolymers* **2010**, 547-574.
43. Yan, M., *Molecularly imprinted materials: science and technology*. CRC press: 2004.
44. Jin, Y.; Chen, N.; Liu, R.; Chen, J.; Bai, L.; Zhang, Y., Preparation and evaluation of molecularly imprinted polymer of olivetol for solid phase extraction. *Se pu= Chinese journal of chromatography/Zhongguo hua xue hui* **2013**, *31* (6), 587-595.
45. Lok, C.; Son, R., Application of molecularly imprinted polymers in food sample analysis—a perspective. *International Food Research Journal* **2009**, *16* (2), 127-140.

46. Jin, Y.; Row, K. H., Adsorption isotherm of ibuprofen on molecular imprinted polymer. *Korean Journal of Chemical Engineering* **2005**, *22* (2), 264-267.
47. Chan, Y. T.; Kuan, W. H.; Chen, T. Y.; Wang, M. K., Adsorption mechanism of selenate and selenite on the binary oxide systems. *Water research* **2009**, *43* (17), 4412-4420.
48. Nishizawa, S.; Shigemori, K.; Teramae, N., A Thiourea-Functionalized Benzo-15-crown-5 for Cooperative Biding of Sodium Ions and Anions. *Chemistry Letters* **1999**, (11), 1185-1186.
49. Shigemori, K.; Nishizawa, S.; Yokobori, T.; Shioya, T.; Teramae, N., Selective binding of very hydrophilic H₂PO₄⁻ anion by a hydrogen-bonding receptor adsorbed at the 1, 2-dichloroethane–water interface. *New journal of chemistry* **2002**, *26* (9), 1102-1104.
50. Aoki, H.; Hasegawa, K.; Tohda, K.; Umezawa, Y., Voltammetric detection of inorganic phosphate using ion-channel sensing with self-assembled monolayers of a hydrogen bond-forming receptor. *Biosensors and Bioelectronics* **2003**, *18* (2), 261-267.
51. Pardeshi, S.; Dhodapkar, R.; Kumar, A., Influence of porogens on the specific recognition of molecularly imprinted poly(acrylamide-co-ethylene glycol dimethacrylate). *Composite Interfaces* **2013**, *21* (1), 13-30.
52. Fitzhenry, L.; Manesiotis, P.; Duggan, P.; McLoughlin, P., Molecularly imprinted polymers for corticosteroids: impact of polymer format on recognition behaviour. *Microchimica Acta* **2013**, *180* (15-16), 1421-1431.
53. Phutthawong, N.; Pattarawarapan, M., Synthesis of highly selective spherical caffeine imprinted polymers via ultrasound - assisted precipitation polymerization. *Journal of Applied Polymer Science* **2013**, *128* (6), 3893-3899.
54. Sathishkumar, M.; Binupriya, A.; Kavitha, D.; Selvakumar, R.; Jayabalan, R.; Choi, J.; Yun, S., Adsorption potential of maize cob carbon for 2, 4-dichlorophenol removal from aqueous solutions: equilibrium, kinetics and thermodynamics modeling. *Chemical Engineering Journal* **2009**, *147* (2), 265-271.
55. Le Noir, M.; Lepeuple, A.-S.; Guieysse, B.; Mattiasson, B., Selective removal of 17β-estradiol at trace concentration using a molecularly imprinted polymer. *Water research* **2007**, *41* (12), 2825-2831.
56. Umpleby li, R. J.; Baxter, S. C.; Bode, M.; Berch Jr, J. K.; Shah, R. N.; Shimizu, K. D., Application of the Freundlich adsorption isotherm in the characterization of molecularly imprinted polymers. *Analytica chimica acta* **2001**, *435* (1), 35-42.
57. Dai, C.-m.; Zhang, J.; Zhang, Y.-l.; Zhou, X.-f.; Duan, Y.-p.; Liu, S.-g., Removal of carbamazepine and clofibrac acid from water using double templates–molecularly imprinted polymers. *Environmental Science and Pollution Research* **2013**, *20* (8), 5492-5501.
58. Matsui, J.; Miyoshi, Y.; Doblhoff-Dier, O.; Takeuchi, T., A molecularly imprinted synthetic polymer receptor selective for atrazine. *Analytical chemistry* **1995**, *67* (23), 4404-4408.
59. Malitesta, C.; Losito, I.; Zambonin, P. G., Molecularly imprinted electrosynthesized polymers: new materials for biomimetic sensors. *Analytical chemistry* **1999**, *71* (7), 1366-1370.
60. Pan, J.; Xu, L.; Dai, J.; Li, X.; Hang, H.; Huo, P.; Li, C.; Yan, Y., Magnetic molecularly imprinted polymers based on attapulgite/Fe₃O₄ particles for the selective recognition of 2, 4-dichlorophenol. *Chemical Engineering Journal* **2011**, *174* (1), 68-75.

61. Liu, Q.-S.; Zheng, T.; Wang, P.; Jiang, J.-P.; Li, N., Adsorption isotherm, kinetic and mechanism studies of some substituted phenols on activated carbon fibers. *Chemical Engineering Journal* **2010**, *157* (2–3), 348-356.
62. Lin, J. M.; Nakagama, T.; Uchiyama, K.; Hobo, T., Temperature effect on chiral recognition of some amino acids with molecularly imprinted polymer filled capillary electrochromatography. *Biomedical Chromatography* **1997**, *11* (5), 298-302.
63. O'Shannessy, D. J.; Ekberg, B.; Mosbach, K., Molecular imprinting of amino acid derivatives at low temperature (0 C) using photolytic homolysis of azobisnitriles. *Analytical biochemistry* **1989**, *177* (1), 144-149.



Chapter 5
Cu isotopic fractionation of
urolithiasis

5. Cu isotopic fractionation of urolithiasis

5.1. introduction

About 25 elements are recognized as essential for human or animal life. Among them, 11 (Co, V, Cr, Mo, Mn, Ni, Cu, Zn, Se, Si, I) are present in trace amounts. Most of them are part of metalloenzymes and participate in biological functions, such as oxygen transport, free radical scavenging, structural organization of macromolecules, and hormonal activity. Other trace elements, such as Al, As, Cd, Hg, and Pb, and even essential ones, in quantities exceeding the needs of the organism, have known toxic effects on human health. Growing concern exists over the possible consequences on human health of new elements, such as Pt, Rh, Pd, Ga, and Ir, now widely used in the electronics industry and in catalytic converters¹. In industrialized societies, symptoms of severe deficiencies of trace elements are rarely seen, although they may occur in association with other pathological conditions, affecting the gastrointestinal absorption of nutrients, such as Crohn's disease, intestinal lymphoma, and gluten-free induced enteropathy¹.

5.1.1. Cu in body

Copper (Cu) is an essential trace metal found in all living organisms in the oxidized Cu(II) and reduced Cu(I) states. It is required for survival and serves as an important catalytic cofactor in redox chemistry for proteins that carry out fundamental biological functions that are required for growth and development^{2,3}. In excess of cellular needs, Cu can be cytotoxic^{4,5}.

Copper is an essential micronutrient. Some enzymes and biological processes where it plays a central role are given in Table 5.1⁶.

Table 5.1 Biological processes involving Cu-binding enzymes or proteins⁶

Function	Enzyme/protein
Iron mobilization	Caeruloplasmin (ferroxidase I), hephaestin
Antioxidant defence	Cu,Zn-superoxide dismutase (SOD1), caeruloplasmin, metallothionein
Cu transport	Caeruloplasmin, albumin, transcuprein, ATP7A, ATP7B, CTR1
Formation of connective tissue	Lysyl oxidase, cartilage matrix glycoprotein
Electron transport	Cytochrome C oxidase (CCO)
Blood clotting	Blood clotting factors V and VIII
Deamination of primary amines	Amine oxidases
α -amidation of neuropeptides	Peptidylglycine monooxygenase
Pigment production e.g. melanin	Tyrosinase
Catecholamine metabolism	Dopamine b-monoxygenase
Oxidation of phenylalanine to tyrosine	Phenylalanine hydroxylase
Metal detoxification	Glutathione
Cu Chaperones	ATOX1: delivery of Cu to ATP7A and ATP7B CCS: delivery of Cu to SOD1 Cox17: delivery of Cu to CCO in mitochondria

In addition, Cu may manifest its toxicity by displacing other metal cofactors from their natural ligands. The replacement of Zn(II) by Cu(II) in the zinc-finger DNA binding domain of the human estrogen receptor renders this protein defective, altering its role in hormone-dependent signal transduction *in vivo*⁷. Thus, precise regulatory mechanisms must be in place to prevent the accumulation of Cu ions to toxic levels⁸. The ingested Cu is absorbed and distributed to copper-requiring proteins. Excretion is the main factor controlling homeostasis. The essential role of Cu in the cardiovascular system has been

demonstrated in many clinical and experimental studies. Most clinical studies identified the correlation between low Cu concentrations and the incidence of cardiovascular diseases⁸.

Although copper deficiency is rare, it may occur when there is a genetic defect in the functioning of a copper transporter (ATP7A), resulting in Menkes disease or the milder Occipital Horn Syndrome. Menkes and Wilson's diseases (WDs), human genetic diseases in Cu transport, have revealed the importance of maintaining appropriate Cu homeostasis⁹. Moreover, Cu is essential for efficient iron uptake and mobilization in mammals^{5,10}.

5.1.2. Isotopic fractionation

5.1.2.1. Stable isotope

Stable isotope ratios of chemical elements in environmental samples contain valuable information on sources and processes which have influenced the history of the samples. A lack of suitable techniques to resolve natural variations in the stable isotope composition of heavy metal elements, prevented further progress for a long time. Analytical developments and methodological improvements over the last two decades have now expanded the feasibility of high-precision stable isotope analyses to almost the entire periodic table and thereby triggered the development of a new scientific field¹¹.

Even though the behavior of the different isotopes of an element is quite similar in most chemical reactions, the small mass differences between the isotopes can cause slight differences in physicochemical properties and reactivity. Most elements in the periodic table contain more than one stable isotopes (only 21 elements have only one stable isotope). The elements that consist of mixtures of two or more stable isotopes have the potential to allow deducing information about their environmental or biological cycling from stable isotope variations¹¹.

Copper has two stable isotopes, ⁶³Cu and ⁶⁵Cu, with relative abundances of 69.2% and 30.8%, resulting in an atomic mass of 63.546 g/mol.

5.1.3. Stable isotope fractionation

Stable isotope variations are reported as relative values compared with reference materials. This has analytical reasons because absolute isotope ratios are more difficult to measure with high precision and accuracy. Additionally, it is essential that results of different laboratories can be related to each other, which requires defining common reference materials as “zero baseline” for isotopic analyses of elements. Therefore, stable isotope data are expressed as delta values (δ) by normalizing isotope ratios in samples to the ratio of a standard material, which can be expressed by the following equation:

$$\delta^x E = \frac{(^x E / ^y E)_{\text{sample}}}{(^x E / ^y E)_{\text{standard}}} - 1 \quad (5-1)$$

where x and y represent isotopes of the element E. Because the resulting values are usually small, delta values are expressed in parts per thousand by multiplying by 1000 and adding the permil sign (‰). Stable isotope ratios are expressed with heavy isotopes in the numerator (x) and light isotopes in the denominator (y), “heavy over light”. Thus, positive values indicate relative enrichments of heavy isotopes and negative values relative enrichments of light isotopes compared with the reference material possessing a value of 0‰.

Stable isotope fractionation causes a shift in the isotope ratio between reactant and product of a reaction. Stable isotope fractionation in natural samples can be divided into kinetic and equilibrium effects. Kinetic isotope effects are caused by different reaction rates of light and heavy isotopes and are only preserved in incomplete processes¹¹. Equilibrium isotope effects occur when two phases react with forward and backward reactions proceeding at equal rates. In this case, the relative isotopic abundance is controlled by energy differences in bonding environments of reaction partners which have reached isotopic equilibrium¹¹.

5.2. Experiments

5.2.1. Reagents and materials

Nitric acid (HNO₃), Optima grade, Fisher Chemical, France

Nitric acid (HNO₃), trace metal grade, J.T. Baker

Nitric acid (HNO₃), technical grade, J.T. Baker

Hydrochloric acid (HCl), 37% Optima grade, Fisher Chemical, France

Hydrochloric acid (HCl), 37% ULTREX[®] ultrapure, J.T. Baker.

Hydrochloric acid (HCl), 37%, trace metal grade, J.T. Baker

Hydrochloric acid (HCl), 37%, technical grade, J.T. Baker

Hydrogen peroxide (H₂O₂), 30% ULTREX[®] ultrapure, J.T. Baker.

Hydrogen peroxide (H₂O₂), 30%, Optima grade, Fisher Chemical, France

5.2.1.1. Certified reference materials

SRM 2976 (NIST), Mussel tissue (trace elements and methylmercury)

SRM 2974a (NIST), Organics in freeze-dried mussel tissue (*mytilus edulis*)

SRM 1566b (NIST), Oyster tissue

SRM1573a (NIST), Tomato leaves

SRM 2977 (NIST), Mussel tissue (organic contaminants and trace elements)

BCR 710 (IRMM), oyster tissue

ERM-CE464 (IRMM), tuna fish

CRM 482 (IRMM), lichen

5.2.1.2. Chromatography materials

Macroporous anion-exchange resin AGMP-1, 100–200 mesh, mesh was purchased from Biorad Laboratories. PolyPrep columns (Bio-Rad Laboratories, Inc.).

Ultra-pure water (resistivity ≥ 18.2 M Ω cm) obtained from a Direct-Q3 system (Millipore, Molsheim, France) was used to prepare all solutions.

All digestion, isolation and dilution protocols were carried out in class-10 clean lab. Savillex[®] PFA vials were used throughout the study for sample handling. Multi-element and single-element standard solutions used for quantitative analysis and the Zn single-

element standard solution used for mass bias correction were prepared from commercially available 1000ppm stock solutions with proper dilution with 2% HNO₃.

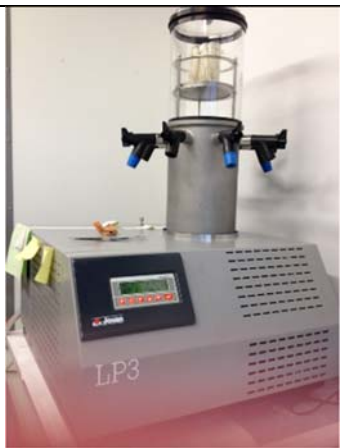
All labware (tips, columns, Savillex[®] PFA vials) was washed successively with 10% analytical grade HNO₃ twice, and 10% trace metal grade HCl.

5.2.2. Equipment and methodology

5.2.2.1. Lyophilizer

The serum and red cell samples were freeze-dried in lyophilizer for 15 hour. When the freeze-drying process was completed, the obtained sample could be used for the digestion procedure. The Freeze-drying works by freezing the material and then reducing the surrounding pressure to allow the frozen water in the material to sublimate directly from the solid phase to the gas phase. Equipment description is specified in table 5.2.

Table 5.2 Lyophilizer employed in the present study.

Equipment	Lyophilizer
Models	PL3
Manufacturer	Jouan, France
Laboratory of analysis	Centre Grup de Tècniques de Separació en Química (GTS),UAB, Barcelona, Spain
Image	

5.2.2.2. High Pressure Asher (HPA)

High Pressure Asher is an ultimate wet digestion device. Wet chemical pressure decomposition has established itself as a versatile, high-performance method for sample preparation for element determination using AAS, ICP-OES, ICP-MS or voltammetry. The samples and acids are placed in closed vessels inside a pressure vessel. This pressure vessel is filled with nitrogen up to 130 bar pressure and heated up to a maximum of 320 °C using a preselected temperature program. The surrounding nitrogen pressure compensates the reaction pressure which arises in the vessels and prevents the vessels opening or bursting. After the reaction, the pressure vessel is cooled down, ventilated and the vessels can be removed without pressure. The HPA-S acid digestion method is an internationally recognized reference procedure and is in operation as a high-performance routine instrument in numerous laboratories. The High Pressure Asher HPA–S is the reference instrument for wet chemical pressure decomposition. The nitrogen in the autoclave ensures the complete seal. In this study the HPA was used for the digestion of the available reference materials (oyster and mussel samples). Equipment description is specified in table 5.3.

Table 5.3 High Pressure Asher employed in the sample digestion.


Equipment	High Pressure Asher
Models	HPA-S
Manufacturer	Anton Paar, Graz, Austria
Laboratory of analysis	Laboratoire de Chimie Analytique Bio-Inorganique et Environnement(LCABIE), Institut Pluridisciplinaire de Recherche sur l'Environnement et les Matériaux, Pau, France



5.2.2.3. Microwave digestion

The microwave digestion system was used to digest the blood sample. The process was accomplished by heating the sample up to 180°C for 90 min. Equipment description is specified in table 5.4.


Table 5.4 Microwave digestion system employed in the extraction procedure.

Equipment	CEM Mars 5 Accelerated Microwave System
Models	Mars 5
Manufacturer	CEM corporation, Matthews, USA
Laboratory of analysis	Centre Grup de Tècniques de Separació en Química (GTS),UAB, Barcelona, Spain
Image	

5.2.2.4. Hot block

The hot block was used to dry and evaporate the sample. The temperature range: from ambient to 105°C. The hot block can heat 36 digestion cups of 50ml at the same time. Equipment description is specified in table 5.5.

Table 5.5 Hot block employed in the present study.

Equipment	Hot block
Models	SC100-36
Manufacturer	Environmental Express, South Carolina, USA
Laboratory of analysis	Laboratoire de Chimie Analytique Bio-Inorganique et Environnement(LCABIE), Pau, France
Image	

5.2.2.5. ICP-MS measurement

ICP-MS is a type of mass spectrometry that is highly sensitive and capable of the determination of a range of metals and several nonmetals at concentrations below one part in 10^{-12} (part per trillion). It is based on coupling together an inductively coupled plasma as a method of producing ions (ionization) with a mass spectrometer as a method of separating and detecting the ions. The elements concentrations of digestion sample were measured by ICP-MS technique. The NexION 300× offers simple operation through PerkinElmer's Syngistix™ software for ICP-MS, a new workflow-based software also designed to improve efficiencies in the laboratory. Equipment description is specified in Table 5.6. For determination of Cu concentration in serum and red cell samples extracted

after microwave digestion, the ICP-MS Element X Series 2 in GTS was used (see Table 3.5 in Chapter 3), the operational conditions and measurement parameters are described in table 5.7. While for the oyster and mussel samples, the ICP-MS NexION 300× in UT2A was used (table 5.6) and the instrumental operating conditions are specified in table 5.8.

Table 5.6 ICP-MS employed in the present study.


Equipment	ICP-MS
Models	NexION 300×
Manufacturer	Perkin Elmer, Inc., USA
Laboratory of analysis	UT2A, Université de Pau et des Pays de l'Adour (UPPA), Pau, France
Image	

Table 5.7 Instrumental operating conditions for ICP-MS system (Thermo X series II)

<i>ICP system</i>	
Instrument	Thermo X series II ICP-MS
RF power	1350W
Auxiliary gas flow	0.92 L min ⁻¹
Coolant gas flow	13.30 Lmin ⁻¹
Nebulizer gas flow	0.89 Lmin ⁻¹
Sample cone	Pt, 1.0 mm orifice
Skimmer cone	Pt, 0.7 mm orifice

Resolution	normal
Nebulizer	concentric nebulizer (Thermo)
<i>Sample introduction system</i>	
Sample uptake flow rate	2 mL min ⁻¹
Delay time	60s
Wash time	50s (HNO ₃ 2%)
<i>Data acquisition parameters</i>	
Analyzer	quadrupole
Scanning mode	peak jumping
Sweep per reading	30
Number of replicates	3
Dwell time	10ms

Table 5.8 Instrumental operating conditions for ICP-MS system (NexION 300×)

<i>ICP system</i>	
Instrument	NexION 300× ICP-MS
RF power	1450W
Auxiliary gas flow	1.2 L min ⁻¹
Plasma gas flow	15 Lmin ⁻¹
Nebulizer gas flow	0.94 Lmin ⁻¹
Analog stage voltage	-1787
Pulse stage voltage	1100
Discriminator threshold	12
Deflector voltage	-4.5
Cell entrance voltage	-6
Cell exit voltage	-6
<i>Data acquisition parameters</i>	

Analyzer	quadrupole
Scanning mode	peak jumping
Sweep per reading	30
Number of replicates	3
Dwell time	25ms


5.2.2.6. Inductively Coupled Plasma Optical Emission Spectrometer (ICP-OES) measurement

Inductively coupled plasma optical emission spectrometry (ICP-OES) is a powerful tool for the determination of metals in a variety of different sample matrices. With this technique, liquid samples are injected into a radiofrequency (RF)-induced argon plasma using one of a variety of nebulizers or sample introduction techniques. The sample mist reaching the plasma is quickly dried, vaporized, and energized through collisional excitation at high temperature. The atomic emission emanating from the plasma is viewed in either a radial or axial configuration, collected with a lens or mirror, and imaged onto the entrance slit of a wavelength selection device. The wavelength of the photons can be used to identify the elements from which they originated. The total number of photons is directly proportional to the concentration of the originating element in the sample.

Simultaneous multielement determinations are performed for up to 70 elements with the combination of a polychromator and an array detector. The analytical performance of such systems is competitive with most other inorganic analysis techniques, especially with regards to sample throughput and sensitivity¹².

In this study the ICP-OES was used to measure the concentration of sodium (Na) and alkaline metals (Ca, Mg) from the sample after column separation in order to make sure the removal of these interferences elements. Equipment description is specified in table 5.9.

Table 5.9 ICP-OES employed in the present study.

Equipment	ICP-OES
Models	Iris advantage 200
Manufacturer	Thermo Jarrel Ash
Laboratory of analysis	Laboratoire de Chimie Analytique Bio-Inorganique et Environnement(LCABIE), Institut Pluridisciplinaire de Recherche sur l'Environnement et les Matériaux, Pau, France
Image	

5.2.2.7. Multicollector-Inductively Coupled Plasma Mass Spectrometer (MC-ICP-MS) Instrumentation

Multicollector-Inductively Coupled Plasma Mass Spectrometer (MC-ICP-MS) is an instrument that measures isotopic ratios that are used in geochemistry, geochronology, and cosmochemistry. A MC-ICP-MS is a hybrid mass spectrometer that combines the advantages of superior ionization of an inductively coupled plasma source and the precise measurements of a magnetic sector multicollector mass spectrometer. The primary advantage of the MC-ICP-MS is its ability to analyze a broader range of elements, including those with high ionization potential that are difficult to analyze by TIMS. The ICP source also allows flexibility in how samples are introduced to the mass spectrometer and allows the analysis of samples introduced either as an aspirated solution or as an aerosol produced by laser ablation.

As a hybrid mass spectrometer, MC-ICP-MS are composed of three primary components (Figure 5.1):

- 1) an inductively coupled plasma ion source, where ions are produced, accelerated, and focused;
- 2) an energy filter and magnetic sector analyzer, where the ions are focused and filtered to produce a beam where the ions have the same approximate energy and can be separated based on their mass/charge ratios; and
- 3) a series of collectors, where the ion beams are measured simultaneously.

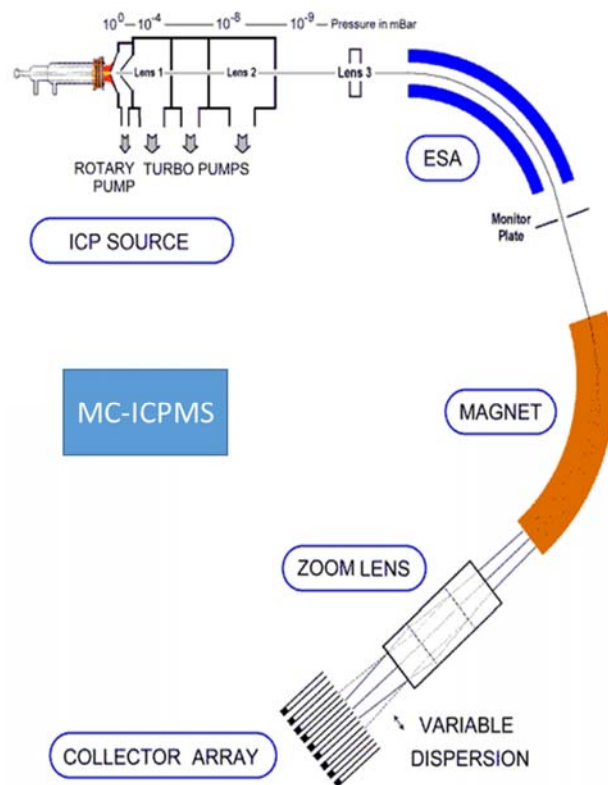


Figure 5.1. Main parts of a MC-ICP-MS

The ions are produced by introducing the sample into an inductively coupled plasma which strips off electrons thereby creating positively charged ions. These ions are accelerated across an electrical potential gradient (up to 10 KV) and focused into a beam via a series of slits and electrostatically charged plates. This ion beam then passes through an energy filter, which results in a consistent energy spectrum in the ion beam and then through a magnetic field where the ions are separated on the basis of their mass to charge ratio. These

mass-resolved beams are then directed into collectors where the ions reaching the collectors are converted into voltage. Isotope ratios are calculated by comparing voltages from the different collectors.

The electronics of these instruments must operate to very close tolerances in order to produce isotope ratios that are precise to 0.01-0.001%. In addition, a high vacuum needs to be maintained along the path of the ion beam in order to avoid scattering of the ions due to interaction with air molecules.

The advantages of MC-ICP-MS compared to other isotope ratio techniques include:

- ✓ the ionization efficiency is very high (near 100%) for most elements which enables analysis of most of the elements of the periodic table, including those with high ionization potential that are difficult to analyze by TIMS.
- ✓ the MC-ICP-MS operates essentially as a steady state system during the analysis resulting in time invariant mass fractionation.
- ✓ there is consistent mass bias variation across the mass range which allows the use of an adjacent element to calculate mass bias for those elements without > 2 stable isotopes
- ✓ the MC-ICP-MS permits flexibility in sample introduction systems. Solutions can be introduced at atmospheric pressure, which allow ease in handling. Laser ablation systems can also be coupled with the MC-ICP-MS, which allows in-situ isotopic measurements in solid materials.

The MC-ICP-MS specified in table 5.10., was the one used in this study to measure the isotopic fractionation. The instrument is designed to measure isotope ratios to high precision. This work was developed during a stay of four months in LCABIE.

Table 5.10 MC-ICP-MS employed in the determination.

Equipment	MC-ICP-MS
Model	Nu Plasma II
Manufacturer	Nu instruments, Wrexham, UK

Laboratory of analysis	Laboratoire de Chimie Analytique Bio-Inorganique et Environnement(LCABIE), Institut Pluridisciplinaire de Recherche sur l'Environnement et les Matériaux, Pau, France
Image	

The Nu Plasma is a double focusing magnetic sector instrument with 12 faraday collectors in fixed positions. The ion beams of the masses of interest are aimed into the collectors by variable dispersion ion optics ('zoom lens'). All collectors have a $10^{11} \Omega$ resistor allowing for a signal range from 0 to 10V. The MC-ICP-MS is operated in low resolution in order to have highest sensitivity.

Measuring conditions was adjusted for maximum sensitivity and stability, plasma robustness and minimum influence of interferences on the target analyte signals are optimized and the conditions and parameters are described in table 5.11.

Table 5.11. Instrumental operating conditions used for isotopic analysis of Cu.

Nu-MC-ICPMS	
RF power	1300W
Instrument resolution	Pseudo-high resolution ~5700(edge resolved power)
Source slit width	0.05 mm
Alpha 1 slit	80 mA
Alpha 2 slit	90 mA
Integration time	5 s

Plasma gas flow rate		13.0 L min ⁻¹													
Auxiliary gas flow rate		0.80 L min ⁻¹													
Nebulizer pressure		28.8 psi													
Faraday cup configuration															
collector	H7	H6	H5	H4	H3	H2	H1	Ax	L1	L2	IC0	L3	IC1	IC2	L4
<i>m/z</i>	65					63			62			61			

5.2.3. Digestion procedure

5.2.3.1. Oyster samples

In order to evaluate the performance of the developed method, 9 Oyster and 1 mussel sample were collected from 7 locations representative of Southern Europe (Figure 5.2). Arcachon and La Rochelle in France. Urdaibai, Ostranor, and Barcelona in Spain. Sado and Aveiro in Portugal. The oyster and mussel samples were collected by oyster farmers and then these samples were treated using following procedure (described in Figure 5.3) before send to the laboratory.



Figure 5.2. Location of oyster and mussel samples collection.

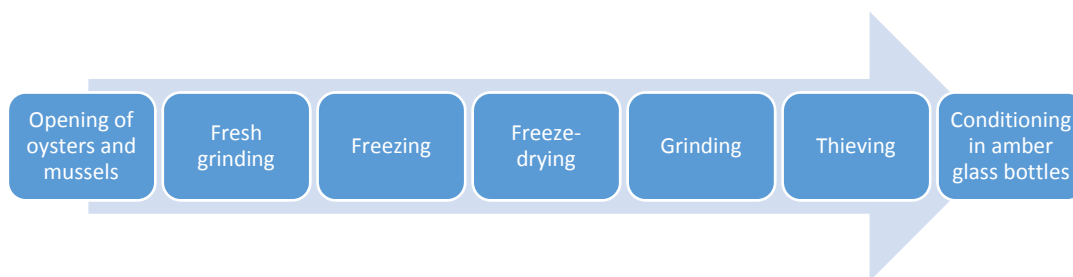


Figure 5.3. Treatment for oyster samples.

5.2.3.2. Oyster sample digestion procedure

For dried and powdered oyster samples and reference materials, 500 mg was weighed out into HPA flasks (50ml, quartz material). For predigestion, 4.5ml HNO₃ (Optima grade) was added overnight. Then 0.5ml 30% H₂O₂ (Optima grade) was added, gently shaken and left about 3 hours to decrease the bubbles. Then the digestion was performed in the high pressure digestion system HPA at 300°C for 4 hours. After the sample was cooled, it was located in ultrasonic bath for 1 hour, covering the flask with Teflon in order to release the dissolved nitrogen gas.

Then the digestion solution was transferred to 12 ml glass vials and 1ml×2times M.Q. water was used to rinse the HPA flask. Then the sample was stored in fridge until analyzed.

5.2.3.3. Blood samples

Blood and urine sample were collected from stone formers patients. The participants were recruited at Hospital Clinic, Barcelona, Spain. Urine samples were also collected. The whole volume of urine was collected in the same plastic bottle (2.2L), mixed and then stored at 4°C until the analysis was done. The blood sample collection was performed in compliance with institutional guidelines. The patients are between 30 and 84 years old, the average age for female donors are 55 years old and male donors are 60 years old. The blood samples were centrifuged at 5000 rpm during 15min to separate the red cells from the blood serum, and the serum was retained for isotope analysis. Blood serum and red cells were

kept at approximately -20°C until use. In this study, all the information(Cu concentration, Cu isotopic information) of the control group came from the research of Albarède et al.¹³.

Table 5.12. Cu concentration of serum and red cells in kidney stone patients.

ID	Gender	Age	Urine volume(ml)
1	woman	51	775
2	man	82	275
3	man	59	1050
6	woman	76	940
7	woman	61	200
8	man	84	810
9	man	52	500
10	man	64	650
11	woman	30	480
12	man	57	920
13	woman	59	665
14	man	74	1020
15	man	72	1350
16	man	50	1900
17	man	40	280
18	man	30	250
19	woman	54	700

5.2.3.4. Sample digestion procedure

2 ml of blood serum samples were first predigested at room temperature in 5 mL 16 M HNO₃, and 3 mL 30% H₂O₂, for 1 hour. Then the samples were digested in a MARS Microwave Digestion System at 200 °C, 300 psi for 90 min. Digested samples were then evaporated in Savillex vials, redissolved in 5 mL 0.1 M HNO₃ and stored in clean vials at

4°C in fridge until use. Three blank and reference material SRM1573a (NIST), tomato leaves were treated under the same condition.

2 ml of red cell samples were first predigested in 5 mL 16 M HNO₃, and 3 mL 30% H₂O₂, for 20 hours. Then the samples were digested a MARS Microwave Digestion System at 180 °C, 300 psi for 90 min. Digested samples were then evaporated in Savillex vials, redissolved in 5 mL 0.1 M HNO₃ and 1 ml 16M HNO₃, stored in clean vials at 4°C in fridge until use.

Sample aliquots of 0.1 mL of the digested solution were used for determination of the total element concentration by ICPMS. The digestion process was evaluated by the recovery of Cu in the reference material. The Cu was separated from these solutions and prepared for isotopic analysis using the method of ion-exchange column separation.

5.2.4. Clean-up procedure

The macroporous anion-exchange resin AGMP-1 100-200 mesh purchased from Bio-rad Laboratories was used as the solid phase to separate the Cu from matrix. Sample preparation and analysis was performed in Class 2 laminar flow hoods in the Class 1000 Clean Room at UAB.

Before the first use, the resin was settled 10 times in M.Q. water and the supernatant was decanted after sufficient settling time in order to eliminate the finest resin particles. The cleaned resin was stored in 0.1 M HCl.

The metals analyzed were separated on bio-rad columns containing 2 mL macroporous anion-exchange resin. The column was washed by acid and only used once in order to avoid contamination¹⁴. Before sample loading, the resin was cleaned three times with 1 M HNO₃ (10 mL) alternating with M.Q. water (2 mL). It was then conditioned with 10 ml of 7M HCl+0.001% H₂O₂. Samples were loaded onto the columns in 7 M HCl +0.001% H₂O₂. The matrix elements are washed off with 7M HCl+0.001% H₂O₂ (10 mL), then Cu was

eluted by the next 20 ml of the same solution. The purification protocol is summarized in Table 5.13. Figure 5.4 shows the column separation of Cu.

Table 5.13. Chromatographic separation sequence^{15,16}

Eluent	Acid Volume (ml)	Purpose
<i>Resin cleaning</i>		
1M HNO ₃	10	Clean
≥18MΩ cm water	2	Rinse
1M HNO ₃	10	Clean
≥18MΩ cm water	2	Rinse
1M HNO ₃	10	Clean
≥18MΩ cm water	10	Rinse
<i>Resin conditioning</i>		
7M HCl+0.001%H ₂ O ₂	10	Conditioning
<i>Sample loading</i>		
7M HCl+0.001%H ₂ O ₂	1	Loading
<i>Elution sequence</i>		
7M HCl+0.001%H ₂ O ₂	10	Matrix(e.g.Mg,Na,Al,Ca,Cr)
7M HCl+0.001%H ₂ O ₂	20	Cu

Resin type: AG MP-1, 100-200 mesh. Resin was loaded into single use, acid washed PolyPrep columns (Bio-Rad Laboratories, Inc.). Resin bed dimensions: height = 4 cm, volume = 2 ml.



Figure 5.4 Cu column separation

After purification, the Cu solutions were evaporated to dryness at 95°C overnight. The residue was dissolved in 7M HNO₃ (1 mL) and then this solution was separated using the same chromatographic procedure once again. Finally, the Cu fractions were evaporated to dryness and dissolved in 5ml 2% HNO₃. The total separated Cu from blood samples were determined using an ICP-MS instrument. The Cu isotopic compositions of samples were determined using a Nu Plasma HR MC-ICP-MS instrument.

5.2.5. Isotopic fractionation measurement

The purified Cu fraction was analyzed by ICP-MS prior to isotope analyses in order to obtain accurate total analyte concentrations, as well as to ensure the absence of interfering elements.

Prior to Cu isotope analysis samples, sample and isotope standards were diluted to a Cu concentration of 200µg L⁻¹ and matrix matched to 2% HNO₃ followed by addition of Zn at 200µg L⁻¹, for on-line mass bias correction. In this study, the NIST SRM 976 was used as delta zero reference material for Cu. No certified Zn reference material being available, the IRMM-3702 was used to correct the mass bias.

In order to calculate Cu isotope ratios from these signals, a linear regression slope (LRS) method, where the signal intensities for ^{65}Cu were plotted against the signal intensities for ^{63}Cu , was used. The slope of the regression curve provides the raw $^{65}\text{Cu}/^{63}\text{Cu}$ ratio, which is later corrected for mass bias applying Russell's exponential law¹⁵.

Results are reported as $\sigma^{65}\text{Cu}$ (Equation 5-2), which is the change in $^{65}\text{Cu}/^{63}\text{Cu}$ ratio in parts per thousand (‰), relative to the isotopic composition of reference material NIST SRM 976. By definition, $\sigma^{65}\text{Cu}_{\text{NIST SRM976}} = 0\text{‰}$.

$$\sigma^{65}\text{Cu} = \left[\left(\frac{^{65}/^{63}\text{Cu}_{\text{sample}}}{^{65}/^{63}\text{Cu}_{\text{NIST SRM976}}} \right) - 1 \right] \times 1000 \quad (5-2)$$

5.3. Results and Discussion

5.3.1. Cu extraction and clean-up procedure optimization

Acid digestion is the most commonly used method for the destruction of organic material in biological samples^{17, 18}. However, conventional hot plate digestion is normally very time-consuming and susceptible to contamination¹⁹. For example, digestion times as long as 3 hours have been needed to achieve complete digestion of urine²⁰. While microwave digestion is a common technique used to dissolve heavy metals in the presence of organic molecules. This technique is usually accomplished by exposing a sample to a strong acid in a closed vessel and raising the pressure and temperature through microwave irradiation.

It is highly recommended to separate the Cu from the blood matrix before isotopic analysis via MC-ICP-MS, not only for avoiding the influence of matrix-induced mass bias, but also because in ICP-MS both Cu isotopes may be subject to spectral overlap due to the occurrence of polyatomic ions with the same mass number. For the biological sample, the very high amount of alkane elements in blood samples is the most serious problem. The major molecular interferences that may be problematic for the isotopic measurement of Cu is listed in Table 5.14. For example, the sodium concentration is in the range of 3000 mg/L, can interfere with Cu at m/z 63 because of the formation of $^{40}\text{Ar}^{23}\text{Na}^+$ in ICP. Magnesium is another less important element which can give rise to $^{40}\text{Ar}^{25}\text{Mg}^+$, interfering with Cu at

m/z 65. ²¹Therefore, before Cu isotopic analysis, column separation of blood samples was carried out twice.

Table 5.14. Main molecular interferences for Cu and Zn isotopic analysis in biological samples.

Element	Mass	interference
Cu	63	²³ Na ⁴⁰ Ar ⁺ , ²⁵ Mg ³⁸ Ar ⁺ , ²⁶ Mg ³⁷ Cl ⁺ , ³¹ P ¹⁶ O ₂ ⁺ , ⁴⁷ Ti ¹⁶ O ⁺
	65	²⁵ Mg ⁴⁰ Ar ⁺ , ³² S ³³ S ⁺ , ³³ S ¹⁶ O ₂ ⁺ , ⁴⁹ Ti ¹⁶ O ⁺ , ¹³⁰ Ba ²⁺
Zn	64	⁴⁸ Ca ¹⁶ O ⁺
	66	⁵⁰ Cr ¹⁶ O ⁺

According to published data, the best way to carry out Cu isolation is by applying ion exchange chromatography, although careful validation of the protocol needs to be carried out as Cu is known to undergo on-column isotope fractionation. In this work, we deployed a separation method based on the use of AG-MP-1 strong anion exchange resin recently developed and validated in our research group for Cu isotopic analysis of oyster samples. It was thus necessary to check the performance of this method for serum samples, which was tested through analysis of one of the control samples for which a sufficient amount was available for performing replicate analyses.

Copper separation and purification was achieved through a column ion exchange chromatography using procedures adapted from Mason¹⁶ and Maréchal¹⁵. Since the blood sample contain significant quantities of Na, Mg, and other constituents, which must be removed to eliminate matrix effects and isobaric interferences.

Na and Mg are the major atomic interferences on Cu (²³Na⁴⁰Ar⁺, ²⁵Mg³⁸Ar⁺, ²⁶Mg³⁷Cl⁺ on ⁶³Cu and ²⁵Mg⁴⁰Ar⁺ on ⁶⁵Cu) and, although these elements are removed in the first column step, we use a second column filled with the same resin to ensure their complete removal. At acid concentrations of 7 M HCl, Cu is retained on the resin while the matrix passes through. The Cu fraction is evaporated to dryness and re-dissolved in 2% HNO₃ in preparation for isotopic analysis.

The resin AG MP-1 is a macroporous form of strongly basic anion exchange resin has higher distribution coefficients for Cu (II) in concentrated HCl than regular AG1. The macroporous resin AG MP-1 is made of chips instead of beads, is very fragile and tends to compact with time.

It was observed previously that the isotopic fractionation happened on resin AG MP-1 and the lighter isotope is preferentially retained on the resin ¹⁵. So this Cu fractionation on the column need purification achieved full recovery and the investigation of the elution curve is quite important. The elution curve of Cu obtained on the ion-exchange resin was shown on the figure 5.5.

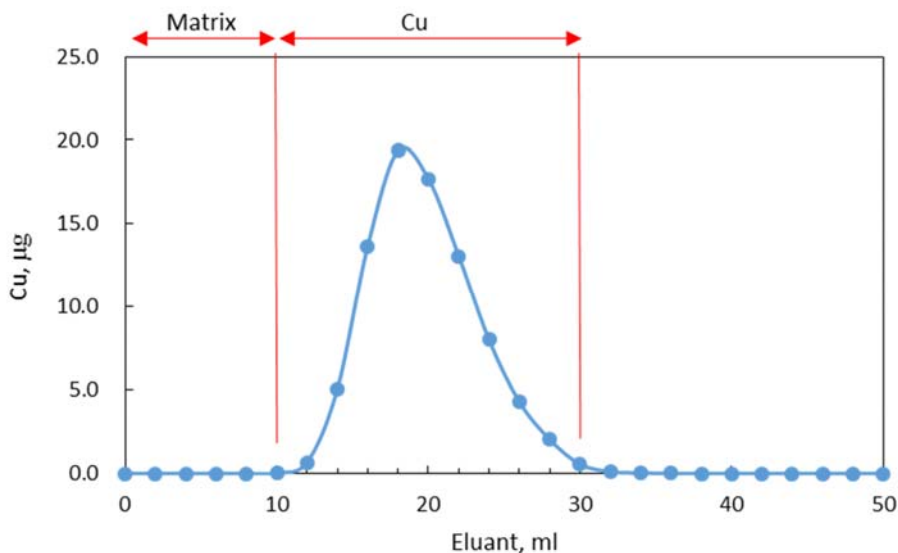


Figure 5.5. Elution curve of Cu on resin.

This separation procedure was validated by the oyster samples and reference materials. Cu recoveries were calculated after analysis of the digests and the eluted Cu fractions by means of ICP-MS, yielding an average of $100 \pm 9\%$ Cu recovery (data are shown in table 5.15), thus avoiding any effect from on-column isotope fractionation. The main interference elements after clean-up separation was also measured by ICP-MS or ICP-OES (data are shown in table 5.16). From table 5.16 we could see that the main interferences elements are eliminated effectively from the matrix. To monitor Cu recoveries along the study, all

of the samples targeted in the investigation were also analyzed for their Cu content after column separation, and the results obtained were compared with previously available concentration values. Near-quantitative Cu yields were obtained in all cases.

Table 5.15. Cu recovery after the clean-up procedure.

Sample	Cu recovery,%
SAMPLE Oyster 1	96
SAMPLE Oyster 2	107
SAMPLE Oyster 3	103
SAMPLE Oyster 4	95
SAMPLE Oyster 5	94
SAMPLE Oyster 6	92
SAMPLE Oyster 7	109
SAMPLE Oyster 8	96
SAMPLE Oyster 9	93
Oyster tissue 1566B	92
Mussel tissue 2976	97
Oyster tissue 1566B	93

Table 5.16. Main interferences elements concentration after the clean-up procedure (in ppm).

Samle	Cd	Zn	Ti	Ce	Sr	P	Mg	Ca	Na
SAMPLE Oyster 1	0.00	0.23	0.02	0.00	0.06	<LOQ	<LOQ	<LOQ	<LOQ
SAMPLE Oyster 2	0.00	-0.15	-0.05	0.00	0.09	<LOQ	<LOQ	<LOQ	<LOQ
SAMPLE Oyster 3	0.00	-0.06	0.01	0.00	-0.02	<LOQ	<LOQ	<LOQ	<LOQ
SAMPLE Oyster 4	0.00	0.09	-0.01	0.00	-0.04	<LOQ	<LOQ	<LOQ	<LOQ
SAMPLE Oyster 5	0.00	-0.17	-0.05	0.00	0.01	<LOQ	<LOQ	<LOQ	<LOQ
SAMPLE Oyster 6	0.00	-0.19	-0.05	0.00	0.02	<LOQ	<LOQ	<LOQ	<LOQ
SAMPLE Oyster 7	0.00	-0.20	-0.04	0.00	0.00	<LOQ	<LOQ	<LOQ	<LOQ
SAMPLE Oyster 8	0.00	-0.11	-0.04	0.00	-0.02	<LOQ	<LOQ	<LOQ	<LOQ
SAMPLE Oyster 9	0.00	-0.13	-0.03	0.00	-0.03	<LOQ	<LOQ	<LOQ	<LOQ
Mussel tissue 2976	0.00	-0.18	-0.03	0.00	-0.02	<LOQ	<LOQ	<LOQ	<LOQ
Mussel tissue 2974a	0.00	-0.20	-0.03	0.00	-0.03	<LOQ	<LOQ	<LOQ	<LOQ
Blank	0.00	-0.14	-0.03	0.00	-0.03	<LOQ	<LOQ	<LOQ	<LOQ
Oyster tissue 1566B	0.00	-0.11	-0.03	0.00	0.00	<LOQ	<LOQ	<LOQ	<LOQ
NIST 3133	0.00	0.00	-0.04	0.00	-0.05	<LOQ	<LOQ	<LOQ	<LOQ

5.3.2. Total Cu concentration in blood.

The Cu concentration of serum and red cell sample from patients and healthy control are summarized in Table 5.17. The differences among the groups are evident. The red cell sample of urolithiasis patients show significantly higher Cu values than the serum sample (either male or female). The Cu concentration in serum ranged between 500-1200 $\mu\text{g/L}$ and in red cell 1600-2600 $\mu\text{g/L}$. The Cu concentration in whole blood found in the bibliography was in the range, 800-1100 $\mu\text{g/L}$ for males and 1000-1400 $\mu\text{g/L}$ for females²². In the present study for males the Cu concentration is in the range, 730-1400 $\mu\text{g/L}$ for serum and 1800-2700 $\mu\text{g/L}$ for red cells. While in the healthy control for males, 350-1200 $\mu\text{g/L}$ for serum and 500-800 $\mu\text{g/L}$ for red cells. In the present study for females the Cu concentration is in the range, 440-1160 $\mu\text{g/L}$ for serum and 1630-2900 $\mu\text{g/L}$ for red cells. While in the healthy control for males, 940-2800 $\mu\text{g/L}$ for serum and 500-1700 $\mu\text{g/L}$ for red cells.

Table 5.17. Cu concentration of serum and red cells in kidney stone patients and control group.

kidney stone patients			Healthy control(data from ¹³)		
Serum		Red cell	Serum		Red cell
ID	Cu conc.,ppb	Cu conc.,ppb	ID	Cu conc.,ppb	Cu conc.,ppb
1	1100	1630	C1	1156	1016
2	1090	2750	C2	1586	962
3	750	2020	C3	976	928
6	570	2220	C4	2816	1705
7	440	1740	C5	2271	1055
8	730	2170	C6	2271	1003
9	820	2740	C7	2165	982
10	1430	2090	C8	896	890
11	1010	2460	C9	1927	1029
12	1200	2710	C10	966	924
13	1160	2890	C11	973	863
14	880	1810	C12	1086	802
15	820	2310	C13	966	766
16	1130	2500	C14	1634	738
17	790	2200	C15	941	701

18	880	2570	C16	1547	606
19	1140	2630	C17	1899	902
			C18	1801	761
			C19	1082	686
			C20	1216	639
			C21	1715	809
			C22	1917	764
			C23	1151	717
			C24	2135	381
			C25	1738	667
			C26		735
			C27		541
			C28		478
			C29	1210	635
			C30	815	557
			C31	701	670
			C32	733	499
			C33	907	687
			C34	675	545
			C35	926	656
			C36	967	591
			C37	750	653
			C38	492	530
			C39	728	716
			C40	698	560
			C41	928	635
			C42	801	713
			C43	875	669
			C44	352	728
			C45	761	670
			C46	753	587
			C47	844	725
			C48	912	761
			C49	883	716

5.3.3. Correction for mass discrimination

Standards solution and samples were measured in 2% HNO₃ solution at the same condition than the blood samples. All the measurements were performed in low-resolution mode. Of the methods available for correcting instrumental mass discrimination, the double spike approach has been shown to be a robust and rigorous technique when applied to isotope systems²³. In this study, Zn standard IRMM-3702 and Cu standard NIST 976 were used for the mass correction. The advantages of using the double-spike method are well known and include elimination of issues concerning differences in the behavior of samples and dopant or standards, used respectively in the doping and standard-bracketing methods, and removing potential fractionation problems induced due to incomplete yield from the column chemistry²⁴.

As long as the f values vary but $f_{\text{Cu}} / f_{\text{Zn}}$ ratio remains constant, the two isotopic ratios of Cu and Zn of a sample should form a linear array in a log – log plot. When $\ln(^{65}\text{Cu}/^{63}\text{Cu})_{\text{meas}}$ (‘meas’ means measure) is plotted against $\ln(^{68}\text{Zn}/^{64}\text{Zn})_{\text{meas}}$, the slope s is

$$s = \frac{f_{\text{Cu}} \ln(65/63)}{f_{\text{Zn}} \ln(68/64)} \quad (5-3)$$

and the intercept y_0

$$y_0 = \ln\left(\frac{^{65}\text{Cu}}{^{63}\text{Cu}}\right)_{\text{true}} - s \times \ln\left(\frac{^{68}\text{Zn}}{^{64}\text{Zn}}\right)_{\text{true}} \quad (5-4)$$

$$f = \frac{\ln(r/R)}{\ln(M_2/M_1)} \quad (5-5)$$

The exponential law was used to describe real instrumental data, for example, if $f_{\text{Cu}}=f_{\text{Zn}}$, then a plot of measured, uncorrected Cu and Zn isotopes in ln-ln space should yield a straight line of a pre-defined slope [$\ln(\text{mass } ^{65}\text{Cu}/\text{mass } ^{63}\text{Cu})/\ln(\text{mass } ^{66}\text{Zn}/\text{mass } ^{64}\text{Zn})$] = 1.015. Isotopic variations of Cu and Zn are shown in figure 5.6 and figure 5.7. In figure 5.6, $\ln(^{68}\text{Zn}/^{64}\text{Zn})$ and $\ln(^{66}\text{Zn}/^{64}\text{Zn})$ are plotted. As it can be seen that the isotopic variations of $^{68}\text{Zn}/^{64}\text{Zn}$ and $^{66}\text{Zn}/^{64}\text{Zn}$ following a mass dependent fractionation relationship with a slope of 2.015 not significantly different from the theoretical value¹⁵. In figure 5.7, $\ln(^{65}\text{Cu}/^{63}\text{Cu})$ and $\ln(^{66}\text{Zn}/^{64}\text{Zn})$ are plotted. As it can be seen that the isotopic variations of

$^{65}\text{Cu}/^{63}\text{Cu}$ and $^{66}\text{Zn}/^{64}\text{Zn}$ following a mass dependent fractionation relationship with a slope of 0.9981 not significantly different from the theoretical value..

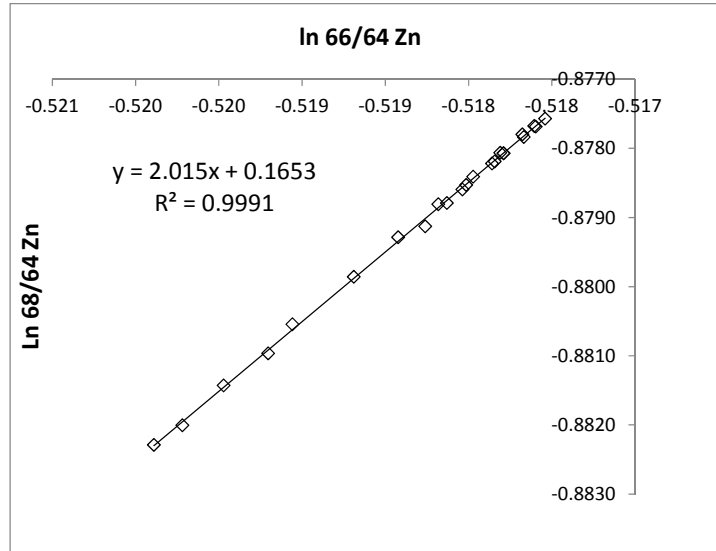


Figure 5.6. Isotopic variations of $^{68}\text{Zn}/^{64}\text{Zn}$ and $^{66}\text{Zn}/^{64}\text{Zn}$ following a mass dependent fractionation relationship with a slope not significantly different from the theoretical value.

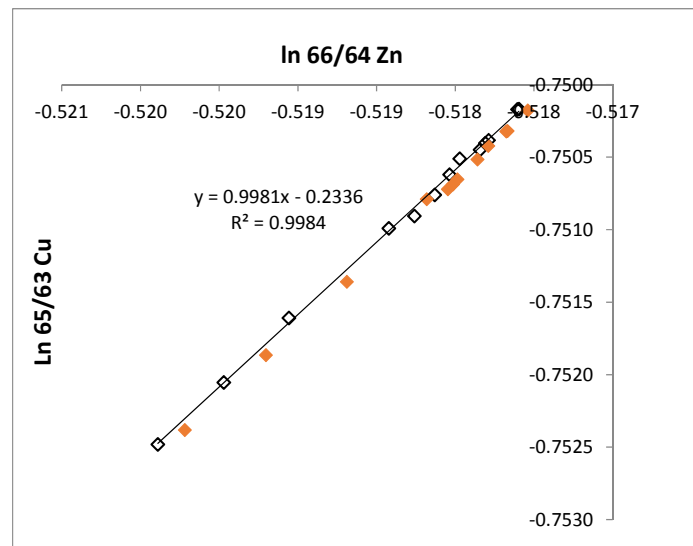


Figure 5.7. Isotopic variations of $^{65}\text{Cu}/^{63}\text{Cu}$ and $^{66}\text{Zn}/^{64}\text{Zn}$ following a mass dependent fractionation relationship with a slope not significantly different from the theoretical value.

In addition, long-term external reproducibility for the digestion, purification and isotope analysis is defined by the processing and analysis of NIST 1573a tomato leaves. This standard was measured as $\delta^{65}\text{Cu} = 0.54$, which is in the range of $\delta^{65}\text{Cu} = 0.63 \pm 0.16 \text{ ‰}$ (mean \pm 2SD) reported by Ryan et al.²⁵.

5.3.4. Cu isotopic analysis of serum and red cell samples

Finally the samples were analyzed following the optimized procedure indicated previously. Due to the low amount of sample available, all samples were analyzed only once. The Cu isotopic composition of serum and red cells for the urolithiasis patients is summarized in Table 5.18 together with the total Cu concentration expressed for the different groups. As seen in this table, all the samples are enriched in the heavier isotope except the serum samples of the control group, as remarks the negative sign, although differences among the groups are evidenced. The serum and red cell samples of urolithiasis patients show significantly higher $\delta^{65}\text{Cu}$ values than the controls (either male or female). For the males, the Cu isotopic fractionation seems to a lesser extent.

Table 5.18 Cu isotopic component of serum and red cell for different groups of individuals studied.

group		serum		red cell	
		Cu conc.	$\delta^{65}\text{Cu}$ (‰)	Cu conc.	$\delta^{65}\text{Cu}$ (‰)
Urolithiasis patients	Males (n=11)	956 \pm 224	0.06 \pm 0.24	2352 \pm 322	0.86 \pm 0.21
	Female (n=6)	903 \pm 316	0.20 \pm 0.24	2262 \pm 499	0.94 \pm 0.22
	Total (n=17)	938 \pm 251	0.11 \pm 0.24	2262 \pm 499	0.90 \pm 0.21
Control group	Males (n=21)	798 \pm 171	-0.28 \pm 0.40	648 \pm 76	0.67 \pm 0.36
	Female (n=28)	1553 \pm 536	-0.24 \pm 0.36	823 \pm 238	0.46 \pm 0.47
	Total (n=49)	1200 \pm 555	-0.26 \pm 0.40	746 \pm 207	0.56 \pm 0.50

Cu concentration in serum of female urolithiasis patients ($903 \pm 316 \mu\text{g l}^{-1}$) were significantly lower than those in healthy control ($1553 \pm 536 \mu\text{g l}^{-1}$). It is need to mention that the age of the female urolithiasis is in the range of 30-76, and the female healthy control is in the range 19-38. However, for male urolithiasis patients the concentration of Cu ($956 \pm 224 \mu\text{g l}^{-1}$) is no significant difference compared with the healthy control ($798 \pm 171 \mu\text{g l}^{-1}$).

These differences among samples from different groups become even more evident when isotopic information is combined with total Cu concentration data, as shown in Figure 5.8 and Figure 5.9. In these figures, a bivariate “Cu concentration” vs. “ $\delta^{65}\text{Cu}$ ” plot, the different groups can be perfectly differentiated.

Data obtained for urolithiasis patients suggest that a possible Cu isotopic drift of the Cu stores is expected to occur because they preferentially retained ^{65}Cu relative to ^{63}Cu .

It was claimed that the low efficiency by which Cu is incorporated into ceruloplasmin in Wilson’s disease patients apparently results in ^{63}Cu enrichment in the serum samples²¹. It was reported that a relationship exists between age and blood $\delta^{65}\text{Cu}$ values, with enrichment in light Cu isotopes in blood of elderly people. We suggest that this observation could be due to the preferential retention of light Cu isotopes by the body^{26,27}.

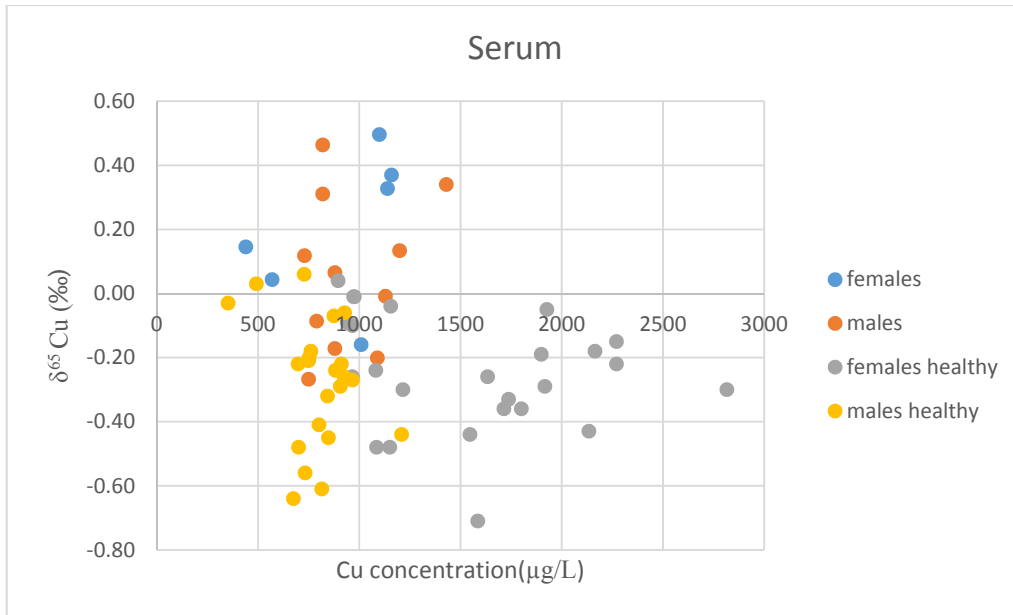


Figure 5.8 “concentration vs. isotopic information” plot for the serum samples of different groups of individuals considered.

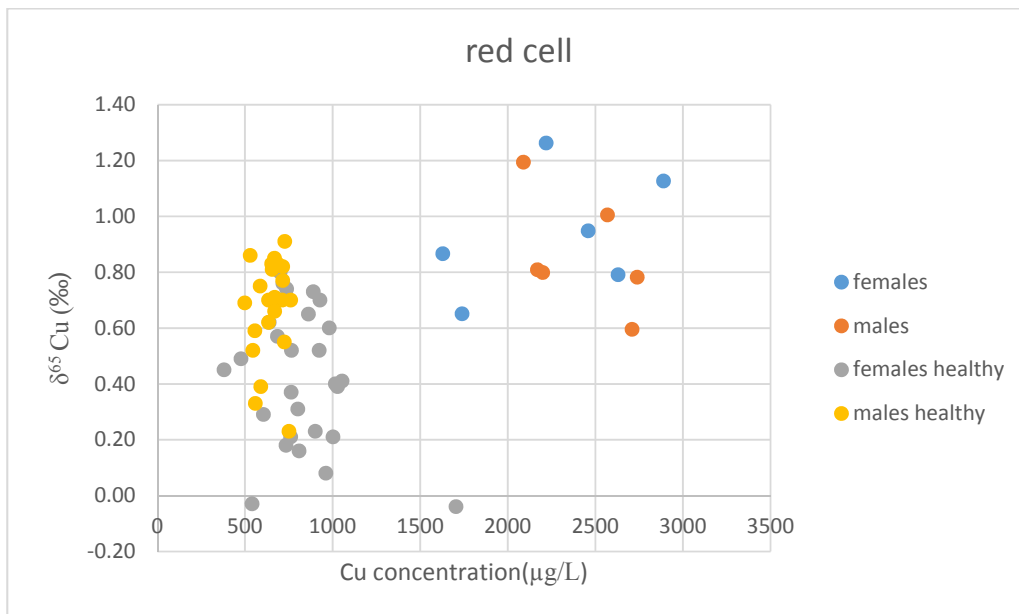


Figure 5.9 “concentration vs. isotopic information” plot for the red cell samples of different groups of individuals considered.

Given the large isotopic dispersion of the results and the low number of samples, isotopic ratio alone cannot account for all the isotopic variability. In the state of the present results, the Cu isotope compositions could be used as a potential isotopic tool for urolithiasis

diagnosis. The renewal of Cu in blood is linked to the erythropoietic process, and takes about 3 months²⁷. The origin of the Cu isotopic fractionations remains unknown in terms of physiological location and biochemical process. This rapid time of residence can explain the large isotopic diverse observed for urolithiasis in human blood.

In order to confirm this assumption, the relationship between Cu isotope compositions and medicine treated patient should be tested. However, this is the first time that a urolithiasis-related isotopic drift is reported. We do not yet know the molecular effects of the evolution of the isotopic ratio shifts, but we believe that this is an avenue to explore in biomedical sciences.

5.4. Conclusion

It was the purpose of this work to investigate the potential use of Cu isotopic analysis for the diagnosis of urolithiasis by analyzing a set of serum samples from different groups such as urolithiasis patients, and normal (supposedly healthy adults). It was found that Cu concentration in serum samples for urolithiasis patients was lower than the healthy control. However, the Cu concentration in red cell of lithiasic patient was much higher than that in healthy control. It was also found that the Cu in serum for lithiasic patients is significantly fractionated towards the heavier isotope when compared to serum samples of control (healthy) individuals. For the population considered in this study, combination of concentration values and isotopic information allows perfect classification of urolithiasis patients and controls into different groups. Although further studies with a larger number of samples are needed, results are encouraging as far as the use of Cu isotopic analysis for early diagnosis of urolithiasis disease is concerned.

5.5. Reference

1. Patriarca, M.; Menditto, A.; Di Felice, G.; Petrucci, F.; Caroli, S.; Merli, M.; Valente, C., Recent developments in trace element analysis in the prevention, diagnosis, and treatment of diseases. *Microchemical journal* **1998**, *59* (2), 194-202.
2. de Romaña, D. L.; Olivares, M.; Uauy, R.; Araya, M., Risks and benefits of copper in light of new insights of copper homeostasis. *Journal of Trace Elements in Medicine and Biology* **2011**, *25* (1), 3-13.
3. Scott, K. C.; Turnlund, J. R., Compartmental model of copper metabolism in adult men. *The Journal of Nutritional Biochemistry* **1994**, *5* (7), 342-350.
4. Linder, M. C.; Hazegh-Azam, M., Copper biochemistry and molecular biology. *The American journal of clinical nutrition* **1996**, *63* (5), 797S-811S.
5. Tapiero, H.; Townsend, D.; Tew, K., Trace elements in human physiology and pathology. Copper. *Biomedicine & pharmacotherapy* **2003**, *57* (9), 386-398.
6. Harvey, L. J.; McArdle, H. J., Biomarkers of copper status: a brief update. *British Journal of Nutrition* **2008**, *99* (S3), S10-S13.
7. Predki, P. F.; Sarkar, B., Effect of replacement of " zinc finger" zinc on estrogen receptor DNA interactions. *Journal of Biological Chemistry* **1992**, *267* (9), 5842-5846.
8. Kang, Y. J., Copper and homocysteine in cardiovascular diseases. *Pharmacology & Therapeutics* **2011**, *129* (3), 321-331.
9. Lalioti, V.; Muruais, G.; Tsuchiya, Y.; Pulido, D.; Sandoval, I. V., Molecular mechanisms of copper homeostasis. *Frontiers in bioscience (Landmark edition)* **2008**, *14*, 4878-4903.
10. Ogra, Y., Molecular mechanisms underlying copper homeostasis in Mammalian cells. *Nihon eiseigaku zasshi. Japanese journal of hygiene* **2013**, *69* (2), 136-145.
11. Wiederhold, J. G., Metal stable isotope signatures as tracers in environmental geochemistry. *Environmental science & technology* **2015**, *49* (5), 2606-2624.
12. Hou, X.; Jones, B. T., Inductively coupled plasma - optical emission spectrometry. *Encyclopedia of Analytical Chemistry* **2000**.
13. Albarède, F.; Télouk, P.; Lamboux, A.; Jaouen, K.; Balter, V., Isotopic evidence of unaccounted for Fe and Cu erythropoietic pathways. *Metallomics* **2011**, *3* (9), 926-933.
14. Shiel, A. E.; Barling, J.; Orians, K. J.; Weis, D., Matrix effects on the multi-collector inductively coupled plasma mass spectrometric analysis of high-precision cadmium and zinc isotope ratios. *Analytica chimica acta* **2009**, *633* (1), 29-37.
15. Maréchal, C. N.; Télouk, P.; Albarède, F., Precise analysis of copper and zinc isotopic compositions by plasma-source mass spectrometry. *Chemical Geology* **1999**, *156* (1), 251-273.
16. Mason, T. F. D. High precision transition metal isotope analysis by plasma-source mass spectrometry and its implications for low temperature geochemistry. Imperial College London (University of London), 2003.

17. Kuwabara, J.; Noguchi, H. In *Development of rapid urine analysis method for uranium*.
18. Turnlund, J. R.; Keyes, W. R.; Kim, S. K.; Domek, J. M., Long-term high copper intake: effects on copper absorption, retention, and homeostasis in men. *The American journal of clinical nutrition* **2005**, *81* (4), 822-828.
19. Atakan, I. H.; Kaplan, M.; Seren, G.; Aktoz, T.; Gül, H.; Inci, O., Serum, urinary and stone zinc, iron, magnesium and copper levels in idiopathic calcium oxalate stone patients. *International urology and nephrology* **2007**, *39* (2), 351-356.
20. Chen, S.-C.; Shiue, M.-Y.; Yang, M.-H., Microwave digestion and matrix separation for the determination of cadmium in urine samples by electrothermal atomization atomic absorption spectrometry using a fast temperature program. *Fresenius' journal of analytical chemistry* **1997**, *357* (8), 1192-1197.
21. Aramendía, M.; Rello, L.; Resano, M.; Vanhaecke, F., Isotopic analysis of Cu in serum samples for diagnosis of Wilson's disease: a pilot study. *Journal of Analytical Atomic Spectrometry* **2013**, *28* (5), 675-681.
22. Iyengar, G., Reevaluation of the trace element content in reference man. *Radiation Physics and Chemistry* **1998**, *51* (4), 545-560.
23. Jaouen, K.; Balter, V., Menopause effect on blood Fe and Cu isotope compositions. *American journal of physical anthropology* **2014**, *153* (2), 280-285.
24. Cameron, V.; Vance, D.; Archer, C.; House, C. H., A biomarker based on the stable isotopes of nickel. *Proceedings of the National Academy of Sciences* **2009**, *106* (27), 10944-10948.
25. Ryan, B. M.; Kirby, J. K.; Degryse, F.; Harris, H.; McLaughlin, M. J.; Scheiderich, K., Copper speciation and isotopic fractionation in plants: uptake and translocation mechanisms. *New Phytologist* **2013**, *199* (2), 367-378.
26. Balter, V.; Zazzo, A.; Moloney, A. P.; Moynier, F.; Schmidt, O.; Monahan, F. J.; Albarede, F., Bodily variability of zinc natural isotope abundances in sheep. *Rapid Communications in Mass Spectrometry* **2010**, *24* (5), 605-612.
27. Jaouen, K.; Gibert, M.; Lamboux, A.; Telouk, P.; Fourel, F.; Albarède, F.; Alekseev, A. N.; Crubézy, E.; Balter, V., Is aging recorded in blood Cu and Zn isotope compositions? *Metallomics* **2013**, *5* (8), 1016-1024.



6. Conclusions

6.1. General conclusion

The thesis work is embedded in the urinary lithiasis field, and includes the use of several techniques, that offer a multiple approach to the challenge posed by this disease. Mainly extraction and separation techniques, and isotopic analysis have been used for the study of urinary disease.

The study presents some results that widen the existing knowledge in urinary lithiasis and provide some useful method and material contribute to the study of urolithiasis. The basic effect has been conducted to the analytical method development for analysis of key inhibitors of urolithiasis. Also through copper isotopic analysis this dissertation provides additional tools to characterize the physiological aspect of urolithiasis.

This chapter will gather the most relevant conclusions, which apply to the study presented along the manuscript. Attending to the structure of the present document, this section will list the conclusions following a similar structure.

6.2. Key inhibitors MAE extraction from food

In this section, the microwave assisted extraction (MAE) method for quantitative extraction key inhibitors (phytic acid and pyrophosphate) from walnuts was developed. MAE proved to be an attractive alternative to conventional extraction methods, such as solid-liquid extraction, for the removal of phytic acid and pyrophosphate from walnuts.

- i. The influence of pH on the column separation was studied, in order to gain precision and accuracy in the final results, the pH of the diluted solution after MAE should adjusted to 6.0.
- ii. The predicted level of total phytic acid extracted with the MAE procedure was similar to those obtained from the traditional procedures reported in previous works.

- iii. The extraction time required for optimal recovery of total phytic acid and pyrophosphate using MAE was significantly less than that required by traditional extraction techniques, thereby showing MAE to be a more rapid and efficient method of extraction.
- iv. The hydrolysis of phytic acid was quite different under different MAE conditions. At the optima extraction MAE condition, the hydrolysis is low than other conditions.
- v. The development of a microwave-assisted extraction method for application in analyzing the concentration of total phytic acid and pyrophosphate may aid in increasing the healthy market potential for walnuts.

6.3. Novel material for determination of key inhibitors

This work demonstrates a new method for extracting phosphorous inhibitors of urolithiasis (phytic acid and pyrophosphate) using molecularly imprinted polymers. The developed polymer can be applied as specific stationary phases in solid-phase extraction or liquid chromatography. The development of methods to extract and recover phosphorous inhibitors from urine is very much desired.

- i. The polymer prepared using MAA as functional monomer showed no affinity for IP₆. The polymer synthesis with N-allylthiourea showed high adsorption for IP₆ with the capacity nearly 4 $\mu\text{mol/g}$, comparing that to the non-imprinted polymer was only 0.1 $\mu\text{mol/g}$.
- ii. The MIP prepared using DEHPA as template show the best adsorption capacity compared with the polymer prepared with pyrophosphoric acid and phenylphosphonic acid.
- iii. The solution pH has a significant effect on the adsorption of IP₆, PPi and Phosphate on the developed MIP.
- iv. The separation of IP₆, PPi and Phosphate was achieved by SPE procedure which using the synthesized MIP as adsorbent.

- v. With improvements in the binding ability and selectivity of the molecularly imprinted polymers proposed in this study, these materials could be put into clinic use.

6.4. Cu isotopic analysis in the blood of urolithiasis patients

The third part of the thesis considers the physiological aspect of urolithiasis. In the literature Copper has shown inhibitory effect on the growth of kidney stone and disordered in copper metabolism may be important in the aetiology of disease. The blood Copper isotope fractionation from urolithiasis patients from Barcelona area was analyzed and compared to healthy controls. The serum and red cell samples Cu isotope compositions was measured by multi-collector ICP-MS after separation and purification by anion exchange chromatography

- i. The Cu column separation process was optimized and validated by the reference materials. Oysters from 7 locations in southern European was used as the reference materials to validate the column separation method.
- ii. Cu concentration in serum of female urolithiasis patients ($903 \pm 316 \mu\text{g L}^{-1}$) were significantly lower than those in healthy control ($1553 \pm 536 \mu\text{g L}^{-1}$).
- iii. However, for male urolithiasis patients the concentration of Cu ($956 \pm 224 \mu\text{g L}^{-1}$) is no significant difference compared with the healthy control ($798 \pm 171 \mu\text{g L}^{-1}$)
- iv. The serum and red cell sample of urolithiasis patients show significantly higher $\delta^{65}\text{Cu}$ values than the controls (either male or female). For the males, the Cu isotopic fractionation seems to a lesser extent.

Annex I

Quantitative analysis of phytic acid and pyrophosphate (phosphorous inhibitors of urolithiasis) from walnuts

Tong LIU^a, Liu HE^a, Manuel VALIENTE^a, Montserrat LÓPEZ-MESAS^{a*}

^aCentre Grup de Tècniques de Separació en Química (GTS), Química Analítica,
Departament de Química, Universitat Autònoma de Barcelona, 08193, Cerdanyola, Spain

*Corresponding author: Montserrat.Lopez.Mesas@uab.cat

Tel: +34 93 581 4938

Fax: +34 93 581 1985

^aAddress: Centre Grup de Tècniques de Separació en Química (GTS), Departament de Química, Facultat de Ciències, Edifici Cn, Universitat Autònoma de Barcelona, Cerdanyola del Vallés, 08193, Barcelona, Spain.

Tong Liu:

Email: liutongyes@gmail.com

Liu He:

Email: heliu2223@gmail.com

Manuel Valiente:

email: Manuel.Valiente@uab.cat

Abstract:

Phytic acid (IP6) and pyrophosphate (PPi) are growing interest in the biomedical field due to their ability as potential inhibitors of urolithiasis among others. A new method to extract both inhibitors from walnuts by microwave-assisted extraction (MAE) and the quantitative analysis was developed. Acid content of extracting solvent, extraction time and temperature were considered to optimize the condition for MAE. After extraction, the sample was purified by an anion exchange solid phase extraction and the phosphorous compounds were analyzed by inductive coupled plasma mass spectrometry. The hydrolysis of phytic acid by microwave treatment was also investigated. The MAE using mixture of H₂SO₄ and HCl shows a better extract ability for both IP6 and PPi and provided results slightly higher than those determined by conventional extraction with no statistical difference. Compared with the conventional acid extraction method, the MAE method reduces extraction time from 3h to 10 min.

Keywords:

phytic acid, microwave-assisted extraction, pyrophosphate, food analysis

1. Introduction

Consumption of nuts has been associated with a decreased risk of cardiovascular disease or events related to heart disease (Sabate, Fraser, Burke, Knutsen, Bennett, & Lindsted, 1993). Nuts have been an important component of human diet from pre-agriculture times to the present day. A recent decline in the consumption of nuts was probably due to concerns about ingesting fatty food. Although total fat intake is related to health risks, there is now general agreement that the more important is the type of fat or fatty acids that are consumed (Amaral, Casal, Pereira, Seabra, & Oliveira, 2003). Compared with most other nuts, walnuts in particular have a unique profile: they are rich in polyunsaturated fatty acids, especially highly enriched in omega-3 polyunsaturated fatty acids, which might have a significant role in the prevention of coronary heart disease (CHD) (Harper & Jacobson, 2001). Other reported results indicated that walnuts provide significant benefits for certain antioxidant capacity and inflammatory markers and had no adverse effects on body weight (Banel & Hu, 2009). The versatility of walnuts, which allow their ready use in the diet as snacks or components of desserts, breads, or entrees, suggests that their consumption would be acceptable to most as part of a cholesterol-lowering diet (Amaral, Casal, Pereira, Seabra, & Oliveira, 2003).

One of the bioactive compounds found in walnuts is phytic acid (myoinositol hexaphosphate, IP6) which is abundantly present in many plant sources and in certain high-fiber diets, such as cereals and legumes. It is claimed to have the ability to enhance the anticancer effect of conventional chemotherapy and control cancer metastases (Rizvi, Riggs, Jackson, Ng, Cunningham, & McFadden, 2006; Somasundar, Riggs, Jackson, Cunningham, Vona-Davis, & McFadden, 2005; Vucenik & Shamsuddin, 2006). In addition, phytic acid acts as an effective inhibitor of calcium salts crystallization in urine and soft

tissues, and prevents the formation of kidney stones (urolithiasis) (Grases, Isern, Sanchis, Perello, Torres, & Costa-Bauza, 2007).

Inorganic pyrophosphate (PPi), can also be present in walnuts and can inhibit the formation of several crystallization reactions as for example the formation of calcium oxalate and hydroxyapatite, chemical composition of the 80% of kidney stones, serving so as natural inhibitor of urolithiasis (Terkeltaub, 2001). In lithiasic patients, lower urinary PPi has been reported (Sharma, Vaidyanathan, Thind, & Nath, 1992) and its intake increase has been recommended (Breslau, Padalino, Kok, Kim, & Pak, 1995) as therapy. Thus, the determination of levels of both natural lithiasic inhibitors, IP6 and PPi, in walnuts is of interest for its healthy use.

The growing interest in the biomedical implications of phytic acid and pyrophosphate and the inherent problems with its poor separation are reflected in the tedious analytical techniques actually described and used in many laboratories. The quantitative extraction of phytate and pyrophosphate from foodstuff is not selective and always co-extract with cations, protein, or other nutrients leading to erroneous estimation, damage to the analytical instruments, or both (Ray, Shang, Maguire, & Knowlton, 2012).

For the determination of phytic acid, many methods have been developed. The frequently used measurement techniques include colorimetric method (Latta & Eskin, 1980), HPLC (Perello, Isern, Munoz, Valiente, & Grases, 2004; Skoglund, Carlsson, & Sandberg, 1998), HPIC (Blaabjerg, Hansen-Møller, & Poulsen, 2010), ³¹P NMR spectroscopy (Kempe, Lommen, De Jonge, Van der Klis, Jongbloed, Mroz, et al., 1999), synchronous fluorescence method (Chen, Chen, Luo, Ma, & Chen, 2009), inductively coupled plasma mass spectrometry (ICP-MS) (Muñoz & Valiente, 2003), and IPC-ICP-MS

(Helfrich & Bettmer, 2004). Indirect determination of phosphate after hydrolysis has been also used for the analysis of pharmaceutical formulations (March, Grases, & Salvador, 1998). The traditional procedures employed for PPI determination are mainly based in chemical (Chang & Denq, 1985) and enzymatic methods (Baykov & Avaeva, 1982). Method including either chromatographic (Yoza, Akazaki, Nakazato, Ueda, Kodama, & Tateda, 1991) or electrophoretic (Hénin, Barbier, & Brack, 1999) separation of PPI have also been reported. A method for the determination of IP6 and PPI in urine by SPE-ICP-MS techniques was developed in our laboratory achieving a simple and easy measurement to simultaneously analyze IP6 and PPI (Munoz, Lopez-Mesas, & Valiente, 2010). But non-laborious method for the extraction and purification of the compounds from a fatty sample has not been developed.

Interest in microwave-assisted extraction (MAE) has increased significantly over the past years as a result of its inherent advantages (reduction in extraction time and solvent volume) over more traditional extraction techniques, such as Soxhlet extraction (Li, Deng, Wu, Liu, Loewen, & Tsao, 2012). Conventional extraction methods have been associated to higher solvent requirements, longer extraction times and increased risk of degradation of thermo-labile constituents. In MAE, the solvent and sample are contained in sealed extraction vessels under controlled temperature and pressure conditions. The closed vessels allow the temperature of the solvent to rise well above its boiling point, which shortens extraction time and subsequently increases extraction efficiency (Eskilsson & Björklund, 2000)(Ballard, Mallikarjunan, Zhou, & O'Keefe, 2010).

Development of robust, inexpensive, and reproducible techniques for accurate quantification of undigested phytate in complex food sample is essential to advance

knowledge of the content of phytic acid and pyrophosphate. The objectives of the current study were to investigate the effects of MAE on the extraction efficiency and optimize the parameters including microwave power, irradiation time and acid solvents. In this paper, we present a rapid and simple procedure for extraction and determination of phytic acid and pyrophosphate content in walnuts.

2. Experiment

2.1. Chemicals and reagents

The walnuts (Lleida, Spain) were purchased from a local supermarket. Tetra-sodium pyrophosphate 10-hydrate (Panreac, Barcelona, Spain), myoinositol hexaphosphoric acid hexasodium salt from corn (Sigma, Steinheim, Germany), hydrochloric acid (J.T. Baker, Deventer, Holland) and sodium dihydrogen phosphate (Panreac, Barcelona, Spain) were of analytical-reagent grade. AG 1x8 200–400 mesh, chloride form, and anion exchange resin was from Bio-Rad Laboratories (Hercules, CA, USA). Purified Milli-Q water of 18mΩ-cm resistivity was used for the preparation of all reagents.

2.2. Preparation of walnut samples

According to the food composition database published by the US Department of Agriculture, 100 g of walnuts contain 15.2 g protein, 65.2 g fat, and 6.7 g dietary fiber (Banel & Hu, 2009). That's means more than half weights of walnuts are fat (fresh weight).

The fat content can reduce the efficiency of the extraction and determination of the analytes so, it is important to defat the walnuts before any procedure and to analyze if the defatting process entails any loss of the analytes.

The walnuts were previously shelled and blended, then dried at 40°C until no further

weight loss and stored into a desiccator until use. Total lipid was extracted from walnut samples by using hexane, based on the modified method of Saad et al. (Saad, Mohd Esa, Ithnin, & Shafie, 2011). To do so, 5 ml of hexane was added to 1 g of walnut and soaked for 16 hours under a hood. Then after filtration, walnuts were evaporated to dryness using a vacuum pump apparatus.

2.3. Microwave-assisted extraction (MAE)

MAE experiments were carried out at a CEM Mars5 Digestion Microwave System (Matthews, USA). Samples (defatted as previously described) were transferred into a set of microwave extraction vessels. The samples were added to hydrochloric acid, sulphuric acid or mixture of both at the selected concentrations. Each mixture was placed in a 100 mL sealed perfluoroalkoxy Teflon reactor vessel and extracted for a certain time at selected temperatures using microwave oven which allowed accurate control of pressure, power and temperature. Three replicates of each sample were extracted at the same time. After certain time of extraction, vessels were allowed to cool down prior to their removal from the extractor.

The obtained creamy extracts were then centrifuged at 5000 rpm for 10 min. The supernatants were collected and used for determination of total phytic acid and pyrophosphate content.

In order to validate the results, the traditional solid-solvent extraction method from the AOAC(AOAC, 1990) was followed. 0.66 M HCl used as extraction solvents. The extraction was carried out at room temperature with constant shaking at medium speed in an orbital mixer for 3 hours. The obtained creamy mixture was then processed in the same way as for the creamy extract obtained by microwave extraction. .

As it is well known, the solvent composition, extraction time and microwave temperature have an effect on the extraction process. The hydrolysis of phytic acid by using a domestic microwave oven has been reported (March, Grases, & Salvador, 1998). In order to minimize the hydrolysis during the MAE process, different acid conditions and microwave parameters have been investigated.

2.4. Separation of IP6 and PPI by SPE

The methodology followed was described elsewhere (Munoz, Lopez-Mesas, & Valiente, 2010). Before separation, the sample was diluted 25 times and then adjusted to pH 6.0 using NaOH solution. To separate IP6 and PPI, 1.0 mL of the obtained cream was transferred quantitatively to a SPE cartridge, packed with 0.2 g of AG 1x8 resin, previously conditioned with 2mL of HCl 10mmol L⁻¹. First phosphate and some other matrix components of sample were eluted with 50 ml of HCl 50 mmol L⁻¹. Then PPI were eluted with a second 5 ml HCl 100 mmol L⁻¹ eluting. Finally the column was washed with 2 mL of HCl 2 mol L⁻¹ to elute phytic acid (IP6). The clean-up process was run by gravity, at a flow rate of 0.33 mL min⁻¹.

2.5. ICP conditions

The determination of PPI and IP6 from the fraction obtained by SPE was carried out through ³¹P analysis of the purified extracts by ICP-MS using ⁴⁵Sc (5 µg L⁻¹) as internal standard. The ICP-MS equipment was X series II ICP-MS (Thermo Scientific, UK) and conditions were set as follows — ICP system: RF power: 1400W; auxiliary gas flow: 0.92 L/min; coolant gas flow: 13.30 L/min; nebulizer: concentric nebulizer (Thermo) at a gas flow rate of 0.90 L/min; sample cone: nickel with 1.0 mm orifice; skimmer cone: nickel

with 0.7 mm orifice; Sample introduction system: sample uptake flow rate 2ml/min; delay time: 60s; wash time: 50s (1% HCl); Data acquisition parameters: analyzer: quadrupole; scanning mode: peak jump; sweeps per reading: 30; dwell time: 10ms; number of replicates: 3.

3. Results and discussion

3.1. Effect of defatting process and acid solvent selection

Since walnuts contain a lot of fat, it is important to investigate the effect of defatting on the extract process. In both traditional acid extraction method procedure (AOAC) and MAE method, it can be observed from table 1 that the non-defatted sample shows about 0.10% of higher content on phytic acid, which means that a small loss of the compound happened during the defatting procedure. According to Oberleas and Harland (Oberleas & Harland, 1986), fat content influences the extractability of phytate from food products and should be lowered below 5% before phytate extraction. As previously said, this kind of sample contains more than 50% weight in fat which can have an adverse effect on any posterior procedure (including SPE and ICP-MS). So it is important to defat the walnuts before the extraction procedure and will be the sample used for subsequent experiment.

Results obtained by the traditional acid extraction method procedure (AOAC method) are shown in table 2. It is observed that after 2 hours of acid extraction the result shows no significant differences as 3 hours of extraction ($P>0.05$), although 3 hours extraction is recommended by the AOAC method. In addition, using sulphuric acid as solvent, 0.52M and 0.94M H₂SO₄ have been tested. It can be observed that 0.52M H₂SO₄ gave the same results as 0.66M HCl on IP₆, while gave lower yield on PPI. In the same extraction condition, compared with 0.52M H₂SO₄, 0.94M H₂SO₄ give a lower yield on IP₆ and a

higher yield on PPI. So, H₂SO₄ will be also tested as acid solvent for the MAE procedure. The amount expected of phytic acid and pyrophosphate in the analyzed walnuts will be compare with 1.04% and 0.14‰ (dry weight).

3.2. Effect of pH

The complexes between phytate and mineral cations are pH sensitive. To minimize the effect of both metals and proteins some researchers treated the samples with NaOH–EDTA (Bos, Verbeek, Van Eeden, Slump, & Wolters, 1991),(Harland & Oberleas, 1985). For several minerals this complexation shows a maximum around pH 6 (Fruhbeck, Alonso, Marzo, & Santidrián, 1995). In that sense, the influence of adjusting the pH on the column separation was studied. pH was adjusted to 6.0 (above the isoelectric point of the proteins) just before the separation procedure (SPE).

From the results (figure 1) it is observed that for the no defatted sample, the pH adjustment has a significant effect ($P<0.05$), obtaining a 0.09% higher content on phytic acid. While for the defatted samples, pH adjustment seems don't have significant difference ($P>0.05$). Nevertheless, it is worthwhile to emphasize the fact that when the pH adjustments were carried out, the standard deviation was lower. For the defatted samples, the pH adjustment does not show a significant effect because this procedure eliminates the possible phytic acid complex (Fruhbeck, Alonso, Marzo, & Santidrián, 1995). Therefore, in order to gain precision and accuracy in the final outcome, the pH of the diluted aliquot was adjusted to 6.0 with 1M NaOH just before running them through the SPE column.

3.3. MAE parameters selection and phytic acid hydrolysis

Three main parameters were considered to optimize the condition for microwave-

assisted extraction: acid concentration of extracting solvent, extraction time and temperature. The results obtained by MAE will be compared with those obtained by the traditional method. As shown in table 3, when using the single acid as the extraction solvent, the 0.52 M H₂SO₄ shows poor extraction ability on PPi under the same condition compare with HCl. On the extract of IP6, 0.66 M HCl and 0.52 M H₂SO₄ didn't show significant different (0.93% and 0.99% respectively). While for the extraction of PPi, the use of 0.66 M HCl only recover 0.08‰ compared with the 0.11‰ of PPi obtained when using 0.52 M H₂SO₄. When temperature was raised from 100 °C to 125 °C, or increased the extraction time from 10 min to 20 min, there was a littler increase on the extraction of IP6 and PPi. Increasing the temperature to 150 °C, the extraction of IP6 was decreased and PPi was increased significantly, due to the hydrolysis of IP6 under this condition, confirmed later on by the study of the hydrolysis (see table 4). The mixture acid solvent of HCl and H₂SO₄ (1:1) was also tested. It is observed that the MAE extraction by the mixture show a good recovery of both IP6 and PPi. The best extraction conditions were found to be 0.52 M H₂SO₄ + 0.66 M HCl at 100°C, 10 min irradiation time, and a solvent volume to walnut ratio of 20 ml/g. For these conditions the hydrolysis was low (see table 4). Mixtures of HCl/H₂SO₄ provided results slightly higher than those determined by conventional extraction with no statistical difference ($P>0.05$) with the advantage that the extraction time decreased from 3 hours to 10 minutes. Compared with the traditional solid-solvent extraction, treatment of the walnut with MAE likely initiated cell rupture, which allowed more of the phytate and pyrophosphate compounds from the bulk to be extracted by the solvent. The dried material used for extraction contains minute traces of moisture and as microwave energy is absorbed and subsequently converted into heat, the moisture begins

to evaporate. The vaporization of water generates pressure within the cell wall that eventually leads to cell rupture, thereby facilitating the leaching out of active constituents into the surrounding solvent and improving extraction efficiency and yield (Ballard, Mallikarjunan, Zhou, & O'Keefe, 2010).

The possible hydrolysis of phytic acid by microwave extraction procedure has been studied under several work conditions to compare the yield of hydrolysis reaction. The MAE work condition and the hydrolysis was list in table 4.

When comparing the different acid concentrations, it can be observed that the hydrolysis of phytic acid increased at lower acid concentration (see experiment 1, 7; 4-6; 8-9), in agreement with the known fact that the absorption of radiation of aqueous acid solutions is more effective at lower acid concentrations. The kinetics of heteropoly acid formation was affected by acidity conditions. Generally the fact is the higher the acid concentration, the faster the reaction. As expected, when comparing at the same molar concentration in acid, it can be observed that at higher temperature higher hydrolysis is observed (see experiments 1-3). The proposed hydrolysis of phytic acid can be compared with other reported hydrolysis method. When hydrolysis is carried out at 120 °C in 2 M HCl, 24 hours is necessary to reach quantitative hydrolysis (de Koning, 1994). In our case, at the MAE condition of 150 °C in 0.1 M HCl, 99% of phytic acid was hydrolyzed in 10 min. When comparing the different inorganic acid at the same microwave treatment conditions, it can be observed that 0.52 M H₂SO₄ gave lower yield of hydrolysis, following by 0.66 M HCl and 0.94 M H₂SO₄. For the purpose of extract phytic acid from walnuts, it is obligate to control the hydrolysis in an accept range. To minimize the hydrolysis of phytic acid in the MAE process, temperature of 100°C during 10 min were recommended.

3.4. Walnuts as a functional food

In developing country situations where cereals and other plant-based foods provide a large proportion of the food consumption, the dietary phytate intake will be greater. Figure 2 shows phytate content of several food (Harland, Smikle-Williams, & Oberleas, 2004; Macfarlane, Bezwoda, Bothwell, Baynes, Bothwell, MacPhail, et al., 1988; Ravindran, Ravindran, & Sivalogan, 1994). Although dietary phytate has been ascribed as a potential way to reduce the risk of mineral deficiency, it exhibits beneficial health effects, such as protection against a variety of cancer and heart-related diseases, diabetes mellitus and renal stones. Pharmaceutical preparations containing phytic acid are used to treat relapsed urolithiasic patients (March, Grases, & Salvador, 1998). These beneficial health effects are more significant for people from developed countries because of the higher incidence of cancer which is associated with higher fat and lower fibre-rich food intakes. Such populations generally do not suffer from mineral deficiencies (Kumar, Sinha, Makkar, & Becker, 2010). Walnuts contains less phytate than other nuts, such as peanut and almond, and rich in polyunsaturated fatty acids, which make it is valuable to develop functional food based on it.

4. Conclusions

MAE proved to be an attractive alternative to conventional extraction methods, such as solid-liquid extraction, for the removal of phytic acid and pyrophosphate from walnuts. The predicted level of total phytic acid extracted with the MAE procedure was similar to those obtained from the traditional procedures reported in previous works. The extraction time required for optimal recovery of total phytic acid and pyrophosphate using MAE was significantly less than that required by traditional extraction techniques, thereby showing

MAE to be a more rapid and efficient method of extraction. The development of a microwave-assisted extraction method for application in analyzing the concentration of total phytic acid and pyrophosphate may aid in increasing the healthy market potential for walnuts.

Acknowledgements

Spanish Ministry MINECO is acknowledged for funding present studies (project ref CTM2012-30970). Tong Liu acknowledges the China Scholarship Council (CSC) for the scholar-grant received.

Table 1. Effect of sample defatting on the extraction of IP6 and PPi content from walnuts

<i>sample</i>	<i>extraction solvent</i>	<i>defatted</i>	<i>Extraction condition</i>	<i>Phytic acid content(% dry wt)</i>	<i>Pyrophosphate content(%o dry wt)</i>
1	0.66M HCl	Yes	2 hours	1.04 ± 0.06	0.13 ± 0.02
2	0.66M HCl	Yes	3 hours	1.04 ± 0.02	0.15 ± 0.03
3	0.66M HCl	No	2 hours	1.16 ± 0.05	0.06 ± 0.02
4	0.66M HCl	Yes	MAE1	0.95 ± 0.02	0.07 ± 0.01
5	0.66M HCl	No	MAE1	1.07 ± 0.03	
6	0.52MH ₂ SO ₄ +0.66MHCl	Yes	MAE2	0.97 ± 0.05	0.09 ± 0.01
7	0.52MH ₂ SO ₄ +0.66MHCl	No	MAE2	1.01 ± 0.05	

MAE1: temperature set: 125 °C, hold time: 10 min; MAE2: temperature set: 50 °C, hold time: 10 min;

Table 2. Study of the solvent nature on the determination of IP6 and PPi content from walnuts

<i>sample</i>	<i>extraction solvent</i>	<i>Extraction time</i>	<i>Phytic acid content(% dry wt)</i>	<i>Pyrophosphate content(%o dry wt)</i>
1	0.66M HCl	2 hours	1.04 ± 0.06	0.13 ± 0.02
2	0.66M HCl	3 hours	1.04 ± 0.02	0.15 ± 0.03
3	0.52M H ₂ SO ₄	0.5 hour	1.04 ± 0.03	0.03 ± 0.01
4	0.52M H ₂ SO ₄	1 hour	1.05 ± 0.06	0.05 ± 0.02
5	0.94M H ₂ SO ₄	0.5 hour	0.90 ± 0.05	0.08 ± 0.02

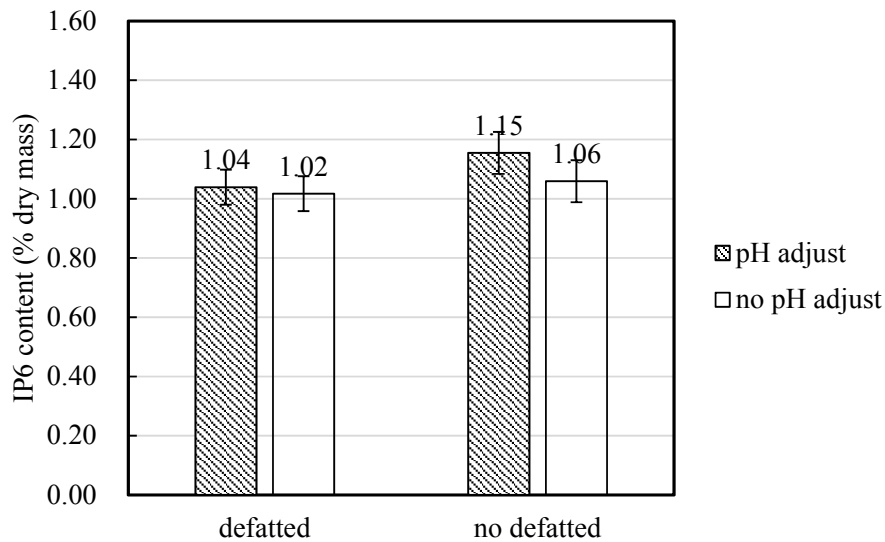


Figure 1. Effect of pH adjustment on separation of phytic acid from walnut

Table 3. Study of the solvent and MAE work condition on the determination of IP6 and PPI content from walnuts

<i>sample</i>	<i>acid content of extracting solvent</i>	<i>MAE condition</i>	<i>Phytic acid content(% dry wt)</i>	<i>Pyrophosphate content(%o dry wt)</i>
1	0.66M HCl	100°C 10 min	0.93 ± 0.08	0.08 ± 0.02
2	0.66M HCl	125°C 10 min	0.95 ± 0.02	0.07 ± 0.01
3	0.66M HCl	125°C 20 min	0.99 ± 0.03	0.09 ± 0.02
4	0.66M HCl	150°C 10 min	0.71 ± 0.08	0.46 ± 0.05
5	0.52M H ₂ SO ₄	100°C 10 min	0.99 ± 0.01	0.11 ± 0.02
6	0.94M H ₂ SO ₄	100°C 10 min	0.98 ± 0.01	0.15 ± 0.03
7	0.52M H ₂ SO ₄ +0.66M HCl	50°C 10 min	0.97 ± 0.05	0.09 ± 0.01
8	0.52M H ₂ SO ₄ +0.66M HCl	80°C 10 min	1.06 ± 0.02	0.14 ± 0.02
9	0.52M H ₂ SO ₄ +0.66M HCl	100°C 10 min	1.13 ± 0.08	0.15 ± 0.04
10	0.52M H ₂ SO ₄ +0.66M HCl	110°C 10 min	1.14 ± 0.02	0.16 ± 0.00

Table 4 Yield of IP6 hydrolysis reaction¹

<i>Experiment</i>	<i>Inorganic acid</i>	<i>Concentration(M)</i>	<i>MAE condition</i>	<i>Hydrolysis (%)</i>
1	HCl	0.1	100°C 10 min	26
2	HCl	0.1	125°C 10 min	33
3	HCl	0.1	150°C 10 min	88
4	HCl	0.1	150°C 20 min	99
5	HCl	0.78	150°C 20 min	85
6	HCl	2.0	150°C 20 min	85
7	HCl	0.66	100°C 10 min	13
8	H ₂ SO ₄	0.52	100°C 10 min	7
9	H ₂ SO ₄	0.94	100°C 10 min	25

¹Initial concentration of phytic acid, 50 mg/L.

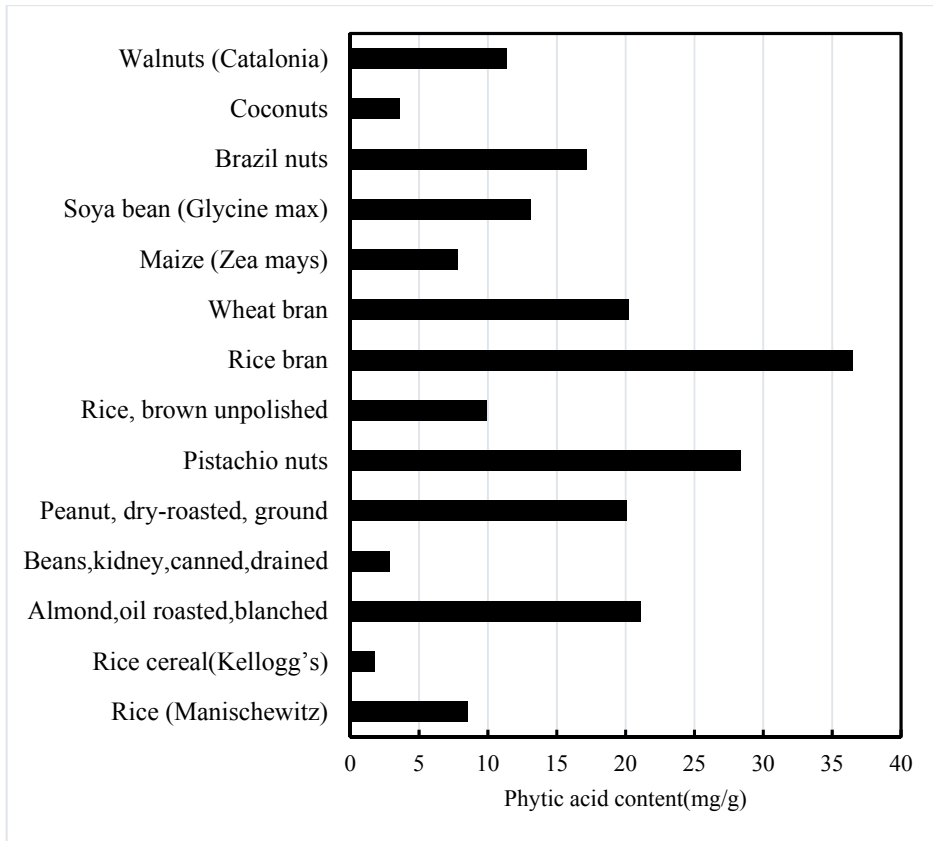


Figure 2. IP6 content of selected foods

References

- Amaral, J. S., Casal, S., Pereira, J. A., Seabra, R. M., & Oliveira, B. P. (2003). Determination of sterol and fatty acid compositions, oxidative stability, and nutritional value of six walnut (*Juglans regia* L.) cultivars grown in Portugal. *Journal of agricultural and food chemistry*, *51*(26), 7698-7702.
- AOAC, W. H. (1990). Official methods of analysis of the Association of Official Analytical Chemists. *Association of Official Analytical Chemists, Arlington, VA, USA*.
- Ballard, T. S., Mallikarjunan, P., Zhou, K., & O'Keefe, S. (2010). Microwave-assisted extraction of phenolic antioxidant compounds from peanut skins. *Food Chemistry*, *120*(4), 1185-1192.
- Banel, D. K., & Hu, F. B. (2009). Effects of walnut consumption on blood lipids and other cardiovascular risk factors: a meta-analysis and systematic review. *Am J Clin Nutr*, *90*(1), 56-63.
- Baykov, A., & Awaeva, S. (1982). A sensitive method for measuring pyrophosphate in the presence of a 10,000-fold excess of orthophosphate using inorganic pyrophosphatase. *Anal Biochem*, *119*(1), 211-213.
- Blaabjerg, K., Hansen-Møller, J., & Poulsen, H. D. (2010). High-performance ion chromatography method for separation and quantification of inositol phosphates in diets and digesta. *Journal of Chromatography B*, *878*(3), 347-354.
- Bos, K. D., Verbeek, C., Van Eeden, C. P., Slump, P., & Wolters, M. G. (1991). Improved determination of phytate by ion-exchange chromatography. *Journal of agricultural and food chemistry*, *39*(10), 1770-1772.
- Breslau, N. A., Padalino, P., Kok, D. J., Kim, Y. G., & Pak, C. Y. (1995). Physicochemical effects of a new slow - release potassium phosphate preparation (UroPhos - K) in absorptive hypercalciuria. *Journal of Bone and Mineral Research*, *10*(3), 394-400.
- Chang, G.-G., & Denq, R.-Y. (1985). Determination of inorganic pyrophosphate concentration in urine. *International Journal of Biochemistry*, *17*(6), 733-735.
- Chen, Y., Chen, J., Luo, Z., Ma, K., & Chen, X. (2009). Synchronous fluorescence analysis of phytate in food. *Microchimica Acta*, *164*(1-2), 35-40.
- de Koning, A. J. (1994). Determination of myo-inositol and phytic acid by gas chromatography using scyllitol

- as internal standard. *Analyst*, *119*(6), 1319-1323.
- Eskilsson, C. S., & Björklund, E. (2000). Analytical-scale microwave-assisted extraction. *Journal of Chromatography A*, *902*(1), 227-250.
- Fruhbeck, G., Alonso, R., Marzo, F., & Santidrián, S. (1995). A modified method for the indirect quantitative analysis of phytate in foodstuffs. *Anal Biochem*, *225*(2), 206-212.
- Grases, F., Isern, B., Sanchis, P., Perello, J., Torres, J. J., & Costa-Bauza, A. (2007). Phytate acts as an inhibitor in formation of renal calculi. *Front Biosci*, *12*(1), 2580-2587.
- Hénin, O., Barbier, B., & Brack, A. (1999). Determination of phosphate and pyrophosphate ions by capillary electrophoresis. *Anal Biochem*, *270*(1), 181-184.
- Harland, B. F., & Oberleas, D. (1985). Anion-exchange method for determination of phytate in foods: collaborative study. *Journal-Association of Official Analytical Chemists*, *69*(4), 667-670.
- Harland, B. F., Smikle-Williams, S., & Oberleas, D. (2004). High performance liquid chromatography analysis of phytate (IP6) in selected foods. *Journal of Food Composition and Analysis*, *17*(2), 227-233.
- Harper, C. R., & Jacobson, T. A. (2001). The fats of life: the role of omega-3 fatty acids in the prevention of coronary heart disease. *Archives of Internal Medicine*, *161*(18), 2185-2192.
- Helfrich, A., & Bettmer, J. (2004). Determination of phytic acid and its degradation products by ion-pair chromatography (IPC) coupled to inductively coupled plasma-sector field-mass spectrometry (ICP-SF-MS). *Journal of Analytical Atomic Spectrometry*, *19*(10), 1330-1334.
- Kemme, P. A., Lommen, A., De Jonge, L. H., Van der Klis, J. D., Jongbloed, A. W., Mroz, Z., & Beynen, A. C. (1999). Quantification of inositol phosphates using ³¹P nuclear magnetic resonance spectroscopy in animal nutrition. *Journal of agricultural and food chemistry*, *47*(12), 5116-5121.
- Kumar, V., Sinha, A. K., Makkar, H. P. S., & Becker, K. (2010). Dietary roles of phytate and phytase in human nutrition: A review. *Food Chemistry*, *120*(4), 945-959.
- Latta, M., & Eskin, M. (1980). A simple and rapid colorimetric method for phytate determination. *Journal of agricultural and food chemistry*, *28*(6), 1313-1315.
- Li, H., Deng, Z., Wu, T., Liu, R., Loewen, S., & Tsao, R. (2012). Microwave-assisted extraction of phenolics with maximal antioxidant activities in tomatoes. *Food Chemistry*, *130*(4), 928-936.

- Macfarlane, B. J., Bezwoda, W. R., Bothwell, T. H., Baynes, R. D., Bothwell, J. E., MacPhail, A. P., Lamparelli, R. D., & Mayet, F. (1988). Inhibitory effect of nuts on iron absorption. *Am J Clin Nutr*, 47(2), 270-274.
- March, J., Grases, F., & Salvador, A. (1998). Hydrolysis of phytic acid by microwave treatment: Application to phytic acid analysis in pharmaceutical preparations. *Microchemical journal*, 59(3), 413-416.
- Muñoz, J. A., & Valiente, M. (2003). Determination of phytic acid in urine by inductively coupled plasma mass spectrometry. *Anal Chem*, 75(22), 6374-6378.
- Munoz, J. A., Lopez-Mesas, M., & Valiente, M. (2010). Minimum handling method for the analysis of phosphorous inhibitors of urolithiasis (pyrophosphate and phytic acid) in urine by SPE-ICP techniques. *Anal Chim Acta*, 658(2), 204-208.
- Oberleas, D., & Harland, B. (1986). Analytical methods for phytate.
- Perello, J., Isern, B., Munoz, J., Valiente, M., & Grases, F. (2004). Determination of Phytate in Urine by High-Performance Liquid Chromatography–Mass Spectrometry. *Chromatographia*, 60(5-6), 265-268.
- Ravindran, V., Ravindran, G., & Sivalogan, S. (1994). Total and phytate phosphorus contents of various foods and feedstuffs of plant origin. *Food Chemistry*, 50(2), 133-136.
- Ray, P., Shang, C., Maguire, R., & Knowlton, K. (2012). Quantifying phytate in dairy digesta and feces: Alkaline extraction and high-performance ion chromatography. *J Dairy Sci*, 95(6), 3248-3258.
- Rizvi, I., Riggs, D. R., Jackson, B. J., Ng, A., Cunningham, C., & McFadden, D. W. (2006). Inositol Hexaphosphate (IP6) Inhibits Cellular Proliferation In Melanoma. *Journal of Surgical Research*, 133(1), 3-6.
- Saad, N., Mohd Esa, N., Ithnin, H., & Shafie, N. H. (2011). Optimization of optimum condition for phytic acid extraction from rice bran. *African Journal of Plant Science*, 5(3), 168-176.
- Sabate, J., Fraser, G. E., Burke, K., Knutsen, S. F., Bennett, H., & Lindsted, K. D. (1993). Effects of walnuts on serum lipid levels and blood pressure in normal men. *New England Journal of Medicine*, 328(9), 603-607.
- Sharma, S., Vaidyanathan, S., Thind, S., & Nath, R. (1992). Urinary excretion of inorganic pyrophosphate by normal subjects and patients with renal calculi in north-western India and the effect of diclofenac

- sodium upon urinary excretion of pyrophosphate in stone formers. *Urologia internationalis*, 48(4), 404-408.
- Skoglund, E., Carlsson, N.-G., & Sandberg, A.-S. (1998). High-performance chromatographic separation of inositol phosphate isomers on strong anion exchange columns. *Journal of agricultural and food chemistry*, 46(5), 1877-1882.
- Somasundar, P., Riggs, D. R., Jackson, B. J., Cunningham, C., Vona-Davis, L., & McFadden, D. W. (2005). Inositol Hexaphosphate (IP6): A Novel Treatment for Pancreatic Cancer¹. *Journal of Surgical Research*, 126(2), 199-203.
- Terkeltaub, R. A. (2001). Inorganic pyrophosphate generation and disposition in pathophysiology. *American Journal of Physiology-Cell Physiology*, 281(1), C1-C11.
- Vucenik, I., & Shamsuddin, A. M. (2006). Protection against cancer by dietary IP6 and inositol. *Nutrition and cancer*, 55(2), 109-125.
- Yoza, N., Akazaki, I., Nakazato, T., Ueda, N., Kodama, H., & Tateda, A. (1991). High-performance liquid chromatographic determination of pyrophosphate in the presence of a 20,000-fold excess of orthophosphate. *Anal Biochem*, 199(2), 279-285.

Annex II

Selective extraction of phytic acid and pyrophosphate (phosphorous inhibitors of urolithiasis) with molecular imprinted polymers

Tong Liu, Liu He, Manuel Valiente, Montserrat López-Mesas*

Centre Grup de Tècniques de Separació en Química (GTS), Química Analítica,
Departament de Química, Universitat Autònoma de Barcelona, Cerdanyola, 08193,
Spain

Abstract:

Introduction & objectives

Phytic acid (IP6) and pyrophosphate (PPi) are natural phosphorous bioactive compounds with growing interest in the biomedical field due to their ability as potential inhibitors of urolithiasis among others. Existing methodologies for their separation and quantitative analysis show inconveniences mainly associated with tedious sample treatment, matrix interferences and lack of resolution. Molecular imprinting technology can be used to generate specific artificial polymeric receptors, i.e., high affinity stationary phases, as already shown for peptides and many other food ingredients. The objective of the present work is the development of a new method to extract both inhibitors by using molecularly imprinted polymer (MIP) as a specific adsorbent.

Materials & Methods

In this work, polymers have been molecularly imprinted using three organophosphorus compound as template, phenylphosphonic acid (PA), Di-(2-ethylhexyl)phosphoric acid (DEHPA) and pyrophosphoric acid. The molecularly imprinted polymer was prepared by thermal polymerization using N-allylthiourea as a functional monomer and ethylene glycol dimethacrylate (EGDMA) as a crosslinker. The polymers based on the three templates and one control polymer which was made without template were also synthesized and tested. The performance of each polymer was compared by absorption capacity. The effects of operating parameters on the adsorption capacity were studied, including the template, contact time, pH, temperature, and initial concentration of target analytes.

Results

Adsorption experimental results showed that the MIP1 using PA as template had the best adsorption capacity for IP6 and PPi compared with non-imprinted polymer, while the MIP2 using DEHPA as template had the best selectivity (IP6>PPi>P). pH have a significant effect on the adsorption capacity of the MIP. When raise the temperature from 20 °C to 65 °C, the adsorption capacity of IP6 change from 3.97µM/g to 3.19µM/g, while PPi changed from 4.55µM/g to 1.44µM/g, and phosphate changed from 2.44µM/g to 0.34µM/g. Based on the molecularly imprinted technology, IP6 and PPi can be separated easily by just changing the pH or temperature.

Conclusions

This work demonstrates a new method for extracting phosphorous inhibitors of urolithiasis (phytic acid and pyrophosphate) using molecularly imprinted polymers and could be used for nephrolithiasis related analysis. The developed polymer can be applied as specific stationary phases in solid-phase extraction or liquid chromatography. The development of methods to extract and recover phosphorous inhibitors from urine is very much desired. With improvements in the binding ability and selectivity of the molecularly imprinted polymers proposed in this study, these materials could be put into clinic use.

1. Introduction

Phytic acid (myoinositol hexaphosphate, IP6) is a naturally occurring compound that is abundantly found in grains, cereals, nuts, and foods that are high in fiber content. It is claimed to have the ability to enhance the anticancer effect of conventional chemotherapy and control cancer metastases^{1,2}. In addition, phytic acid acts as an effective inhibitor of calcium salts crystallization in urine and soft tissues, and prevents the formation of kidney stones (urolithiasis)³.

Inorganic pyrophosphate (PPi), can inhibit the formation of several crystallization reactions as for example the formation of calcium oxalate and hydroxyapatite, chemical composition of the 80% of kidney stones, serving so as natural inhibitor of urolithiasis⁴. In lithiasic patients, lower urinary PPi has been reported⁵ and its intake increase has been recommended⁶ as therapy. Thus, the determination of levels of both natural lithiasic inhibitors, IP6 and PPi, in urine is of interest for its healthy use.

The growing interest in the biomedical implications of phytic acid and pyrophosphate and the inherent problems with its poor separation are reflected in the tedious analytical techniques actually described and used in many laboratories. The quantitative extraction of phytate and pyrophosphate from urine is not selective and always co-extract with cations, protein, or other nutrients leading to erroneous estimation, damage to the analytical instruments, or both⁷.

For the determination of phytic acid, many methods have been developed. The frequently used measurement techniques include colorimetric method⁸, HPLC^{9,10,11,12}, HPIC¹³, ³¹P NMR spectroscopy¹⁴, synchronous fluorescence method¹⁵, inductively coupled plasma mass spectrometry (ICP-MS)¹⁶, and IPC-ICP-MS¹⁷. Indirect determination of phosphate after hydrolysis has been also used for the analysis of pharmaceutical formulations¹⁸. The traditional procedures employed for PPi determination are mainly based in chemical¹⁹ and enzymatic methods²⁰. Method

including either chromatographic²¹ or electrophoretic²² separation of PPi have also been reported. A method for the determination of IP6 and PPi in urine by SPE-ICP-MS techniques was developed in our laboratory achieving a simple and easy measurement to simultaneously analyze IP6 and PPi²³. But a non-laborious method for the extraction and purification from a fatty sample has not been developed.

Interest in molecularly imprinted polymer technique has increased significantly over the past few years as a result of its inherent advantages over more traditional extraction techniques. It has been demonstrated in many cases that MIP adsorption is an effective method to extract and separate molecular from matrix, but only few papers about IP6 separation using MIP were published, and the separation of PPi using the MIP adsorbent has also hardly been reported. Furthermore, the MIP mentioned above were prepared using single template and thus these MIP could not exhibit high selectivity for most of compounds especially belonging to different groups.

The main advantage of MIPs are their high affinity and selectivity for the target molecule (template). MIPs have higher physical strength, robustness, resistance to elevated pressure and temperature and inertness against various chemicals (organic solvents, acids, bases, and metal ions) compared to biological media such as proteins and nucleic acids. Furthermore, their production costs are low and their lifetimes can be as long as several years at room temperature²⁴.

2. Experimental

Reagents:

Compounds used for the synthesis of MIP and the nonimprinted polymer (NIP) were N-Allylthiourea (functional monomer), ethylene glycol dimethacrylate (EGDMA) (crosslinker), phenylphosphonic acid (template molecule), pyrophosphoric acid (template molecule) and Di-(2-ethylhexyl)phosphoric acid (DEHPA)(template molecule). All these compounds were purchased from Sigma-Aldrich (Steinheim, Germany). 2,2'-azobisisobutyronitrile (AIBN), from Acros Organics (Geel, Belgium), was used as the free radical initiator. Myoinositol hexaphosphoric acid hexasodium salt from corn (Sigma, Steinheim, Germany), hydrochloric acid (J.T. Baker, Deventer, Holland) and sodium dihydrogen phosphate (Panreac, Barcelona, Spain) were of analytical-reagent grade. Purified Milli-Q water of 18mΩ-cm resistivity was used for the preparation of all reagents.

Preparation of Molecular Imprinted Polymer

The MIP synthesized using as functional monomer N-allylthiourea was prepared following the literature²⁵ with a few modification. A certain amount of template (0.5mmol or 1 mmol), the functional monomer N-Allylthiourea (464.8mg, 4.0mmol), and cross-linker EGDMA (3.96g, 20mmol) were dissolved in ACN (4.0mL). The

preassembly solution was degassed in a sonicating bath for 5 min to get the prepolymerization solution. After sonication, AIBN (30mg, 0.18mm) was added into the prepolymerization solution as an initiator, purged with nitrogen for 10 min and sealed. The polymerization was carried out in a thermostatic water bath at 60 °C for 16 h, followed by heating at 80 °C for 3 h under nitrogen atmosphere. After the polymerization process, the obtained polymer was ground and sieved to yield a particle size of 50-100µm. In order to remove the template molecules, the polymer particles were washed. To do so, the polymer was placed in a Soxhlet apparatus and washed with water/acetic acid (4:1, v/v) for 24 h, and then with ethanol for 24 h more. The polymer was washed to elute the template and then complete elution of template was confirmed from the eluent by ICPMS. As a reference, non-imprinted polymer (NIP), was prepared in parallel to the MIP by using the same procedure without addition of template. As previously, the MIP synthesized using as functional monomer MAA was prepared following the literature with modification²⁶. A certain amount of template (phytic acid, 0.5-1mmol), the functional monomer (MAA, 5-16mmol), cross-linker (MBAm, EGDMA, or MBA+ ACM) were dissolved in suitable porogenic solvent and ammonium persulfate as an initiator added. The reaction mixture was degassed in a sonicating bath for 20 min, purged with nitrogen for 10 min and sealed. The polymerization was carried out in a thermostatic water bath (see table 4.2) at 40 °C for 24 h. The polymer was ground and sieved to yield a particle size of 28-75µm. To wash the polymer, it was placed in a Soxhlet apparatus and washed with water/acetic acid (4:1, v/v) for at least 48 h, followed by water for others 48 hours and then ethanol 48 h more. Non-imprinted polymer (NIP) was prepared in parallel to the MIP by using the same procedure, in order to use it as a reference.

Batch mode studies

The experimental parameters affecting the adsorption of IP₆ such as pH, contact time, initial concentration of IP₆ and temperature were studied in batch mode. Stock solutions (IP₆, PPi and P) were prepared by dissolving the reagents in Mill-Q water. 10mg of sorbent (MIPs or NIPs) was dispersed in standard solution of corresponding analyte (2 mL). The system was properly shaken on a rotary mixer at 25 rpm. After the desired time, MIPs and NIPs were isolated through 0.22µm Millipore filters (Millex-GS, Millipore, Ireland), and the concentration of analytes in the solvent phase was determined by ICP-MS.

Influence of the initial pH

The effect of initial pH on the equilibrium uptake of analytes (IP₆, PPi and P) was investigated in the pH range from 1.0 to 6.0. The solution pH was adjusted by the addition of 0.1 M HCl or 0.1 M NaOH, alternatively. In this study, each initial analyte concentration is 25 µM. 2 ml of this solution, at each selected pH, was agitated by a rotary mixer with 10 mg of MIP for 1 hour. The temperature was conducted at 20°C.

Influence of temperature

In order to study the temperature effect on the adsorption capacity of MIP, batch experiment also did at different temperatures (20°C, 50°C and 70°C). Experiments are all conducted at pH 4.0, and other conditions were kept equal as mentioned above.

Isotherm Studies

Adsorption isotherm is critical to evaluate the sorption capacity of adsorbents as well as understand the sorbate–sorbent interactions. Two commonly used model, the Langmuir and Freundlich²⁷ equations were used to describe the experimental data of adsorption isotherms. The Langmuir isotherm model can be expressed by the following equation:

$$Q_e = \frac{Q_m K_L C_e}{1 + K_L C_e} \quad (1)$$

Where C_e is the equilibrium concentration ($\mu\text{mol L}^{-1}$) of adsorbate in solution, Q_e represents the amount of IP6 adsorbed at equilibrium ($\mu\text{mol g}^{-1}$), Q_m is the maximum adsorption capacity and K_L is the Langmuir constants related to adsorption capacity and energy of adsorption.

The Freundlich isotherm model is given as follows:

$$Q_e = K_F C_e^{1/n} \quad (2)$$

Where K_F is a constant representing the adsorption capacity ($\mu\text{mol g}^{-1}$), and n is a constant depicting the adsorption intensity.

To carry out the assays, 10mg of MIP or NIP were added to 2 ml aqueous solution of phytic acid in the range of 0-100 μM of different concentrations and stirred for 1 hour at room temperature. The polymer particles were filtered off and filtrate was analyzed for phytic acid by ICP-MS. The quantity of phytic acid bounded was determined by subtracting the equilibrium amount of the compound to the initial measured quantity. The experimental binding data were fitted to the Langmuir-Freundlich (L-F) adsorption models.

Kinetics studies

The pseudo-first-order kinetic model can be generally described in the following equation:

$$\ln(q_{eq} - q_t) = \ln Q_e - k_1 t \quad (2)$$

Where q_{eq} and q_t are the amounts (mmol/g) of adsorbed analytes on the imprinted polymer at equilibrium and at time t , respectively. k_1 is the first order rate constant (1/min).

The pseudo-second-order kinetic model is expressed by Eq. (3).²⁸

$$dq_t/dt = k_2 (q_{eq} - q_t)^2 \quad (3)$$

where q_{eq} is the sorption capacity at equilibrium and q_t is the loading of the compound at time t . k_2 ($\text{g mg}^{-1} \text{h}^{-1}$) represents the pseudo-second-order rate constant for the kinetic

model. By integrating Eq. (3) with the boundary conditions of $q_t=0$ at $t=0$ and $q_t=q_t$ at $t=t$, the following linear equation can be obtained:

$$\frac{t}{q_t} = \frac{1}{V_0} + \frac{1}{q_{eq}} t \quad (4)$$

$$V_0 = k_2 q_{eq}^2 \quad (5)$$

Where V_0 ($\text{mg g}^{-1} \text{h}^{-1}$) is the initial sorption rate. Therefore, the V_0 and q_{eq} values of kinetic tests can be determined experimentally by plotting t/q_t versus t .

To perform the adsorption kinetic experiments, 40 ml of IP₆ 25 μM was added to 200 mg of MIP. The suspension was set at pH 5.6 and shaken for 120 min. Aliquots of 1 ml were taken at different times.

ICP conditions

The determination of PPI and IP₆ was carried out through ³¹P analysis of the purified extracts by ICP-MS using ⁴⁵Sc (5 $\mu\text{g L}^{-1}$) as internal standard. The ICP-MS equipment was X series II ICP-MS (Thermo Fisher Corp., USA) and conditions were set as table 1.

Table 1 Instrumental operating conditions for ICPMS system

<i>ICP system</i>	
Instrument	Thermo X series II ICP-MS
RF power	1350W
Auxiliary gas flow	0.92 L min ⁻¹
Coolant gas flow	13.30 Lmin ⁻¹
Nebulizer gas flow	0.89 Lmin ⁻¹
Sample cone	Pt, 1.0 mm orifice
Skimmer cone	Pt, 0.7 mm orifice
Resolution	normal
Nebulizer	concentric nebulizer (Thermo)
<i>Sample introduction system</i>	
Sample uptake flow rate	2 mL min ⁻¹
Delay time	60s
Wash time	50s (HCl 1%)
<i>Data acquisition parameters</i>	
Analyzer	quadrupole
Scanning mode	peak jumping
Sweep per reading	30
Number of replicates	3
Dwell time	10ms

3. Results and discussion

The choice of monomer and cross-linker

The choice of functional monomer is very important in order to forming more stable complexes with the template to generate MIPs with template-specific cavities.

The thiourea group has been used in the literature as anion binding sites through the hydrogen bond donors to recognize anions²⁹. It is known to have a strong binding ability to phosphate in hydrophilic solvent and aqueous media^{30,31}. For the present study, it was necessary to develop the molecularly imprinted polymers that had effective binding in a hydrophilic condition. For this purpose, functional monomer with a thiourea group, N-allylthiourea was chosen to prepare the molecularly imprinted polymer and the binding activities of the imprinted polymers was evaluated.

Methacrylic acid (MAA) is a conventional functional monomer in molecular imprinting. Three different cross linkers N, N'-Methylenebisacrylamide (MBAm), ethylene glycol dimethacrylate (EGDMA), Acrylamide (ACM), were used to synthesize the imprinted polymers in order to evaluate the imprinting effect.

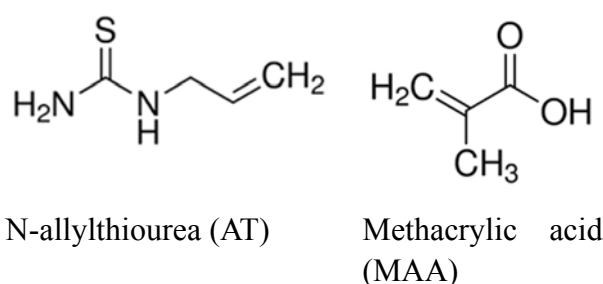


Figure 1. Structures of monomer used in this study

Table 2 shows the polymers prepared imprinted (MIP) or non-imprinted (NIP) with the amount and type of functional monomer, solvent and crosslinker used.

Table 2. Imprinted and non-imprinted polymers prepared in this study

<i>Polymer</i>	<i>Template (mmol)</i>	<i>Functional monomer (mmol)</i>	<i>Crosslinker (mmol)</i>	<i>Solvent (ml)</i>
M3	Phytic acid (1.0)	MAA(16.0)	MBAm (12.5)	Water/ethane (3:1, V/V) 10ml
N3	None	MAA(16.0)	MBAm (12.5)	Water/ethane (3:1, V/V) 10ml
M13*	Phytic acid (1.0)	MAA(16.0)	EGDMA (20)	Water/ACN (80/8ml)
N13*	None	MAA(16.0)	EGDMA (20)	Water/ACN (80/8ml)
M15*	Phytic acid (0.5)	MAA(5.0)	MBA (12.5)+ ACM(5)	Water/ethane (3:1, V/V) 10ml
N15*	None	MAA(5.0)	MBA (12.5)+ ACM(5)	Water/ethane (3:1, V/V) 10ml
M29	DEHPA (1.0)	AT(4.0)	EGDMA (20)	ACN 4ml
N29	None	AT(4.0)	EGDMA (20)	ACN 4ml

Note* imprinted polymer prepared by suspension method due to the solubility of the template.

Results are shown in Figure 2. It is observed how one of the MIP has an adsorption capacity higher than the rest (M29) and differentiated from the corresponding NIP (N29) what indicates the effect of imprinting.

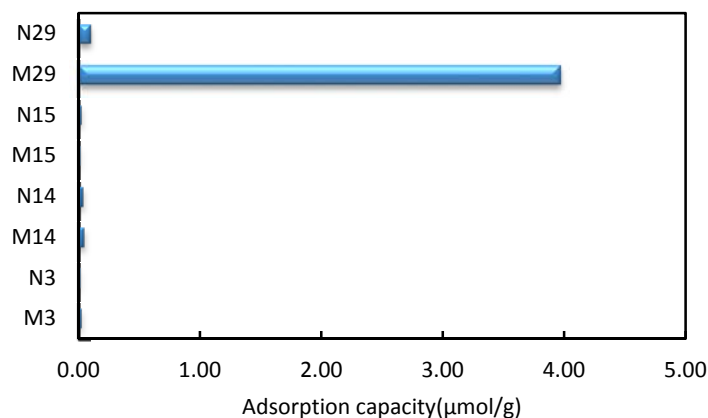


Figure 2. Binding activities of imprinted polymers towards IP6 in water solutions.

When using N-allylthiourea as the functional monomer, the amount of IP6 binding to the imprinted polymers was nearly 4 µmol/g, comparing that to the non-imprinted polymer was only 0.1 µmol/g (Fig.2).

However, for MAA none of the polymers showed affinity to IP6. Though methacrylic acid is a powerful functional monomer in molecular imprinting in the organic solution system, the binding activities were quite low in aqueous media. N-allylthiourea, as the functional monomer, has both the strong binding ability to IP6 in an aqueous condition and hydrophilicity. Thus, the imprinted polymer would successfully interact with IP6²⁵.

The effect of steric factors on recognition

To prepare the MIP different compounds were used as template: DEHPA, pyrophosphoric acid and phenylphosphonic. The different MIPs prepared are shown in Table 3.

Comparing the imprinted polymers M-1, M-2, M-3, M-4 and M-5, bulk polymer prepared in the same functional monomer and cross-linker but using different templates, the synthesized polymer had different adsorption capacity for IP6, PPI and P. The adsorption capacity of all the imprinted polymers is shown in Figure 6. It indicated that M-5 have the best adsorption capacity for IP6, PPI, and P. This means that the imprinted polymer using DEHPA as template has the best specific adsorption ability which means the template has a great effect on the binding capacity of MIP for the adsorption of IP6. . This can be explained by the presence of steric factors in the template. This possibility of recognition based on steric factors was further suggested by the adsorption capacity of imprinted polymers. The template DEHPA is much bigger than phenylphosphonic acid and pyrophosphoric acid which may leave larger binding site on the surface of

imprinted polymers. The effect of molecular shape on recognition was particularly pronounced in the case of imprinted polymer M-5 which had the highest adsorption capacity for IP₆, PPI and P.

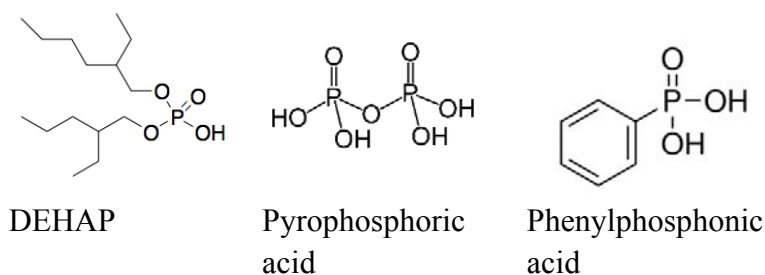


Figure 3. Structures of templates used in this study

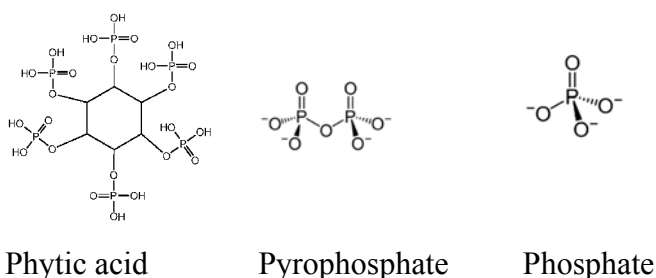


Figure 4. Structures of the objective analytes used in this study

Table 3. Imprinted and non-imprinted polymers prepared in this study

<i>Polymer</i>	<i>Template (mmol)</i>	<i>Functional monomer (mmol)</i>	<i>Crosslinker (mmol)</i>	<i>Solvent (ml)</i>
M-1	DEHPA (0.4)	AT(4.0)	EGDMA (16)	Acetonitrile 4ml
M-2	Pyrophosphoric acid (1.5)	AT(4.0)	EGDMA (16)	Acetonitrile 4ml + ethanol 1.5ml
M-3	Pyrophosphoric acid (1.5)	AT(4.0)	EGDMA (16)	Ethanol 4ml
M-4	Phenylphosphonic acid (1.0)	AT(4.0)	EGDMA (20)	Acetonitrile 4ml
M-5	DEHPA (1.0)	AT(4.0)	EGDMA (20)	Acetonitrile 4ml
NIP	None	AT(4.0)	EGDMA (20)	Acetonitrile 4ml

The impact of porogenic solvent

Nature and volume of the porogenic solvent is also a vital factor in molecular imprinting synthesis³². The typically solvents used were toluene, dichloromethane, chloroform, and acetonitrile. Less polar solvents are believed to enhance the complex formation by ensuring strong interactions such as hydrogen bonds²⁴. Although acetonitrile was shown by preliminary studies³³ to be the optimum porogen for synthesizing EGDMA system polymers, in the present study, polymers M-2 and M-3 were prepared with the addition of ethanol as porogen solvent because the pyrophosphoric has a poor solubility

in acetonitrile. Compared with acetonitrile, ethanol is a more polar solvent. The presence of ethanol reduced the imprinting effect which was observed in the adsorption capacity of M-2 (ethanol and ACN), which was better than M-3 (only ethanol) for all three compounds. These results suggest that the use of correct porogen can have a significant effect on the chemical performance.

Given the poor performance of these polymers, no further studies were carried out on it, yet it is worthy to mention the binding ability compared with the NIP polymer.

The characterization of MIP

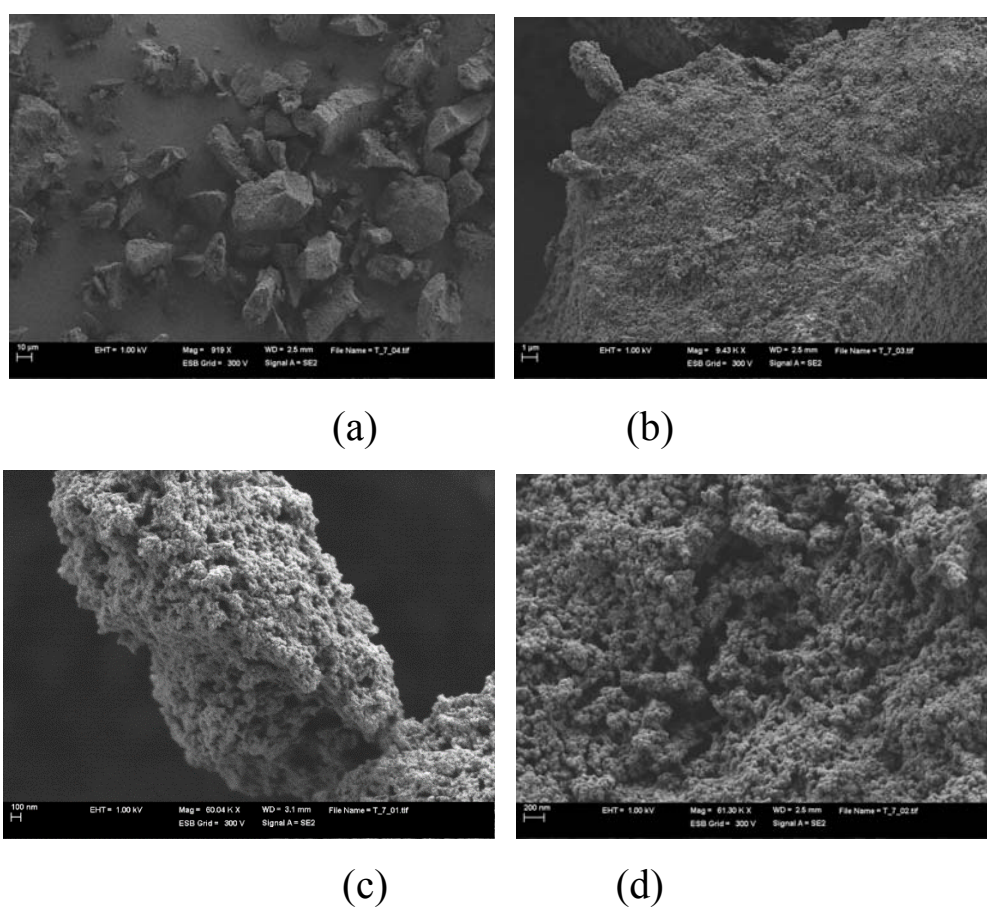


Figure 5. SEM of prepared by bulk polymerization method

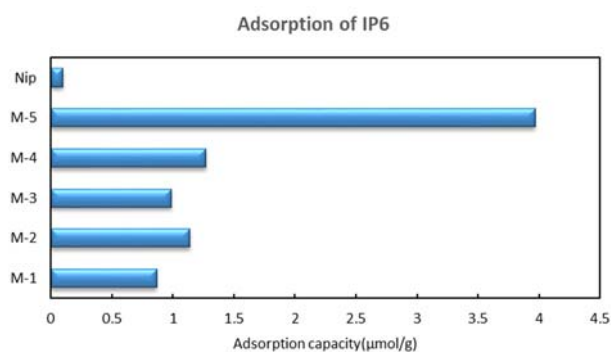
The SEM image of M-29 shows irregular shaped and agglomerated particles with 25 μm size are observed in the SEM images of (a). Fig. 5 (a) to (d) depicts the SEM images from 1000× to 61.30K× respectively. The morphology of these MIPs is highly agglomerated and irregularly shaped with particle size in nanometers. We could observe a lot of holes on the surface of the polymer.

The impact of molar ratio

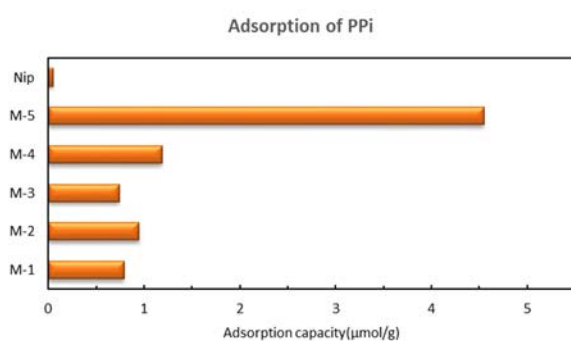
It is known that the molar ratio template: functional monomer: cross-linker affects polymer porosity which determines the substrate accessibility, size and shape of active binding site, which at the end will affect the sorption capacity. On the other hand, the arrangement of functional groups in the recognition sites of the polymeric network will

determine the degree of specific binding interactions³⁴.

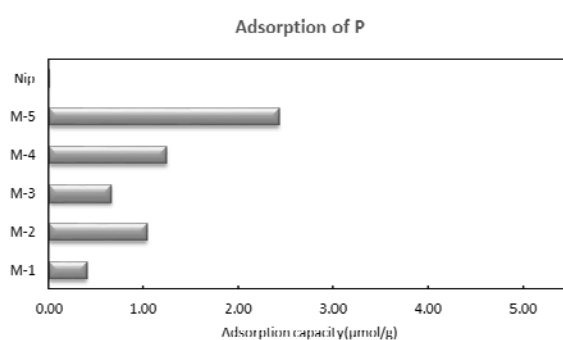
This can be observed comparing M1 and M5 (figure 6), where the same template but with different molar ratio were used (0.4:4:16 and 1:4:20 respectively). For the second polymer a higher performance is obtained being the best molar ratio 1:4:20 which was the chosen in the present work.



(a)



(b)



(c)

Figure 6. adsorption capacity of MIP for polymers shown in Table 1

The effect of pH

Solution pH usually influences the adsorption to a large extent, as it affects the properties of both adsorbent and adsorbate. Optimization of pH value for adsorption medium plays a vital role in the adsorption studies. The pH of the adsorption medium is the most significant parameter in the treatment of phytic acid by the adsorbent. The

pH of the solution affects the degree of ionization and speciation of phytic acid which subsequently leads to a change in adsorption kinetics and equilibrium characteristics³⁵. Then, the effect of pH on the adsorption of phytic acid was study and results are shown in Fig. 7.

It was observed that adsorption of IP6 between pH 2.0 to 5.6 did not cause any change in adsorption capacity. Fig. 7 also showed that adsorption of IP6 at pH 1.0 was significantly low and indicates that the MIP loss the adsorption capacity. The fact neutral molecules of phytic acid are benefit for the adsorption process has also been reported previously for other sorbent by Muños et al.²³. For subsequent studies, pH 5.6 was selected for the adsorption medium since is the pH closer to the natural pH of environmental water samples and urine.

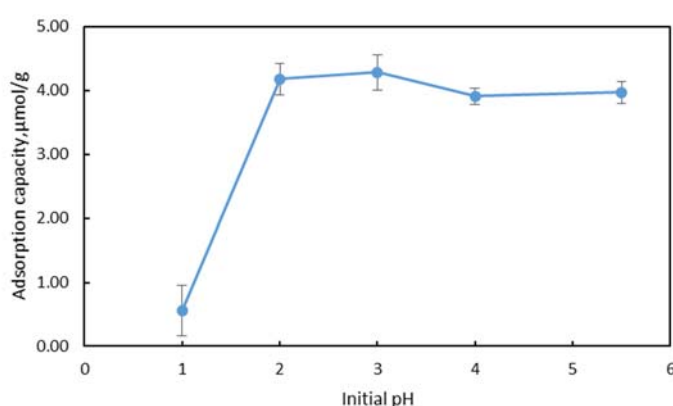


Figure 7. Effect of pH on adsorption of IP6.

Adsorption isotherms

From previous results, MIP 5 was selected as the best for the adsorption and separation of phytic acid and so isotherm study was performed on it.

Langmuir isotherm

The Langmuir adsorption isotherm has been successfully applied to many MIP adsorption processes and has been the most widely used to describe the adsorption of a solute from a liquid solution. A basic assumption of the Langmuir theory is that adsorption takes place at specific homogeneous sites on the surface of the adsorbent. It is then assumed that once adsorbate molecule occupies a site, no further adsorption can take place at that site. The rate of adsorption to the surface should be proportional to a driving force and area. The driving force is the concentration in the solution, and the area is the amount of bare surface³⁵.

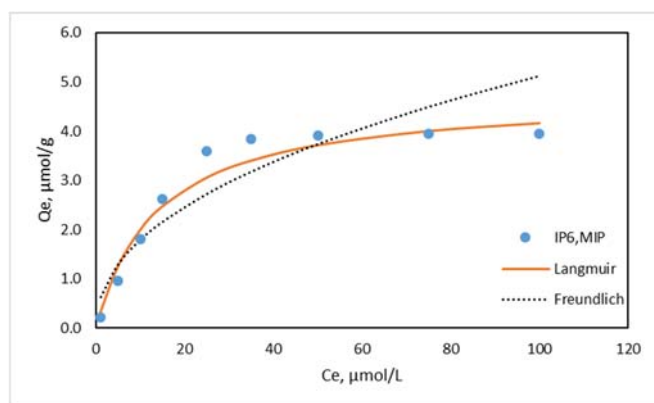


Figure 8. Adsorption isotherm of the imprinted polymer.

In order to investigate the binding properties of the IP6 imprinted polymer, the saturation adsorption experiments were carried out and the corresponding adsorption isotherms were shown in Figure 8.

In Figure 8, the adsorption capacity, Q_e is shown against initial concentrations of IP6. From Figure 3, when the concentration of IP6 increased, the adsorption capacity (Q_e) firstly increased sharply, then increased slowly, to finally reach a saturation profile at higher concentration. It could be ascribed to the molecular-imprinting effect, which could recognize the templates via multiple point electrostatic interaction and shape complementarity formed in the MIP by the polymerization³⁶.

It shows (figure 8) the adsorption isotherms of the MIP adsorbents for IP6, and Langmuir and Freundlich models. As shown the adsorption isotherms of IP6 on the MIP can be fitted better by the Langmuir model than the Freundlich. Freundlich isotherm has been observed for a wide range of heterogeneous surfaces, including activated carbon, silica, clays, metals, and polymers³⁷. Freundlich equation is suitable for heterogeneous surfaces and has been applied in the adsorption process using the non-covalently imprinted polymers. In this study, the correlation coefficients suggest that the Langmuir isotherm model is suitable for describing the adsorption equilibrium of IP6 by the imprinted polymer. The fitting data in table 3 shows that the maximum adsorption capacity (Q_{max}) for IP6 was $4.675 \mu\text{mol/g}$.

Table 4. Parameters in adsorption isotherm of imprinted polymer

Isotherm models	Constants	
Langmuir equation	$Q_m(\mu\text{mol g}^{-1})$	4.675
	$K_L(L \mu\text{mol}^{-1})$	0.074
	r^2	0.9783
Freundlich equation	$K_F(\mu\text{mol g}^{-1})$	0.633
	n^{-1}	0.454
	r^2	0.8199

Adsorption properties and Scatchard analysis

The adsorption capacity of MIP is an important parameter to determine the amount of

MIP required to quantitatively adsorb a specific amount of imprinted templates from solution³⁸.

Scatchard analysis is a method to linearize data from a saturation binding experiment in order to determine binding constants. To investigate the binding ability of the imprinted polymer in aqueous media, a Scatchard analysis was carried out. This tool has been already applied in molecularly imprinted polymer in the bibliography³⁹.

Scatchard analysis was conducted using the following equation⁴⁰:

$$\frac{Q_e}{F} = \frac{Q_{max} - Q_e}{K_D} \quad (6)$$

Where Q_e ($\mu\text{mol/g}$) is the amount of IP6 bounded to the polymer and F ($\mu\text{mol/L}$) is equilibrium concentration of free IP6 in solution (approximated by the analytical concentration of IP6). Q_{max} ($\mu\text{mol/g}$) is the apparent maximum number of binding sites of the polymer and K_D ($\mu\text{mol/L}$) represents the dissociation constant of the complex IP6-MIP.

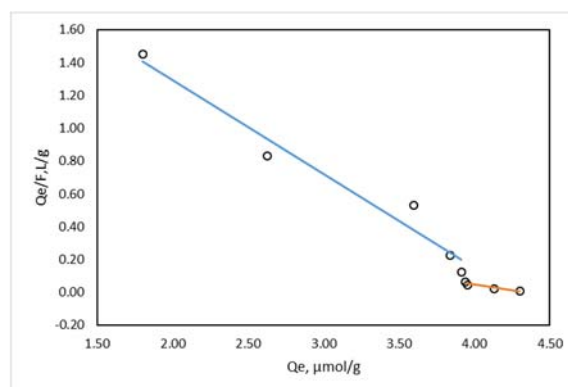


Figure 9. Scatchard plot of the imprinted polymer to estimate the binding ability calculated from the saturation profile.

The Scatchard plot was shown in Fig.9. The dissociation constant K_D and the number of binding sites Q_{max} can be estimated from the obtained binding data which was plotted in Figure 9. As shown in the Scatchard plot, the relationship between Q_e/F and Q_e was not a single linear curve, but consisted of two linear curves with different slopes, suggesting that the binding sites in MIP are heterogeneous in respect to the affinity for IP6³⁹. Since there are two distinct parts within the plot which can be considered as straight lines, it would be reasonable to assume that the binding sites configuration in the MIP can be classified into two distinct groups with specific binding properties. This kind of non-intervalence-type molecular imprinting polymer has been reported by other researches⁴¹. Under the assumptions, the respective dissociation constant, K_D , was estimated by Scatchard analysis calculated from the saturation profile. The K_D of the highest affinity binding site was estimated to be 1.75 μM and 7.32 μM . The respective theoretical binding site, Q_{max} were calculated on 4.26 $\mu\text{mol/g}$ and 4.34 $\mu\text{mol/g}$ of dry polymer.

Adsorption kinetics

The kinetics of adsorption that describe the solute adsorption rate governing the residence time of the sorption reaction is one of the important characteristics that define the efficiency of adsorption.

Fig. 10 shows the adsorption kinetics of IP₆ on the MIP at different time intervals and the simulation of the pseudo-second-order kinetic model. It can be seen that the adsorption equilibrium was almost achieved after 10 min. Adsorption of IP₆ on the MIP approach pseudo-equilibrium rapidly. For IP₆, more than 70% removal of IP₆ was achieved within 1 min of contact and the adsorption equilibrium was approached in 10 min. The greater surface area and smaller particle size raise the probability of the adsorption reactions. The sorption amount of the MIP for IP₆ reached 3.85 $\mu\text{mol g}^{-1}$ after 10 min sorption, suggesting the good imprinting effect of the MIP. The short contact time needed to reach equilibrium as well as the high adsorption capacity suggests that the MIP possess highly potential applications for the removal of IP₆ from urine.

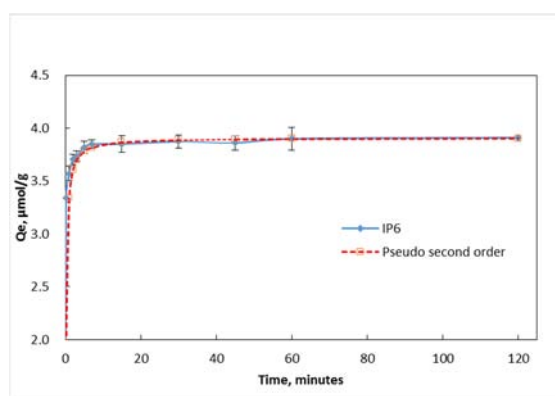


Figure 10. Adsorption kinetics of IP₆ on the MIP at pH5.6.

Table 5 shows the determination coefficients (r^2) and the other parameters obtained from the pseudo-second-order kinetic model by the plot of t versus t/q_t to determine the V_0 and q_{eq} values for all the media. The pseudo-second-order model fits the kinetic data in our system very well ($r^2 > 0.999$). The initial adsorption rate of IP₆ over MIP is $23.3 \mu\text{mol g}^{-1} \text{h}^{-1}$. The fitting data show that the MIP has a good affinity for IP₆, which takes less time to reach equilibrium in the process.

Table 5. Kinetic parameters of a pseudo-second-order kinetic model fitting IP₆ adsorption by the MIP.

system	V_0 $\mu\text{mol g}^{-1} \text{h}^{-1}$	q_{eq} $\mu\text{mol g}^{-1}$	k_2 $\text{g } \mu\text{mol}^{-1} \text{h}^{-1}$	r^2
IP ₆ /MIP	23.25	3.91	1.52	0.99998

The effect of temperature

The temperature has two major effects on the adsorption process. Increasing the temperature is known to increase the rate of diffusion of the adsorbate molecules across the external boundary layer and in the internal pores of the adsorbent particle, owing to

the decrease in the viscosity of the solution. In addition, changing the temperature will change the equilibrium capacity of the adsorbent for a particular adsorbate³⁵. In this phase study, a series of experiments were conducted at 20, 50, and 70°C to study the effect of temperature on the rate and the kinetics. The results are present in Fig.6. As can be seen, the uptake decrease with the rise of temperature, indicating the exothermic nature of these adsorptions⁴².

Also we can see that PPI have a little more capacity than IP6, this is may be because the size the PPI is smaller than IP6, so it is easier to go into the MIP body and occupy a lot of the active space. P is less adsorb on MIP and well release from MIP as the temperature arise.

Since these prepared imprinted polymer could be used in high performance liquid chromatography (HPLC) or capillary electrochromatography (CEC) for the separations of phosphate compounds, there will have some obstacles leading to loss of separation power, such as the effects of temperature on the polymer syntheses and chiral recognition characters⁴³. Since host functional monomers binding to the specific guest templates are chemically solidified by cross-linking polymerization, the host-guest complexation mechanism is also a kinetically driven process. The temperature effect is assumed to be an important factor for CEC filled with molecularly imprinted polymer since there potential Joule heating within the capillary under usual voltage setting of 5–30 kV⁴³.

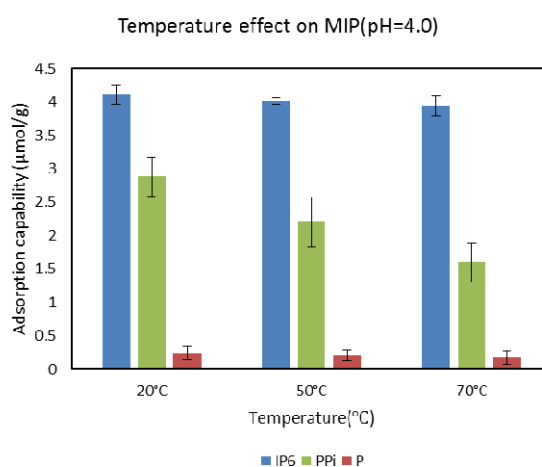


Figure 11. IP6, PPI and P adsorption capacity on MIP at different temperature at pH=4.0

Separation section

Since we found the pH have a significant effect on the adsorption of IP6 on the developed MIP, therefore, a separation procedure based on acid elution was developed. For this purpose, different concentrations of HCl were used (0.1 M, 0.01M and 0.005M) and the obtained results were compared. With the addition of acid solution, the non-specific interactions established between the analytes and the MIP was disrupted so that the adsorbed analytes were almost completely eluted upon the introduction of the washing step.

The effect of pH

In order to selectively elute the IP6, PPI and P from the SPE column, it is necessary to investigate the effect of pH on the adsorption of MIP which will be used for the separation procedure. It is indicated in figure 12(a) that the MIP start to desorb the IP6 below pH 2.0, and 95% of the IP6 was desorbed form the imprinted polymer at pH 1.0. While for PPI, desorption started below pH 6 slowly and sharply desorbed from pH 3.0 to pH 2.0. Figure 12(c) show that the P cannot adsorbed on the imprinted blow pH 4.0. This phenomena let us to think about separate the three compounds by just tuning the pH of the elute solution.

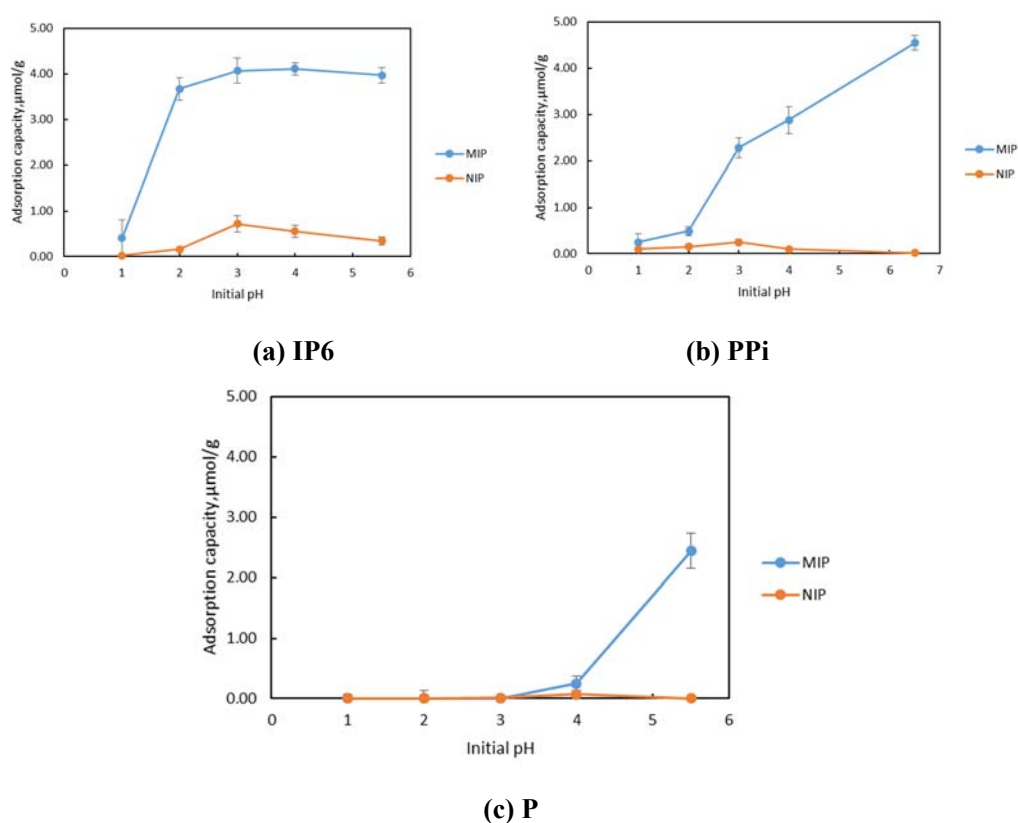


Figure 12. IP6, PPI and P adsorption capacity on MIP at different pH

This can be explained by the different dissociate constant of these three compounds. IP6 is highly selectively adsorbed in the imprinted polymer as a consequence of its strongest dissociation at low pH values ($pK_{a1} = -0.15$, $pK_{a2} = 0.41$, $pK_{a3} = 0.85$, $pK_{a4} = 1.84$). PPI is strongly dissociated at low pH values ($pK_{a1} = 0.85$, $pK_{a2} = 1.49$, $pK_{a3} = 5.77$, $pK_{a4} = 8.22$) being strongly retained by the resin, whereas Pi ($pK_{a1} = 2.12$, $pK_{a2} = 7.20$, $pK_{a3} = 12.36$) is easier desorbed from the polymer by lower the pH or use diluted HCl. Thus, separation is pH-dependent and a suitable selection of the eluting condition according to their acidity will lead to highly purified extracts of PPI and IP6, respectively²³. Due to the different dissociation degree of the phosphorous species depending on the pH a separation system based on pH gradient can be designed where P can be separated from IP6 and PPI at pH 3.0 and the PPI can be separated from IP6 at the pH 2.0, then the IP6 could eluted at pH 1.0 by the use of molecularly imprinted

polymer solid phase extraction system.

SPE-MIP separation system

Based on the discovery of the effect of pH, we did the SPE separation to separate IP6, PPI and P by elute the cartridge with HCl solution. In order to do this, the prepared MIP-SPE cartridge loaded with IP6 and PPI just by passing the defined concentration of standard analytes through the cartridge. After a washing step with HCl, the analytes were eluted with different concentration of HCl. All fractions were collected and analyzed by ICP-MS. All results were confirmed by triplicated experiments.

After loaded the PPI, the 1mM HCl can only elute 6.5% of the loaded analytes, this means the acid are not strong enough the disrupt the interaction between PPI and MIP(table 6). While when increase the HCl to 5mM, 71.9% of the PPI can be eluted and this recovery increase to 97.8% at 10mM HCl. From figure 4.18 we can clearly observed that the PPI can be efficiently eluted from the matrix by HCl solution (concentrated more than 10mM (pH=3)), since at this pH the MIP has very poor adsorption capacity which observed in the batch experiments. While for the IP6, under the condition of 10mM HCl, the recovery is only 38.2% that means at this condition the MIP still can adsorb the IP6 well. However, when we using the more concentrated HCl, at 100mM conditions, the recovery of IP6 can achieve 103.7% which means all of the IP6 has release to the acid solution.

Table 6. Recovery of IP6 and PPI by the SPE process under different elute condition.

analyte	elute solution	recovery,%
PPI	1mM	6.5
	5mM	71.9
	10mM	97.8
	50mM	107.5
IP6	10mM	38.2
	100mM	103.7
	200mM	113.6

4. Conclusions

MIP were successfully synthesized using the bulk polymerization method. The polymer prepared using MAA as functional monomer showed no affinity for IP6. The polymer synthesis with N-allylthiourea showed high adsorption for IP6 with the capacity nearly 4 $\mu\text{mol/g}$, comparing that to the non-imprinted polymer was only 0.1 $\mu\text{mol/g}$. The MIP prepared using DEHPA as template show the best adsorption capacity compared with the polymer prepared with pyrophosphoric acid and phenylphosphonic acid. The solution pH has a significant effect on the adsorption of IP6, PPI and Phosphate on the

developed MIP. The separation of IP6, PPi and Phosphate was achieved by SPE procedure which using the synthesized MIP as adsorbent.

This work demonstrates a new method for extracting phosphorous inhibitors of urolithiasis (phytic acid and pyrophosphate) using molecularly imprinted polymers and could be used for nephrolithiasis related analysis. The developed polymer can be applied as specific stationary phases in solid-phase extraction or liquid chromatography. The development of methods to extract and recover phosphorous inhibitors from urine is very much desired. With improvements in the binding ability and selectivity of the molecularly imprinted polymers proposed in this study, these materials could be put into clinic use.

Reference

1. Rizvi, I.; Riggs, D. R.; Jackson, B. J.; Ng, A.; Cunningham, C.; McFadden, D. W., Inositol Hexaphosphate (IP6) Inhibits Cellular Proliferation In Melanoma. *Journal of Surgical Research* **2006**, *133* (1), 3-6.
2. Somasundar, P.; Riggs, D. R.; Jackson, B. J.; Cunningham, C.; Vona-Davis, L.; McFadden, D. W., Inositol Hexaphosphate (IP6): A Novel Treatment for Pancreatic Cancer1. *Journal of Surgical Research* **2005**, *126* (2), 199-203.
3. Grases, F.; Isern, B.; Sanchis, P.; Perello, J.; Torres, J. J.; Costa-Bauza, A., Phytate acts as an inhibitor in formation of renal calculi. *Front Biosci* **2007**, *12* (1), 2580-7.
4. Terkeltaub, R. A., Inorganic pyrophosphate generation and disposition in pathophysiology. *American Journal of Physiology-Cell Physiology* **2001**, *281* (1), C1-C11.
5. Sharma, S.; Vaidyanathan, S.; Thind, S.; Nath, R., Urinary excretion of inorganic pyrophosphate by normal subjects and patients with renal calculi in north-western India and the effect of diclofenac sodium upon urinary excretion of pyrophosphate in stone formers. *Urologia internationalis* **1992**, *48* (4), 404-408.
6. Breslau, N. A.; Padalino, P.; Kok, D. J.; Kim, Y. G.; Pak, C. Y., Physicochemical effects of a new slow - release potassium phosphate preparation (UroPhos - K) in absorptive hypercalciuria. *Journal of Bone and Mineral Research* **1995**, *10* (3), 394-400.
7. Ray, P.; Shang, C.; Maguire, R.; Knowlton, K., Quantifying phytate in dairy digesta and feces: Alkaline extraction and high-performance ion chromatography. *Journal of dairy science* **2012**, *95* (6), 3248-3258.
8. Latta, M.; Eskin, M., A simple and rapid colorimetric method for phytate determination. *Journal of Agricultural and Food Chemistry* **1980**, *28* (6), 1313-1315.
9. Skoglund, E.; Carlsson, N.-G.; Sandberg, A.-S., High-performance chromatographic separation of inositol phosphate isomers on strong anion exchange columns. *Journal of agricultural and food chemistry* **1998**, *46* (5), 1877-1882.
10. Rounds, M.; Nielsen, S., Anion-exchange high-performance liquid chromatography with post-column detection for the analysis of phytic acid and other inositol phosphates. *Journal of Chromatography A* **1993**, *653* (1), 148-152.
11. Perello, J.; Isern, B.; Munoz, J.; Valiente, M.; Grases, F., Determination of Phytate in Urine by High-

- Performance Liquid Chromatography–Mass Spectrometry. *Chromatographia* **2004**, *60* (5-6), 265-268.
12. Sandberg, A. S.; Ahderinne, R., HPLC Method for Determination of inositol Tri - , Tetra - , Penta - , and Hexaphosphates in Foods and Intestinal Contents. *Journal of Food Science* **1986**, *51* (3), 547-550.
 13. Blaabjerg, K.; Hansen-Møller, J.; Poulsen, H. D., High-performance ion chromatography method for separation and quantification of inositol phosphates in diets and digesta. *Journal of Chromatography B* **2010**, *878* (3), 347-354.
 14. Kemme, P. A.; Lommen, A.; De Jonge, L. H.; Van der Klis, J. D.; Jongbloed, A. W.; Mroz, Z.; Beynen, A. C., Quantification of inositol phosphates using ³¹P nuclear magnetic resonance spectroscopy in animal nutrition. *Journal of agricultural and food chemistry* **1999**, *47* (12), 5116-5121.
 15. Chen, Y.; Chen, J.; Luo, Z.; Ma, K.; Chen, X., Synchronous fluorescence analysis of phytate in food. *Microchimica Acta* **2009**, *164* (1-2), 35-40.
 16. Muñoz, J. A.; Valiente, M., Determination of phytic acid in urine by inductively coupled plasma mass spectrometry. *Analytical chemistry* **2003**, *75* (22), 6374-6378.
 17. Helfrich, A.; Bettmer, J., Determination of phytic acid and its degradation products by ion-pair chromatography (IPC) coupled to inductively coupled plasma-sector field-mass spectrometry (ICP-SF-MS). *Journal of Analytical Atomic Spectrometry* **2004**, *19* (10), 1330-1334.
 18. March, J.; Grases, F.; Salvador, A., Hydrolysis of phytic acid by microwave treatment: Application to phytic acid analysis in pharmaceutical preparations. *Microchemical journal* **1998**, *59* (3), 413-416.
 19. Chang, G.-G.; Denq, R.-Y., Determination of inorganic pyrophosphate concentration in urine. *International Journal of Biochemistry* **1985**, *17* (6), 733-735.
 20. Baykov, A.; Avaeva, S., A sensitive method for measuring pyrophosphate in the presence of a 10,000-fold excess of orthophosphate using inorganic pyrophosphatase. *Analytical biochemistry* **1982**, *119* (1), 211-213.
 21. Yoza, N.; Akazaki, I.; Nakazato, T.; Ueda, N.; Kodama, H.; Tateda, A., High-performance liquid chromatographic determination of pyrophosphate in the presence of a 20,000-fold excess of orthophosphate. *Analytical biochemistry* **1991**, *199* (2), 279-285.
 22. Hénin, O.; Barbier, B.; Brack, A., Determination of phosphate and pyrophosphate ions by capillary electrophoresis. *Analytical biochemistry* **1999**, *270* (1), 181-184.
 23. Munoz, J. A.; Lopez-Mesas, M.; Valiente, M., Minimum handling method for the analysis of phosphorous inhibitors of urolithiasis (pyrophosphate and phytic acid) in urine by SPE-ICP techniques. *Analytica chimica acta* **2010**, *658* (2), 204-8.
 24. Cheong, W. J.; Yang, S. H.; Ali, F., Molecular imprinted polymers for separation science: a review of reviews. *Journal of separation science* **2013**, *36* (3), 609-28.
 25. Kugimiya, A.; Takei, H., Preparation of molecularly imprinted polymers with thiourea group for phosphate. *Analytica chimica acta* **2006**, *564* (2), 179-183.
 26. Cirillo, G.; Curcio, M.; Parisi, O. I.; Puoci, F.; Iemma, F.; Spizzirri, U. G.; Picci, N., Gastro-intestinal sustained release of phytic acid by molecularly imprinted microparticles. *Pharmaceutical development and technology* **2010**, *15* (5), 526-31.
 27. Jin, Y.; Row, K. H., Adsorption isotherm of ibuprofen on molecular imprinted polymer. *Korean Journal of Chemical Engineering* **2005**, *22* (2), 264-267.
 28. Chan, Y. T.; Kuan, W. H.; Chen, T. Y.; Wang, M. K., Adsorption mechanism of selenate and selenite on the binary oxide systems. *Water research* **2009**, *43* (17), 4412-4420.
 29. Nishizawa, S.; Shigemori, K.; Teramae, N., A Thiourea-Functionalized Benzo-15-crown-5 for

- Cooperative Biding of Sodium Ions and Anions. *Chemistry Letters* **1999**, (11), 1185-1186.
30. Shigemori, K.; Nishizawa, S.; Yokobori, T.; Shioya, T.; Teramae, N., Selective binding of very hydrophilic H₂PO₄⁻ anion by a hydrogen-bonding receptor adsorbed at the 1, 2-dichloroethane–water interface. *New journal of chemistry* **2002**, 26 (9), 1102-1104.
31. Aoki, H.; Hasegawa, K.; Tohda, K.; Umezawa, Y., Voltammetric detection of inorganic phosphate using ion-channel sensing with self-assembled monolayers of a hydrogen bond-forming receptor. *Biosensors and Bioelectronics* **2003**, 18 (2), 261-267.
32. Pardeshi, S.; Dhodapkar, R.; Kumar, A., Influence of porogens on the specific recognition of molecularly imprinted poly(acrylamide-co-ethylene glycol dimethacrylate). *Composite Interfaces* **2013**, 21 (1), 13-30.
33. Fitzhenry, L.; Manesiotis, P.; Duggan, P.; McLoughlin, P., Molecularly imprinted polymers for corticosteroids: impact of polymer format on recognition behaviour. *Microchimica Acta* **2013**, 180 (15-16), 1421-1431.
34. Phutthawong, N.; Pattarawarapan, M., Synthesis of highly selective spherical caffeine imprinted polymers via ultrasound - assisted precipitation polymerization. *Journal of Applied Polymer Science* **2013**, 128 (6), 3893-3899.
35. Sathishkumar, M.; Binupriya, A.; Kavitha, D.; Selvakumar, R.; Jayabalan, R.; Choi, J.; Yun, S., Adsorption potential of maize cob carbon for 2, 4-dichlorophenol removal from aqueous solutions: equilibrium, kinetics and thermodynamics modeling. *Chemical Engineering Journal* **2009**, 147 (2), 265-271.
36. Le Noir, M.; Lepeuple, A.-S.; Guieysse, B.; Mattiasson, B., Selective removal of 17 β -estradiol at trace concentration using a molecularly imprinted polymer. *Water research* **2007**, 41 (12), 2825-2831.
37. Umpleby Ii, R. J.; Baxter, S. C.; Bode, M.; Berch Jr, J. K.; Shah, R. N.; Shimizu, K. D., Application of the Freundlich adsorption isotherm in the characterization of molecularly imprinted polymers. *Analytica chimica acta* **2001**, 435 (1), 35-42.
38. Dai, C.-m.; Zhang, J.; Zhang, Y.-l.; Zhou, X.-f.; Duan, Y.-p.; Liu, S.-g., Removal of carbamazepine and clofibric acid from water using double templates–molecularly imprinted polymers. *Environmental Science and Pollution Research* **2013**, 20 (8), 5492-5501.
39. Matsui, J.; Miyoshi, Y.; Doblhoff-Dier, O.; Takeuchi, T., A molecularly imprinted synthetic polymer receptor selective for atrazine. *Analytical chemistry* **1995**, 67 (23), 4404-4408.
40. Malitesta, C.; Losito, I.; Zambonin, P. G., Molecularly imprinted electrosynthesized polymers: new materials for biomimetic sensors. *Analytical chemistry* **1999**, 71 (7), 1366-1370.
41. Pan, J.; Xu, L.; Dai, J.; Li, X.; Hang, H.; Huo, P.; Li, C.; Yan, Y., Magnetic molecularly imprinted polymers based on attapulgite/Fe₃O₄ particles for the selective recognition of 2, 4-dichlorophenol. *Chemical Engineering Journal* **2011**, 174 (1), 68-75.
42. Liu, Q.-S.; Zheng, T.; Wang, P.; Jiang, J.-P.; Li, N., Adsorption isotherm, kinetic and mechanism studies of some substituted phenols on activated carbon fibers. *Chemical Engineering Journal* **2010**, 157 (2–3), 348-356.
43. Lin, J. M.; Nakagama, T.; Uchiyama, K.; Hobo, T., Temperature effect on chiral recognition of some amino acids with molecularly imprinted polymer filled capillary electrochromatography. *Biomedical Chromatography* **1997**, 11 (5), 298-302.

Annex III

Cu isotopic fractionation in blood of kidney stone patients

1. Introduction

About 25 elements are recognized as essential for human or animal life. Of these, 11 (Co, V, Cr, Mo, Mn, Ni, Cu, Zn, Se, Si, I) are present in trace amounts. Most of them are part of metalloenzymes and participate in biological functions, such as oxygen transport, free radical scavenging, structural organization of macromolecules, and hormonal activity. Other trace elements, such as Al, As, Cd, Hg, and Pb, and even essential ones, in quantities exceeding the needs of the organism, have known toxic effects on human health. Growing concern exists over the possible consequences on human health of new elements, such as Pt, Rh, Pd, Ga, and Ir, now widely used in the electronics industry and in catalytic converters¹. In industrialized societies symptoms of severe deficiencies of trace elements are rarely seen, although they may occur in association with other pathological conditions, affecting the gastrointestinal absorption of nutrients, such as Crohn's disease, intestinal lymphoma, and gluten-free induced enteropathy¹.

Copper (Cu) is an essential trace metal found in all living organisms in the oxidized Cu(II) and reduced Cu(I) states. It is required for survival and serves as an important catalytic cofactor in redox chemistry for proteins that carry out fundamental biological functions that are required for growth and development^{2,3}. In excess of cellular needs, Cu can be cytotoxic^{4,5}. Most clinical studies identified the correlation between low Cu concentrations and the incidence of cardiovascular diseases⁶. Copper is an essential micronutrient. As with iron (Fe), it can undergo valency changes, from Cu (II) to Cu (I), and this ability to either accept or donate electrons makes it an important part of many catalytic processes⁷. Some enzymes and biological processes where it plays a central role⁸.

It was the goal of this work to investigate the potential use of Cu isotope ratios in biological fluids for diagnosis of urolithiasis disease. For this purpose, the Cu isotopic

composition of a set of serum and red cell samples from urolithiasis patients was determined by means of MC-ICP-MS, after chromatographic isolation of Cu. Considering the difficulty in finding representative samples for this kind of study, this type of sample is collected so that is sufficiently large for a pilot study.

2. Experiments

2.1. Reagents and standards

All digestion, isolation and dilution protocols were carried out in class-10 clean lab. Savillex[®] PFA vials were used throughout the study for sample handling. Optima grade nitric acid (HNO₃), Optima grade hydrochloric (HCl) produced by Fisher. Hydrogen peroxide (H₂O₂ 30% ULTREX[®] ultrapure reagent) and hydrochloric acid (ULTREX[®] ultrapure reagent) were purchased from J.T.Baker. Ultra-pure water (resistivity ≥ 18.2 M Ω cm) obtained from a Direct-Q3 system (Millipore, Molsheim, France), was used to prepare all solutions. Multi-element and single-element standard solutions used for quantitative analysis and the Zn single-element standard solution used for mass bias correction.

All labware (tips, columns, Savillex[®] PFA vials) was washed successively with 10% analytical grade HNO₃ twice, and 10% trace metal grade HCl. Macroporous anion-exchange resin AGMP-1 100–200 mesh was purchased from Bio-rad Laboratories.

For isolation of the Cu from matrix, Poly-Prep chromatography columns (2 mL resin bed, 10 mL reservoir) were filled with AG-MP-1 (100–200 mesh) strong anion exchange resin. Both the columns and the resin were acquired from Bio-Rad (Hercules, CA, USA).

2.2. Sample

Blood and urine sample were collected from stone formers patients. The participants were recruited at Hospital Clinic, Barcelona, Spain. 24 hour urine samples were also collected. The whole volume of urine was collected in the same plastic bottle (2.2L), mixed and then stored at 4°C until the analysis was done. The blood sample collection

was performed in compliance with institutional guidelines. The patients are between 30 and 84 years old, female donors are 55 ± 2.2 years old and male donors are 60 ± 20 years old. The blood samples were centrifuged at 5000 rpm during 15min to separate the red cells from the blood serum, and the serum was retained for isotope analysis. Blood serum and red cells were kept at approximately -20°C until use. In this study, all the information(Cu concentration, Cu isotopic information) of the control group came from the research of Albarède et al.⁹.

2.3. Sample digestion

2 ml of blood serum samples were first predigested at room temperature in 5 mL 16 M HNO_3 , and 3 mL 30% H_2O_2 , for 1 hour. Then the samples were digested in a MARS Microwave Digestion System at 200°C , 300 psi for 90 min. Digested samples were then evaporated in Savillex vials, redissolved in 5 mL 0.1 M HNO_3 and stored in clean vials at 4°C in fridge until use. Three blank and reference material SRM1573a (NIST), tomato leaves were treated under the same condition.

2 ml of red cell samples were first predigested in 5 mL 16 M HNO_3 , and 3 mL 30% H_2O_2 , for 20 hours. Then the samples were digested a MARS Microwave Digestion System at 180°C , 300 psi for 90 min. Digested samples were then evaporated in Savillex vials, redissolved in 5 mL 0.1 M HNO_3 and 1 ml 16M HNO_3 , stored in clean vials at 4°C in fridge until use.

Sample aliquots of 0.1 mL of the digested solution were used for determination of the total element concentration by ICPMS. The digestion process was evaluated by the recovery of Cu in the reference material. The Cu was separated from these solutions and prepared for isotopic analysis using the method of ion-exchange column separation.

2.4. Column separation of Cu from the matrix

The macroporous anion-exchange resin AGMP-1 100-200 mesh purchased from Bio-rad Laboratories was used as the solid phase to separate the Cu from matrix. Sample

preparation and analysis was performed in Class 2 laminar flow hoods in the Class 1000 Clean Room at UAB.

Before the first use, the resin was settled 10 times in M.Q. water and the supernatant was decanted after sufficient settling time in order to eliminate the finest resin particles. The cleaned resin was stored in 0.1 M HCl.

The metals analyzed were separated on bio-rad columns containing 2 mL macroporous anion-exchange resin. The column was washed by acid and only used once in order to avoid contamination¹⁰. Before sample loading, the resin was cleaned three times with 1 M HNO₃ (10 mL) alternating with M.Q. water (2 mL). It was then conditioned with 10 ml of 7M HCl+0.001% H₂O₂. Samples were loaded onto the columns in 7 M HCl +0.001% H₂O₂. The matrix elements are washed off with 7M HCl+0.001% H₂O₂ (10 mL), then Cu was eluted by the next 20 ml of the same solution. The purification protocol is summarized in Table 1.

Table 1. Chromatographic separation sequence^{11,12}

Eluent	Acid Volumn (ml)	Purpose
<i>Rensin cleaning</i>		
1M HNO ₃	10	Clean
≥18MΩ cm water	2	Rinse
1M HNO ₃	10	Clean
≥18MΩ cm water	2	Rinse
1M HNO ₃	10	Clean
≥18MΩ cm water	10	Rinse
<i>Rensin conditioning</i>		
7M HCl+0.001%H ₂ O ₂	10	Conditioning
<i>Sample loading</i>		
7M HCl+0.001%H ₂ O ₂	1	Loading
<i>Elution sequence</i>		
7M HCl+0.001%H ₂ O ₂	10	Matrix(e.g.Mg,Na,Al,Ca,Cr)
7M HCl+0.001%H ₂ O ₂	20	Cu

2.5. Isotopic fractionation measurement

The purified Cu fraction was analyzed by ICP-MS prior to isotope analyses in order to obtain accurate total analyte concentrations, as well as to ensure the absence of interfering elements.

Prior to Cu isotope analysis samples, sample and isotope standards were diluted to a Cu concentration of $200\mu\text{g L}^{-1}$ and matrix matched to 2% HNO_3 followed by addition of Zn at $200\mu\text{g L}^{-1}$, for on-line mass bias correction. In this study, the NIST SRM 976 was used as delta zero reference material for Cu. No certified Zn reference material being available, the IRMM-3702 was used to correct the mass bias.

In order to calculate Cu isotope ratios from these signals, a linear regression slope (LRS) method, where the signal intensities for ^{65}Cu were plotted against the signal intensities for ^{63}Cu , was used. The slope of the regression curve provides the raw $^{65}\text{Cu}/^{63}\text{Cu}$ ratio, which is later corrected for mass bias applying Russell's exponential law¹¹.

Results are reported as $\sigma^{65}\text{Cu}$ (Equation 1), which is the change in $^{65}\text{Cu}/^{63}\text{Cu}$ ratio in parts per thousand (‰), relative to the isotopic composition of reference material NIST SRM 976. By definition, $\sigma^{65}\text{Cu}_{\text{NIST SRM976}} = 0\text{‰}$.

$$\sigma^{65}\text{Cu} = \left[\left(\frac{^{65}/^{63}\text{Cu}_{\text{sample}}}{^{65}/^{63}\text{Cu}_{\text{NIST SRM976}}} \right) - 1 \right] \times 1000 \quad (1)$$

The purified Cu fraction was analyzed by ICP-MS (Element2, Thermo Fisher Scientific, Bremen, Germany) prior to isotope analyses in order to obtain accurate analyte concentrations, as well as to ensure the absence of interfering elements. Operational conditions and measurement parameters are described in table1.

Prior to Cu isotope analysis samples, working-and isotope standards were diluted to a Cu concentration of $200\mu\text{g L}^{-1}$ and matrix matched to 2% HNO_3 followed by addition of Zn at $200\mu\text{g L}^{-1}$, for on-line mass bias correction. In this study, the NIST SRM 976 was used as delta zero reference material for Cu¹³. No certified Zn reference material being available, the IRMM-3702 was used¹⁴ to correct the mass bias¹⁵.

Measuring conditions was adjusted for maximum sensitivity and stability, plasma robustness and minimum influence of interferences on the target analyte signals are optimized and the conditions and parameters are described in table 2.

Table 2. Instrumental operating conditions used for isotopic analysis of Cu.

Nu-MC-ICPMS															
RF power		1300W													
Instrument resolution		Pseudo-high resolution ~5700(edge resolved power)													
Source slit width		0.05 mm													
Alpha 1 slit		80 mA													
Alpha 2 slit		90 mA													
Integration time		5 s													
Plasma gas flow rate		13.0 L min ⁻¹													
Auxiliary gas flow rate		0.80 L min ⁻¹													
Nebulizer pressure		28.8 psi													
Faraday cup configuration															
collecto	H	H	H	H	H	H	H	A	L	L	IC	L	IC	IC	L
r	7	6	5	4	3	2	1	x	1	2	0	3	1	2	4
<i>m/z</i>	65					63			62			61			

3. Results and Discussion

3.1. The Cu column separation optimization

Acid digestion is the most commonly used method for the destruction of organic material in biological samples¹⁴, ¹³. However, conventional hot plate digestion is normally very time-consuming and susceptible to contamination¹⁵. For example, digestion times as long as 3 hours have been needed to achieve complete digestion of urine¹⁶. While microwave digestion is a common technique used to dissolve heavy metals in the presence of organic molecules. This technique is usually accomplished by

exposing a sample to a strong acid in a closed vessel and raising the pressure and temperature through microwave irradiation.

It is highly recommended to separate the Cu from the blood matrix before isotopic analysis via MC-ICP-MS, not only for avoiding the influence of matrix-induced mass bias, but also because in ICP-MS both Cu isotopes may be subject to spectral overlap due to the occurrence of polyatomic ions with the same mass number. For the biological sample, the very high amount of alkane elements in blood samples is the most serious problem. The major molecular interferences that may be problematic for the isotopic measurement of Cu is listed in Table 3. For example, the sodium concentration is in the range of 3000 mg/L, can interfere with Cu at m/z 63 because of the formation of $^{40}\text{Ar}^{23}\text{Na}^+$ in ICP. Magnesium is another less important element which can give rise to $^{40}\text{Ar}^{25}\text{Mg}^+$, interfering with Cu at m/z 65. ¹⁷Therefore, before Cu isotopic analysis, column separation of blood samples was carried out twice.

Table 3. Main molecular interferences for Cu and Zn isotopic analysis in biological samples.

Element	Mass	interference
Cu	63	$^{23}\text{Na}^{40}\text{Ar}^+$, $^{25}\text{Mg}^{38}\text{Ar}^+$, $^{26}\text{Mg}^{37}\text{Cl}^+$, $^{31}\text{P}^{16}\text{O}_2^+$, $^{47}\text{Ti}^{16}\text{O}^+$
	65	$^{25}\text{Mg}^{40}\text{Ar}^+$, $^{32}\text{S}^{33}\text{S}^+$, $^{33}\text{S}^{16}\text{O}_2^+$, $^{49}\text{Ti}^{16}\text{O}^+$, $^{130}\text{Ba}^{2+}$
Zn	64	$^{48}\text{Ca}^{16}\text{O}^+$
	66	$^{50}\text{Cr}^{16}\text{O}^+$

According to published data, the best way to carry out Cu isolation is by applying ion exchange chromatography, although careful validation of the protocol needs to be carried out as Cu is known to undergo on-column isotope fractionation. In this work, we deployed a separation method based on the use of AG-MP-1 strong anion exchange resin recently developed and validated in our research group for Cu isotopic analysis of oyster samples. It was thus necessary to check the performance of this method for serum samples, which was tested through analysis of one of the control samples for which a sufficient amount was available for performing replicate analyses.

Copper separation and purification was achieved through a column ion exchange chromatography using procedures adapted from Mason¹² and Maréchal¹¹. Since the blood sample contain significant quantities of Na, Mg, and other constituents, which must be removed to eliminate matrix effects and isobaric interferences.

Na and Mg are the major atomic interferences on Cu ($^{23}\text{Na}^{40}\text{Ar}^+$, $^{25}\text{Mg}^{38}\text{Ar}^+$, $^{26}\text{Mg}^{37}\text{Cl}^+$ on ^{63}Cu and $^{25}\text{Mg}^{40}\text{Ar}^+$ on ^{65}Cu) and, although these elements are removed in the first column step, we use a second column filled with the same resin to ensure their complete removal. At acid concentrations of 7 M HCl, Cu is retained on the resin while the matrix passes through. The Cu fraction is evaporated to dryness and re-dissolved in 2% HNO₃ in preparation for isotopic analysis.

The resin AG MP-1 is a macroporous form of strongly basic anion exchange resin has higher distribution coefficients for Cu (II) in concentrated HCl than regular AG1. The macroporous resin AG MP-1 is made of chips instead of beads, is very fragile and tends to compact with time.

It was observed previously that the isotopic fractionation happened on resin AG MP-1 and the lighter isotope is preferentially retained on the resin¹¹. So this Cu fractionation on the column need purification achieved full recovery and the investigation of the elution curve is quite important.

This separation procedure was validated by the oyster samples and reference materials. Cu recoveries were calculated after analysis of the digests and the eluted Cu fractions by means of ICP-MS, yielding an average of $100 \pm 9\%$ Cu recovery, thus avoiding any effect from on-column isotope fractionation. To monitor Cu recoveries along the study, all of the samples targeted in the investigation were also analyzed for their Cu content after column separation, and the results obtained were compared with previously available concentration values. Near-quantitative Cu yields were obtained in all cases.

3.2. Total Cu concentration in blood.

The Cu concentration of serum and red cell sample from patients and healthy control are summarized in Table 4. The differences among the groups are evident. The red cell sample of urolithiasis patients show significantly higher Cu values than the serum sample (either male or female). The Cu concentration in serum ranged between 500-1200 µg/L and in red cell 1600-2600 ug/L. The Cu concentration in whole blood found in the bibliography was in the range, 800-1100µg/L for males and 1000-1400µg/L for females¹⁸. In the present study for males the Cu concentration is in the range, 730-1400 µg/L for serum and 1800-2700 µg/L for red cells. While in the healthy control for males, 350-1200 µg/L for serum and 500-800 µg/L for red cells. In the present study for females the Cu concentration is in the range, 440-1160 µg/L for serum and 1630-2900 µg/L for red cells. While in the healthy control for males, 940-2800 µg/L for serum and 500-1700 µg/L for red cells.

Table 4. Cu concentration of serum and red cells in kidney stone patients and control group.

kidney stone patients			Healthy control(data from ⁹)		
Serum		Red cell	Serum		Red cell
ID	Cu conc.,ppb	Cu conc.,ppb	ID	Cu conc.,ppb	Cu conc.,ppb
1	1100	1630	C1	1156	1016
2	1090	2750	C2	1586	962
3	750	2020	C3	976	928
6	570	2220	C4	2816	1705
7	440	1740	C5	2271	1055
8	730	2170	C6	2271	1003
9	820	2740	C7	2165	982
10	1430	2090	C8	896	890
11	1010	2460	C9	1927	1029
12	1200	2710	C10	966	924
13	1160	2890	C11	973	863
14	880	1810	C12	1086	802
15	820	2310	C13	966	766
16	1130	2500	C14	1634	738
17	790	2200	C15	941	701
18	880	2570	C16	1547	606
19	1140	2630	C17	1899	902
			C18	1801	761
			C19	1082	686

C20	1216	639
C21	1715	809
C22	1917	764
C23	1151	717
C24	2135	381
C25	1738	667
C26		735
C27		541
C28		478
C29	1210	635
C30	815	557
C31	701	670
C32	733	499
C33	907	687
C34	675	545
C35	926	656
C36	967	591
C37	750	653
C38	492	530
C39	728	716
C40	698	560
C41	928	635
C42	801	713
C43	875	669
C44	352	728
C45	761	670
C46	753	587
C47	844	725
C48	912	761
C49	883	716

3.3. Correction for mass discrimination

Standards solution and samples were measured in 2% HNO₃ solution at the same condition than the blood samples. All the measurements were performed in low-resolution mode. Of the methods available for correcting instrumental mass discrimination, the double spike approach has been shown to be a robust and rigorous technique when applied to isotope systems¹⁹. In this study, Zn standard IRMM-3702 and Cu standard NIST 976 were used for the mass correction. The advantages of using the double-spike method are well known and include elimination of issues concerning

differences in the behavior of samples and dopant or standards, used respectively in the doping and standard-bracketing methods, and removing potential fractionation problems induced due to incomplete yield from the column chemistry²⁰.

As long as the f values vary but $f_{\text{Cu}}/f_{\text{Zn}}$ ratio remains constant, the two isotopic ratios of Cu and Zn of a sample should form a linear array in a log – log plot. When $\ln(^{65}\text{Cu}/^{63}\text{Cu})_{\text{meas}}$ ('meas' means measure) is plotted against $\ln(^{68}\text{Zn}/^{64}\text{Zn})_{\text{meas}}$, the slope s is

$$s = \frac{f_{\text{Cu}} \ln(65/63)}{f_{\text{Zn}} \ln(68/64)} \quad (2)$$

and the intercept y_0

$$y_0 = \ln\left(\frac{^{65}\text{Cu}}{^{63}\text{Cu}}\right)_{\text{true}} - s \times \ln\left(\frac{^{68}\text{Zn}}{^{64}\text{Zn}}\right)_{\text{true}} \quad (3)$$

$$f = \frac{\ln(r/R)}{\ln(M_2/M_1)} \quad (4)$$

The exponential law was used to describe real instrumental data, for example, if $f_{\text{Cu}}=f_{\text{Zn}}$, then a plot of measured, uncorrected Cu and Zn isotopes in ln-ln space should yield a straight line of a pre-defined slope $[\ln(\text{mass } ^{65}\text{Cu}/\text{mass } ^{63}\text{Cu})/\ln(\text{mass } ^{66}\text{Zn}/\text{mass } ^{64}\text{Zn})] = 1.015$. Isotopic variations of Cu and Zn are shown in figure 1 and figure 2. In figure 1, $\ln(^{68}\text{Zn}/^{64}\text{Zn})$ and $\ln(^{66}\text{Zn}/^{64}\text{Zn})$ are plotted. As it can be seen that the isotopic variations of $^{68}\text{Zn}/^{64}\text{Zn}$ and $^{66}\text{Zn}/^{64}\text{Zn}$ following a mass dependent fractionation relationship with a slope of 2.015 not significantly different from the theoretical value¹¹. In figure 2, $\ln(^{65}\text{Cu}/^{63}\text{Cu})$ and $\ln(^{66}\text{Zn}/^{64}\text{Zn})$ are plotted. As it can be seen that the isotopic variations of $^{65}\text{Cu}/^{63}\text{Cu}$ and $^{66}\text{Zn}/^{64}\text{Zn}$ following a mass dependent fractionation relationship with a slope of 0.9981 not significantly different from the theoretical value..

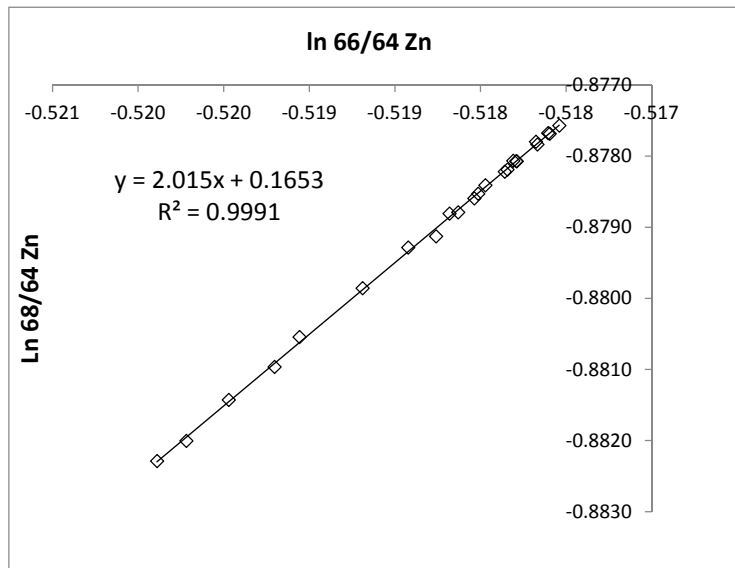


Figure 1. Isotopic variations of $^{68}\text{Zn}/^{64}\text{Zn}$ and $^{66}\text{Zn}/^{64}\text{Zn}$ following a mass dependent fractionation relationship with a slope not significantly different from the theoretical value.

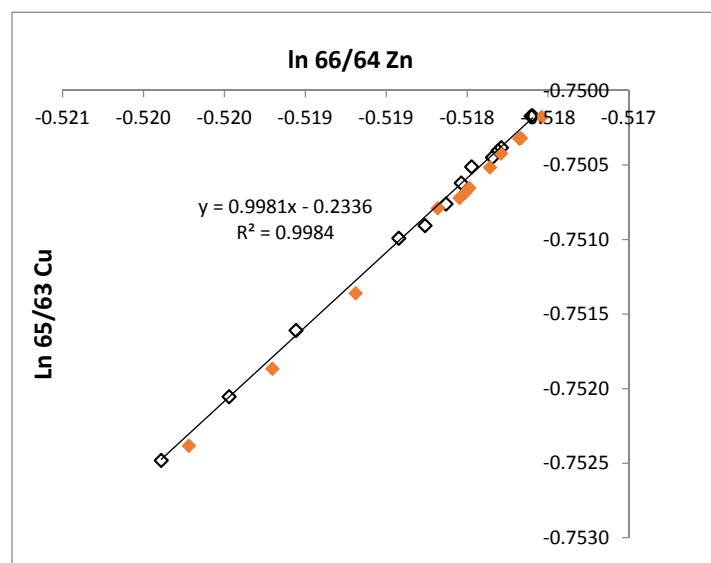


Figure 2. Isotopic variations of $^{65}\text{Cu}/^{63}\text{Cu}$ and $^{66}\text{Zn}/^{64}\text{Zn}$ following a mass dependent fractionation relationship with a slope not significantly different from the theoretical value.

In addition, long-term external reproducibility for the digestion, purification and isotope analysis is defined by the processing and analysis of NIST 1573a tomato leaves. This standard was measured as $\delta^{65}\text{Cu} = 0.54$, which is in the range of $\delta^{65}\text{Cu} = 0.63 \pm 0.16$ ‰ (mean \pm 2SD) reported by Ryan et al.²¹.

3.4. Cu isotopic analysis of the serum and red cell samples

Finally the samples were analyzed following the optimized procedure indicated previously. Due to the low amount of sample available, all samples were analyzed only once. The Cu isotopic composition of serum and red cells for the urolithiasis patients is summarized in Table 5 together with the total Cu concentration expressed for the different groups. As seen in this table, all the samples are enriched in the heavier isotope except the serum samples of the control group, as remarks the negative sign, although differences among the groups are evidenced. The serum and red cell samples of urolithiasis patients show significantly higher $\delta^{65}\text{Cu}$ values than the controls (either male or female). For the males, the Cu isotopic fractionation seems to a lesser extent.

Cu concentration in serum of female urolithiasis patients ($903 \pm 316 \mu\text{g l}^{-1}$) were significantly lower than those in healthy control ($1553 \pm 536 \mu\text{g l}^{-1}$). It is need to mention that the age of the female urolithiasis is in the range of 30-76, and the female healthy control is in the range 19-38. However, for male urolithiasis patients the concentration of Cu ($956 \pm 224 \mu\text{g l}^{-1}$) is no significant difference compared with the healthy control ($798 \pm 171 \mu\text{g l}^{-1}$).

Table 5. Cu isotopic component of serum and red cell for different groups of individuals studied.

		serum		red cell	
	group	Cu conc.	$\delta^{65}\text{Cu}$ corr. (‰)	Cu conc.	$\delta^{65}\text{Cu}$ corr. (‰)
urolithiasis	Males (n=11)	956 ± 224	0.06 ± 0.24	2352 ± 322	0.86 ± 0.21
	Female (n=6)	903 ± 316	0.20 ± 0.24	2262 ± 499	0.94 ± 0.22
	Total (n=17)	938 ± 251	0.11 ± 0.24	2262 ± 499	0.90 ± 0.21
control	Males (n=21)	798 ± 171	-0.28 ± 0.40	648 ± 76	0.67 ± 0.36
	Female (n=28)	1553 ± 536	-0.24 ± 0.36	823 ± 238	0.46 ± 0.47
	Total (n=49)	1200 ± 555	-0.26 ± 0.40	746 ± 207	0.56 ± 0.50

These differences among samples from different groups become even more evident when isotopic information is combined with total Cu concentration data, as shown in

Figure 3 and Figure 4. In these figures, a bivariate “Cu concentration” vs. “ $\delta^{65}\text{Cu}$ ” plot, the different groups can be perfectly differentiated.

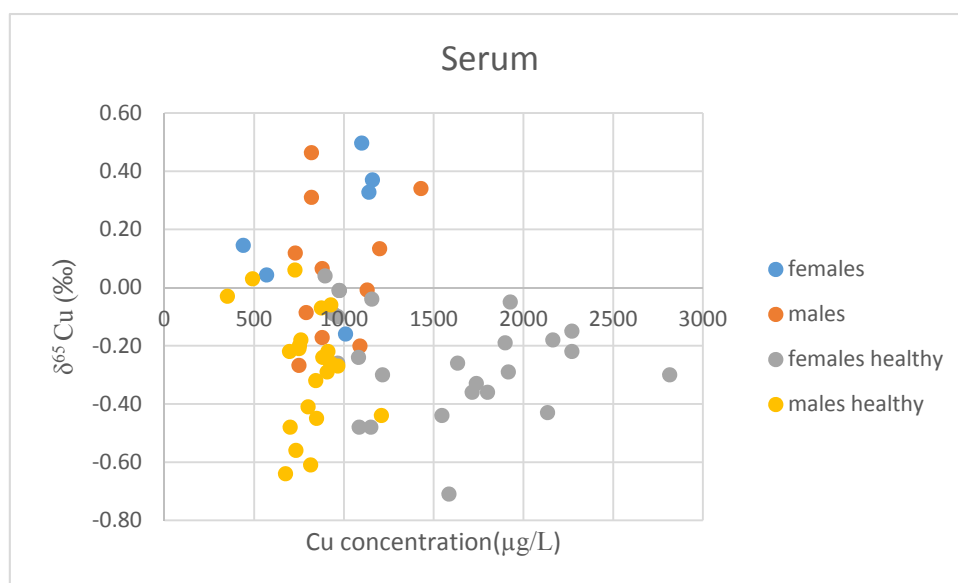


Figure 3 “concentration vs. isotopic information” plot for the serum samples of different groups of individuals considered.

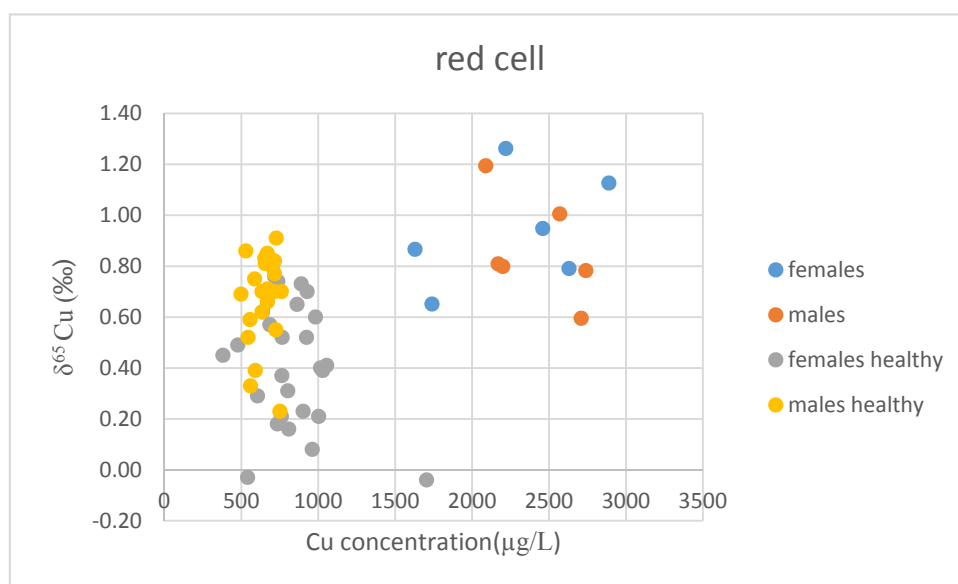


Figure 4 “concentration vs. isotopic information” plot for the red cell samples of different groups of individuals considered.

Data obtained for urolithiasis patients suggest that a possible Cu isotopic drift of the Cu stores is expected to occur because they preferentially retained ^{65}Cu relative to ^{63}Cu .

It was claimed that the low efficiency by which Cu is incorporated into ceruloplasmin in Wilson’s disease patients apparently results in ^{63}Cu enrichment in the serum samples¹⁷. It was reported that a relationship exists between age and blood $\delta^{65}\text{Cu}$ values,

with enrichment in light Cu isotopes in blood of elderly people. We suggest that this observation could be due to the preferential retention of light Cu isotopes by the body^{22, 23}.

Given the large isotopic dispersion of the results and the low number of samples, isotopic ratio alone cannot account for all the isotopic variability. In the state of the present results, the Cu isotope compositions could be used as a potential isotopic tool for urolithiasis diagnosis. The renewal of Cu in blood is linked to the erythropoietic process, and takes about 3 months²³. The origin of the Cu isotopic fractionations remains unknown in terms of physiological location and biochemical process. This rapid time of residence can explain the large isotopic diverse observed for urolithiasis in human blood.

In order to confirm this assumption, the relationship between Cu isotope compositions and medicine treated patient should be tested. However, this is the first time that a urolithiasis-related isotopic drift is reported. We do not yet know the molecular effects of the evolution of the isotopic ratio shifts, but we believe that this is an avenue to explore in biomedical sciences.

4. Conclusion

It was the purpose of this work to investigate the potential use of Cu isotopic analysis for the diagnosis of urolithiasis by analyzing a set of serum samples from different groups such as urolithiasis patients, and normal (supposedly healthy adults). It was found that Cu concentration in serum samples for urolithiasis patients was lower than the healthy control. However, the Cu concentration in red cell of lithiasic patient was much higher than that in healthy control. It was also found that the Cu in serum for lithiasic patients is significantly fractionated towards the heavier isotope when compared to serum samples of control (healthy) individuals. For the population considered in this study, combination of concentration values and isotopic information allows perfect classification of urolithiasis patients and controls into different groups. Although further studies with a larger number of samples are needed, results are

encouraging as far as the use of Cu isotopic analysis for early diagnosis of urolithiasis disease is concerned.

Reference

1. Patriarca, M.; Menditto, A.; Di Felice, G.; Petrucci, F.; Caroli, S.; Merli, M.; Valente, C., Recent developments in trace element analysis in the prevention, diagnosis, and treatment of diseases. *Microchemical journal* **1998**, *59* (2), 194-202.
2. de Romaña, D. L.; Olivares, M.; Uauy, R.; Araya, M., Risks and benefits of copper in light of new insights of copper homeostasis. *Journal of Trace Elements in Medicine and Biology* **2011**, *25* (1), 3-13.
3. Scott, K. C.; Turnlund, J. R., Compartmental model of copper metabolism in adult men. *The Journal of Nutritional Biochemistry* **1994**, *5* (7), 342-350.
4. Linder, M. C.; Hazegh-Azam, M., Copper biochemistry and molecular biology. *The American journal of clinical nutrition* **1996**, *63* (5), 797S-811S.
5. Tapiero, H.; Townsend, D.; Tew, K., Trace elements in human physiology and pathology. Copper. *Biomedicine & pharmacotherapy* **2003**, *57* (9), 386-398.
6. Kang, Y. J., Copper and homocysteine in cardiovascular diseases. *Pharmacology & Therapeutics* **2011**, *129* (3), 321-331.
7. Wiederhold, J. G., Metal stable isotope signatures as tracers in environmental geochemistry. *Environmental science & technology* **2015**, *49* (5), 2606-2624.
8. Harvey, L. J.; McArdle, H. J., Biomarkers of copper status: a brief update. *British Journal of Nutrition* **2008**, *99* (S3), S10-S13.
9. Albarède, F.; Télouk, P.; Lamboux, A.; Jaouen, K.; Balter, V., Isotopic evidence of unaccounted for Fe and Cu erythropoietic pathways. *Metallomics* **2011**, *3* (9), 926-933.
10. Shiel, A. E.; Barling, J.; Orians, K. J.; Weis, D., Matrix effects on the multi-collector inductively coupled plasma mass spectrometric analysis of high-precision cadmium and zinc isotope ratios. *Analytica chimica acta* **2009**, *633* (1), 29-37.
11. Maréchal, C. N.; Télouk, P.; Albarède, F., Precise analysis of copper and zinc isotopic compositions by plasma-source mass spectrometry. *Chemical Geology* **1999**, *156* (1), 251-273.
12. Mason, T. F. D. High precision transition metal isotope analysis by plasma-source mass spectrometry and its implications for low temperature geochemistry. Imperial College London (University of London), 2003.
13. Turnlund, J. R.; Keyes, W. R.; Kim, S. K.; Domek, J. M., Long-term high copper intake: effects on copper absorption, retention, and homeostasis in men. *The American journal of clinical nutrition* **2005**, *81* (4), 822-828.
14. Kuwabara, J.; Noguchi, H. In *Development of rapid urine analysis method for uranium*.
15. Atakan, I. H.; Kaplan, M.; Seren, G.; Aktoz, T.; Gül, H.; Inci, O., Serum, urinary and stone zinc, iron, magnesium and copper levels in idiopathic calcium oxalate stone patients. *International urology and nephrology* **2007**, *39* (2), 351-356.
16. Chen, S.-C.; Shiue, M.-Y.; Yang, M.-H., Microwave digestion and matrix separation for the determination of cadmium in urine samples by electrothermal atomization atomic absorption spectrometry using a fast temperature program. *Fresenius' journal of analytical chemistry* **1997**, *357* (8),

1192-1197.

17. Aramendía, M.; Rello, L.; Resano, M.; Vanhaecke, F., Isotopic analysis of Cu in serum samples for diagnosis of Wilson's disease: a pilot study. *Journal of Analytical Atomic Spectrometry* **2013**, *28* (5), 675-681.
18. Iyengar, G., Reevaluation of the trace element content in reference man. *Radiation Physics and Chemistry* **1998**, *51* (4), 545-560.
19. Jaouen, K.; Balter, V., Menopause effect on blood Fe and Cu isotope compositions. *American journal of physical anthropology* **2014**, *153* (2), 280-285.
20. Cameron, V.; Vance, D.; Archer, C.; House, C. H., A biomarker based on the stable isotopes of nickel. *Proceedings of the National Academy of Sciences* **2009**, *106* (27), 10944-10948.
21. Ryan, B. M.; Kirby, J. K.; Degryse, F.; Harris, H.; McLaughlin, M. J.; Scheiderich, K., Copper speciation and isotopic fractionation in plants: uptake and translocation mechanisms. *New Phytologist* **2013**, *199* (2), 367-378.
22. Balter, V.; Zazzo, A.; Moloney, A. P.; Moynier, F.; Schmidt, O.; Monahan, F. J.; Albarede, F., Bodily variability of zinc natural isotope abundances in sheep. *Rapid Communications in Mass Spectrometry* **2010**, *24* (5), 605-612.
23. Jaouen, K.; Gibert, M.; Lamboux, A.; Telouk, P.; Fourel, F.; Albarède, F.; Alekseev, A. N.; Crubézy, E.; Balter, V., Is aging recorded in blood Cu and Zn isotope compositions? *Metallomics* **2013**, *5* (8), 1016-1024.